## *Molecular pharmacological characterisation of recombinant and native NR2B- and NR3B- containing NMDA receptors*

Chaffey, Heather Emily

# Molecular Pharmacological Characterisation of Recombinant and Native NR2B– and NR3B–containing NMDA Receptors

PhD Thesis

2008



Heather Emily Chaffey

School of Biological and Biomedical Sciences

Durham University



# Abstract

NMDA receptors are ionotropic, glutamate receptors which mediate fast excitatory transmissions within the central nervous system. They form tetrameric or pentameric heterologous complexes from seven NMDA receptor subunits NR1, NR2A-D and NR3A-B which each convey distinct expression patterns, functional and pharmacological properties to the receptor complex. Due to its involvement in excitatory transmission, over-excitation of the NMDA receptor, particularly the NR2B subunit, has been the focus of pharmaceutical therapeutic targeting for neurodegenerative conditions and chronic pain. This thesis discusses the potential importance and clinical effectiveness of targeting NMDA receptors and the difficulties in drug development arising from the receptor's heteromeric nature.

The work herein focuses on the pharmacological characterisation of two novel NR2B-selective antagonists Compound A and Compound B, the physiological and pharmacological effects of NR3 subunit inclusion in the NMDA receptor complex, and the modifications of NMDA receptor physiology and subunit expression during chronic pain states.

This research provides novel evidence to suggest that Compound A and Compound B bind with a high selectivity and affinity towards NR1/NR2B containing receptors. It provides novel evidence for a differential cytoprotective effect of the NR3 subunits showing significant cytoprotection in NR1/NR2B, but not NR1/NR2A, receptors and shows that NR3B inclusion in the receptor can differentially modulate the binding affinities of NR2B-selective antagonists.

This study also shows evidence for increased activity of spinal and supra-spinal NR2B-containing receptors indicating NMDA receptor modulation and involvement in a chronic pain model.

# Candidates Declaration



All animal studies in this thesis were performed with full Home Office ethical (Durham University - Project licence PPL-6003437) and GSK (Harlow) in house project licence.

All human material was obtained with full Home Office ethical approval (under Newcastle University LREC 2002/295).

# Acknowledgements

I'd like to start by saying a huge thank you to all those who have helped and supported me throughout the course of my PhD.

I would particularly like to say a huge thank you to my supervisor Dr Paul Chazot for his continued guidance, support and encouragement throughout the three (nearly four!) years, and for the many opportunities he's given me.
I'd also very much like to thank the girls in the lab in Durham; Fiona, Andrea, Sawsan, Becca and Steph for all their help and advice and for being really great friends.

I'd also like to say a huge thank you to my industrial supervisor Dr Martin Gunthorpe, again for all his support and guidance and for giving me the opportunity to go and work in his lab at GSK, learn a great technique and meet some lovely people. I'd like to thank all the ephys team at GSK for being so friendly and welcoming, and in particular Jon for all his help and patience!

I also want to thank all of my friends and family, especially my mum, for all her encouragement, and Markus for his amazing support and endless enthusiasm.

# Contents

## Chapter 1 Introduction


| | | |
|---|---|---|
| 1.1 | Neurotransmitters within the central nervous system | 1 |
| 1.2 | Glutamate receptors within the central nervous system | 1 |
| 1.3 | The NMDA receptor | 3 |
| 1.3.1 | NMDA receptor activation and modulatory binding sites | 3 |
| 1.3.2 | NMDA channel kinetics | 4 |
| 1.3.3 | NMDA receptor subunit structure | 6 |
| 1.3.3.1 | The NR1 subunit structure | 7 |
| 1.3.3.2 | The NR2 subunit structure | 8 |
| 1.3.3.3 | The NR3 subunit structure | 9 |
| 1.4 | Regional distribution of the NMDA receptor subunits | 10 |
| 1.4.1 | NR1 expression | 11 |
| 1.4.2 | NR2A expression | 11 |
| 1.4.3 | NR2B expression | 11 |
| 1.4.4 | NR2C expression | 12 |
| 1.4.5 | NR2D expression | 12 |
| 1.4.6 | NR3A-B expression | 13 |
| 1.5 | NMDA receptor subunit co-assembly | 14 |
| 1.6 | Physiological and functional properties of NR2B and NR3B receptors | 15 |
| 1.6.1 | Physiological properties of NR2B-containing receptors | 15 |
| 1.6.2 | Physiological properties of NR3-containing receptors | 18 |
| 1.7 | NMDA receptor signalling and trafficking | 20 |
| 1.8 | Pharmacological targeting of the NMDA receptor | 21 |
| 1.8.1 | Non-selective NMDA antagonists | 22 |
| 1.8.2 | NR2B subunit selective antagonists | 23 |
| 1.9 | NMDA receptor associations with pathology | 29 |
| 1.9.1 | Calcium-dependent excitotoxicity | 29 |
| 1.9.2 | Huntington's Disease | 30 |
| 1.9.3 | Schizophrenia | 31 |
| 1.9.4 | Parkinson's Disease | 32 |
| 1.9.5 | Alzheimer's Disease | 33 |
| 1.9.6 | Amyotrophic lateral sclerosis (Motor neuron disease) | 34 |
| 1.9.7 | Chronic Pain | 35 |
| 1.9.8 | NMDA receptor and central sensitisation | 37 |
| 1.9.9 | NR2B as an analgesic target | 39 |

| | | |
|---|---|---|
| 1.10 | Hypotheses, Aims and Objectives | 41 |

**Chapter 2 Materials and Methods**

| | | |
|---|---|---|
| 2.0 | Materials | 43 |
| 2.1 | Preparation of standard solutions | 43 |
| 2.1.1 | Acrylamide gels | 43 |
| 2.1.2 | APS (Ammonium Persulfate) | 43 |
| 2.1.3 | Coumeric Acid | 43 |
| 2.1.4 | DMEM F12 Media | 43 |
| 2.1.5 | DTT | 43 |
| 2.1.6 | Electrode Buffer | 44 |
| 2.1.7 | Extracellular solution for patch-clamping | 44 |
| 2.1.8 | Extracellular solution for $Ca^{2+}$ permeability experiments | 44 |
| 2.1.9 | Homogenisation buffer | 44 |
| 2.1.10 | Intracellular solution for patch-clamping | 44 |
| 2.1.11 | Intracellular solution for $Ca^{2+}$ permeability experiments | 44 |
| 2.1.12 | Lowry assay reagents | 44 |
| 2.1.13 | Luminol | 45 |
| 2.1.14 | Lysis Buffer | 45 |
| 2.1.15 | Phosphate buffered saline (PBS) | 45 |
| 2.1.16 | Radioligand Binding Assay buffer | 45 |
| 2.1.17 | Radioligand Binding Wash buffer | 45 |
| 2.1.18 | Running gel buffer | 45 |
| 2.1.19 | Sample buffer | 45 |
| 2.1.20 | Solubilisation buffer 1% sodium deoxycholate | 45 |
| 2.1.21 | Solubilisation buffer using sodium dodecyl sulphate | 45 |
| 2.1.22 | Stacking gel buffer | 46 |
| 2.1.23 | Stacking gel | 46 |
| 2.1.24 | Tris/EDTA (TE) buffer | 46 |
| 2.1.25 | Transfer buffer | 46 |
| 2.1.26 | Tris buffered saline (TBS) | 46 |
| 2.1.27 | Tyrodes Buffer for FLIPR | 46 |
| 2.2 | Methods | 47 |
| 2.2.1 | Glutaraldehyde method for conjugating peptides to carrier proteins | 47 |
| 2.2.2 | The 3-Maleimimdobenzoic acid N-hydroxysuccinimide (MBS) method of conjugating peptides to carrier proteins (cysteine coupling). | 47 |
| 2.2.3 | Inoculation procedure | 49 |
| 2.2.4 | Generation of an NR3B peptide affinity column | 49 |
| 2.2.5 | Immunopurification of anti-NR3B using an NR3B peptide affinity | 50 |

| | | |
|---|---|---|
| | column | |
| 2.2.6 | Homogenised membrane preparation | 51 |
| 2.2.7 | Lowry Assay to determine protein concentration | 52 |
| 2.2.8 | SDS-PAGE and Western blotting | 53 |
| 2.2.8.1 | Preparation of the samples | 53 |
| 2.2.8.2 | SDS-PAGE | 53 |
| 2.2.8.3 | Western blotting-Transfer | 54 |
| 2.2.8.4 | Incubating the nitrocellulose | 54 |
| 2.2.8.5 | Developing the nitrocellulose | 55 |
| 2.2.9 | Cryostat sectioning of rat spinal cord and whole brain | 55 |
| 2.2.9.1 | Frozen preparations | 55 |
| 2.2.9.2 | Formaldehyde fixed preparations | 55 |
| 2.2.10 | Immunohistochemistry on adult rat and human spinal cord | 56 |
| 2.2.11 | Optimised method for immunohistochemistry on adult rat spinal cord tissue | 57 |
| 2.2.12 | Solubilisation and immunopurification of NMDA receptors | 58 |
| 2.2.12.1 | Solubilisation using 1% sodium deoxycholate (DOC) | 58 |
| 2.2.12.2 | Solubilisation using sodium dodecyle sulphate (SDS) | 59 |
| 2.2.12.3 | Immunopurification | 59 |
| 2.2.12.4 | Immunoprecipitation using Seize X Protein A Immunoprecipitation Kit | 61 |
| 2.2.13 | Chloroform/Methanol Procedure for protein precipitation | 61 |
| 2.2.14 | Radioligand Binding | 62 |
| 2.2.14.1 | Competition Binding | 62 |
| 2.2.14.2 | Saturation Binding | 65 |
| 2.2.15 | Plasmid DNA preparation | 66 |
| 2.2.15.1 | Transformation of HB101 competent *E.coli* cells | 66 |
| 2.2.15.2 | Preparing glycerol stocks of transformed competent *E.Coli* cells | 66 |
| 2.2.15.3 | Amplification and preparation of plasmid DNA | 67 |
| 2.2.15.4 | Harvesting the large-scale culture and purification of plasmid DNA using the Qiagen plasmid maxi-kit | 67 |
| 2.2.15.5 | Quantification and determination of purity of the DNA yield | 68 |
| 2.2.16 | Preparation of tissue culture medium | 69 |
| 2.2.17 | Sub-culturing HEK293 cells | 69 |
| 2.2.18 | Transfection of HEK293 cells using lipofectamine reagent | 69 |
| 2.2.18.1 | Harvesting transfected HEK293 cells | 71 |
| 2.2.19 | CytoTox 96 Non-radioactive Assay | 71 |

| | | |
|---|---|---|
| 2.2.20 | Whole-cell patch-clamp electrophysiology on recombinant NMDA receptors expressed in HEK293 cells. | 72 |
| 2.2.21 | [$^3$H] Ro-256981 Autoradiography on rat spinal cord and whole brain | 73 |
| 2.2.22 | Fluorescence imaging plate reader (FLIPR). | 74 |


## Chapter 3 - Pharmacological characterisation of two novel NR2B-selective antagonists COMPOUND A and COMPOUND B


| | | |
|---|---|---|
| 3.1 | Introduction | 78 |
| 3.2 | Results | |
| 3.2.1 | Competition binding to investigate the displacement of [$^3$H] Ro-256981 by ifenprodil in adult Sprague-Dawley rat forebrain membranes. | 80 |
| 3.2.2 | Competition binding to investigate displacement of [$^3$H] Ro-256981 with COMPOUND A in adult Sprague-Dawley rat forebrain | 81 |
| 3.2.3 | Competition binding to investigate the displacement of [$^3$H] Ro-256981 with COMPOUND B, in adult Sprague-Dawley rat forebrain | 82 |
| 3.2.4 | Competition assay investigating the displacement of [$^3$H] CP-101606 binding by COMPOUND A in adult rat forebrain membranes | 83 |
| 3.2.5 | Competition assay investigating the displacement of [$^3$H] CP-101606 binding with COMPOUND B in adult rat forebrain tissue | 84 |
| 3.2.6 | Confirmation of recombinant NMDA receptor subunit expression | 85 |
| 3.2.7 | Competition binding assay to investigate the displacement of [$^3$H] Ro-256981 by COMPOUND A in recombinant NR1/NR2B receptor complexes | 86 |
| 3.2.8 | Competition assay investigating the displacement of [$^3$H] Ro-256981 by COMPOUND B in recombinant NR1/NR2B receptors | 87 |
| 3.2.9 | Competition binding assay to investigate the influence of COMPOUND A upon the binding of [$^3$H] CP-101606 in recombinant NR1/NR2B receptors | 88 |
| 3.2.10 | Competition assay to show the influence of COMPOUND B upon the binding of [$^3$H] CP-101606 towards recombinant NR1/NR2B receptors | 89 |
| 3.2.11 | Competition curve to investigate the competitive binding between [$^3$H] MK-801 and ifenprodil in adult rat forebrain tissue. | 91 |
| 3.2.12 | Competition assay to investigate the influence of COMPOUND A upon the binding of [$^3$H] MK-801 to adult rat forebrain tissue | 92 |
| 3.2.13 | Competition binding assay investigating the influence of COMPOUND B on the specific binding of [$^3$H] MK-801 in adult rat forebrain tissue | 93 |

3.3 Discussion 95

## Chapter 4 - Investigating NR3B co-expression and co-assembly in rat and human spinal cord using subunit-selective antibodies

4.0 Introduction 103
4.1 Results 107
4.1.1 Rodent anti-NR3B characterization 107
4.1.2 Immunopurification of polyclonal rodent anti-NR3B 107
4.1.3 Characterisation of anti-rodent NR3B antibody via western blotting with recombinant NMDA receptor subunits 108
4.1.4 Characterisation of anti-rodent NR3B using western blotting with native and recombinant NMDA receptors 109
4.1.5 Characterisation of the specificity of the anti-rodent NR3B with antigenic peptide blockade. 110

4.2 Anti-human NR3B characterization 111
4.2.1 Immunoaffinity purification of polyclonal anti-human NR3B 111
4.2.2 Characterisation of the anti-human NR3B antibody using western blotting on native NMDA receptors 112
4.2.3 Characterisation of anti-human NR3B in both human and rat native tissue with antigenic peptide blockade 113

4.3 Characterisation of the commercial anti-rat NR3B Upstate 114

4.4 Co-expression of the NMDA receptor subunits NR1, NR2A, NR2B and NR3B in the adult rat and adult human spinal cord 115
4.4.1 Purification of subunit selective anti-NMDA antibodies 115
4.4.2 Immunohistochemical investigations of NMDA subunit co-expression in the rat spinal cord. 117
4.4.2.1 Expression of NR1, NR3B, NR2A and NR2B in adult rat cervical spinal cord 119
4.4.2.2 Expression of NR1, NR2A, NR2B and NR3B in adult rat thoracic spinal cord. 122
4.4.2.3 Expression of NR1, NR2A, NR2B and NR3B in the adult rat lumbar spinal cord 125
4.4.2.4 Qualitative summary of NMDA subunit expression in the dorsal and ventral horns spanning the three different upper regions of the adult rat spinal cord. 128

4.4.3 NMDA subunit expression in human cervical spinal cord 130
4.4.4 Qualitative summary of NMDA receptor subunit expression in the dorsal and ventral horns of the adult human cervical spinal cord 133

4.5 Co-associations of NMDA subunits in the rat spinal cord 135
4.5.1 Solubilisation and immunopurification of adult rat spinal cord 135

| | | |
|---|---|---|
| | receptors using 1% SDS. | |
| 4.5.1.1 | Immunopurification of 1% SDS solubilised adult rat spinal cord homogenate using an anti-NR1 immunoaffinity column | 136 |
| 4.5.1.2 | Optimisation of SDS solubilisation between 0.75 and 0.05%. | 138 |
| 4.5.1.3 | Optimisation of SDS solubilisation between 0.5 and 0.2%. | 139 |
| 4.5.1.4 | Immunopurification of 0.3% SDS solubilised material from adult rat cervical spinal cord using anti-NR1 and anti-NR2A immunoaffinity columns | 140 |
| 4.5.1.5 | Immunopurification using an anti-NR1 affinity column | 140 |
| 4.5.1.6 | Immunopurification using an anti-NR2A affinity column | 140 |
| 4.6 | NR2A, NR2B and NR3B protein expression levels in different spinal cord regions | 143 |
| 4.7 | Discussion | 145 |

**Chapter 5 - The influence of NR3 subunits on NMDA receptor cytotoxicity, physiology and pharmacology**

| | | |
|---|---|---|
| 5.1 | Introduction | 157 |
| 5.1.1 | Effect of NR3 subunits upon NMDA-mediated cytotoxicity | 157 |
| 5.1.2 | Effect of NR3 upon the functional and biophysical characteristics of the NR1/NR2B receptor channel | 158 |
| 5.1.3 | Pharmacological influences of the NR3B subunit upon NR1/NR2B receptors | 159 |
| 5.2 | Results | 160 |
| 5.2.1 | Differential cytoprotective effects of NR3A and NR3B upon cell death mediated by NR1/NR2A and NR1/NR2B receptors expressed in HEK 293 cells | 160 |
| 5.2.1.1 | Differential cytotoxicity of various recombinant NMDA receptors | 161 |
| 5.2.2 | Functional influence of NR3B upon NR1/NR2B receptor physiology | 163 |
| 5.2.2.1 | Peak NMDA current amplitude of cells transfected with NR1/NR2B and NR1/NR2B/NR3B receptors | 164 |
| 5.2.2.2 | Reversal potentials of cells transfected with NR1/NR2B and NR1/NR2B/NR3B receptors | 165 |
| 5.2.2.3 | Calcium permeability experiments investigating the shift in reversal potentials of HEK 293 cells transfected with NR1/NR2B and NR1/NR2B/NR3B receptors | 166 |
| 5.2.2.4 | Sensitivity of NR1/NR2B and NR1/NR2B/NR3B receptor complexes to magnesium blockade using current/voltage (I/V) relationship | 167 |
| 5.2.2.5 | Investigating the sensitivity of NR1/NR2B and NR1/NR2B/NR3B receptor complexes towards 100μM magnesium blockade | 168 |
| 5.2.2.6 | Investigation the sensitivity of NR1/NR2B and NR1/NR2B/NR3B | 169 |

receptors towards 20μM magnesium blockade

5.2.3 Pharmacological influence of NR3B upon NR2B subtype selective antagonists 170
5.2.3.1 Cytoprotective effect of NR2B-selective antagonists upon NR1/NR2B and NR1/NR2B/NR3B receptors expressed in HEK293 cells 170
5.2.3.2 Investigating the influence of the NR3B subunit upon the NR2B subtype-selective antagonist CP-101,606 (10 μM) in recombinant NR1/NR2B and NR1/NR2B/NR3B receptors 173
5.2.3.3 Investigating the influence of the NR3B subunit upon the activity of the selective NR2B antagonist CP-101,606 (300nM, 10 seconds) in recombinant NR1/NR2B and NR1/NR2B/NR3B receptors 174
5.2.3.4 Investigating the influence of the NR3B subunit upon the activity of the selective NR2B antagonist CP-101,606 (300nM, 60 seconds) in recombinant NR1/NR2B and NR1/NR2B/NR3B receptors 175
5.2.3.5 Investigating the influence of the NR3B subunit upon the activity of the selective NR2B antagonist CP-101,606 (30nM, 60 seconds) in recombinant NR1/NR2B and NR1/NR2B/NR3B receptors 176
5.2.3.6 Investigating the influence of the NR3B subunit upon the activity of the selective NR2B antagonist Ro-256981 (10μM, 10 seconds) in recombinant NR1/NR2B and NR1/NR2B/NR3B receptors 177
5.2.3.7 Investigating the influence of the NR3B subunit upon the activity of the selective NR2B antagonist Ro-256981 (30nM, 60 seconds) in recombinant NR1/NR2B and NR1/NR2B/NR3B receptors 178
5.2.3.8 Competition binding to investigate the pharmacological influence of NR3B expression upon the displacement of [$^3$H] CP-101606 by COMPOUND A 179
5.2.3.9 Competition binding to investigate the pharmacological influence of NR3B upon the displacement of [$^3$H] CP-101606 by COMPOUND B 180
5.2.3.10 Radioligand binding assay investigating the specific binding of [$^3$H] Ro-256981 in recombinant NR1/NR2B and NR1/NR2B/NR3B receptors. 181
5.2.3.11 Radioligand binding assay investigating the specific binding of [$^3$H] CP-101606 in recombinant NR1/NR2B and NR1/NR2B/NR3B receptors 182

5.3 Discussion 184

## Chapter 6 - NMDA subunit expression in a chronic pain model

6.1 Introduction 197
6.2 Results 200
6.2.1 Immunohistochemical characterisation of subunit expression in the spinal cord of adult male rats subjected to a novel chronic pain model 200

| | | |
|---|---|---|
| 6.2.1.1 | NR1 expression | 202 |
| 6.2.1.2 | NR2A expression | 203 |
| 6.2.1.3 | NR2A phosphorylation | 204 |
| 6.2.1.4 | NR2B expression | 206 |
| 6.2.1.5 | NR2B phosphorylation | 207 |
| 6.2.1.6 | NR3B expression | 209 |
| 6.2.1.7 | Post-synaptic density 95 (PSD-95) expression | 210 |
| 6.2.1.8 | Qualitative summary of NMDA receptor subunit expression and phosphorylation state in the lumbar and thoracic regions of spinal cord from control and model tissue | 211 |
| 6.2.2 | Autoradiographical analysis of the distribution and density of NR2B-containing receptors in the CNS of adult male rats exposed to a chronic pain model | 212 |
| 6.2.2.1 | Analysis of autoradiography on the adult rat spinal cord | 212 |
| 6.2.2.1.1 | Mapping the expression of functional NR2B-containing receptors in the spinal cord of sham and FCA treated adult rats using [$^3$H] Ro-256981 | 214 |
| 6.2.2.2 | Analysis of autoradiography on the adult rat brain | 216 |
| 6.2.2.2.1 | Mapping the expression of functional NR2B-containing receptors in the spinal cord of sham and FCA treated adult rats using [$^3$H] Ro-256981 | 218 |
| 6.3 | Discussion | 222 |

**Chapter 7 - Overall discussion and further work**

| | | |
|---|---|---|
| 7.1 | Characterisation of COMPOUND A and COMPOUND B | 233 |
| 7.2 | Expression and differential cytoprotective effects of NR3 subunits | 235 |
| 7.3 | Physiological impact of NR3B in NR1/NR2B receptors | 238 |
| 7.4 | Pharmacological impact of NR3B in NR1/NR2B receptors | 239 |
| 7.5 | NMDA receptor modulation in a chronic pain model | 241 |
| 7.6 | Overall findings | 243 |
| | **References** | 245 |

# List of Figures


| Figure | Title | Page |
|---|---|---|
| | **Chapter 1** | |
| 1.1 | A schematic diagram representing the two classes of glutamate receptor (A)(Verkhratsky and Kirchoff, 2007). | 2 |
| 1.2 | Schematic diagram showing an NMDA receptor channel in the closed and open positions (A) and the predicted transmembrane topology of individual subunit (B) showing the extracellular amino terminals, the intracellular carboxyl terminals , the membrane domains (M1-4) and the agonist and NR2B-selective antagonist binding sites. | 7 |
| 1.3 | Phylogenic tree (A) showing NMDA receptor subunit homology and polypeptide sequences (B) showing transmembrane domains (black and grey boxes) and regions of alternative splicing (asterisks). Taken from Cull-Candy *et al.*, 2001. | 10 |
| 1.4 | Schematic representation of the bi-lobular LIVBP ifenprodil binding site on the NR2B subunit showing the significant amino acids (Chazot, 2004). | 25 |
| 1.5 | Chemical structures of early NR2B-selective antagonists (Williams, 2001) and the channel blocker MK-801 (Nikam and Meltzer, 2002). | 26 |
| 1.6 | Chemical structures of second generation NR2B-selective antagonists (Nikam and Meltzer, 2002). | 27 |
| 1.7 | Schematic diagram representing afferent Aδ and C-fibre input to the dorsal root ganglion, through the cord and into the spinothalamic tracts (Anaesthesia, UK, www.frca.co.uk). | 36 |
| | **Chapter 2** | |
| 2.1 | Schematic diagram showing anti-NR3B purification via specific NR3B peptide-affinity. The specific anti-NR3B antibodies bind to the peptide conjugated to the column and | 51 |

are eluted. The non-peptide specific antibodies are washed away.

2.2 Schematic diagram showing immunopurification of NR1-containing receptors from detergent-solubilised material. Only those receptor complexes containing NR1 subunits will bind to the specific anti-NR1 antibodies and be purified. The monomeric non-functional NR2A and NR2B subunits are washed away. 60

2.3 Schematic diagram representing the induction of fluorescence when Fluo-4 reacts with calcium in cells. The influx of calcium via NMDA receptors and calcium released from intracellular stores contribute to the fluorescent signal detected by the FLIPR machine. 75

**Chapter 3**

3.1 Competition binding experiment showing ifenprodil displacement of [$^3$H] Ro-256981 in adult rat forebrain membranes, best fit to a one-site binding model. Non-specific binding was defined with ifenprodil (1mM). 80

3.2 Competition binding experiment showing one-site displacement of [$^3$H] Ro-256981 binding by COMPOUND A in adult rat forebrain membranes. Non-specific binding was defined with ifenprodil (1mM). 81

3.3 Competition binding experiment showing one-site displacement of [$^3$H] Ro-256981binding by COMPOUND B in adult rat forebrain membranes. Non-specific binding was defined with ifenprodil (1mM). 82

3.4 Competition binding experiment showing COMPOUND A displacement of [$^3$H] CP-101,606 in adult rat forebrain membranes, best fit to a one-site binding model. Non-specific binding was defined using ifenprodil (1mM). 83

3.5 Competition binding experiment showing COMPOUND B displacement of [$^3$H] CP-101,606 in adult rat forebrain tissue fitted to a one-site binding model. Non-specific 84

binding was defined with ifenprodil (1mM).

3.6 Immunoblot confirming the expression of NR1 and NR2B subunits in HEK293 cells for use in radioligand binding experiments. Lanes 1+2 HEK 293 cells expressing NR1/NR2B receptors and probed with anti-NR1 (2μg/ml). Lanes 3+4 HEK 293 cells expressing NR1/NR2B receptors probed with anti-NR2B (2μg/ml). Representative blot from n=3 experiments. 85

3.7 Competition binding showing two-site displacement of [$^3$H] Ro-256981 by COMPOUND A in recombinant NMDA NR1/NR2B receptors expressed in HEK293 cells. Non-specific binding was defined with ifenprodil (1mM). 86

3.8 Competition binding experiment showing two-site displacement of [$^3$H] Ro-256981 by COMPOUND B in recombinant NR1/NR2B receptors expressed in HEK293 cells. Non-specific binding was defined with ifenprodil (1mM). 87

3.9 Competition binding showing the two-site displacement of [$^3$H] CP-101,606 by COMPOUND A in recombinant NR1/NR2B receptors expressed in HEK 293 cells. Non-specific binding was defined with ifenprodil (1mM). 88

3.10 Competition binding experiment showing one-site high affinity displacement of [$^3$H] CP-101,606 by COMPOUND B in recombinant NR1/NR2B receptors expressed in HEK293 cells. Non-specific binding was defined using ifenprodil (1mM). 89

3.11 Competition binding experiment showing low affinity ifenprodil displacement of [$^3$H] MK-801 binding in adult rat forebrain membranes. Non-specific binding was defined with ketamine (1mM) and the reaction terminated after 30, 60 and 90 minutes. 91

3.12 Competition binding experiments showing the COMPOUND A displacement of [$^3$H] MK-801 binding in adult rat forebrain, terminating the reaction after 30, 60 and 92

90minutes. Non-specific binding was defined with ketamine (1mM).

3.13 Competition binding experiments showing the COMPOUND B displacement of [$^3$H] MK-801 binding in adult rat forebrain, terminating the reaction after 30, 60 and 90minutes. Non-specific binding was defined with ketamine (1mM). 93

**Chapter 4**

4.1 Schematic diagram of immunoglobulin structure 104

4.2 Immunoblot showing recombinant NR3B, NR3A and NR1 subunits expressed in HEK 293 cells. Probed with anti-rodent NR3B (2μg/ml). Representative from n=3 experiments. 108

4.3 Immunoblot showing adult rat forebrain (1) and spinal cord (2) membranes (30μg) and recombinant NR3B expressed in HEK 293 cells (3+4), probed with anti-rodent NR3B (2μg/ml). Representative from n=3 experiments. 109

4.4 Immunoblot showing adult rat forebrain (1+4) and spinal cord (2+5) (30μg, respectively), and recombinant NR3B (3+6) subunits expressed in HEK 293 cells probed overnight with anti-rodent NR3B (2μg/ml). Representative from n=2 experiments. 110

4.5 Immunoblot showing post-mortem human putamen membranes (1) (50μg) and adult rat forebrain membranes (2) (30μg) probed with anti-human NR3B (2μg/ml). representative from n=3 experiments. 112

4.6 Immunoblot (n=1) showing adult rat spinal cord membranes (1+6), adult rat forebrain membranes (2+7) (30μg) and human putamen membranes (4,5,8+9)(50μg) probed with anti-human NR3B (2μg/ml). Lane 3 was loaded 113

with sample buffer.

4.7 Representative immunoblot (n=2) showing adult rat forebrain membranes (1) and adult rat spinal cord membranes (2) (30μg) and recombinant NR3B expressed in HEK 293 cells (3+4) probed with commercial anti-NR3B (1:1000). 114

4.8 Representative immunoblots (n=3) showing adult rat forebrain membranes (25μg) (Lane 1) and adult rat spinal cord membranes (25μg) (Lane 2), probed overnight with anti-rNR1 (2μg/ml) (A), anti-rNR2A (2μg/ml) and anti-rNR2B (2μg/ml). 116

4.9 Schematic diagram showing the laminae layers in the dorsal and ventral regions of the rodent lumbar spinal cord. 117

4.10 Control sections showing the immunoreactivity in tissue in the absence of primary antibodies in the cervical dorsal horn (A), the lumbar dorsal horn (B) and the thoracic ventral horn (C). Low resolution image of the cervical cord showing NR1 immunostaining (Bigini *et al.*, 2006) with red arrows highlighting the dorsal and ventral areas of the cord focused upon in this study. 118

4.11 Expression of NR1 (probed anti-rNR1 2μg/ml) (A), NR3B (commercial anti-rNR3B 1:1000) (B) in the dorsal horns laminae I, II, III and ventral horns showing the motor neurons (MN) of the cervical rat spinal cord (n=2). Scale bars represent 100μm. 120

4.12 Expression of NR2A (anti-rNR2A 2μg/ml) (C) and NR2B (anti-rNR2B 2μg/ml) (D) in the dorsal horn laminae I, II, III and ventral horns showing the motor neurons (MN) of the cervical rat spinal cord (n=2). 121

4.13 Expression of NR1 (probed anti-rNR1 1μg/ml) (A), NR3B (commercial anti-rNR3B 1:1000) (B) in the dorsal horn laminae I, II, III and ventral horns showing the motor neurons (MN) of the thoracic rat spinal cord (n=2). Scale bars represent 100μm. 123

| | | |
|---|---|---|
| 4.14 | Expression of NR2A (anti-rNR2A 2μg/ml) (C) and NR2B (anti-rNR2B 2μg/ml) (D) in the dorsal horn laminae I, II, III and ventral horns showing the motor neurons (MN) of the thoracic rat spinal cord (n=2). Scale bars represent 100μm. | 124 |
| 4.15 | Expression of NR1 (probed anti-rNR1 1μg/ml) (A), NR3B (commercial anti-rNR3B 1:1000) (B) in the dorsal horn laminae I, II, III and ventral horns showing the motor neurons (MN) of the lumbar rat spinal cord (n=2). Scale bars represent 100μm. | 126 |
| 4.16 | Expression of NR2A (anti-rNR2A 2μg/ml) (C) and NR2B (anti-rNR2B 2μg/ml) (D) in the dorsal horn laminae I, II, III and ventral horns showing the motor neurons (MN) of the lumbar rat spinal cord (n=2). Scale bars represent 100μm. | 127 |
| 4.17 | Expression of NR1 (probed anti-hNR1 1μg/ml) (A), NR3B (commercial anti-rNR3B 1:1000) (B) in the dorsal horn laminae I, II, III and ventral horns showing the motor neurons (MN) of the cervical human spinal cord (n=1). Scale bars represent 100μm. | 131 |
| 4.18 | Expression of NR2A (anti-rNR2A 2μg/ml) (C) and NR2B (anti-rNR2B 2μg/ml) (D) in the dorsal horn laminae I, II, III and ventral horns showing the motor neurons (MN) of the cervical human spinal cord (n=1). Scale bars represent 100μm. | 132 |
| 4.19 | Representative immunoblots (n=2) showing solubilised membranes (lane 1) and unsolubilised membranes (lane 2) probed overnight with anti-rNR1 (2μg/ml) (A), anti-rNR2B (2μg/ml) (B), anti-rNR2A (2μg/ml) (C) and anti-rNR3B (1:1000) (D). | 136 |
| 4.20 | Immunoblot showing adult rat spinal cord homogenate (25μg/ml) (SC), solubilised membranes (S), unsolubilised membranes (DT), unbound material (UB) and elutions 1-5 (E1-5), probed overnight with anti-NR1 (2μg/ml), anti-NR2A (2μg/ml), anti-NR2B (2μg/ml) and anti-NR3B (1:1000). Representative immunoblots from n=3 experiments. | 137 |

4.21 Immunoblots (n=1) showing solubilised and unsolubilised membranes at 0.75% [SDS] (1+2), solubilised and unsolubilised membranes at 0.5% [SDS] (3+4), solubilised and unsolubilised membranes at 0.25% [SDS] (5+6), solubilised and unsolubilised membranes at 0.1% [SDS] and solubilised and unsolubilised membranes at 0.05% [SDS]. Probed with anti-NR1 (2μg/ml) (A), anti-NR2A (2μg/ml) (B), anti-NR2B (2μg/ml) and anti-NR3B (1:1000). 138

4.22 Immunoblots (n=1) showing solubilised and unsolubilised membranes at 0.5% [SDS] (1+2), solubilised and unsolubilised membranes at 0.4% [SDS] (3+4), solubilised and unsolubilised membranes at 0.3% [SDS] (5+6), solubilised and unsolubilised membranes at 0.2% [SDS]. Probed with anti-NR1 (2μg/ml) (A), anti-NR2A (2μg/ml) (B), anti-NR2B (2μg/ml) and anti-NR3B (1:1000). 139

4.23 Representative immunoblots (n=2) showing purified fractions from an anti-NR1 affinity column. Spinal cord homogenate (25μg/ml) (SC), solubilised membranes (S), unsolubilised membranes (DT), unbound material (UB) and elutions 1-5 (E1-5). Probed with anti-NR1 (2μg/ml) (A), anti-NR2A (2μg/ml) (B), anti-NR2B (2μg/ml) and anti-NR3B (1:1000). 141

4.24 Representative immunoblots (n=2) showing purified fractions from an anti-NR2A affinity column. Spinal cord homogenate (25μg/ml) (SC), solubilised membranes (S), unsolubilised membranes (DT), unbound material (UB) and elutions 1-5 (E1-5). Probed with anti-NR1 (2μg/ml) (A), anti-NR2A (2μg/ml) (B), anti-NR2B (2μg/ml) and anti-NR3B (1:1000). 142

4.25 Representative immunoblots (n=3) showing adult rat forebrain membranes (20μg) (1), adult rat cervical cord membranes (20μg) (2) and adult rat thoracic/lumbar cord membranes (20μg) (3). Probed with anti-rNR2A (2μg/ml), anti-rNR2B (2μg/ml) and anti-rNR3B (1:1000). 144

4.26 Re-probing the immunoblots in figure 4.22 with anti-mouse β-actin (1:1000). Immunoblot showing adult rat forebrain membranes (20μg) (1), adult rat cervical cord membranes (20μg) (2) and adult rat thoracic/lumbar cord membranes 144

(20μg) (3).

**Chapter 5**

5.1 Schematic diagram representing electrode position and cell placement in the microscope bath beneath the barrels used for rapid agonist and antagonist application (From Jon Spencer, GSK). 158

5.2 The percentage cytotoxicity of HEK 293 cells expressing various combinations of NMDA receptor subunits *p<0.05, **p<0.01, ***p<0.001 one way ANOVA. 162

5.3 Electrophysiological traces of peak amplitudes (pA) obtained from recombinant NR1/NR2B (A), NR1/NR2B/NR3B (B) and NR1 (C) receptors. Histogram (D) and data range charts (E) show the mean ± SD for 25 individual experiments. 164

5.4 Current/voltage (IV) relationships for NR1/NR2B (A) and NR1/NR2B/NR3B (B) receptors expressed in HEK 293 cells, showing no statistical differences between channel characteristics. 165

5.5 Calcium permeability experiments, measuring the shift in reversal potential of the receptor channel between 0.3 and 30mM extracellular calcium. 166

5.6 Characterisation of magnesium sensitivity of recombinant NR1/NR2B (A) (n=8) and NR1/NR2B/NR3B (B) (n=6) receptors using current/voltage (I/V) relationships. 167

5.7 Electrophysiological traces depicting the sensitivity of NR1/NR2B (A) and NR1/NR2B/NR3B (B) receptors towards 100uM concentrations of magnesium and a histogram (C) representing the mean ± SD of data from all experiments. 168

5.8 Electrohysiological traces representing the signals measured from NR1/NR2B (A) and NR1/NR2B/NR3B (B) receptor complexes when exposed to 20μM magnesium chloride, and a histogram (C) showing the mean± SD of all data sets. 169

| | | |
|---|---|---|
| 5.9 | Differential cytoprotective effects of the NR2B-selective antagonists ifenprodil (A), COMPOUND B (B) and COMPOUND A (C) upon NR1/NR2B and NR1/NR2B/NR3B receptor complexes * p=<0.05, **p=<0.01 Two-tailed T-Test. | 172 |
| 5.10 | Electrophysiological traces representing inhibition of signals from recombinant NR1/NR2B (A) and NR1/NR2B/NR3B (B) receptors. Figure C represents the mean ± SD of percentage inhibition from all data sets. | 173 |
| 5.11 | Electrophysiological traces representing the inhibition of NR1/NR2B (A) and NR1/NR2B/NR3B (B) receptor activity by 300nM CP-101606. Figure C shows the mean ± SD of percentage inhibition from all data sets. | 174 |
| 5.12 | Electrophysiological traces representing the inhibition of NR1/NR2B (A) and NR1/NR2B/NR3B (B) receptor activity by 300nM CP-101606. Figure C shows the mean ± SD of percentage inhibition from all data sets. | 175 |
| 5.13 | Electrophysiological traces representing the inhibition of NR1/NR2B (A) and NR1/NR2B/NR3B (B) receptor activity by 30nM CP-101606. Figure C shows the mean ± SD of percentage inhibition from all data sets. | 176 |
| 5.14 | Electrophysiological traces showing the inhibition of NR1/NR2B (A) and NR1/NR2B/NR3B (B) receptor activity by the NR2B-selective antagonist Ro 256981 (10μM 10 seconds). Figure C shows the mean ± SD of percentage inhibition from all data sets. | 177 |
| 5.15 | Electrophysiological traces showing the inhibition of NR1/NR2B (A) and NR1/NR2B/NR3B (B), by recombinant receptor activity by Ro-256981 (30nM, 60seconds). Figure C, shows signal from NR1/NR2B receptors before antagonist application, Figure E, shows signal from NR1/NR2B/NR3B receptors before antagonist application. Figure D, shows the mean ± SD of percentage inhibition from all data sets. | 178 |
| 5.16 | Competition binding showing two-site displacement of [$^3$H] CP-101606 by COMPOUND A in recombinant NR1/NR2B and NR1/NR2B/NR3B receptors. The results displayed are mean ± SD of three individual experiments and non-specific | 179 |

binding was defined using 1mM ifenprodil.

5.17 Competition binding experiments showing the displacement of [$^3$H] CP-101606 by COMPOUND B in recombinant NR1/NR2B and NR1/NR2B/NR3B receptors. Data shown is mean ± SD for two individual experiments and non-specific binding was defined using 1mM ifenprodil. 180

5.18 Histogram representing specific binding data for [$^3$H] Ro-256981 in recombinant NR1/NR2B and NR1/NR2B/NR3B receptors. The data shown is mean ± SD for two individual experiments. Non-specific binding was defined using 1mM ifenprodil. 181

5.19 Histogram to represent the specific binding data for [$^3$H] CP-101606 in recombinant NR1/NR2B and NR1/NR2B/NR3B receptors. The data shows the mean ± SD for two individual experiments. Non-specific binding was defined with 1mM ifenprodil 182

**Chapter 6**

6.1 Schematic (Tolle *et al.*, 1993) and low resolution images (Liu *et al.*, 1994) of the cord highlighting the dorsal (outer lamina) and ventral regions (motor neurons) investigated in this study (A) and control sections showing the immunoreactivity in tissue in the absence of primary antibodies in the lumbar dorsal horn (B), the lumbar ventral horn (C), the thoracic dorsal horn (D) and the thoracic ventral horn (E). 201

6.2 Expression of NR1 protein in the dorsal (A) and ventral (B) horns of the thoracic cord in a sham animal probed with anti-NR1 (1μg/ml). The outer laminae I, II, III are labelled in the dorsal horn (A) and cell bodies of motor neurons (MN) in laminae IX in the ventral horn (B). Scale bar represents 100nm. 202

6.3 Expression of NR2A protein in the ventral horns of lumbar spinal cord in sham (A) and FCA model (B) animals, probed with anti-NR2A (2μg/ml). The cell bodies of the motor neurons (MN) within laminae IX show high levels of NR2A 203

protein expression. Scale bar represents 100nm.

6.4 Expression of phosphorylated NR2A subunit at tyrosine residue 1325 in the dorsal horn of sham (A) and FCA (B) lumbar cord tissue. Weak immunoreactivity is present particularly in the outer laminae (I, II and III) of the dorsal horn. Scale bar represents 100nm. 205

6.5 Expression of phosphorylated NR2A subunit at tyrosine 1387 in the dorsal horn of sham (A) and FCA (B) lumbar cord tissue. Initial evidence for increased phosphorylation of NR2A at tyrosine 1387 in the outer laminae (I, II and III) during the inflammatory response. Scale bar represents 100nm. 205

6.6 Expression of NR2B protein within the dorsal horns of lumbar spinal cord in sham (A) and FCA (B) tissue. NR2B shows expression in the outer laminae (I, II and III) in both sham and model tissue showing involvement in sensory inputs to the cord. Scale bar represents 100nm. 206

6.7 Expression of phosphorylated NR2B at tyrosine 1252 within the dorsal horn of lumbar sham (A) and FCA (B) tissue. Similar levels of immunoreactivity suggest no alteration in phosphorylation of Nr2B at this residue in the outer laminae I, II and III of the dorsal horns. Scale bar represents 100nm. 207

6.8 Expression of phosphorylated NR2B at residue y1336 within the dorsal horn of lumbar sham (A) and FCA (B) tissue. Initial evidence for increased phosphorylation of NR2B at this residue in the outer laminae I, II and III, suggesting potentiation of sensory NR2B-mediated transmission. Scale bar represents 100nm. 208

6.9 Expression of phosphorylated NR2B at residue y1472 within the dorsal horn of lumbar sham (A) and FCA (B) tissue. Initial evidence for enhanced phosphorylation of the NR2B subunit at residue 1472, in outer laminae I, II and III, important for blockade of receptor internalisation. Scale bar represents 100nm. 208

6.10 Expression of NR3B protein within the dorsal horns of the lumbar spinal cord in sham (A) and FCA (B) tissue. Initial evidence for increased NR3B expression in outer laminae I, II and III following onset of the inflammatory response. Scale bar represents 100nm. 209

6.11 Expression of PSD-95 within the ventral horns of the lumbar cord in sham (A) and FCA (B) tissue. Initial evidence for increased expression of PSD-95 in the motor neuronal soma (MN) of FCA model tissue (B) in comparison with sham tissue (A). Scale bar represents 100nm. 210

6.12 Representative autoradiograms of adult rat lumbar spinal cord using [$^3$H] Ro-256981 in sham (A) and FCA treated (B) animals. Representative image showing non-specific binding defined using ifenprodil (1mM) (C). 213

6.13 Autoradiographical data showing [$^3$H] Ro-256981 binding within the dorsal and ventral horns of sham and FCA spinal cord.
Data shown are the mean values ± standard deviation for n=4 sham and n=4 FCA spinal cords. Sham and FCA tissue is compared in the dorsal horn of the lumbar cord (A), the ventral horn of the lumbar cord (B), the dorsal horn of the thoracic cord (C) and the ventral horn of the thoracic cord (D). Levels of [$^3$H] Ro-256981 binding are higher in the lumbar region than the thoracic region, consistent with NR2B immunoreactivities in IHC experiments. 215

6.14 Representative horizontal (A+B) and coronal (C+D) autoradiograms showing [$^3$H] Ro-256981 binding within sham and FCA-treated rat brains. Non-specific binding was defined using 1mM ifenprodil (E). 217

6.15 Autoradiographical data showing [$^3$H] Ro-256981 binding within the whole brain of sham and FCA-treated animals.
Data shown are the means ± standard deviation of between n=3/4 sham and n=3/4 FCA whole brains. Sham and FCA tissue is compared in $1^0$ somatosensory cortex (A), the $2^0$ somatosensory cortex (B), the cingulate cortex (C), the periaqueductal grey (D). 219

6.16 Autoradiographical data showing [$^3$H] Ro-256981 binding within the whole brains of sham and FCA treated animals. Data shown are the means ± standard deviation of between n=3/4 sham and n=3/4 FCA whole brains. Sham and FCA tissue is compared in hippocampal regions CA1 (E), CA2 (F), CA3 (G), the dentate gyrus (H).* p=< 0.05 Unpaired Two-tailed T-Test. 220

6.17 Autoradiographical data showing [$^3$H] Ro-256981 binding within the whole brains of sham and FCA-treated animals. Data shown are the means ± standard deviation of between n=3/4 sham and n=3/4 FCA whole brains. Sham and FCA tissue is compared in the thalamus (I) and all brain regions in both hemispheres combined (p=0.05) (J). * p=<0.05 Unpaired Two tailed T-Test. 221

**Chapter 7**

7.1 Schematic diagram showing the binding affinities and selectivity towards NR2B-containing receptors of Ro-256981, CP-101606, COMPOUND A and COMPOUND B, and the potential allosteric interaction of COMPOUND B with the channel pore. 234

7.2 A schematic diagram showing the differential protective effect of the NR3 subunits upon the proposed NMDA-mediated calcium toxicity in NR1/NR2A and NR1/NR2B receptors. 236

7.3 A schematic diagram showing that the inclusion of an NR3B subunit into the receptor complex may have an allosteric effect upon the LIVBP binding domain of the NR2B-selective antagonists. 240

7.4 A schematic diagram showing the pathway of chronic pain transmission from the spinal cord, through the brainstem and into the cortex (Analgesia, UK) and the changes in the NMDA receptor which may contribute to the persistent response. 242

# List of tables

## Chapter 1

1.1 Modulatory properties inferred by the various NR2 and NR3 subunits on the receptor complex, data obtained from Gibb and Colquhoun, (1991), Cull-Candy *et al.*, 2001 and Priestley, (2002). 5

## Chapter 2

2.1 Preparation of standard solutions for lowry assay. 52

2.2 Preparation of scintillation tubes for competition radioligand binding assays 63

2.3 Preparation of transfection reagents 70

## Chapter 3

3.1 Summary of the competitive binding data obtained for the novel compounds COMPOUND A and COMPOUND B 94

## Chapter 4

4.1 Anti-rodent NR3B antibody yield (μg/ml) from each collection of antisera 107

4.2 Anti-human NR3B antibody yield (μg/ml) from each collection of antisera 111

4.3 Qualitative summary of the average intensity of immunoreactivity for each subunit in the cervical, thoracic and lumbar regions of adult rat spinal cord. 129
(+) = Very weak expression, + = Weak expression, ++ = Moderate expression, +++ = Strong sxpression, ++++ = Very strong expression.

4.4 Qualitative summary of the average intensity of immunoreactivity for each subunit in the cervical region of adult human spinal cord. 134
(+) = Very weak expression, + = Weak expression, ++ = Moderate expression,
+++ = Strong expression, ++++ = Very strong expression.

## Chapter 5

5.1 Summarising the pharmacological influence of the NR3B subunit upon NR2B-selective antagonists ifenprodil, Ro-256981, CP-101606, COMPOUND A and COMPOUND B. 183

## Chapter 6

6.1 Qualitative summary of the average intensity of immunoreactivity detected with each of the antibodies, in the lumbar and thoracic regions of the spinal cord. (+) = Very weak expression, + = Weak expression, ++ = Moderate expression, +++ = Strong sxpression, ++++ = Very strong expression. 211

# Chapter 1

# Introduction

## 1.1 Neurotransmitters within the central nervous system

Essential signalling mechanisms within the central nervous system (CNS) rely upon selective release of neurotransmitters and their interactions with specific receptors. As the primary excitatory neurotransmitter in the CNS, glutamate and its receptors are a major target for combating many disease states, which can manifest due to hyper or hypo-activation of these receptors. Widely expressed throughout the CNS, the N-methyl-D-aspartate (NMDA) receptor is a glutamate receptor that mediates neurotransmission via calcium influx upon neuronal depolarisation. As such it is vital for normal neuronal function and any modulations to this balanced system may cause disease.

This introduction will discuss the NMDA receptor, its multiple subunit structure, distribution, co-assembly, physiology and pharmacology in detail with particular focus on the specific properties of NR2B and NR3 subunits.

## 1.2 Glutamate receptors within the central nervous system

The amino acid L-glutamate is the most ubiquitous excitatory neurotransmitter in the central nervous system, mediating its effects via a large family of ionotropic and metabotropic receptors.

Metabotropic glutamate receptors are seven transmembrane-domain G-protein-coupled receptors that control intracellular signalling cascades (Nakanishi, 1994; Jordan *et al.*, 1999; Roche *et al.*, 1999; Chan *et al.*, 2001) and provide modulatory and regulatory roles in neurotransmission (Takanishi *et al.*, 1993; Malherbe *et al.*, 1999; Kew and Kemp, 2005). Eight family members (mGluR1-8) have been

identified to date, which have subsequently been divided into three groups according to sequence homology, secondary messenger coupling and pharmacology. As shown in Figure 1, group I, containing mGluR1 and R5, predominantly couple to phospholipase C (PLC), whereas groups II (mGlu-R2 and R3) and III (mGlu-R4, R6, R7 and R8) regulate adenylyl cyclase activity (Kew and Kemp, 2005).

Ionotropic glutamate receptors (iGluRs) are ligand-gated channels divided into three groups (AMPA, Kainate and NMDA) and named according to the pharmacological tools used to selectively activate them. AMPA and kainate receptors display predominance for sodium and potassium permeability, whereas NMDA receptors are predominantly calcium permeable.

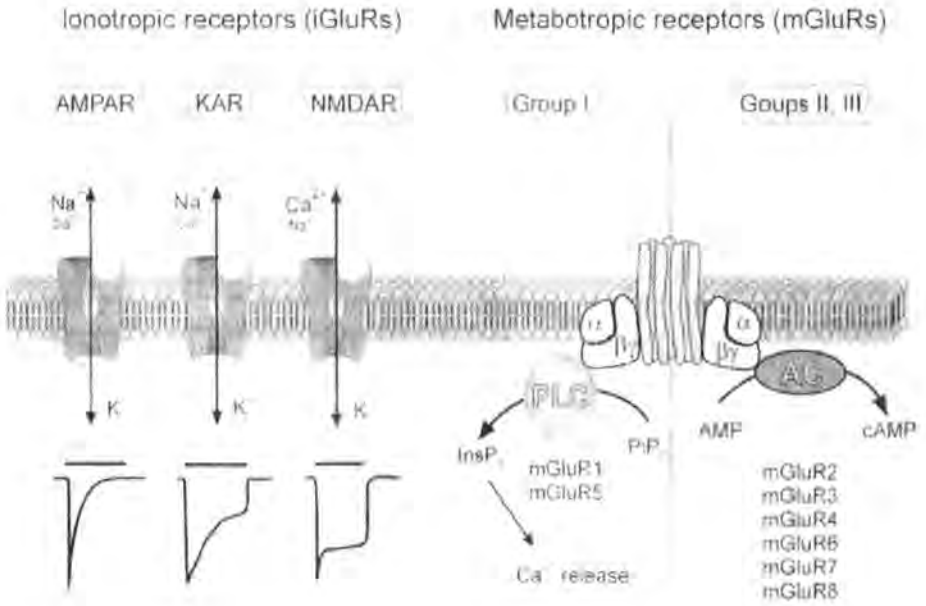


**Figure 1.1 A schematic diagram representing the two classes of glutamate receptor (A) (Verkhratsky and Kirchoff, 2007).**

## 1.3 The NMDA receptor

Located throughout the central nervous system, the NMDA receptor forms a major subclass of excitatory L-glutamate receptor (Chazot and Stephenson, 1997; Stephenson 2001). NMDA receptors are heterologous complexes of essential and modulatory subunits, co-assembled in various tetrameric or pentameric arrangements (Wafford *et al.*, 1993; Sheng *et al.*, 1994; Chazot *et al.*, 1994). Seven NMDA receptor subunits have been identified to date, each providing specific modulatory influences on the receptor complex. Initial cloning of the NR1 subunit by Moriyoshi *et al.*, 1991 was followed rapidly by the identification and cloning of the four NR2 subunits NR2A, NR2B, NR2C and NR2D (Kutsuwada *et al.*, 1992; Monyer *et al.*, 1992; Ishii *et al.*, 1993) and the two NR3 subunits: NR3A (Ciabarra *et al.*, 1995; Sucher *et al.*, 1995) and NR3B (Nishi *et al.*, 2001; Matsuda *et al.*, 2002).

The NR1 subunit is obligatory for NMDA receptor function and at least one NR1 subunit is therefore always incorporated into the receptor complex. The NR1 combines with at least one modulatory NR2 (A-D) subunit and more infrequently a modulatory NR3 (A-B) subunit.

This heterologous nature confers a huge potential capacity for flexible modulation of the nervous system with different heteromers displaying individual biological and pharmacological characteristics.

### 1.3.1 NMDA receptor activation and modulatory binding sites

In addition to the complexity of NMDA receptors arising from multiple subunit co-assembly, two co-agonists glutamate and glycine, must be present in order to activate the receptor channel.

Early research expressing homomeric NR1 subunits (Boeckman *et al.*, 1994) and homomeric NR2 subunits (Kutsuwada *et al.*, 1992) failed to produce functional receptors fuelling the theory that neither subunit possessed the ability to function in isolation and that they must form heteromeric complexes. Research using site directed mutagenesis has since shown that the glycine binding site is present on the NR1 subunit (Kuryatov *et al.*, 1994), with the glutamate binding site on the NR2 subunit (Laube *et al.*, 1998). It is thought that the agonists bind to the S1 and S2 regions (see section 1.3.3), inducing conformational changes and folding of the proteins, inducing channel opening (Priestley, 2002).

The synthetic compound N-methyl-D-aspartate, an analogue of L-glutamate is frequently used as an agonist for research and it was the initial activation of these receptors by NMDA which led to its nomenclature.

The receptor complex also has many other binding sites available for allosteric modulators such as a redox site, $Zn^{2+}$ and endogenous polyamine binding sites. There are also multiple phosphorylation and glycosylation sites on the cytoplasmic tail, which are very important for regulation of NMDA activity (Zigmond *et al.*, 1999; Kew and Kemp, 2005).

### 1.3.2 NMDA channel kinetics

NMDA receptors are membrane-bound, ligand-gated, non-selective cation channels characterised by voltage-dependent activity, high calcium permeability and comparatively slow activation/deactivation kinetics (Cull-Candy *et al.*, 2001; Stephenson, 2001; Takai *et al.*, 2003). NMDA receptor channel kinetics are largely influenced by subunit combination with each NR2 and NR3 subunit conferring

different modulatory properties on the receptor complex (see table 1.1). For example NR1/NR2A receptors show very fast (millisecond) deactivation following excitatory currents, whereas NR1/NR2D receptors deactivate much more slowly (seconds) (Cull-Candy *et al.*, 2001; Wyllie *et al*, 1998).

| | Channel kinetics | Channel conductance (picosiemens) | $Mg^{2+}$ sensitivity |
|---|---|---|---|
| **NR2A** | Fast deactivation ($\tau$ decay ~90ms) High permeability $Ca^{2+}$ | High principal conductance state ~50pS | High sensitivity |
| **NR2B** | Slower deactivation ($\tau$ decay ~370-400ms) High permeability $Ca^{2+}$ | High principal conductance state ~50pS | High sensitivity |
| **NR2C** | Slower deactivation, ($\tau$ decay ~370-400ms) Lowered permeability $Ca^{2+}$ | Lower principal conductance state ~30pS | Reduced sensitivity |
| **NR2D** | Very slow deactivation ($\tau$ decay ~4800ms) Lowered permeability $Ca^{2+}$ | Lower principal conductance state ~30pS | Reduced sensitivity |
| **NR3A/B** | Low permeability $Ca^{2+}$ | Lower conductance | Reduced sensitivity |

**Table 1.1 Modulatory properties inferred by the various NR2 and NR3 subunits on the receptor complex, data obtained from Gibb and Colquhoun, (1991), Cull-Candy *et al.*, 2001 and Priestley, (2002).**

At negative membrane potentials, current flux through the NMDA receptors is vastly reduced in the presence of micromolar concentrations of magnesium, forming a voltage-dependent magnesium block (Nowak and Wright 1992) which is relieved

when the membrane is depolarized beyond ~40mV. An asparagine residue in the pore-forming region has been shown to play a major role in the magnesium sensitivity particularly in the NR2 subunits where NR2A and NR2B-containing receptors display higher sensitivities towards magnesium blockade than NR2C and NR2D-containing receptors (Cull-Candy *et al*, 2001). Research by Williams *et al.*, 1998 also showed the importance of a tryptophan residue in the same region of the M2 domain for $Mg^{2+}$ sensitivity, with mutations to this residue greatly attenuating the magnesium blockade of NR2B-containing receptors.

The voltage dependence and degree of $Mg^{2+}$ inhibition can be modulated by permeant ions (Qian and Johnson, 2006; Antonov and Johnson, 1999), a factor which is thought to be important in receptor function and modulation of synaptic transmissions. Studies by Hori and Carpenter, (1994) and Zhang *et al.*, (1996) show that large fluctuations in the concentration of permeant ions under pathological conditions can also alter $Mg^{2+}$ inhibition (Qian and Johnson, 2006), thereby modulating receptor role and function.

### 1.3.3 NMDA receptor subunit structure

Structurally, NMDA receptor subunits have a large extracellular N-terminal region followed by three transmembrane domains (M1, 3, 4) and a pore-forming domain (M2) which forms a re-entrant loop (Dingledine *et al.*, 1999). The M2 domain contains an asparagine residue in a sequence of three amino acids, the QRN site (amino acid position between 598 and 612 depending on specific subunit) which is critical for $Ca^{2+}$ permeability and $Mg^{2+}$ sensitivity (Nishi *et al.*, 2001; Stephenson, 2001; Matsuda *et al.*, 2002). The third and fourth transmembrane domains share a large extracellular loop (S2 region), which forms the agonist binding domain with

the extracellular N-terminal (S1 region) (Armstrong *et al.*, 1998; Dingledine *et al.*, 1999; Kew and Kemp, 2005; Stephenson, 2001). The cytoplasmic C-terminus varies in size depending on the subunit and contains multiple sites for interaction with intracellular proteins (Dingledine *et al.*, 1999).

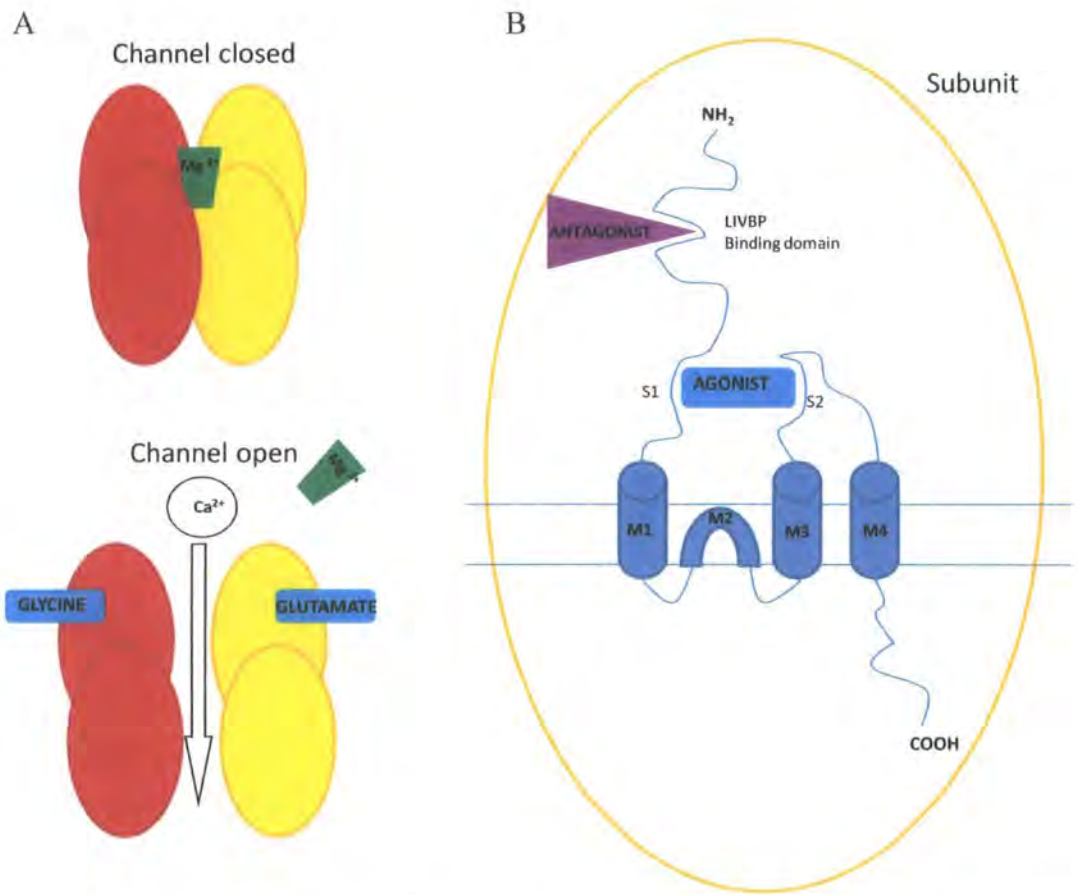


**Figure 1.2 Schematic diagram showing an NMDA receptor channel in the closed and open positions (A) and the predicted transmembrane topology of individual subunit (B) showing the extracellular amino terminals, the intracellular carboxyl terminals , the membrane domains (M1-4) and the agonist and NR2B-selective antagonist binding sites.**

### 1.3.3.1 The NR1 subunit structure

The 120KDa NR1 subunit is essential for channel formation and incorporates the binding site for the receptor co-agonist glycine. The NR1 gene consists of 22 exons

that give rise to eight distinct splice variants, namely NR1-1a, NR1-1b to NR1-4a and NR1-4b, due to three sites of alternative splicing (Stephenson, 2001; Cull-Candy *et al.*, 2001; Blahos and Wenthold, 1996). The splice variants can be characterised by the presence or absence of exon 5 (21 amino acid sequence) in the N-terminal region and by differential splicing of exons 21 (C1) and 22 (C2) in the C-terminal region (Stephenson, 2001). Studies investigating the influence of each variant have shown that different splice variants can co-exist within the same receptor complex (Chazot and Stephenson, 1997b) and that there is no preferential assembly of NR2 subunits and particular NR1 variants (Blahos and Wenthold, 1996). Research has shown the existence of intracellular pools of unassembled NR1-C2-exon-containing NR1 subunits (Chazot and Stephenson, 1997b) and that homomeric complexes of NR1 subunits containing the C2 exon can be expressed at the cell surface (Standley *et al.*, 2000) and bind the NMDA selective antagonist MK-801 (Chazot *et al.*, 1991) fuelling speculation that they can form glycine receptors that function independently of glutamate binding (Stephenson, 2001).

#### 1.3.3.2 The NR2 subunit structure

In order to form a functional NMDA receptor, NR1 must co-assemble with at least one of four modulatory NR2 subunits (2A-D), which are essential for glutamate binding. The NR2 subunits are larger than NR1, with molecular masses of ~170-180KDa for NR2A and NR2B (Kopke *et al.*, 1993; McBain and Mayer, 1994) and ~150KDa for NR2C and NR2D (Akesson *et al.*, 2000). The quaternary structure of the NMDA receptor is therefore potentially very large, with masses ranging from 630-850 KDa (Wenthold *et al.*, 1992; Brose *et al.*, 1993; Chazot *et al.*, 1994; Blahos and Wenthold, 1996). There is approximately 70% amino acid sequence homology

between the NR2A and NR2B subunits, with a similar degree of homology between the NR2C and NR2D subunits (see figure 1.3A). However, this homology decreases to approximately 55% between the two pairs of subunits. (Stephenson 2001). Both the NR2C and NR2D subunit genes undergo alternative splicing to form two isoforms (Ishii *et al.* 1993; Suchanek *et al.* 1995) though the functional significance of these variations is largely unknown (see figure 1.3B).

#### 1.3.3.3 The NR3 subunit structure

NR3A and NR3B make up the most recently discovered NMDA receptor subunit family. NR3A was first identified from the mouse genome in 1995 (Ciabarra *et al.*, 1995; Sucher *et al.*, 1995) and was so named due to its similarity to known NMDA receptor subunits (27% homology to NR1 and NR2). The human NR3A gene (*GRIN3A*) shows 92.7% sequence identity to rat NR3A and is localized to chromosome 9q34 in the region 13-34 and translates into a protein with a molecular mass ~100KDa (Andersson *et al.*, 2001). NR3B was then discovered in 2001 in the human and mouse genomes (Nishi *et al.*, 2001; Matsuda *et al.*, 2002) following identification of a unique sequence showing significant homology to the glutamate receptor family (Nishi *et al.*, 2001) and particularly with NR3A with which it shares 62% homology (Matsuda *et al.*, 2002). The human gene (*GRIN3B*) contains eight coding exons, is localised to chromosome 19p13.3 and the protein product has a molecular weight of ~100KDa (Andersson *et al.*, 2001).

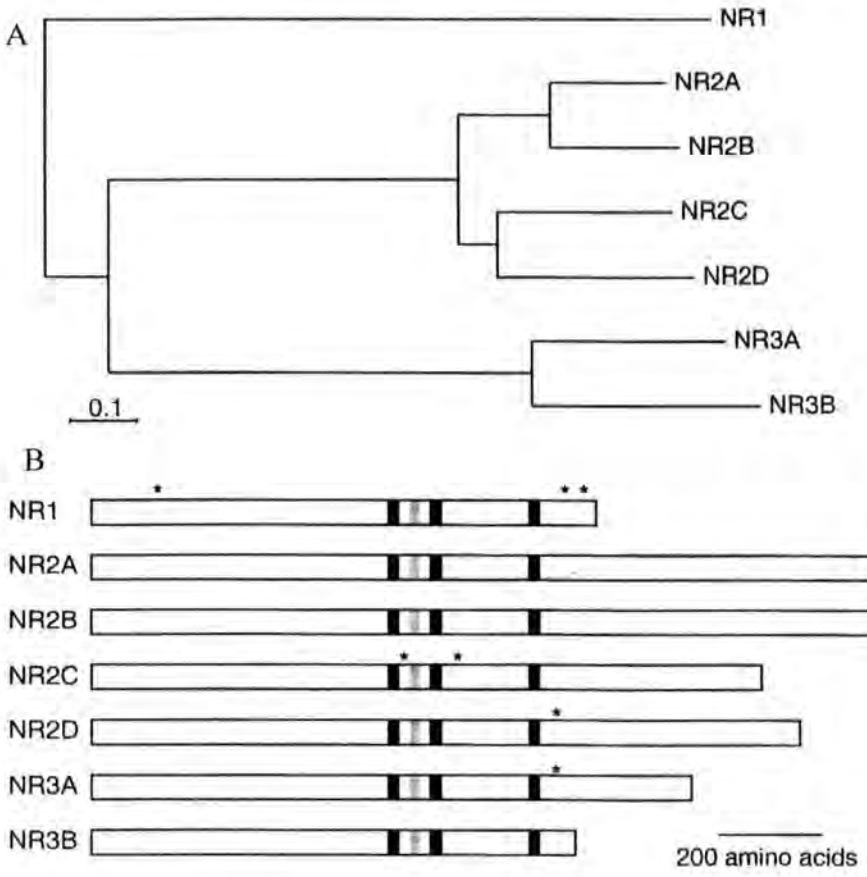


**Figure 1.3 Phylogenic tree (A) showing NMDA receptor subunit homology and polypeptide sequences (B) showing transmembrane domains (black and grey boxes) and regions of alternative splicing (asterisks). Taken from Cull-Candy *et al.*, 2001.**

## 1.4 Regional distribution of the NMDA receptor subunits

In the early 90's the regional expression of NMDA receptor subunits was a focus for many research groups (Monyer *et al.* 1992; Buller *et al.*, 1994, Akazawa *et al.*, 1994 and Sucher *et al.*, 1995) using in situ hybridisation and immunohistochemical techniques. Since then, studies have been carried out using genetic, immunological and pharmacological probes to investigate NMDA receptor subunit expression and co-association in different regions of the CNS.

### 1.4.1 NR1 expression

The NR1 subunit is ubiquitously expressed throughout the central nervous system in mature tissue. *In situ* hybridisation studies to map NR1 mRNA levels throughout development found that in the foetal brain, NR1 expression was low and restricted to the cortex and hippocampus but expression increased and became more widespread as development progressed (Takai *et al.*, 2003).

### 1.4.2 NR2A expression

NR2 subunits display distinct expression patterns throughout development: NR2A subunit mRNA expression shows a similar distribution pattern to that of the NR1 subunit; it is highly expressed throughout the forebrain in the hippocampus, cerebral cortex, thalamus and in the cerebellum (Monyer *et al.*, 1992; Wenzel *et al.*, 1996). At embryonic days 18-20, NR2A expression was evident throughout forebrain regions with expression increasing into the neonate and adult (Takai *et al.*, 2003). In the cerebellum, low expression levels in the neonate increase steadily, reaching adult levels by post-natal day 22 (Wang *et al.*, 1995). In the rodent (Nagy *et al.*, 2004) and human lumbar spinal cord (Sundstrom *et al.*, 1997), NR2A mRNA and protein expression have been shown in the dorsal horn, particularly laminae III-IV with varying levels in the ventral horn.

### 1.4.3 NR2B expression

NR2B is expressed predominantly in forebrain areas in adult tissue, particularly in the hippocampus, cerebral cortex and thalamic regions. *In situ* hybridisation studies show high levels of NR2B mRNA expression by embryonic day 17 in the cerebral cortex, thalamus and spinal cord, with levels increasing after birth in these regions

and the hippocampus, olfactory bulbs and striatum (Monyer *et al.*, 1994; Wang et al., 1995). Protein expression studies show a similar distribution of the NR2B subunit (Loftis and Janowsky, 2003). Laurie *et al.*, 1997 showed that NR2B protein expression increased from birth to postnatal day 20 before declining slightly in whole neonatal rat brains. NR2B expression in the cerebellum is present until postnatal day 22 when levels are no longer detectable (Wang *et al.*, 1995). Loftis and Janowsky, 2003 suggest a developmental role for granule cell maturation from this early down-regulation of NR2B expression which seemingly is replaced with NR2C expression (Monyer *et al.*, 1994).

In the rodent and primate spinal cord, NR2B shows expression in the superficial laminae of the lumbar dorsal horn and the motor neurons of the ventral horn (Nagy *et al.*, 2004; Mutel *et al.*, 1998; Rigby *et al.*, 2002). Although overall, NR2B is expressed to a lesser extent than NR2A.

### 1.4.4 NR2C expression

The NR2C subunit is almost exclusively expressed in the cerebellum, particularly in Purkinje and granule cells (Rigby *et al.*, 2002; Kew and Kemp, 2005; Stephenson, 2001) with almost no expression in forebrain regions. Tolle *et al.*, (1993) describe very weak detection of NR2C mRNA in the dorsal horn of the rat spinal cord and in the periaqueductal grey. One study by Sundstrom *et al.*, (1997) detected NR2C expression in human lumbar-sacral cord via immunoblotting, possibly suggesting differences in expression between species.

### 1.4.5 NR2D expression

The NR2D subunit is expressed highly in the embryo and newly-born rat, but

expression levels decline with maturity with low levels in the adult brainstem, midbrain thalamus, subthalamic nucleus and substantia nigra (Wenzel *et al.* 1996; Wenzel *et al.* 1995; Monyer *et al.*, 1992). Primate studies show NR2D expression in the adult thalamus (Jones *et al.*, 1998) and human hippocampus (Scherzer *et al.*, 1998). Rodent studies show weak but diffuse NR2D expression in the spinal cord (Watanabe *et al.*, 1994; Rigby *et al.*, 2002), with a similar intensity of expression and distribution in human studies (Sundstrom *et al.*, 1997; Rigby *et al.*, 2002).

### 1.4.6 NR3A-B expression

Differing expression patterns of NR3A and NR3B suggest separate roles and importance throughout various stages of development. In the rat, NR3A is widely expressed during development particularly in the cortex, midbrain and hippocampus (Al-Hallaq *et al.*, 2002) reaching peak expression between postnatal days 7 and 10 thereafter decreasing substantially in adult animals with limited expression in nuclei in the thalamus, amygdala and the olfactory tract (Nishi *et al.*, 2001; Ciabarra *et al.*, 1995; Sucher *et al.*, 1995). Expression has also been detected in the mouse cerebellum at post-synaptic sites where it may form symmetrical synapses between climbing fibre terminals and cerebellar interneurons (Fukaya and Watanabe, 2007). A recent study revealed some interesting species differences between rodent and human expression of NR3A. Eriksson *et al.*, (2002) show that NR3A is expressed in both embryonic and adult human brain tissue, with a similar distribution pattern to a post-natal rat, calling into question the accuracy and comparable nature of rodent models with human receptors.

NR3B is highly expressed in somatic motor neurons in the brain, brainstem and spinal cord beginning at postnatal day 10-14 and continuing to maximal levels into

adulthood (Fukaya *et al.*, 2005; Matsuda *et al.*, 2003; Nishi *et al.*, 2001). Expression within the motor neurons is mainly concentrated within the neuronal cell bodies rather than the dendrites which may indicate areas of intracellular NR3B storage (Matsuda *et al.*, 2003) or an extrasynaptic location of NR3B containing receptors which may be activated following synaptic stimulation (Clark and Cull Candy 2002). A recent immunolocalisation study revealed evidence for more widespread expression of NR3B in the cortex, cerebellum, hippocampus and in spiny projection neurons of the striatum (Wee *et al.*, 2007).

### 1.5 NMDA receptor subunit co-assembly

The specific expression patterns of the NMDA receptor subunits suggests that specific NMDA receptor subunit co-assembly is regulated in a spatio-temporal manner to fulfil specialised roles throughout the CNS enhancing the complexity and heterologous nature of the receptor.

Many studies have investigated the subunits contained within native receptor assemblies, particularly in the rodent forebrain to look at the influence of specific sub-populations. According to these studies native NMDA receptors are composed of at least one NR1 subunit, one or more NR2 subunits (e.g NR1/NR2B or NR1/NR2A/NR2B) (Luo *et al.*, 1997; Chazot and Stephenson, 1997) and possibly one or more NR3 subunits (e.g. NR1/NR2B/NR3B) (Al-Hallaq *et al.*, 2002) with some debate as to whether the subunits co-assemble to form tetrameric and/or pentameric structures (Chazot, 2004).

In forebrain structures immunoprecipitation and immunopurification studies have shown co-association between NR1/NR2A, NR1/NR2B, NR1/NR2A/NR2B (Chazot and Stephenson, 1997; Blahos and Wenthold, 1996) and NR1/NR2D,

NR1/NR2A/NR2D, NR1/NR2B/NR2D (Dunah *et al.*, 1998; Stephenson, 2001). Research into subunit combinations in the spinal cord has been more limited. One group used solubilisation and immunoprecipitation of NMDA receptors from human lumbar-sacral regions finding co-associations between NR1, NR2A, NR2C and NR2D (Sundstrom *et al.*, 1997). The native associations of the NR3 subunits and the other subunits with which they assemble have yet to be elucidated but would provide important information about NMDA receptor function and pharmacology.

## 1.6 Physiological and functional properties of NR2B and NR3B receptors

### 1.6.1 Physiological properties of NR2B-containing receptors

As discussed previously, subunit composition plays a critical role in receptor function and activity. NMDA receptors containing NR2B subunits therefore display distinctive properties such as a high sensitivity to magnesium blockade and increased sensitivity to glutamate (Fuller *et al*, 2006; Cull-Candy *et al.*, 2001). Electrophysiological measurements investigating channel kinetics showed that NR2B-containing receptors desensitise more slowly and take longer to recover than NR2A-containing receptors, thereby increasing the duration of channel opening (Vicini *et al.*, 1998; Chen *et al.*, 1999; Loftis and Janowsky, 2003; Fuller *et al.*, 2006) and hence receptor activation.

During synaptic development two populations of NMDA receptor develop, those which cluster at synapses and those which remain extrasynaptic (Cottrell *et al.*, 2000; Thomas *et al.*, 2006), though recent research suggests a more fluid movement of receptors between synaptic and extrasynaptic sites along the postsynaptic membrane (Choquet and Triller, 2003; Zhao *et al.*, 2008). It is thought that these populations of

receptors may have different intracellular interactions with trafficking proteins and signalling cascades and therefore may have distinct roles in synaptic plasticity (Massey *et al.*, 2004) and neuronal cell death (Hardingham *et al.*, 2000) with extrasynaptic receptors potentially shutting down survival promoting pathways in the cell (Hardingham *et al.*, 2000). It has been shown that extrasynaptic NMDA receptors promote neuronal plasticity via a key contribution to the calcium signal necessary to induce these changes (Harris and Pettit, 2007).

Previous research has shown that NR2B-containing receptors occur both synaptically and extrasynaptically providing the potential for increased NMDA receptor activity via glutamate release both within and external to the synapse (Tovar and Westbrook, 1999; Liu *et al.*, 2004; Thomas *et al.*, 2006).

Via their key involvement in long-term potentiation (LTP) (Bliss and Lømo, 1973) and long-term depression (LTD), persistent activity-dependent increases and decreases in synaptic strength, NR2B-containing receptors are vital for information storage and synaptic plasticity in the brain (Yang *et al.*, 2005). The NR2B subunit has been associated with vital behavioural and physiological functions such as feeding, learning and memory (Bliss and Collingridge, 1993; Stanley *et al.*, 1996, Kahn *et al.*, 1999; Chazot, 2004). For example, NR2B-defective mice lack the suckling response and die shortly after birth (Kutsuwada *et al.*, 1996) and over-expression results in mice that exhibit superior ability in learning and memory tasks when compared to controls (Loftis and Janowsky, 2003).

The NR2B subunit is important for localisation of the receptor, anchoring it to the membrane and connecting the receptor with specific intracellular signalling mechanisms that modulate receptor functions (Loftis and Janowsky, 2003). The last five residues of the C-terminal domain of the NR2B complex are thought to be

important for binding to the PDZ domain of PSD-95/SAP102 (Neithammer *et al.*, 1996; Lim *et al.*, 2002) and are therefore critical for formation of multi-protein signalling complexes. Via PSD-95, NR2B is linked to many enzymes responsible for signal transduction within the cell, such as those essential for phosphorylation. NR2B is the most prominently tyrosine phosphorylated protein in the PSD fraction (Chazot 2004; Gardoni and DiLuca, 2006) which can contribute to potentiation and enhancement of receptor responses and alter intracellular signalling events (Lee, 2006). An internalisation motif (YEKL) is located on the C-terminal of the NR2B subunit close to the binding site for PSD-95. Prybylowski *et al.*, (2005) propose that phosphorylation of the tyrosine on this motif may inhibit internalisation of the receptor complex, thereby potentiating receptor localisation at the cell membrane and enhancing signal transmissions.

NR2B also interacts with growth factors and hormones such as brain-derived neurotrophic factor (BDNF) via post-synaptic trkB receptors and tyrosine phosphorylation of the subunit (Levine and Kolb, 2000; Lin *et al.*, 1999). It is reported that exposure to BDNF via these receptors increases single channel open probability, potentiating receptor activity.

NR2B-containing receptors are also proposed to stabilise and maintain the intracellular enzyme serine/threonine kinase CaMKII in an active conformation (Bayer *et al.*, 2001). This enzyme is activated by NMDA receptor mediated $Ca^{2+}$ influx and by increasing phosphorylation of NMDA subunits and reducing desensitisation of NR2B-containing receptors it is thought to contribute to long-term potentiation (LTP) (Bayer *et al.*, 2001; Lisman *et al.*, 2002; Colbran *et al.*, 2004.).

### 1.6.2 Physiological properties of NR3-containing receptors

The modulatory properties of the NR3A or NR3B subunits are the most poorly characterised of all the NMDA receptor subunits, although initial studies show interesting differences between the NR2 and NR3 subunits.

Critically, in the NR3 subunits, the asparagine residue at the QRN site of the second hydrophobic transmembrane domain is replaced with glycine followed by arginine at the N+1 site, properties which may be associated with reducing the $Ca^{2+}$ permeability and altering the magnesium sensitivity of the receptor (Matsuda *et al.*, 2002; Nishi *et al.*, 2001). Co-expression of mouse NR3A with NR1 and NR2A *in vitro* reduced glutamate-induced whole cell current and single channel conductance (Ciabarra *et al.*, 1995; Das *et al.*, 1998; Sucher *et al.*, 1995; Perez-Otano *et al.*, 2001) and in NR3A-/- mice the amplitude of NMDA receptor currents was increased in comparison to wild type neurons (Das *et al.*, 1998). It has also been proposed that the NR3A doesn't undergo extensive molecular rearrangement upon channel gating due to symmetrical alignment of the M3 segments of NR1 and NR3A. The M3 segments of both subunits form a narrow constriction in the outer vestibule of the receptor channel modulating the passage of cations (Wada *et al.*, 2006) and therefore possibly reducing calcium influx.

Nishi *et al.*, (2001) also describe suppressed glutamate-induced current when mouse NR3B was co-expressed in HEK 293 cells with NR1/NR2A subunits, referring to NR3B as a dominant-negative subunit. In partial contrast to this study, research carried out by Matsuda *et al.*, (2002) found no significant reduction in current amplitude in HEK 293 cells co-expressing mouse NR3B with NR1 and NR2A, although they did find reduced $Ca^{2+}$ permeability of NMDA receptor channels in these cells.

Research to date has found that NR3A and NR3B co-associate with NR1 and NR2A in heterologous cells and cultured neurons (Nishi *et al.*, 2001; Matsuda *et al.*, 2002, Das *et al.*, 1998; Ciabarra *et al.*, 1995; Sucher *et al.*, 1995). Under native conditions the mechanisms behind NR3B trafficking and incorporation into the receptor complex remain unclear. It is known from recombinant work in mammalian cell models that expression of a functional receptor requires NR1 for formation of the channel pore and trafficking to the membrane. Co-transfection of NR3B with NR2A or NR3B alone failed to produce functional receptors, however there remains some debate as to whether NR1 and NR3 co-transfection results in functional glycine receptor formation (Chatterton *et al.*, 2002). Evidence showing that NR3A has a soluble ligand binding domain with a high affinity for glycine (Kd 40nM) compared to a very low affinity for glutamate (Kd 9.6mM) (Yao and Mayer, 2006) fuels speculation for formation of such glycine channels in NR1/NR3 complexes. NR1/NR3B glycine-activated cation channels have been recorded in both oocytes (Chatterton *et al.*, 2002) and mammalian cells (Pina-Crespo and Heinemann, 2004) though Perez-Otano *et al.*, (2001) and Matsuda *et al.*, (2002) found no such activity in their mammalian systems. Both NR3A (Perez-Otano *et al.*, 2001) and NR3B (Matsuda *et al.*, 2003) require association with NR1 in order to exit from the endoplasmic reticulum and express on the cellular surface. Within the C-terminal of the NR3B subunit, it is thought that amino acids 952-985 are important for receptor trafficking and may be able to mask the endoplasmic reticulum (ER) retention signal of the NR1 subunit (Matsuda *et al.*, 2003). It is therefore possible that a receptor complex consisting of NR1/NR3B subunits may be actively transported to the membrane but full investigation of this controlled trafficking and specific subunit co-assembly has yet to be carried out.

The evidence currently available suggests important modulatory influences of the NR3 subunits on the NMDA receptor complex. Changes from NR3A to NR3B expression throughout development in the rodent may be important for regulation of calcium permeability throughout maturity and critical for maintaining control of intracellular calcium concentrations in NMDA receptors.

### 1.7 NMDA receptor signalling and trafficking

The precise mechanisms governing NMDA receptor delivery to the synapse are complex and yet to be fully elucidated. However, their expression at the cell surface is known to be subject to plastic changes depending on the neuronal environment (Prybylowski and Wenthold, 2004). These alterations in NMDA receptor numbers and expression patterns are mediated via delivery, internalisation and translocation between synaptic and extrasynaptic sites (Prybylowski and Wenthold, 2004).

In order to ensure that only functional NMDA receptors are delivered to the cell membrane, endoplasmic reticulum (ER) retention signals exist on the individual subunits. These retention motifs are masked upon formation of functional complexes and the receptor is able to exit the ER. Fukaya *et al.*, 2003, showed that NR1 was vital for the release of NR2 subunits from the ER in hippocampal pyramidal cells *in vivo*: in the absence of NR1, the NR2 subunits are retained and aggregated into intracisternal granules.

NMDA subunits associate with members of the membrane-associated guanylate kinases (MAGUKs) family, namely SAP102 (synapse associated protein) and PSD95 (post-synaptic density), which form scaffolding molecules linking the

receptor with intracellular enzymes and signalling molecules (Van Zundert *et al.*, 2004). Research suggests associations with protein complexes differ according to subunit composition of the receptor and its synaptic or extrasynaptic localisation, resulting in potentially different signalling cascades and functions (Van Zundert *et al.*, 2004). PSD-95 binds directly to important signalling proteins such as GTPase-activating protein, neuronal nitric oxide synthase (nNOS), Fyn and $Ca^{2+}$ ATPases (Van Zundert *et al.*, 2004). Associations of PSD-95 with kinesin motors KIF18 and KIF17 are important for NMDA receptor delivery to the synapse (Mok *et al.*, 2002; Guillaud *et al.*, 2003) and linkage of the protein huntingtin to PSD-95 provides some evidence for NMDA associated excitotoxicity in Huntington's disease models (Zeron *et al.*, 2002; Prybylowski and Wenthold, 2004). Linkage with PSD-95 also enables phosphorylation of the subunits via enzymes such as tyrosine kinases and protein kinase C, important for movement of receptors from synaptic to extrasynaptic locations (Fong *et al.*, 2002) and inhibiting internalisation of NR2B-containing receptor complexes (Prybylowski *et al.*, 2005).

Recent data shows association of NR3A with microtubule-associated protein 1S (MAP1S), which links this subunit with cytoskeletal proteins, possibly facilitating its anchoring and stabilization within the synapse and its potential for movement between synaptic and extra-synaptic sites (Eriksson *et al.*, 2002).

### 1.8 Pharmacological targeting of the NMDA receptor

NMDA receptors play a vital role in excitatory transmissions within the central nervous system and therefore have long been implicated in disease pathogenesis. In the late 1980's Choi *et al.*, 1988 noted toxic effects of NMDA receptor activation in

primary cultured neurons which could be protected by NMDA antagonists. NMDA receptor mediated glutamate toxicity is now well documented with both *in vitro* and *in vivo* experiments.

### 1.8.1 Non-selective NMDA antagonists

The first generation of NMDA antagonists were developed to treat stroke and trauma patients (Wang and Shuaib, 2005) and were either non-selective, non-competitive channel blockers such as phencyclidine (PCP), (+)-5-methyl-10,11-dihydro-5-H-dibenzo[a,d]cyclohepten-5,10-imine (MK-801) (Kemp *et al.*, 1987), memantine and ketamine, or competitive antagonists which act at the agonist glutamate or glycine binding domains. Some of the first compounds discovered such as (R)-2-amino-5-phosphonopentanoate (R-AP5) (Paoletti and Neyton, 2006) and cis-4-phosphonomethyl-2-piperidine carboxylic acid (CGS-19, 755) (Bennett *et al.*, 1990; Murphy *et al.*, 1988) are examples of competitive antagonists acting at the glutamate binding site on the NR2 subunits. They show good selectivity for NMDA receptors over other ionotropic glutamate channels but show modest selectivity variations between the NR2 subunits. Compounds acting at the co-agonist glycine binding site such as 5-nitro-6,7-dichloro-1,4-dihydro-2,3-quinoxalinedione (ACEA-1021 (Leeson and Iversen, 1994) and 5, 7-dichlorokynurenic acid (5,7-DCKA) (Hess *et al.*, 1998) also show minimal receptor subtype selectivity as they are targeting binding sites on the NR1 subunit. Animal studies using the channel blockers memantine and ketamine (Carlton and Hargett, 1995; Qian *et al.*, 1996) have shown encouraging effects for treatment of neuropathic and inflammatory pain, which have also been seen in human studies (Mercadante *et al.*, 1995; Eisenberg *et al.*, 1998) and indeed, recently memantine and amantadine have been approved for treatment of late-stage

Alzheimer's and Parkinson's diseases (Roesler *et al*, 2003). However, the non-selective nature of these compounds and the resultant level of unacceptable side effects at analgesic doses such as psychomimetic effects, impaired learning, memory and motor function have limited their widespread use and resulted in largely unsuccessful clinical trials.

Subunit specific, activity-dependent modulators are therefore greatly favoured, as they have potential for increased therapeutic indices based on selectivity for specific sub-populations such as NR2B-containing receptors.

### 1.8.2 NR2B subunit selective antagonists

The heterogeneous nature of the NMDA receptor complex and the pharmacological modulations and specific regional distribution provided by the various subunit co-assemblies has enabled more selective NMDA receptor targeting.

Pharmacologically, the NR2B subunit has become important as a target for subunit specific antagonists, which can potentially block or reduce the excitatory effects of the receptors (Williams 2001, Zhuo 2002, Chazot *et al.*, 2002). It is thought that the more restricted expression patterns and the particularly low expression levels in the cerebellum may enhance therapeutic action whilst limiting the risk of serious motor side effects (McCauley 2005). NR2B-containing NMDA receptors have been implicated in many CNS pathologies such as stroke, drug-induced dyskinesias, dementias and chronic pain (Chizh *et al.*, 2001; Chazot, 2004) due to their specific distribution in affected brain areas and physiological properties. For example, high expression levels of NR2B-containing receptors in pain related structures such as the forebrain and dorsal horn of the spinal cord (Monyer *et al.*, 1994; Boyce *et al.* 1999)

make it a therapeutic target. A large proportion of NR2B-containing receptors are located extrasynaptically, which is thought to be important as their excess stimulation by glutamate diffusing from the synaptic cleft can result in glutamate-induced toxicity. Toxicity as a result of $Ca^{2+}$ influx leads to loss of mitochondrial membrane potential, free radical production and hyper-excitation (Sattler and Tymianski, 2000; Chazot 2004). It has been shown that over-expression of NR2B in the anterior cingulate and insular cortices of mice results in selective enhancement of persistent pain (Wei *et al*, 2001) and that gene knockdown of NR2B reduces formalin induced nociception (Tan *et al.*, 2005), implying that NR2B-containing receptors in the forebrain play an important role in chronic pain (Chizh *et al.*, 2001; Wei *et al.*, 2001; Petrenko *et al.*, 2003; Chazot 2004).

In the 1980s, it was discovered that ifenprodil (a phenylethanolamine originally developed as a vasodilating agent) (Williams, 2001) acted as an NMDA receptor antagonist, displaying neuroprotective effects but without the serious side-effect profile of other antagonists (Carter *et al.*, 1988; Williams *et al.*, 1993). Ifenprodil is a non-competitive, voltage independent, activity-dependent antagonist (Williams, 1993; Kew *et al*, 1996; Chenard and Menniti, 1999), which is highly sensitive to extracellular pH and displays a high level of NR2B selectivity (Williams *et al.*, 1993), having a 400-fold higher affinity for NR1/NR2B than for NR1/NR2A receptors (Williams 1993; Kew *et al.*, 1996). Inhibition with ifenprodil is activity dependent with a 40-fold higher affinity for the agonist-bound activated state (possibly present in excitotoxic conditions) than the inactivated state thereby increasing its side effect profile in comparsion to the channel blockers (Williams *et*

*al.*, 1993; Kew *et al.*, 1996). However, side effects such as hyperventilation, motor impairment and ptosis were seen (Boyce *et al.*, 1999) partly as it has a high affinity for α1-adrenergic, sigma and serotonin receptors (Williams, 1993; Chenard *et al.*, 1995) and is therefore not exclusively NMDA specific.

The binding site of the ifenprodil molecule is distinct from the channel pore, the glutamate, glycine or the polyamine site (Grimwood *et al.*, 2000). It is located within the N-terminal leucine/isoleucine/valine binding protein-like domain (LIVBP-like domain) (Perin-Dureau *et al.*, 2002). 3D mapping of this domain showed a cleft with a 'venus fly trap' mode of action (Perin-Dureau *et al.*, 2002; Chazot, 2004). The presence of an aspartate and two phenylalanine residues within the lobes of the cleft appear to be essential for high affinity ifenprodil binding (Chazot, 2004).

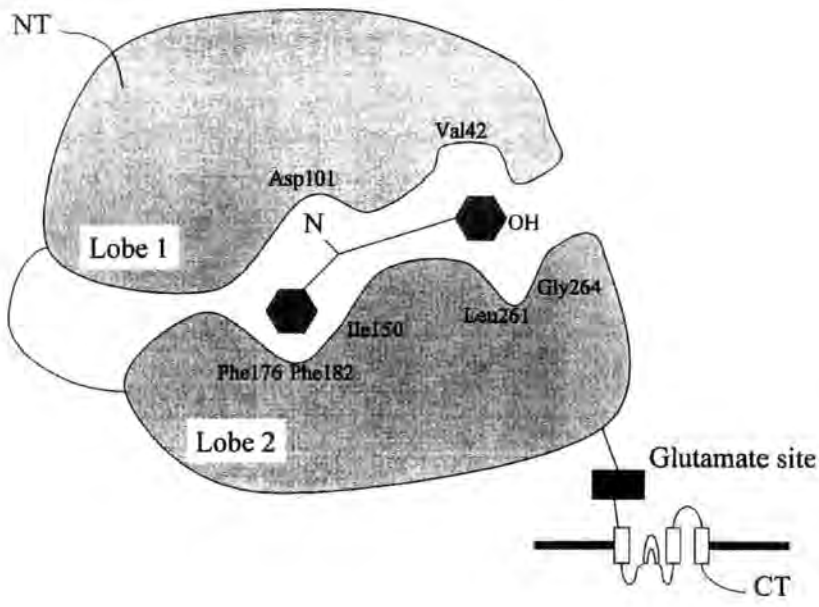


**Figure 1.4 Schematic representation of the bi-lobular LIVBP ifenprodil binding site on the NR2B subunit showing the significant amino acids (Chazot, 2004).**

Ifenprodil and its early analogues haloperidol and eliprodil still had problems with non-specific targeting and side-effects preventing their use clinically, though they

became very useful tools along with channel blockers like MK-801 to investigate receptor pharmacology and allosteric properties of binding sites.

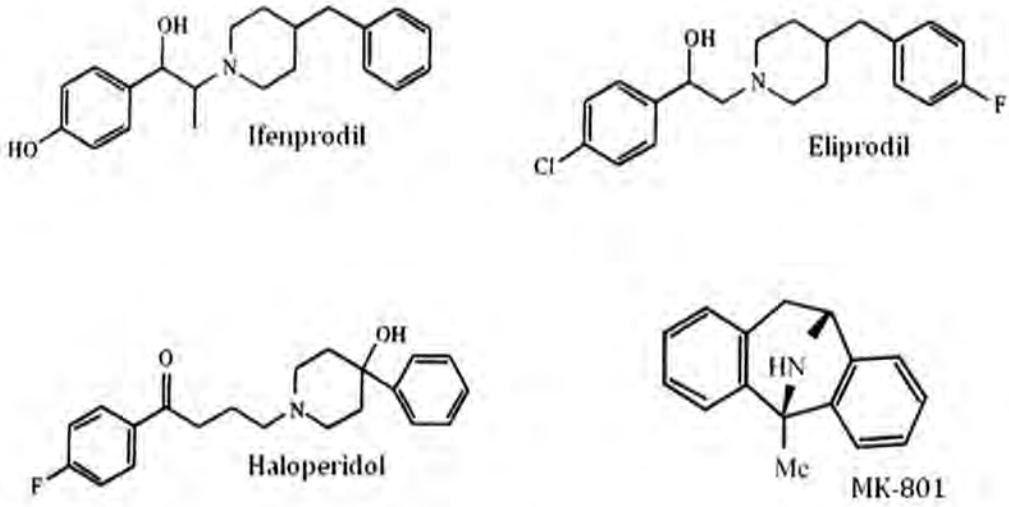


**Figure 1.5 Chemical structures of early NR2B-selective antagonists (Williams, 2001) and the channel blocker MK-801 (Nikam and Meltzer, 2002).**

The ifenprodil molecule subsequently became the congener for second generation NR2B antagonist development with a number of analogues such as Ro-256981, Ro-04-5595 (Roche) and CP-101,606 (Pfizer) (Chazot, 2004). These compounds have been developed to display a higher affinity for NR2B-containing receptors with a reduced affinity for α1-adrenergic receptors (Chenard *et al.*, 1995). They work to enhance inhibition of the NMDA receptor (Lynch and Guttman, 2001) by increasing the effects of extracellular protons and possibly by decreasing the affinity of the receptor for co-agonist glycine binding (Williams, 2001).

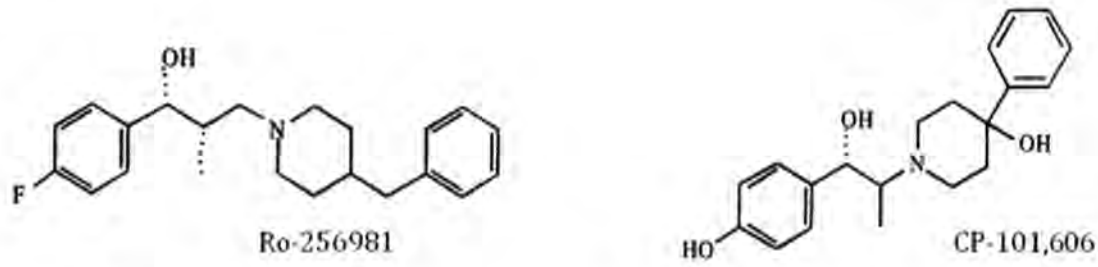


**Figure 1.6 Chemical structures of second generation NR2B-selective antagonists (Nikam and Meltzer, 2002).**

Both CP-101,606 (Menniti *et al.*, 1997) and Ro-256981 (Fischer *et al.*, 1997) are piperidine-containing compounds (B-linker analogues with hydroxyl functionality) and display structural similarity to ifenprodil, binding to the ifenprodil site on rat forebrain membranes with high affinities ($K_D$) of 9.4nM and (Kd) of 10nM for Ro-256981 and CP-101,606 respectively (Chazot *et al.*, 2002).

Further work to identify the binding characteristics and subtype selectivity of these two compounds discovered two separate classes of antagonists. Ro-256981 binds to NR2B-containing receptors irrespective of the presence of another NR2 subunit, whereas CP-101,606 binding is highly affected by the presence of alternative NR2 subunits within the receptor complex (Chazot *et al.*, 2002). The heterogeneity of the receptor complex is therefore very important in defining antagonist affinities (Chazot and Stephenson, 1997).

Both Ro-256981 and CP-101,606 have shown potent neuroprotective activity against glutamate-induced NMDA receptor-mediated toxicity *in vitro* and *in vivo* (Fischer *et al.*, 1997; Tsuchida *et al.*, 1997; Boyce *et al.*, 1999; Chizh and Headley, 2005). *In vivo* studies by Boyce *et al.*, 1999 showed potent anti-nociceptive activity upon mechanical allodynia following nerve injury in rats with neither compound inducing

motor impairment at analgesic doses (3-10mg/kg), however some impairment of rotarod performance at high doses of Ro-256981 (up to 100mg/kg) were noted and they concluded that CP-101,606 had the best therapeutic window (Boyce *et al.*, 1999; Boyce and Rupniak, 2002).

Other studies showing CP-101,606 induced neuroprotection in primary neuronal cultures (Menniti *et al.*, 1997) and in *in vivo* animal models of ischaemic brain injury (Di *et al.*, 1997; Tsuchida *et al.*, 1997; Wang and Shuaib, 2005) and chronic pain displayed reversal of mechanical hyperalgesia and reduced excitation of dorsal horn neurons following windup (Taniguchi *et al.*, 1997; Boyce *et al.*, 1999) with an improved side-effect profile in comparison to ifenprodil. The encouraging profile of CP-101,606 in animals led to clinical trials in humans for the treatment of traumatic brain injury and haemorrhagic stroke (Menniti *et al.*, 1998). Phase I tolerability studies in healthy volunteers showed no adverse effects at therapeutic doses (200ng/ml) with the maximum tolerated plasma concentration of 4200ng/ml after which adverse effects included amnesia, dizziness and confusion (Menniti *et al.*, 1998; Boyce and Rupniak, 2002) were reported. An open-label phase I study in subjects with severe traumatic brain injury or intracerebral haemorrhage showed good penetration to the CSF and that CP-101,606 infusion for 24 or 72 hours was well tolerated with improvements on the Glasgow outcome score (Bullock *et al.*, 1999) and a double blind, placebo-controlled study of 53 subjects with traumatic head injuries showed good tolerability of the drug with no significant cardiovascular abnormalities reported (Merchant *et al.*, 1999).

To date, despite the improved safety profiles of these ifenprodil-like NR2B-selective compounds and promising data from clinical trials, they have not yet been approved for human use due to potential potassium channel mediated cardiotoxicity, poor oral

bioavailability (Kew and Kemp, 2005) and heterogeneity in the patient populations tested and therefore novel compounds structurally unrelated to ifenprodil are being developed (Claiborne *et al.*, 2003).

There are many other NR2B selective compounds in development and recently Merck and Co have disclosed a class of hydroxybenzimidazoles (McCauley *et al.*, 2004) and Gideon and Richter have a compound RGH-896, of undisclosed structure, entering phase IIa clinical trials for neuropathic pain (Farkas *et al.*, 2003).

### 1.9 NMDA receptor associations with pathology

Tightly regulated control of NMDA receptor expression and function is required for normal physiological processing within the central nervous system. Their essential role and widespread distribution means disruption of NMDA receptor physiology is often evident in neuronal pathologies. Specific patterns of receptor heterogeneity may therefore provide therapeutic targets for many chronic conditions.

#### 1.9.1 Calcium-dependent excitotoxicity

Excessive glutamate-mediated calcium entry into cells can lead to excitotoxicity and neuronal cell death. It is a mechanism of neuronal loss implicated in both acute disease such as ischaemia and chronic neurodegenerative diseases such as amyotrophic lateral sclerosis (Arundine and Tymianski, 2003).

Within a cell calcium ions are vital for normal physiological processes such as signalling and synaptic activity, and therefore under normal conditions, homeostatic regulation of cytosolic $Ca^{2+}$ is tightly controlled (Arundine and Tymianski, 2003). Excessive glutamate release from synapses triggers NMDA, AMPA and Kainate

receptor channel opening and $Ca^{2+}$ and $Na^{+}$ influx. Increased internal $Ca^{2+}$ concentrations from excessive influx and release from intracellular stores overcome the regulatory mechanisms, the metabolic processes within the cell begin to fail and the cell dies (Choi, 1988; Sattler and Tymianski, 2000). The source-specificity hypothesis for $Ca^{2+}$ toxicity was proposed by Tymianski *et al.*, 1993 and states that neurotoxicity in cells requires specific signalling pathways triggered by $Ca^{2+}$ entry at specific receptors to be activated. Their experiments showed high levels of toxicity when $Ca^{2+}$ entered via NMDA receptors, whereas $Ca^{2+}$ entry via voltage-sensitive channels was tolerated (Tymianski *et al.*, 1993; Arundine and Tymianski, 2003). It is thought that this specific toxicity via NMDA receptors results from the formation of a ternary complex between NMDA receptors, PSD-95/SAP90 (post-synaptic density-95/synapse associated protein 90) and nNOS (nitric oxide synthase) (Sattler *et al.*, 1999) increasing nNOS activity and thereby toxicity. The evidence from these studies therefore supports the potential beneficial effects of NMDA receptor therapeutic targeting.

### 1.9.2 Huntington's Disease

NMDA-mediated excitotoxicity and specific associations with the mutated huntingtin protein have been investigated as possible links with disease aetiology. Huntington's disease manifests as a hyperkinetic movement disorder with cognitive and psychiatric dysfunction and affects 5-10/100,000 population worldwide (Li *et al.*, 2003). An autosomal dominantly inherited condition, it is caused by expanded CAG repeats in the first exon of the Huntington's disease gene (Li *et al.*, 2003). Co-expression of the mutant gene huntingtin with NR1/NR2B receptors increases current amplitudes and may increase the number of receptors expressed at the cell

surface (Chen *et al.*, 1999b) potentiating NMDA activation and potential for toxic calcium accumulation within the cell. Cytotoxicity studies have also shown increased levels of cytotoxicity when NR1/NR2A and more so NR1/NR2B were co-expressed with the full length mutant huntingtin-138Q (Zeron *et al.*, 2001) providing evidence for NMDA involvement in potential neuropathologies associated with the disease. Interestingly, NR2A and NR2B gene variations have recently been linked to modification of age onset in Huntington's disease accounting for 7.2% additional variance in the age of onset in patients (Arning *et al.*, 2007).

### 1.9.3 Schizophrenia

Glutamatergic transmission via NMDA receptors has been implicated in some of the pathogenic mechanisms behind schizophrenia (Stefani and Moghaddam, 2004; Heresco-Levy and Javitt, 1998; Gao *et al.*, 2000) based on observations that hypofunction of receptors as a result of NMDA antagonist treatment causes some transient psychotic states in healthy individuals (Du Bois and Huang, 2007; Loftis and Janowsky, 2003). Studies investigating the potential mechanisms of NMDA involvement have found abnormal glutamate receptor expression (Beneyto *et al.*, 2007). Grimwood *et al.*, 1999 discovered up-regulation of NR2B-containing receptors in the superior temporal cortex using radioligand binding with [$^3$H] ifenprodil. Gao *et al.*, 2000 showed a 40% increase in NR2B mRNA in the CA2 hippocampal region of schizophrenic post-mortem tissue in comparison to controls and elevated levels of NR3A were shown in the dorsolateral prefrontal cortex and inferior temporal neocortex in schizophrenic tissue in comparison to controls (Mueller *et al.*, 2004). It has also been shown that inhibition of NMDA receptor activity during cortical development produces cognitive deficits phenotypically

relevant to schizophrenia in the adult (Stefani and Moghaddam, 2004) providing evidence for NMDA involvement in cognitive disorders and showing their importance for normal physiological development.

### 1.9.4 Parkinson's Disease

Parkinson's disease is a progressive neurodegenerative condition manifesting in dyskinetic effects with tremor, rigidity and cognitive dysfunction. Affecting millions of people world-wide, parkinsonian diseases arise due to dopamine-glutamate imbalances within the striatothalamocortical loop, reducing stimulation of the motor cortex (Ulas *et al.*, 1994). Reduced formation of dopamine in the substantia nigra causes increased activity of the striatal pathway to the external pallidum, lack of regulated inhibition of the subthalamic nucleus and glutamatergic hyperactivity in the basal ganglia (Albin *et al.*, 1989; Loschmann *et al.*, 2004). It has been proposed that this over-excitation at glutamatergic synapses may be NMDA receptor mediated as it is known that these receptors are vital in both the basal ganglia and striatum for normal physiological processes (Hallett and Standaert, 2004). In addition it has been shown that receptor structure, function and abundance in the striatum of Parkinson's disease patients is altered by dopamine depletion (Hallett and Standaert, 2004) with selective increases in NMDA-sensitive glutamate binding (Ulas *et al.*, 1994). Attempts to combat this up-regulation of NMDA receptors in diseased patients with selective antagonists has been a major focus for many studies with some success in animal models, where, for example, the NR2B-selective compounds Ro-256981 (Loschmann *et al.*, 2004) and CP-101,606 (Wessell *et al.*, 2004) showed anti-parkinsonian activities. Development of NMDA

antagonists with increased selectivity and reduced side-effect profiles may therefore provide real potential for future treatments.

### 1.9.5 Alzheimer's Disease

Alzheimer's disease is the most prevalent neurodegenerative condition affecting millions worldwide. Few cases of familial early onset disease have been documented, however the majority of cases are sporadic with later-stage onset generally in the 6$^{th}$ decade of life. Manifesting as progressive cognitive decline with neuropsychiatric symptoms, amyloid plaques and neurofibrillary tangles in the brain remain indicative of this dementia. The aetiology behind disease onset is still not fully understood with many approaches such as pathophysiological mechanisms behind the misfolding of amyloid-beta and genetic mutations being explored (Albensi *et al.*, 2004). Pharmacological therapies have mainly relied upon cholinergic inhibitors which partially enhanced patient cognitive states (Doraiswamy, 2003; Lipton, 2007) though recently therapeutic focus has shifted to NMDA receptor antagonism to combat the glutamatergic excitotoxicity and subsequent neuronal death seen in dementia (Albensi *et al.*, 2004; Lipton, 2007). Memantine is a non-competitive, low-affinity NMDA receptor open channel blocker which has been clinically approved in Europe and the USA for the treatment of moderate-severe Alzheimer's disease (Doraiswamy, 2003; Albensi *et al.*, 2004). The preferential binding of memantine to excessively activated NMDA receptors seems to reduce the adverse side-effect profile seen with other antagonists because normal physiological activity isn't disrupted to a high degree (Lipton, 2007) and there is some evidence to suggest memantine up-regulates production of BDNF, promoting

neuronal survival (Albensi *et al.*, 2004). Second generation memantine derivatives are currently in development and it is hoped their safety profile and neuroprotective efficacy will be improved for more wide-spread use in neurodegenerative conditions.

### 1.9.6 Amyotrophic lateral sclerosis (Motor neuron disease)

Amyotrophic lateral sclerosis (ALS) is a progressive, fatal neurodegenerative disease characterised by the selective loss of somatic motor neurons in the spinal cord, brainstem and motor cortex (Samarasinghe *et al.*, 1996; Shaw *et al.*, 1994). The pathophysiology behind the disease and its rapid progression to paralysis and death remain largely unknown though advances, particularly in genetic techniques have increased knowledge and stimulated further research.

90% of cases develop sporadically generally in older patients, though 10% of cases are familial with some genetic mutations in the Cu/Zn superoxide dismutase 1 enzyme (SOD1). This SOD1 enzyme is a homodimeric cytosolic protein (Gorman *et al.*, 1996) which breaks down highly toxic superanion radicals into harmless products making it very important for the cell's defence against free radical damage and excitotoxicity.

Glutamate-mediated excitotoxicity via AMPA and NMDA (Samarasinghe *et al.*, 1996; Shaw *et al.*, 1994) receptors as well as deficiencies in astrocytic glutamate uptake (Rao and Weiss, 2004) and damage to glutamate transporters (Rodriguez *et al.*, 1997) have all been proposed as potential pathological mechanisms in both sporadic and familial diseases. All of these factors could lead to neuronal cell death via $Ca^{2+}$ toxicity disrupting metabolic processes, inducing proteolysis, stimulating free radical production and damaging mitochondrial membranes (Rodriguez *et al.*, 1997). Motor neurons are also particularly susceptible to $Ca^{2+}$ overload as they

naturally have reduced levels of calcium binding proteins and AMPA GluR2 receptors which can flux $Ca^{2+}$ so the effect is exacerbated in these cells.

Research into NMDA receptor expression levels found reduced density of NMDA receptor expression, up to 50% reduction in NR1 mRNA expression in the ventral horn (Virgo and De Belleroche, 1995) in motor neuron disease patients in comparison to control tissue (Shaw *et al.*, 1994; Samarasinghe *et al.*, 1996). These data are likely to reflect the overall loss of motor neurons from the spinal cord of diseased patients, however they confirm the presence of NMDA receptors on motor neurons and a study by Samarasinghe *et al.*, 1996 highlights the possibility of modification in the composition of receptor subunits with widespread loss of the NR2A subunit in both dorsal and ventral horns of diseased patients in comparison to controls.

A mouse model carrying the SOD1 mutation has been developed which displays similar disease pathology and clinical symptoms to MND patients. Wang and Zhang, (2005) have found that treatment of these mutant mice with the NMDA antagonist memantine significantly delayed disease progression and increased the lifespan of the mice in comparison to controls, indicating that NMDA mediated excitotoxicity may be involved in MND pathogenesis and may therefore be a target for future therapies.

### 1.9.7 Chronic Pain

Chronic pain is a serious debilitating condition resulting from prolonged tissue injury or more commonly from prolonged hypersensitisation of nociceptive neurons. It is estimated that over 20% of the world's adult population are affected by persistent pain resulting in healthcare costs of €200 billion per annum.

At present, despite advances in the understanding of the pathophysiological mechanisms of chronic pain, the underlying neuronal and neurochemical mechanisms involved in inducing, maintaining and processing nociceptive information are complex and still not fully understood.

It is known that upon activation of peripheral nociceptors, pain transduction is conducted through myelinated Aδ and unmyelinated C fibres to the dorsal root ganglion in the spinal cord (see figure 1.7). Signals are then transmitted via the spinothalamic tract to the thalamus and cortex for modulation of sensory input (Markenson, 1996) and motor responses. However, prolonged activation of nociceptors and a reduction in transduction threshold can lead to chronic stimulation. Since the late 1980s the major research focus has been on the identification of molecules involved in pain perception in order to develop analgesic treatments.

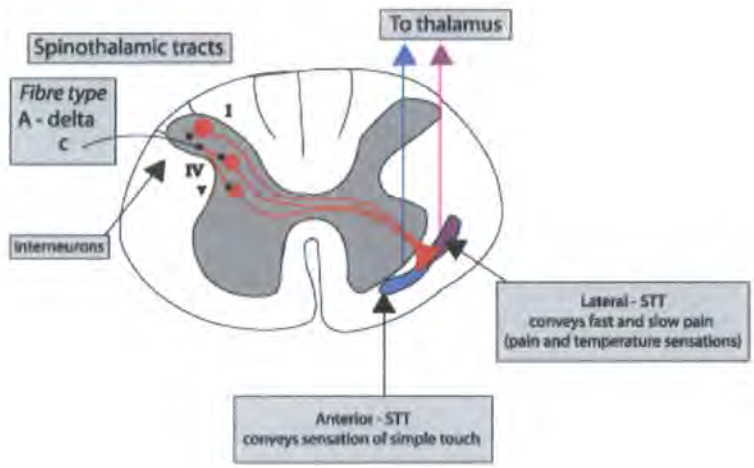


**Figure 1.7 Schematic diagram representing afferent Aδ and C-fibre input to the dorsal root ganglion, through the cord and into the spinothalamic tracts (Anaesthesia UK, www.frca.co.uk).**

### 1.9.8 NMDA receptor and central sensitisation

Glutamate is known to be a major excitatory neurotransmitter in the central nervous system (Petrenko *et al.*, 2003; Chizh, 2002; Kemp and McKernan, 2002) and plays a major role in excitatory synaptic transmission and sensitisation. Glutamatergic synapses therefore play important roles in both acute and chronic nociceptive processing at both normal and pathophysiological levels. Upon acute noxious stimulation primary afferent terminals in the spinal cord release glutamate which primarily activates AMPA receptors on second order neurons (Chizh, 2002). However, prolongued activation of nociceptors stimulates continuous release of glutamate and neuropeptides, causing long-lasting membrane depolarisation, removal of the voltage-dependent magnesium block on the NMDA receptor and thus sustained receptor activation and persistent pain response (Chizh, 2002; Haley *et al.*, 1990; Ma and Woolf, 2002).

Tissue injury or inflammation generating pain hypersensitivity can often have a protective effect, reducing the pain threshold to prevent further injury; however in some circumstances this hypersensitivity can become pathological. An example is neuropathic pain associated with damage to the nervous system (Ma and Woolf, 2002), which can arise secondarily from conditions such as viral infections, chemotherapy or traumatic injuries (Boyce *et al.*, 1999). This hypersensitivity mechanistically can result from two sources, peripheral or central sensitisation (Ma and Woolf, 2002). Peripheral sensitisation restricts increases in pain sensitivity to the site of injury (Ji *et al.*, 2003) increasing sensitivity of primary afferent nociceptors (Zhuo, 2002; Ma and Woolf, 2002). There is some evidence that the numbers of NMDA receptors are thought to increase upon peripheral sensitization, enhancing transmissions (Petrenko *et al.* 2003). Central sensitisation involves the

hyper-excitation of nociceptive neurons within the central nervous system, particularly in the dorsal horn of the spinal cord (Ma and Woolf, 2002; Woolf, 1983; Cook *et al.*, 1987) where the receptive field and responsiveness of the dorsal horn neurons are increased and their activation threshold is reduced (Cook *et al*, 1987; Ji *et al.*, 2003).

Biochemical, electrophysiological and behavioural data (Medvedev *et al.*, 2004) indicate that the NMDA receptor can mediate long-term synaptic plastic changes lasting from hours to days (Zhuo, 2002), phenomena termed long-term potentiation (Bliss and Lømo, 1973) and long-term depression, and the NMDA receptor is therefore essential for the development of central sensitisation (Ultenius *et al.*, 2006) and thus chronic pain.

It is thought that NMDA receptors play a major role in central sensitisation due to their ability to alter neuronal membrane excitability via activation of protein kinase C (Ma and Woolf, 2002). Upon membrane depolarization, $Ca^{2+}$ influx allows the translocation of protein kinase C from the cytosol to the membrane. Protein kinase C is then able to phosphorylate receptors including the NMDA receptor and in turn potentiate their activation, amplifying the NMDA response in a positive feedback manner greatly contributing to central sensitization (Zhen *et al.* 1997).

In the 1980's two groups Davies *et al.*, 1987 and Dickenson *et al.*, 1987 first provided evidence for the role of NMDA receptors in nociception and their potential as analgesic targets observing that 'spinal delivery of NMDA receptor antagonists inhibited the hyper-excitability of the spinal cord nociceptive neurons induced by C-fibre stimulation'. Many animal pain models have subsequently provided evidence for NMDA mediated nociceptive responses (Medvedev *et al.*, 2004; Ultenius *et al.*, 2006; Boyce *et al.*, 1999; Massey *et al.*, 2004) which have initiated the current level

of biomedical and pharmacological interest in NMDA receptors driven by the potential therapeutic possibilities of NMDA receptor antagonists.

### 1.9.9 NR2B as an analgesic target

NR2B-containing NMDA receptors have been a target for analgesic compounds since the requirement for subunit selective compounds with higher binding affinities and improved safety profiles became crucial. Studies have shown selective NR2B antagonist induction of anti-nociception without motor dysfunction demonstrating the improved safety profile and effectiveness of these compounds (Boyce *et al.*, 1999).

Also, as knowledge of the physiological properties of NR2B-containing receptors has improved, evidence of their potential role in hyper-excitation and central sensitisation has increased.

Expression studies using anti-NR2B antibodies, *in situ* hybridisation techniques and radiolabelled binding assays (Nagy *et al.*, 2004; Tolle *et al.*, 1993; O'Donnell *et al.*, 2004; Mutel *et al.*, 1998; Chazot and Sheahan unpublished) have demonstrated the localisation of NR2B-containing receptor expression in pain-related structures such as the dorsal horn of the spinal cord, particularly in the outer laminae I-II (Nagy *et al*, 2004), primary sensory fibres (Ma and Hargreaves, 2000), and forebrain structures such as the anterior cingulate cortex (Wei *et al.*, 2001), cortex and thalamus (Sheahan and Chazot, unpublished). Research carried out by Wei *et al.*, (2001) demonstrated that over-expression of NR2B in mice can lead to enhanced pain behaviour in comparison with control animals, possibly caused by the slow receptor desensitisation and increased affinity for glutamate of NR2B-containing receptors, enhancing channel opening time and hence increasing activity.

The extra-synaptic localisation of NR2B-containing receptors also contributes to the potential for enhancing NMDA receptor activation as excessive glutamate release within the synaptic cleft could lead to glutamate spillover, which preferentially activates high-affinity NMDA receptors, enhancing responsiveness of the network (Momiyama 2000; Van Zundert *et al.*, 2004; Lambe and Aghajanian 2006). A recent study by Liu *et al.*, (2007) suggests that activation of synaptic or extrasynaptic NR1/NR2B receptors increases NMDA activity and potentially initiates apoptotic signalling cascades promoting neuronal cell death.

Increased tyrosine phosphorylation of the NR2B subunit, which potentiates activity, has also been recorded following induction of long-term potentiation, providing evidence for this subunits involvement in synaptic plasticity and potential hyperexcitation (Rosenblum *et al.*, 1996; Rostas *et al.*, 1996; Lee, 2006). Also an important study by Abe *et al.*, (2005) shows evidence suggesting Fyn kinase-mediated phosphorylation of Tyr 1472 on the NR2B subunit is essential for maintenance of neuropathic pain via post-translational modifications up-regulating receptor activity, (Chazot, 2004) by blocking endocytosis, again providing evidence for the suitability of targeting NR2B-containing receptors.

It has also been proposed that NR2B interaction with BDNF enhances channel open probability (discussed in section 1.6.3), increasing evidence for potential over-activation of NR2B-containing receptors (Levine and Kolb, 2000; Loftis and Janowsky, 2003) and increasing their association with diseases such as chronic pain.

This thesis discusses the potential importance and clinical effectiveness of targeting

NMDA receptors, the difficulties in drug development arising from the heteromeric nature of the receptor and the inferred functional and pharmacological implications.

## 1.10 Hypotheses, Aims and Objectives

To investigate the physiological and pharmacological characterisation of NR2B and NR3B-containing NMDA receptors and evaluate the influence of receptor heterogeneity on NMDA antagonist development, the following hypotheses were addressed in this study;

- NR2B-selective antagonists display differential pharmacological properties and are influenced by NMDA receptor heterogeneity.
- The NR3B subunit influences the physiological function and pharmacology of NMDA receptor complexes.
- Chronic pain states elicit alterations of NMDA receptor physiology through changes in subtype expression and/or protein post-translational modification.

To address these hypotheses, this study aimed to;

- Investigate two novel NR2B subunit-selective antagonists developed by GlaxoSmithKline (COMPOUND A and COMPOUND B), characterising their binding properties and using them as tools to explore the pharmacological influences of NMDA receptor subunit heterogeneity.
- Generate rodent and human anti-NR3B polyclonal antibodies and utilise them with a panel of selective NMDA antibodies to determine the distribution and complex associations of NMDA receptors, particularly NR3B-containing receptors in adult rat and human spinal cord.

- Investigate the functional implications of NR3 subunit inclusion in the NMDA receptor complex upon cytotoxicity, physiology and pharmacology.
- Investigate the distribution, expression and phosphorylation of NMDA receptor subunits in rodent spinal cord and whole brain from a chronic pain model and compare with controls.

# Chapter 2

# Materials and Methods

## 2.0 Materials

All chemicals and solutions were supplied by Sigma-Aldrich Company, UK and Gibco Ltd, UK except where specified.

## 2.1 Preparation of standard solutions

### 2.1.1 Acrylamide gels

| Reagent | 6% | 7.5% | 10% |
|---|---|---|---|
| Running Gel Buffer | 3ml | 3ml | 3ml |
| Stock Acrylamide | 2.4ml | 3ml | 4ml |
| $dH_2O$ | 6.6ml | 6ml | 5ml |
| TEMED | 6µl | 6µl | 6µl |
| APS | 60µl | 60µl | 60µl |

### 2.1.2 APS (Ammonium Persulphate)

0.228g in 1ml deionised $H_2O$ ($dH_2O$).

### 2.1.3 Coumeric Acid

11mg coumeric acid in 1ml dimethyl sulphoxide (DMSO).

### 2.1.4 DMEM F12 Media

DMEM F12 Ham's F-12 (1:1 MIX), 2x50ml foetal calf serum (FCS), 300µl gentomycin (5mg/ml), 40ml sodium bicarbonate (pH 7.6).

### 2.1.5 DTT

200mM DTT in 1ml $dH_2O$.

**2.1.6 Electrode Buffer**

6g tris-HCl, 28.8g glycine, 0.67g EDTA, 1g SDS in 1L $dH_2O$.(pH 8.8)

**2.1.7 Extracellular solution for patch-clamping**

130mM NaCl, 5mM KCl, 2mM $CaCl_2$, 30mM glucose, 25mM HEPES (pH 7.3, osmolarity 330).

**2.1.8 Extracellular solution for $Ca^{2+}$ permeability experiments**

**0.3mM $Ca^{2+}$ solution:** 100mM NaCl, 10mM HEPES, 10mM glucose, 80mM sucrose, 0.3mM $CaCl_2$. (pH 7.3 osmolarity ~310).

**30mM $Ca^{2+}$ solution:** 100mM NaCl, 10mM HEPES, 10mM glucose, 30mM $CaCl_2$ (pH 7.3 osmolarity ~310).

**2.1.9 Homogenisation buffer**

50mM tris-HCl, 5mM EDTA, 5mM EGTA, 320nM sucrose in 200ml $dH_2O$ (pH 7.4).

**2.1.10 Intracellular solution for patch-clamping**

140mM CsCl, 4mM $MgCl_2$, 10mM EGTA, 10mM HEPES (pH 7.3 with CsOH (pH 7.3 osmolarity 312).

**2.1.11 Intracellular solution for $Ca^{2+}$ permeability experiments**

140mM NaCl, 10mM HEPES, 1.1mM EGTA (pH 7.3 osmolarity ~290).

**2.1.12 Lowry assay reagents:**

**Reagent A:** 2% $Na_2CO_3$, 0.1M NaOH, 0.5% SDS in $dH_2O$.

**Reagent B:** 2% Sodium potassium tartrate in $dH_2O$.

**Reagent C:** 1% $CuSO_4$ in $dH_2O$.

**2.1.13 Luminol**

100mM tris-HCl, 22mg luminol in 100ml $dH_2O$ (pH 8.5).

**2.1.14 Lysis Buffer**

TBS, 2mM EDTA (pH 8), 1:100 protease inhibitor cocktail set III

**2.1.15 Phosphate buffered saline (PBS)**

8g NaCl, 0.2g KCl, 1.44g $Na_2HPO_4$, 0.24g $KH_2PO_4$ in 1L $dH_2O$ (pH 7.4).

**2.1.16 Radioligand Binding Assay buffer**

50mM tris-HCl, 5mM EDTA, 5mM EGTA in 500ml $dH_2O$ (pH 7.1).

**2.1.17 Radioligand Binding Wash buffer**

40mM $NaH_2PO_4$-NaOH in 1L $dH_2O$ (pH 7.4).

**2.1.18 Running gel buffer**

1.5M tris, 8mM EDTA, 0.4% SDS (pH 8.8).

**2.1.19 Sample buffer**

30mM sodium hydrogen phosphate, 30% (v/v) glycerol. 0.05% (v/v) bromophenol blue, 7.5% (w/v) SDS in $dH_2O$ (pH 7.0).

**2.1.20 Solubilisation buffer 1% sodium deoxycholate**

50mM tris, 1% (w/v) deoxycholic acid, 0.15M NaCl, 5mM EDTA. 5mM EGTA, 1mM phenylmethylsulphonyl fluoride, 1:100 Protease Inhibitor Cocktail III in $dH_2O$.

**2.1.21 Solubilisation buffer using sodium dodecyl sulphate**

50mM tris, various [SDS], 0.15M NaCl, 5mM EDTA, 5mM EGTA, 1mM phenylmethylsulphonyl fluoride, 1:100 protease inhibitor cocktail III.

**2.1.22 Stacking gel buffer**

0.5M tris, 8mM EDTA, 0.4% SDS in 100ml $dH_2O$ (pH 6.8)

**2.1.23 Stacking gel**

2.3ml $dH_2O$, 0.65ml acrylamide, 1ml stacking gel buffer, 5µl TEMED, 80µl ammonium persulphate (APS) (10%).

**2.1.24 Tris/EDTA (TE) buffer**

10mM tris, 1mM EDTA (pH 8.0) in $dH_2O$.

**2.1.25 Transfer buffer**

25mM tris, 192mM glycine, 20% (v/v) methanol in 1L$dH_2O$.

**2.1.26 Tris buffered saline (TBS)**

50mM tris-HCl, NaCl 0.9% in 1000ml $dH_2O$ (pH 7.4).

**2.1.27 Tyrodes Buffer for FLIPR**

145mM NaCl, 2.5mM KCl, 10mM HEPES, 10mM glucose, 1.5mM $CaCl_2$ (pH 7.3 Osmolarity ~320).

## 2.2 Methods

### 2.2.1 Glutaraldehyde method for conjugating peptides to carrier proteins.

Method as previously described by Stephenson and Duggan, 1991.

This procedure was used to conjugate the following rodent NR3B peptide (ISL, Paignton, UK) to thyroglobulin (carrier protein) through its amino terminal (N) residue.

NR3B Rodent Peptide T G P P E G Q Q E R A E Q E C –amide

Equal amounts (4mg) of peptide and carrier protein were dissolved in 2ml 0.1M $NaHCO_3$ buffer containing 0.5% (v/v) glutaraldehyde (freshly thawed). The peptide protein mixture was incubated in a glass tube for 16hrs at RT with vigorous mixing. 200µl of 1M glycine ethyl ester (pH 8) terminated the reaction. The peptide-protein conjugate was separated from the uncoupled peptide by dialysis against PBS for 4hrs at 4°C (4x500ml), diluted to a final concentration of 1mg/ml and stored in 100µl aliquots at -20°C.

### 2.2.2 The 3-Maleimimdobenzoic acid N-hydroxysuccinimide (MBS) method of conjugating peptides to carrier proteins (cysteine coupling).

Method as previously described by Stephenson and Duggan, 1991.

This procedure was used to conjugate the following human NR3B peptide (ISL, Paignton, UK) to thyroglobulin through its amino-terminal cysteine residue.

NR3B Human C T G P P E G S K E E T A E A E-amide

4mg of thyroglobulin were dissolved in $KH_2PO_4$ buffer (pH 7.2) containing 10mM $Na_2HPO_4$ to a final concentration of 20mg/ml and the solution dialyzed overnight against 500ml 10mM $KH_2PO_4$ buffer containing 10mM $Na_2HPO_4$ (pH 7.2) at 4°C. 50µl of 10mM $KH_2PO_4$ buffer (pH 7.2) containing 10mM $Na_2HPO_4$ was added to 4mg (200µl) of dialysed carrier protein, which was then activated by addition of 85µl stock MBS (3mg/ml of diamethylformanide). This mixture was then incubated at RT for 30mins on an orbital shaker.

The activated carrier protein was separated from free MBS by dialysis against 50mM $KH_2PO_4$ buffer (pH6), containing 50mM $Na_2HPO_4$ for 2hrs at RT (2x 1litre changes).

1ml of 4mg/ml peptide, dissolved in 10mM $KH_2PO_4$, pH 7.2, containing 10mM $Na_2HPO_4$ was added to the dialysed activated carrier protein and incubated overnight at RT with gentle mixing. The peptide conjugate was separated from the uncoupled peptide by dialysis against PBS for a total of 4hrs at 4°C (4x500ml changes).

The dialysed peptide-protein conjugate was diluted with PBS to a final concentration of 1mg/ml and stored in 100µl aliquots at -20°C.

### 2.2.3 Inoculation procedure.

200µl of sterile PBS was mixed with 100µg (100µl) of freshly thawed peptide-conjugated carrier protein. This mixture was then emulsified with an equal volume (300µl) of Freunds complete adjuvant. This was mixed thoroughly using a wide bore syringe, until a viscous emulsion was obtained.

The preparation was then injected intramuscularly into both hind legs of a New Zealand rabbit. Primary immunization was performed with Freunds complete adjuvant, whereas subsequent immunizations, at 1 month intervals, were performed with incomplete Freunds adjuvant.

Rabbits were bled from the marginal ear vein 7-10 days post-booster injections, where 10-15ml of blood was collected. The blood was allowed to stand at RT for 2hrs followed by clot contraction for 16hrs at 4°C. The cellular material was removed by centrifugation at 12000xg for 10mins at 4°C and the serum stored in 1ml aliquots at -20°C.

### 2.2.4 Generation of an NR3B peptide affinity column.

The use of a peptide-carrier protein conjugate necessitates the affinity purification of the anti-peptide antibodies from the antiserum in order to remove non-specific binding from the anti-carrier protein antibodies.

The synthesis of the peptide affinity columns is described by Stephenson and Duggen (1991) and was carried out using an Immunopure rProtein A IgG Orientation Kit (Pierce, UK).

0.3g of activated CH-sepharose was incubated in 100ml water at RT for 15minutes to swell, before being applied to a 25ml column and washed under gravity with 100ml HCl (1mM) at 4°C. The sepharose was then equilibrated with 25ml 0.1M $NaHCO_3$ (pH 8.0) containing 0.3M NaCl and transferred to a capped tube in 1ml of equilibration buffer. 1ml of 5mg/ml of the respective peptide was dissolved in equilibration buffer and incubated with the sepharose beads for 1hr at RT with gentle mixing.

25ml wash with equilibration buffer terminated the reaction and all the remaining active sites were blocked by incubation with 3ml 0.1M Tris-HCl (pH 8.0) containing 0.5M NaCl for 1 hr at RT with gentle mixing. The sepharose beads were then washed alternately with 4x 0.1M $CH_3COOH$ (acetic acid pH 4.0), containing 0.5M NaCl and 0.1M Tris-HCl (pH 8.0) containing 0.5M NaCl.

The column was then equilibrated and washed with 20ml PBS and stored in 10ml PBS containing 0.02% $NaN_3$ at $4^0$C until use.

### 2.2.5 Immunopurification of anti-NR3B using an NR3B peptide affinity column

The NR3B peptide column was washed with 100ml TBS before application of 5ml of serum. The column was batch mixed for 2 hrs at room temperature and then the unbound serum was collected and retained. The column was then washed under gravity with 100ml of TBS. The anti-NR3B antibody was then eluted in 1ml fractions using 50mM glycine pH 2.3 and immediately neutralized with15µl of 2M Tris. Eight fractions in total were collected.

The absorbance of each fraction was measured at 280nm using a Jenway Genova spectrophotometer and the peak fractions containing the antibody were pooled and

dialyzed overnight in 300ml TBS. The dialysate was collected and the optical density (OD) was measured at 280nm. The absorbance value was divided by 1.35, to give the concentration in mg/ml. 0.02% $NaN_3$ was then added to the purified antibody as a preservative and stored in the fridge at 4°C. The column was then washed and stored in TBS containing 0.02% $NaN_3$.

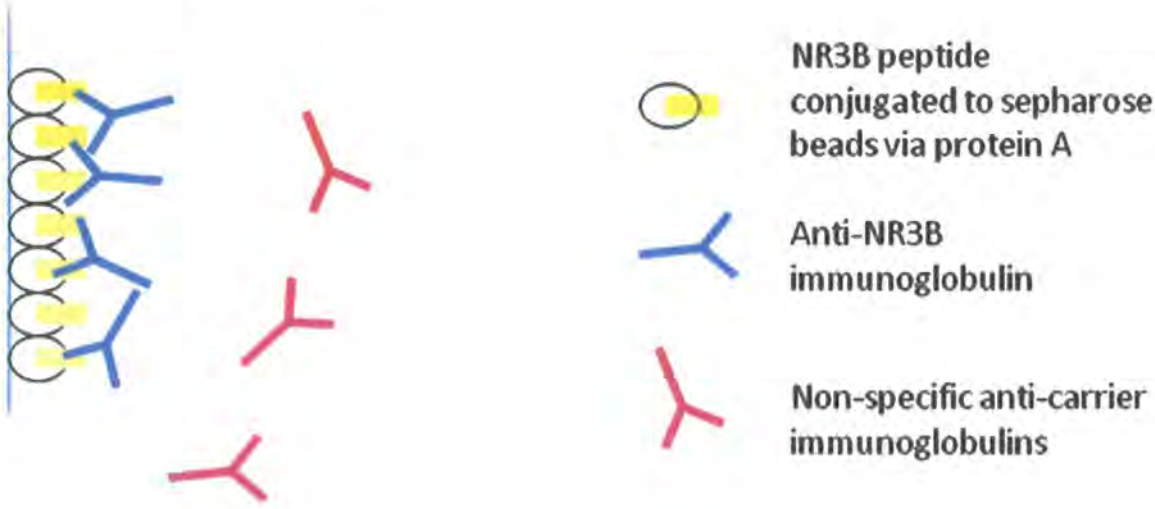


**Figure 2.1 Schematic diagram showing anti-NR3B purification via specific NR3B peptide-affinity. The specific anti-NR3B antibodies bind to the peptide conjugated to the column and are eluted. The non-peptide specific antibodies are washed away.**

### 2.2.6 Homogenised membrane preparation

All animal studies were performed with full ethical and Home Office approval (Project licence PPL-6003437).

Adult male Sprague-Dawley Rat forebrains (whole brain minus the cerebellum) or spinal cords (cervical, thoracic and/or lumbar regions) were homogenized.

2ml of cold homogenization buffer (solutions 2.1.9) was used to homogenize each brain or spinal cord using a Dounce glass homogenizer. All the homogenized tissue was placed into JA20 centrifuge tubes and centrifuged at 2200rpm, 4°C for 10 minutes.

Following removal of the supernatant, the pellet was re-suspended in homogenization buffer, and the previous two steps repeated. The supernatant was removed and pooled together in a clean JA20 centrifuge tube. The supernatants were centrifuged at 15000rpm at 4°C for 30 minutes.

The supernatant was then discarded and the pellet re-suspended in homogenization buffer.

The amount of buffer in which to re-suspend the pellet was calculated as follows: The initial weight of the tissue x 5ml =11.6g x 5ml buffer = 58ml.

The re-suspended pellet was gently homogenized to a smooth mixture, aliquoted and frozen at -20°C.

### 2.2.7 Lowry Assay to determine protein concentration

The reagents A, B, C and D (solutions 2.2.12) required for the assay were prepared, with a 1mg/ml stock of bovine serum albumin (BSA).

A series of standard solutions were prepared as follows:

| [BSA] mg/ml | Vol. BSA (µl) | Vol. $dH_2O$ (µl) |
|---|---|---|
| 0 | 0 | 100 |
| 20 | 20 | 80 |
| 40 | 40 | 60 |
| 60 | 60 | 40 |
| 80 | 80 | 20 |
| 100 | 100 | 0 |

**Table 2.1 Preparation of standard solutions for Lowry assay.**

Each concentration of BSA and a series of test protein (5 µl protein +95µl $dH_2O$) were made up in triplicate and vortexed.

0.5ml of reagent D was added to each tube, vortexed and left to stand at RT for 10mins. 50µl of Folin:$dH_2O$ was then added to each tube, vortexed and left to stand at RT for 30 minutes. Addition of 0.5ml $dH_2O$ terminated the reaction. The absorbance at 750nm was then measured and analysed. A standard curve of absorbance against concentration was plotted and the concentrations of the samples being assayed calculated.

### 2.2.8 SDS-PAGE and Western blotting

#### 2.2.8.1 Preparation of the samples:

5-10µl of rat forebrain or spinal cord preparation, 5µl of sample buffer (3x), 2µl DTT (3mg/ml) (10x) and 8µl $dH_2O$.

The samples were then pulsed at 6000rpm and placed in a 95°C heat block for 5 minutes to denature the proteins. They were then pulsed again at 6000rpm, vortexed, and loaded into the wells using a Hamilton page loader.

#### 2.2.8.2 SDS-PAGE:

The stacking gel was prepared (solutions 2.1.22), excess water drained and the stacking gel quickly poured, with the comb set in place. 10-15 minutes was allowed for the stacking gel to set, before rinsing again with water. The tank was then filled with electrode buffer (solutions 2.1.6) and the samples loaded. The gel was then run at 10mA, 180V for 30 minutes before increasing the current to 15mA for 1.5-2hrs.

**2.2.8.3 Western blotting-Transfer**:

Hybond nitrocellulose membrane (Amersham International, Buckinghamshire, UK) was soaked in transfer buffer for 10 minutes prior to the transfer. The transfer system was built up on the white side of the cassette as follows; sponge, 2 pieces of blotting paper (Amersham International, Buckinghamshire, UK), nitrocellulose (Amersham International, Buckinghamshire, UK), gel, 2 pieces of blotting paper, sponge. The cassette was placed into transfer buffer (solutions 2.1.25) and transfer started at 50V, 220mA for 2.5 hours.

**2.2.8.4 Incubating the nitrocellulose**:

The nitrocellulose was removed from the transfer tank and blocked to inhibit any endogenous reactive sites with 5% marvel (w/w), 0.2% Tween 20 (w/v) in TBS and 50µl 2M NaOH, for 1 hr at RT.

The nitrocellulose was incubated in primary antibody against the protein of interest at varying concentrations. 2.5% (w/w) marvel in TBS buffer + 1°Ab (0.5-2µg/ml) overnight at 4°C.

Unbound primary antibody was washed (4x10 min) with 2.5% marvel (w/w), 0.2% Tween 20 (w/v) in TBS. The nitrocellulose was then incubated in secondary (2°) anti-rabbit horseradish-peroxidase linked antibody (Amersham International, Buckinghamshire, UK) (1:2000 dilution) for 1hr at RT.

The 2 °antibody was washed (4x10 min) with 2.5% marvel (w/w), 0.2% Tween 20 (w/v) in TBS, followed by rinsing in TBS.

**2.2.8.5 Developing the nitrocellulose:**

In order to visualize the proteins on the blot the nitrocellulose was exposed to 6µl $H_2O_2$, 10ml luminol (solutions 2.1.13) and 100µl coumaric acid (solutions 2.1.3) in order to complete the enzyme (2° antibody) -substrate ($H_2O_2$) reaction at RT for 1 minute. The blot was covered with clingfilm, taped inside the cassette and then exposed to the film. Following 1-5 minutes of exposure (antibody dependent) the film was removed and placed in Polymax RT developer and replenisher and Polymax RT fixer and replenisher (Kodak Professional, UK) and water.

**2.2.9 Cryostat sectioning of rat spinal cord and whole brain.**

**2.2.9.1 Frozen preparations**

Whole spinal cords and brains were dissected from adult male Sprague-Dawley rats weighing approximately 270g and immediately frozen on dry ice and stored at -20$^0$C until sectioning.

The frozen tissue was orientated and mounted onto a specimen block at -20$^0$C using Tissue-Tek$^{TM}$ adhesive and Cryofreeze aerosol (Agar Scientific). The cryostat was adjusted and maintained at -20$^0$C, with 20µm sections mounted directly onto poly-D-lysine coated microscope slides.

**2.2.9.2 Formaldehyde fixed preparations**

Whole spinal cords dissected from adult male Sprague-Dawley rats weighing approximately 270g, were fixed using 4% paraformaldehyde and stored at 4$^0$C. Three days prior to sectioning, the tissue was placed in10% sucrose solution for cryoprotection.

Immediately prior to sectioning, the fixed tissue was frozen in liquid nitrogen -70$^0$C for 1 minute in isopentane before being orientated and mounted onto a specimen block with Tissue-Tek$^{TM}$ adhesive and Cryofreeze aerosol (Agar Scientific). Transverse sections of the spinal cord were sliced at 20μm and stored in 1ml PBS in 24-well plates or mounted directly onto poly-D-lysine coated microscope slides.

**2.2.10 Immunohistochemistry on adult rat and human spinal cord.**

Tissue sections were either processed in 24-well plates (Iwaki, Japan) (with 0.5ml solution/well) or directly on the slides post-mounting (in coplin jars). The procedure was carried out at room temperature except where stated.

The procedure was carried out on approximately 20 spinal cord sections (20μm) each run, with variation of the primary antibody at concentrations ranging from 0.01-2μg/ml. The sections were incubated in 10% methanol, 3% hydrogen peroxide in 10ml TBS buffer for 10 minutes with shaking. 0.2% glycine, 0.2% Tween 20 in 50ml TBS buffer was then added to the wells for 15 minutes with shaking, followed by 0.2% Triton-X-100 in TBS for a further 15 minutes.

50mM sodium citrate pH8.4 was added to each well and incubated for 30 minutes at room temperature before being replaced by 50mM sodium citrate pH8.4 at 80°C for 30 minutes. A wash step in 0.2% Triton-X-100 in TBS followed for 15 minutes before a blocking step using 2% serum, 0.2% Tween 20 in TBS for 60 minutes incubation. Primary antibody (0.01-2μg/ml) in 1% serum in TBS was then added to the tissue for an overnight incubation at 4°C.

The tissue sections were then washed in 1% serum in TBS (3x0.5ml) followed by addition of secondary biotinylated antibody (0.1%) in 1% serum in TBS. The sections were washed in 1% serum in TBS (3x0.5ml). The vector ABC solution (made up 10 minutes prior to use) was then applied for 5 minutes with shaking before washing steps in TBS (5x0.5ml). Diaminobenzidine (DAB) developing solution (1 DAB tablet per 10ml TBS and 6µl hydrogen peroxide) was added to the wells for 10 minutes incubation in the dark. DAB was removed and the sections washed in $dH_2O$ before mounting onto plain microscope slides (0.8x1.0mm) for drying. Once the tissue was dry the coverslips were applied using DPX histological mountant.

**2.2.11 Optimised method for immunohistochemistry on adult rat spinal cord tissue.**

Tissue sections were either processed in 24-well plates (Iwaki, Japan) (with 0.5ml solution/well) or directly on the slides post mounting (in coplin jars). The procedure was carried out at room temperature except where stated.

Tissue was incubated with 10% methanol in PBS, with 3% $H_2O_2$ for 30 minutes before washing (3x 5minutes) with PBS-Triton-X-100 (PBS-T, 0.2%, v/v) pH 7.4. The tissue sections were then inbubated in PBS-glycine (0.2% w/v) pH 7.4 for 30 minutes to quench excess fixative before 1 hour incubation with blocking buffer (PBS-Triton plus 10% goat serum). The sections were then incubated in primary antibody (diluted in PBS+ 1% goat serum) overnight (concentrations ranging from 0.5-2µg/ml, depending on the antibody). The tissue sections were then thoroughly washed (3x5 minutes with PBS-triton X 100, before incubation for 2 hours with the appropriate biotinylated secondary antibody from the vecta-stain ABC kit (1 drop in 10ml PBS/1% serum). 30

minutes before the end of this incubation, the ABC solution was prepared (100µl solution A and 100µl solution B in 5ml PBS) and then applied to the tissue for an hour incubation. The tissue was then washed with PBS-TritonX100 (3x5minutes) and then with PBS (2x5minutes) before the developing steps using DAB developing kit for approximately 10 minutes or until staining occurs.

### 2.2.12 Solubilisation and immunopurification of NMDA receptors

#### 2.2.12.1 Solubilisation using 1% sodium deoxycholate (DOC)

Male Sprague-Dawley adult rat forebrain preparation (3mg/ml) or spinal cord (1.5mg/ml) was used for this assay.

6 x 1ml aliquots of homogenized membranes (3mg/ml) were centrifuged at 13000rpm for 3 minutes, the supernatant removed and discarded. The pellet was re-suspended in solubilisation buffer (solutions 2.1.20) to obtain a final concentration of 1.5mg of protein/ml. The samples were pooled together and the re-suspended mixture stirred batch wise at either 4 or 37°C for 1hour. Following this incubation, the samples were centrifuged at 10000g for 30minutes at 4°C. The supernatant containing the solubilised membranes was collected, and the pellet re-suspended in solubilisation buffer (detergent-treated membranes) - a sample of each was retained for blotting.

The solubilised membranes were then dialyzed against 2 x 1L of dialysis buffer for 1.5 hours each at 4°C. This dialyzed material then became the source of the NMDA receptors. The same procedure was also carried out at 37°C in order to investigate optimal solubilisation conditions.

### 2.2.12.2 Solubilisation using sodium dodecyl sulphate (SDS)

Male Sprague-Dawley adult rat forebrain preparation (3mg/ml) or spinal cord (1.5mg/ml) was used for this assay.

2x1ml (1.5mg/ml) aliquots of homogenized membranes were centrifuged at 13000rpm for 3 minutes and the supernatant discarded. The pellet was re-suspended in solubilisation buffer (solutions 2.1.21) to obtain a final concentration of 1.5mg protein/ml. This solubilisation/protein mixture was incubated at RT, 4 or 37°C for 3 minutes with shaking. 5 volumes of ice-cold Triton-x-100 were used to dilute the [SDS] and the mixture was centrifuged at 13000rpm for 10 minutes. The supernatant containing the solubilised receptors was removed and dialysed against 2x1L of dialysis buffer for 3hrs at 4°C. The unsolubilised fraction remaining in the pellet was resuspended in solubilisation buffer.

Following dialysis, the solubilised membranes were purified via an immunoaffinity column or via immunoprecipitation with anti-NR3B antibodies.

### 2.2.12.3 Immunopurification

The dialyzed solubilised material was then purified via an anti-NR1 immunoaffinity column. Purification is achieved as NR1-containing receptors covalently couple to the anti-NR1 column, which is then washed and the receptors eluted. The solubilised receptors were incubated on the column for 20 hours at 4°C, using a peristaltic pump for constant circulation at a rate of 10ml/hr. Following incubation, any unbound receptors were drained from the column and retained to calculate uptake efficiency and the column washed with 50ml wash buffer.

The NMDA receptors were eluted using glycine pH 2.3. 8x1ml fractions were collected and neutralized with 2M tris to a final pH 7.4. In order to identify the receptor-containing fractions, immunoblotting was carried out using anti-NR1, anti-NR2A, anti-NR2B and anti-NR3B antibodies.

The same procedure was also carried out using an anti-NR2A column in order to isolate NR2A-containing receptors.

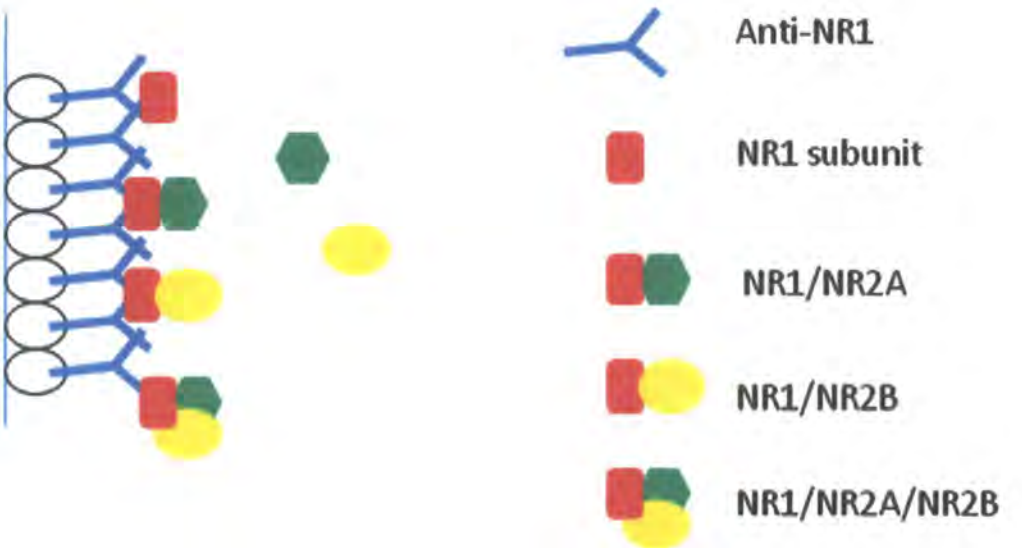


**Figure 2.2 Schematic diagram showing immunopurification of NR1-containing receptors from detergent-solubilised material. Only those receptor complexes containing NR1 subunits will bind to the specific anti-NR1 antibodies and be purified. The monomeric non-functional NR2A and NR2B subunits are washed away.**

**2.2.12.4 Immunoprecipitation using Seize X Protein A Immunoprecipitation Kit (Pierce, Rockford, IL 61105).**

Following the manufacturers instructions, 200µg of rat anti-NR3B antibody was cross-linked with DSS (disuccinimidyl suberate) to Immunopure® Immobilized Protein A before antigen precipitation.

Adult male Sprague-Dawley rat spinal cord homogenate (1.5mg/ml) was solubilised with 0.5% sodium deoxycholate (see 2.2.12.1) before solubilised membranes were applied to the immobilized antibody for either 4 hours or 16 hours incubation at $4^0$C. Immunoprecipitated receptors were then eluted from the column using ImmunoPure® Elution Buffer and the fractions analyzed using SDS-PAGE.

**2.2.13 Chloroform/Methanol Procedure for protein precipitation**

50µl of sample were made up to 100µl with $dH_2O$, to which 4xvolume (4x100µl) methanol was added. The samples were vortexed and pulsed up to 13000rpm. 100µl of chloroform was added, after which the samples were again pulsed at 13000rpm. 300µl $dH_2O$ was added and the samples centrifuged for 1 minute at 13000rpm.

The top layer of the sample was removed ensuring no disturbance to the intermediate phase (containing the protein).

100µl of methanol was again added, and the samples vortexed and centrifuged for 4 minutes at 13000rpm. The supernatant was removed and the pellet allowed to air dry for 30 minutes at RT before dissolving in sample buffer and loading for SDS-PAGE analysis.

### 2.2.14 Radioligand Binding

#### 2.2.14.1 Competition Binding

Competitive binding experiments measure the binding of a single concentration of radioligand in the presence of various concentrations of unlabelled ligand (Motulsky 1995) to determine the affinity of unlabelled ligands for receptors.

During the experiment, both radiolabelled and unlabelled compounds compete for the available receptor binding sites providing a measurement of compound affinities. Once an equilibrated state of reaction has been attained, the amount of radiolabelled ligand bound to the receptor was measured following separation from the free, unbound radiolabelled ligand via filtration. The affinity of the unlabelled compound was then measured indirectly via its ability to compete with and displace the radiolabelled ligand. The parameters obtained are the concentration of unlabelled compound that inhibits the binding of the radiolabelled ligand by 50% ($IC_{50}$) and subsequently the dissociation constant for the unlabelled compound ($K_i$).

During binding experiments it is possible for the compounds to bind to non-specific sites distinct from the site of interest. It is therefore important to measure non-specific binding in the presence of a high concentration of unlabelled compound, that binds to all receptor sites of interest and subtract this value from the total binding to give specific binding.

1mM ifenprodil was used to define non-specific binding for [$^3$H] CP-101,606 and [$^3$H] Ro-256981 assays and 1mM ketamine defined non-specific binding in [$^3$H] MK-801 assays. All assays were also carried out in the presence of DTG (10μM), a sigma-site antagonist to avoid non-specific binding, particularly in rat forebrain tissue.

A series of dilutions ($10^{-3}$ -$10^{-10}$ M) of the compound to be analyzed was prepared from a 10mM ($10^{-2}$ M) stock solution of compound dissolved in either 50mM Tris-HCL, 5mM EDTA and 5mM EGTA (pH 7.1) or DMSO depending on the compound.

Adult male Sprague-Dawley rat homogenized forebrain was used as the source of NMDA receptors at a concentration of 1mg/ml. (For recombinant receptors the forebrain is replaced with harvested recombinant NMDA receptors expressed in HEK293 cells).

[$^3$H] Ro-256981, [$^3$H] CP-101606 and [$^3$H] MK-801 were utilized as radioligands in order to compare the pharmacology of both compounds COMPOUND A and COMPOUND B (GlaxoSmithKline, Harlow, UK). Addition of 1mM DTG (a sigma site antagonist) to the assay prevented non-specific binding to sigma sites.

The scintillation tubes were set up as follows with a total of 200µl/tube.

| | Protein (1mg/ml) | Compound ($10^{-3}$ to $10^{-9}$) | Radioligand | Assay buffer | DTG (1mM) |
|---|---|---|---|---|---|
| **Total** | 100µl | - | 20µl | 60µl | 20µl |
| **Compound** | 100µl | 20µl | 20µl | 40µl | 20µl |
| **Non-Specific** | 100µl | 20µl | 20µl | 40µl | 20µl |

**Table 2.2 Preparation of scintillation tubes for competition radioligand binding assays.**

Following incubation on ice for 2hrs, the reaction was terminated and bound radioligand washed with ice-cold 10mM sodium phosphate buffer and collected by rapid filtration through Whatman GF/B filters (Semat International, UK) using a Brandle Harvester. The filters were then collected and immersed in Ecoscint A liquid scintillation fluid (National Diagnostics, UK) overnight at RT before quantification using Packard tri-Carb 1600TR spectrophotometer. The data was analyzed using GraphPad Prism version 4.0

to plot competition experiments as a one-site or two-site sigmoidal dose response curve with a variable slope.

From these experiments the concentration of unlabelled ligand that inhibits the binding of the radioactive compound by 50% is the $IC_{50}$ value, calculated as follows:

For a one-site binding competition model:

$$y = \text{Nonspecific} + \frac{(\text{Total-Nonspecific})}{1+10^{(log\,[D] - \log(IC50)}}$$

For a two-site binding competition model:

$$y = \text{Nonspecific} + \frac{\text{Total-Nonspecific}}{\left(\frac{\text{Fraction 1}}{1+10^{(x-\log IC_{50}\,1)}}\right)}$$

$y$ = the specific binding at a fixed concentration of displacing drug

$x$ = $\log_{10}$ concentration of the displacer

log[D] =logarithm of concentration of unlabelled drug on $x$- axis

Fraction 1 = The fraction of binding to the first type of receptor

From the $IC_{50}$ values, the inhibition constants ($K_i$) for the unlabelled ligand were calculated using the Cheng and Prusoff equation (Cheng and Prusoff, 1973; Deupree and Bylund).

$$Ki = \frac{IC_{50}}{1+\frac{[\text{radioligand}]}{K_d}}$$

$B_{max}$ can be calculated by the law of mass action

where: $B_{max} = B_0 (K_d + [L] )/ [L]$

$IC_{50}$ = concentration of unlabelled ligand that inhibits 50% binding of radiolabeled ligand

$K_d$ = the affinity of the radiolabelled ligand for the receptor

$B_0$ = the specific binding of the radioligand.

### 2.2.14.2 Saturation Binding

Saturation binding experiments were performed to determine the affinity ($K_d$) of a specific radioligand for a receptor and the density of receptor sites in a preparation ($B_{max}$) (Deupree and Bylund).

Adult male Sprague-Dawley rat forebrain homogenate (1mg/ml) was again used as the source of NMDA receptors. A concentration range (0-30nM) of [$^3$H] Ro-256981 or [$^3$H] CP-101,606 was prepared with 10mM sodium phosphate buffer and incubated with 100µl forebrain homogenate (200µl total) for 2 hours on ice. Bound radioligand was then washed and collected via rapid filtration and quantified (see 2.2.14.1).

Saturation binding experiments were also analyzed using GraphPad Prism version 4.

The affinity ($K_d$) of the radiolabelled compound for the receptor was calculated as follows:

$$y = \frac{B_{max}\, x}{K_d + x}$$

Where:

$y$ = specifically bound radiolabelled compound

$x$ = concentration of radiolabelled compound

$B_{max}$ = density of receptor sites

### 2.2.15 Plasmid DNA preparation

#### 2.2.15.1 Transformation of HB101 competent *E.coli* cells

This method is essentially as previously described by Dagert and Ehrlich (1979).

A 100µl aliquot of frozen HB101 competent cells (Promega Ltd, UK) was thawed on ice for 5 minutes. 20ng/µl of plasmid DNA to amplify was added to the competent cells and mixed gently. This cell mixture was then incubated on ice for 30 minutes before heat shocking the cells at 42°C for 1 min. The cells were incubated on ice for a further 2 minutes, followed by addition of 900µl LB broth (47g broth in 1L $dH_2O$) to the transformed cells. This mixture was then incubated for an hour on a shaker at 37°C.

100µl of the cell suspension was spread onto previously prepared culture plates containing 1.5% (w/v) agar in LB broth containing ampicillin (50µg/ml). The culture plates were then incubated at 37°C for 18-20 hrs in an inverted position to prevent the build-up of condensation.

#### 2.2.15.2 Preparing glycerol stocks of transformed competent *E.Coli* cells

500µl of terrific broth supplemented with 50% (v/v) sterile glycerol and 50µg/ml ampicillin to 500µl of the small overnight culture. Aliquots were then stored at -80°C in cryogenic vials until use.

#### 2.2.15.3 Amplification and preparation of plasmid DNA

$B_{max}$ = density of receptor sites

### 2.2.15 Plasmid DNA preparation

#### 2.2.15.1 Transformation of HB101 competent *E.coli* cells

This method is essentially as previously described by Dagert and Ehrlich (1979).

A 100µl aliquot of frozen HB101 competent cells (Promega Ltd, UK) was thawed on ice for 5 minutes. 20ng/µl of plasmid DNA to amplify was added to the competent cells and mixed gently. This cell mixture was then incubated on ice for 30 minutes before heat shocking the cells at 42°C for 1 min. The cells were incubated on ice for a further 2 minutes, followed by addition of 900µl LB broth (47g broth in 1L $dH_2O$) to the transformed cells. This mixture was then incubated for an hour on a shaker at 37°C.

100µl of the cell suspension was spread onto previously prepared culture plates containing 1.5% (w/v) agar in LB broth containing ampicillin (50µg/ml). The culture plates were then incubated at 37°C for 18-20 hrs in an inverted position to prevent the build-up of condensation.

#### 2.2.15.2 Preparing glycerol stocks of transformed competent *E.Coli* cells

500µl of terrific broth supplemented with 50% (v/v) sterile glycerol and 50µg/ml ampicillin to 500µl of the small overnight culture. Aliquots were then stored at -80°C in cryogenic vials until use.

#### 2.2.15.3 Amplification and preparation of plasmid DNA

Preparation of small-scale culture of plasmid DNA.

10ml of terrific broth containing ampicillin (50μg/ml) was inoculated with one isolated colony from the culture plates using a sterile loop and incubated for 18-20hrs on a shaker at 37°C.

Preparation of large-scale culture of plasmid DNA.

3mls of the small overnight culture were used to inoculate 500ml of terrific broth containing ampicillin (50μg/ml). This large culture was then incubated for 18-20hrs on a shaker at 37°C.

**2.2.15.4 Harvesting the large-scale culture and purification of plasmid DNA using the Qiagen plasmid maxi-kit** (Qiagen, Crawley, West Sussex, UK).

To harvest the transformed *E.coli* cells, the large-scale overnight culture was transferred into two ice-cold centrifuge tubes, and spun at 6500xg for 10 minutes at 4°C. The supernatant was discarded, and the remaining pellet re-suspended in ice-cold P1 buffer (10ml).

In order to lyse the bacteria containing the plasmid, 10ml of P2 buffer was added and mixed by gentle inversion, before incubation at RT for 5minutes. The mixture was neutralized with chilled P3 buffer (10ml) and mixed with gentle inversion before incubating on ice for 20 minutes. This solution was centrifuged at 14000xg for 30 minutes at 4°C, before the clear lysate was transferred to a clean tube.

During centrifugation, a Qiagen 500 tip was equilibrated with QBT buffer (10ml). The cell lysate was poured into the column and allowed to pass through under gravity flow.

The column was washed twice with QC buffer (30ml) and the plasmid DNA eluted using 15ml QF buffer. 10.5ml of ice-cold isopropanol (0.7 vol) was used to elute the DNA, and the solution centrifuged again at 14000g for 30 minutes at 4°C. The remaining pellet was washed carefully with ice-cold ethanol (1ml) and allowed to air dry for approximately 30 minutes. The purified DNA was dissolved in 500µl TE buffer (solutions 2.1.24) and stored at 4°C until the purity of the DNA was calculated.

**2.2.15.5 Quantification and determination of purity of the DNA yield**

The purity and the concentration of the plasmid DNA was determined by measuring the optical density at λ 260nm and λ 280nm. The ratio of the optical densities at these two wavelengths was determined. ($OD_{\lambda}$ 260 nm / $OD_{\lambda}$ 280 nm) should be within the range 1.8-2.0.

The plasmid DNA concentration is at λ 260 nm. Therefore this absorbance relating to plasmid DNA concentration was multiplied by 50 as an OD of 1 corresponds to approximately 50µg/ml for dsDNA. After calculating the plasmid DNA concentration in µg/µl, the final concentration was diluted to 1µg/µl in TE buffer. The plasmid DNA was then stored in 100µl aliquots at -20°C until use.

Once thawed, the DNA was stored at 4°C to prevent freeze/thaw denaturation.

**2.2.16 Preparation of tissue culture medium**

The tissue culture medium was prepared using 500ml Gibco DMEM F12 (1:1) (Cambrex Bio Science Verviers, Belgium) plus glutamate, 20ml sodium bicarbonate, 50ml foetal calf serum and 10ml penicillin/streptomycin solution. The pH was adjusted to pH 7.6 before being filter sterilized (Nalgene$^{TM}$ 500ml filter unit).

### 2.2.17 Sub-culturing HEK293 cells.

The culture media was aspirated and the cells washed with 10ml PBS. 2ml trypsin/EDTA was added, the flask tapped and replaced in the incubator for approximately 30 seconds to remove cells. 10ml of pre-warmed new media was then added to the cells and the suspension titrated thoroughly to prevent aggregation. 2ml of this suspension was then seeded into each new flask or culture dish.

For cell counting, the cell suspension was first centrifuged at 200g/5 min and the cell pellet resuspended in 10ml pre-warmed media. 1ml of the resuspended cell mixture was then used to count number of cells/ml.

### 2.2.18 Transfection of HEK293 cells using lipofectamine reagent

Transfections were carried out in 35mm culture dishes for western blotting, cytotoxicity assay and in 25cm$^2$ culture flasks for radioligand binding.

cDNA mixtures were prepared in ratios of 1:3 e.g, NR1:NR1/2B or 1:3:3 NR1/NR1/2B:NR1/2B/3B.

The transfection reagents were prepared as follows.

| | Tube 1 | Tube 2 |
|---|---|---|
| **Culture dishes** | 6µl PLUS reagent | 5µl Lipofectamine |
| | 1µg Plasmid cDNA | 150µl Optimem-I media |
| | 150µl Optimem-I media | |
| **Culture Flasks** | 30µl PLUS reagent | 25µl Lipofectamine |
| | 5µg Plasmid cDNA | 750µl Optimem-I media |
| | 750µl Optimem-I media | |

**Table 2.3 Preparation of transfection reagents**

Following a15minutes incubation at RT, the contents of the lipofectamine tube 2, were transferred into tube 1 and incubated for a further 15 minutes at RT.

During the second 15 minute incubation, the HEK293 cells were washed (3x 2ml for dishes) (3x10ml for flasks) with Optimem-I medium. The contents of the remaining tubes were diluted with 2ml (35mm dishes) or 10ml (25cm$^2$ flasks) with Optimem-I medium, and added gently to the washed HEK293 cells. The cells were incubated in the transfection medium for 5 hrs (5% $CO_2$, 37°C). Following this incubation, the optimem-I medium containing the plasmid DNA was replaced with the usual tissue culture growth medium (sections 2.2.16) and incubated for 48 hrs (5% $CO_2$, 37$^0$C) before harvesting. 1mM ketamine was added as an NMDA antagonist to those transfection mixtures which would be used in functional studies, to prevent cytotoxicity.

The above method was adapted for transfections for electrophysiology and FLIPR assays as follows: cells were seeded onto poly-D-lysine coated coverslips in 35mm culture dishes to be transfected for electrophysiology and in T175 culture flasks for FLIPR assays. Lipofectamine 2000 reagent replaced Lipofectamine PLUS reagent and incubation times were adjusted according to the manufacturer's instructions.

#### 2.2.18.1 Harvesting transfected HEK293 cells

Each culture dish/flask was drained and the cells re-suspended in cold homogenization buffer (solutions 2.1.9) containing protease inhibitor cocktail III (Calbiochem) (1:100). The cells were scraped off the culture dish/flask and transferred to a glass-dounce homogenizer and homogenized for 30 strokes. The cell homogenate was then centrifuged at 13000 rpm for 5 minutes at 4°C. The supernatant was removed and the pellet re-suspended in homogenization buffer (1ml per dish, 5ml per flask) and homogenized again. The transfected cells were stored in 100µl aliquots at -20°C.

### 2.2.19 CytoTox 96 Non-radioactive Assay (Promega Ltd, UK).

1.5ml of media was removed from the cells and centrifuged for 2minutes at 13000rpm and the supernatant retained. This supernatant contains lactate dehydrogenase (LDH) released from the lysed cells. The pellet was re-suspended in 1ml PBS and placed on the cells in the culture dish. The dish was then frozen for 2hrs at -20°C. The cells were thawed, centrifuged again (2minutes, 13000rpm) and the supernatant retained, the contents of which was the total LDH.

A 1:10 and a 1:20 dilution of each of the supernatants were prepared for the assay. Tissue culture medium DMEM:F12 was used as calibrator for the assay, with each dilution measured in triplicate (undiluted supernatant, 1:10 and 1:20). 50µl of substrate mix (Cytotox$^{96}$ Promega) was added to each dilution before incubation for 30 minutes at RT in the dark. LDH was then quantified with absorbency readings at 490nm.

### 2.2.20 Whole-cell patch-clamp electrophysiology on recombinant NMDA receptors expressed in HEK293 cells.

HEK293 cells were passaged approximately every 3 days when cells were ~80% confluent. HEK293 cells were seeded onto poly-D-lysine coated coverslips in 35mm culture dishes 24hrs prior to transfection and incubated under normal conditions.

Recombinant NMDA receptors (NR1, NR1/NR2B and NR1/NR2B/NR3B) labelled with GFP (green fluorescent protein), were transiently expressed in WT HEK293 cells using an optimized Lipofectamine$^{TM}$ protocol as described previously (section 2.2.18). Following 24hr incubation in the presence of the NMDA antagonist ketamine (1mM), successfully transfected (GFP-positive) cells were chosen for electrophysiology.

Patch microelectrodes (GC120F-10 resistance 2-5MΩ) were fabricated on a Sutter instruments P-87 electrode puller (Sutter Instruments Company, Novato, CA) whilst extracellular (solutions 2.1.8) and intracellular (solutions 2.1.11) solutions were warmed to RT (20-24$^0$C) in a water bath. Solutions were set up to provide continual perfusion of the recording chamber with extracellular solution and alternating perfusion with the co-agonists (100µM Glutamate and 10µM Glycine) and antagonists (CP-101606 and Ro-

256981 10μM and 300nM) through a multi-channel automated fast-switching solution exchange system (SF-77B; Warner Instrument, Hamden, CT). All experiments were conducted in the absence of extracellular magnesium to avoid voltage blockade of the receptor channel.

HEK293 cells successfully transfected with NMDA receptor subunit combinations were identified using GFP and manipulated in the recording chamber into position beneath the perfusion barrels. The microelectrode was filled with intracellular solution and placed onto the head stage before being positioned onto the cell to make a seal. Whole-cell patch clamp recordings were carried out at RT in voltage-clamp mode using an Axopatch 200B amplifier, controlled via the pClamp8/pClamp9 software suite (Axon Instruments Inc., Union City, CA).

### 2.2.21 [$^3$H] Ro-256981 Autoradiography on rat spinal cord and whole brain

Essentially as described previously by Mutel *et al*, 1998.

Selected slides were removed from the freezer and allowed to equilibrate to room temperature. The slides were incubated 2x 10 minutes in Tris buffer (solutions 2.1.24) at RT followed by 1.5hr incubation in [$^3$H] Ro-256981 in Tris buffer (20nM). Slides were then washed in tris buffer (2x5minutes, 1x15 minutes) on ice. In order to define non-specific binding, two slides were incubated in [$^3$H] Ro-256981 (20nM) containing ifenprodil ($10^{-3}$M) for 1.5hrs on ice before repeating the washing steps detailed above. Following the washing steps, the slides were briefly dipped in ice-cold $dH_2O$ (1L) before air drying on the bench overnight.

The slides were then taped into a Kodak developing cassette with Amersham tritium hypersensitive film and stored for 5 weeks at RT, before fixing (Kodak GBX fixer and replenisher) and developing (Kodak GBX developer and replenisher) (Kodak Professional, UK).

The autoradiograms were analysed 'blind' using the ImageJ program, where [$^3$H] Ro-256981 binding density was measured and calculated from a tritium standard mini-scale (Amersham, UK), developed along-side the samples.

### 2.2.22 Fluorescence imaging plate reader (FLIPR).

The FLIPR assay enables measurement of changes in the concentration of free intracellular calcium using fluorophores which bind and react to calcium, emitting fluorescence in a concentration-dependent manner, when excited by an argon laser. This assay was used to measure the concentration of intracellular calcium in HEK293 cells expressing recombinant NMDA receptors.

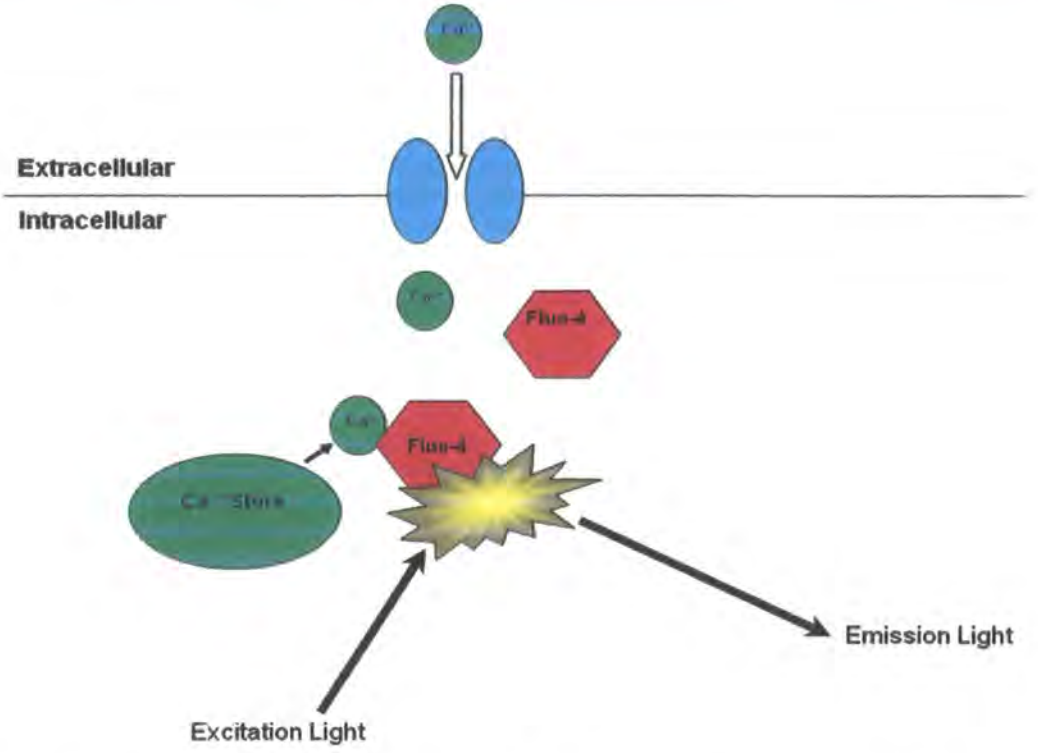


**Figure 2.3 Schematic diagram representing the induction of fluorescence when Fluo-4 reacts with calcium in cells. The influx of calcium via NMDA receptors and calcium released from intracellular stores contribute to the fluorescent signal detected by the FLIPR machine.**

48hrs prior to FLIPR assay, HEK293 cells were transfected as described previously (section 2.2.18) with NR1, 3B, NR1/2B and NR1/2B/3B subunits. 24hrs post-transfection, cells were removed from the culture flasks with trypsin/EDTA, centrifuged (200g/5minutes), re-suspended in pre-warmed fresh culture medium and counted. Approx 40000 cells/well were seeded onto Cornell™ black walled, clear bottomed poly-D-lysine coated 96-well plates as shown below and returned to the incubator for a further 24hrs.

| | 1 | 2 | 3 | 4 | 5 | 6 | 7 | 8 | 9 | 10 | 11 | 12 |
|---|---|---|---|---|---|---|---|---|---|---|---|---|
| **WT** | | | | | | | | | | | | |
| **NR1** | | | | | | | | | | | | |
| **NR1/2B** | | | ~40,000 cells/well | | | | | | | | | |
| **NR1/2B** | | | | | | | | | | | | |
| **NR1/2B** | | | | | | | | | | | | |
| **NR1/2B/3B** | | | | | | | | | | | | |
| **NR1/2B/3B** | | | | | | | | | | | | |
| **NR1/2B/3B** | | | | | | | | | | | | |

Prior to the assay the FLIPR system (Molcular Devices, UK) was switched on and allowed to equilibrate for 30minutes. The water system, CCD camera and the computer were initiated followed by the laser according to manufacturer's instructions and a yellow test plate signal generated and stored.

Dye loading of the cells:

An aliquot of Fluo 4 was thawed slowly and protected from direct light. The Fluo 4 was diluted to a final concentration of 1mM (equated to 60µl/10ml) in Tyrode's buffer (solutions 2.1.27) (without magnesium) and 50µl/well applied to the cell plate using a multi-channel pipette. Cells were then incubated at RT in the dark for 1-2hrs.

Following the dye loading, the cells were washed 4x150µl rinses with Tyrodes buffer using a Denley Cell washer system which leaves the cells in 125µl of fresh buffer after washing.

For agonist studies, 50µl of each agonist was added to the respective wells of the cell plate within the FLIPR system. Each agonist dose-response curve is made up of 12 half-log concentrations. Prior to agonist addition a single image of the cell plate is taken as a signal test. During the run 60 images were taken at 1 second intervals followed by a further 24 images at 5 second intervals with agonist addition being made 20 seconds after the first image was taken. Agonist induced receptor activation was therefore detected as an increase in fluorescence.

For antagonist studies, following the washing step, 25µl of antagonist was added to the respective wells of the cell plate and incubated for 20minutes at RT in the dark. As above, addition of the agonist was carried out in the FLIPR system and signals recorded with multiple time resolved images as previously described. Functional antagonism was indicated by a suppression of agonist induced increases in fluorescence.

The fluorescence measurements were extracted and tabulated using an ASCII text file and analysed using Microsoft Excel.

# Chapter 3

# Pharmacological characterisation of two novel NR2B-selective antagonists COMPOUND A and COMPOUND B

## 3.1 Introduction

NMDA receptors have been a potential therapeutic target for the treatment of neuropathologies since the 1980's when it was noted that application of NMDA antagonists attenuated glutamate induced toxicity in primary neurons (Choi *et al.*, 1988). Their widespread distribution, expression in disease related areas of the nervous system and potential for mediating toxic effects via over-activation, has led to focused research and interest in pharmaceutical intervention into NMDA receptor function.

Initially developed as universal non-selective channel-binding antagonists, compounds such as MK-801, Phencyclidine (PCP) and AP-5 showed an unacceptably high side-effect profile rendering them inappropriate for clinical use. Therefore the focus of research shifted to increasing the specificity and selectivity of receptor targeting, utilising the heterogeneous nature of the receptor.

Modulation of the receptor complex by the inclusion of the NR2B subunit has been specifically implicated in many disease pathologies including chronic pain, dementia, schizophrenia, stroke and neurodegenerative conditions (Chazot and Hawkins, 1999; Chazot, 2004). NR2B-containing receptors potentiate NMDA receptor activation and therefore antagonising them specifically may be therapeutically beneficial, whilst limiting the adverse side-effect profile.

The development of NR2B subunit selective compounds such as ifenprodil and its analogues eliprodil, CP-101606 and Ro-256981 have provided important research tools for the pharmacological characterisation of the NMDA receptor complex, which enhance the potential for increasing specificity of pharmaceutical intervention.

In 2005, McCauley reviewed the new patents and patent applications put forward in 2001-2004 for novel compounds developed as a result of new structural diversities in small molecule NR2B antagonists. Currently Gideon Richter have promising preclinical data for the novel compound RGH-96 (Bradford and Chazot, unpublished), which is entering phase IIa clinical trials for the treatment of neuropathic pain. Merck & Co and Pfizer have also disclosed new compounds showing that despite problematic side-effects, the targeting of NR2B-containing NMDA receptors remains a pharmaceutical focus.

This chapter will review and characterise the pharmacological profile of two novel NR2B-selective antagonists developed by GlaxoSmithKline; COMPOUND A and COMPOUND B. Radioligand binding assays (2.2.14) will be used to investigate the binding affinity of these compounds and propose potential binding sites of the ligands in native adult rat forebrain (2.2.6, 2.2.7) and recombinant receptor populations (2.2.15-18). The ifenprodil analogues CP-101606 and Ro-256981 and the channel blocker MK-801 will be utilised as radioligands for displacement assays and to compare the selectivity and binding kinetics of the novel drugs.

## 3.2 Results

### 3.2.1 Competition binding to investigate the displacement of [$^3$H] Ro-256981 by ifenprodil in adult Sprague-Dawley rat forebrain membranes.

Adult rat forebrain membranes (100µg protein/tube) were used as the source of native NMDA receptors in this experiment where ifenprodil displacement of [$^3$H] Ro-256981 was fitted to a 1-site sigmoidal variable slope model. This experiment acted as a control to demonstrate the effective displacement of the [$^3$H] Ro-256981 ligand by the batch of ifenprodil which would be used in subsequent experiments. A steep hillslope (-0.9) and sigmoidal curve with $K_i$ = 52 ± 1.0nM demonstrates high affinity displacement of [$^3$H] Ro-256981 by ifenprodil and therefore high affinity binding towards receptor sites. The data shown is the average ± SD of three individual experiments, each performed in triplicate.

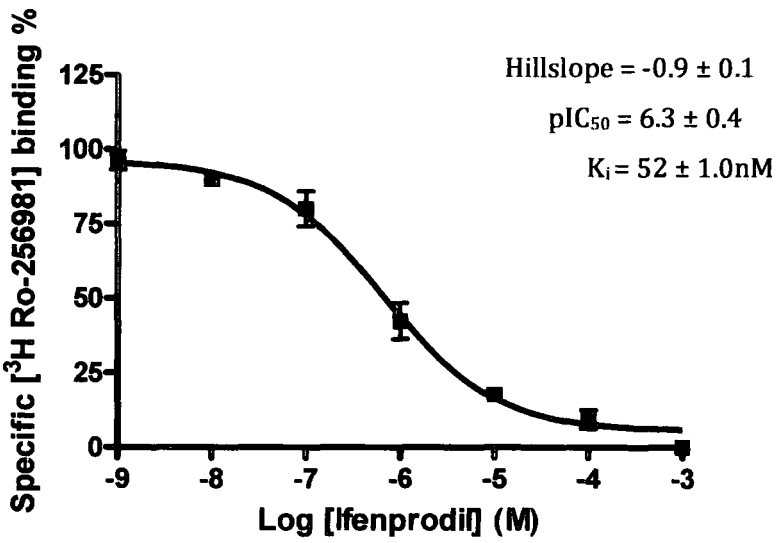


**Figure 3.1 Competition binding experiment showing ifenprodil displacement of [$^3$H] Ro-256981 in adult rat forebrain membranes, best fit to a one-site binding model. Non-specific binding was defined with ifenprodil (1mM).**

### 3.2.2 Competition binding to investigate displacement of [$^3$H] Ro-256981 with COMPOUND A in adult Sprague-Dawley rat forebrain.

Adult rat forebrain membranes (100μg protein/tube) were used as the source of native NMDA receptors in this competition assay with COMPOUND A [$10^{-3}$M-$10^{-10}$M]. Displacement of [$^3$H] Ro-256981 by COMPOUND A ($10^{-3}$-$10^{-10}$M) was fitted to a 1-site sigmoidal variable slope showing one low affinity binding site $pIC_{50}$ 4 ± 0.4 with a $K_i$ = 158 ± 14μM. The hillslope (-0.8) and low affinity binding may indicate heterogeneous receptor populations containing alternative NR2 subunits, to which COMPOUND A doesn't readily bind. Despite the presence of DTG, a sigma site antagonist, approximately 20% non-specific binding is evident.

The data shown are an average ± SD of three individual experiments each carried out in triplicate.

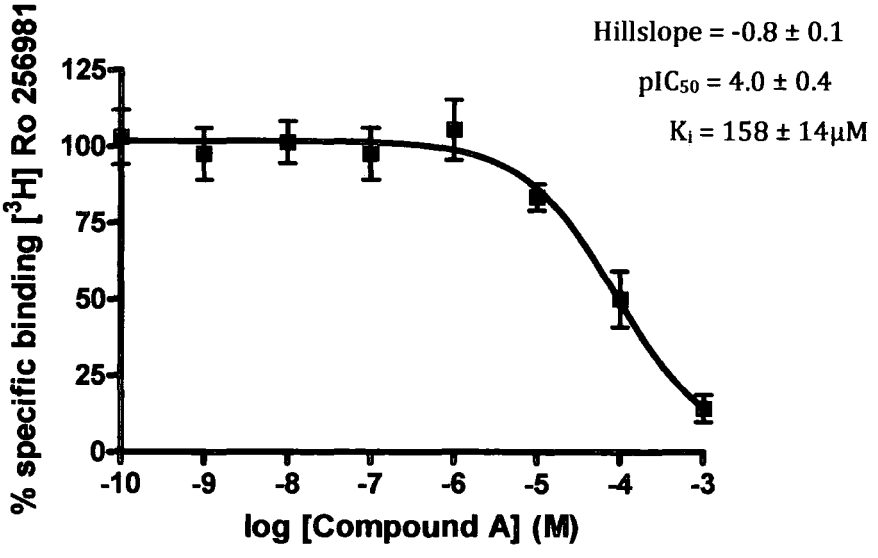


**Figure 3.2 Competition binding experiment showing one-site displacement of [$^3$H] Ro-256981 binding by COMPOUND A in adult rat forebrain membranes. Non-specific binding was defined with ifenprodil (1mM).**

### 3.2.3 Competition binding to investigate the displacement of [$^3$H] Ro-256981 with COMPOUND B, in adult Sprague-Dawley rat forebrain.

Adult male Sprague-Dawley rat forebrain membranes (100μg protein/tube) were used as the source of NMDA receptors in this competition assay with COMPOUND B [$10^{-3}$M-$10^{-10}$M]. The COMPOUND B displacement curve of [$^3$H] Ro-256981 binding was best fitted to a one-site binding model with low affinity binding ($K_i$ = 180 ± 7μM). Again this low affinity binding may indicate that [$^3$H] Ro-256981 is binding to alternative sites within the native tissue, to which COMPOUND B is largely insensitive. The data presented are an average ± SD of three individual experiments, each performed in triplicate. Again, despite the presence of DTG, a sigma site antagonist, approximately 20% insensitive binding is evident. These experiments were performed with three different batches of radioligand (from different sources) and produced consistent results (not shown).

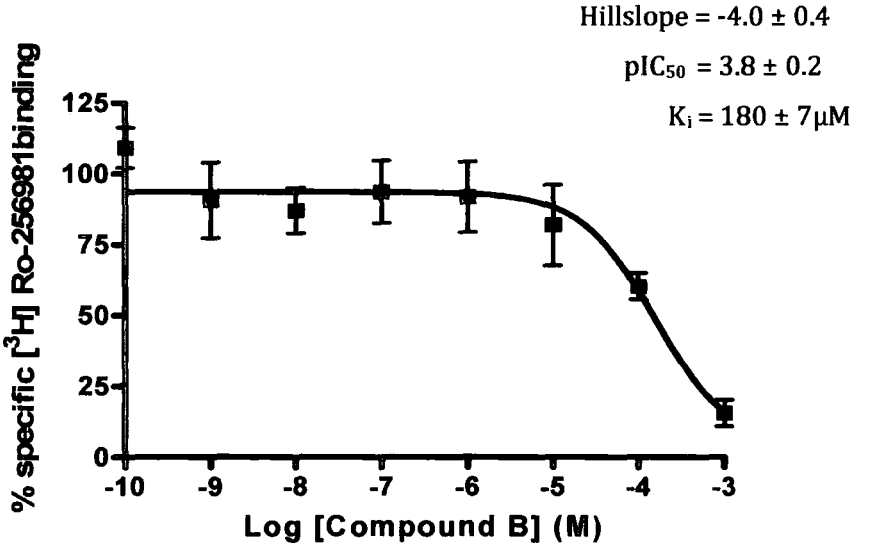


**Figure 3.3 Competition binding experiment showing one-site displacement of [$^3$H] Ro-256981 binding by COMPOUND B in adult rat forebrain membranes. Non-specific binding was defined with ifenprodil (1mM).**

### 3.2.4 Competition assay investigating the displacement of [$^3$H] CP-101606 binding by COMPOUND A in adult rat forebrain membranes.

Adult male Sprague-Dawley rat forebrain membranes (100µg protein/tube) were the source of NMDA receptors in this competition assay investigating COMPOUND A [$10^{-3}$M-$10^{-10}$M].

The high affinity ($K_i$ = 6 ± 2nM) displacement of [$^3$H] CP-101606 binding by COMPOUND A was fitted to a one-site variable sigmoidal curve model and shows that this novel compound displays high affinity binding towards NMDA receptors composed of only NR1/NR2B subunits. There is some evidence for low affinity binding to a second site at high concentrations of COMPOUND A, which may be other NMDA receptor populations, or alternative, non-sigma receptor sites present in the native tissue. The data shown are an average ± SD of two individual experiments each carried out in triplicate.

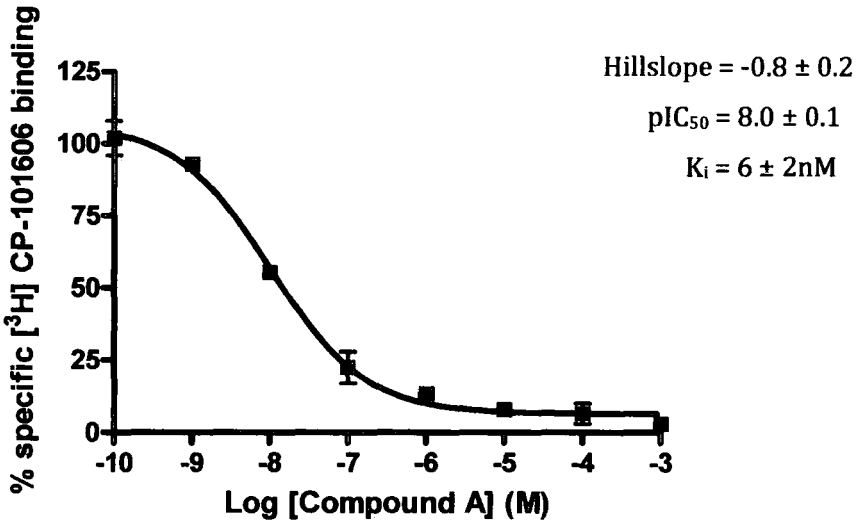


**Figure 3.4 Competition binding experiment showing COMPOUND A displacement of [$^3$H] CP-101,606 in adult rat forebrain membranes, best fit to a one-site binding model. Non-specific binding was defined using ifenprodil (1mM).**

### 3.2.5 Competition assay investigating the displacement of [$^3$H] CP-101606 binding with COMPOUND B in adult rat forebrain tissue.

Adult Sprague-Dawley rat forebrain membranes were used as the source of NMDA receptors in this competition study investigating COMPOUND B [$10^{-3}$M - $10^{-10}$M]. COMPOUND B bound with a high affinity ($K_i$ = 8 ± 9nM) to native NR2B-containing NMDA receptors displacing [$^3$H] CP-101606 in a model best fitted to a sigmoidal variable slope, one-site model. This data suggests similarity between the novel compounds and CP-101606 with a seemingly high affinity for only NR1/NR2B receptors and the same site of action. Complete displacement of [$^3$H] CP-101606 was not achieved at milimolar concentrations of COMPOUND B, indicating that this compound maybe more highly selective for NMDA receptors than CP-101606. This data may indicate that COMPOUND B and COMPOUND A differ in pharmacological interaction with the receptor complex in the brain. The data shown are an average ± SD of two experiments, each carried out in triplicate.

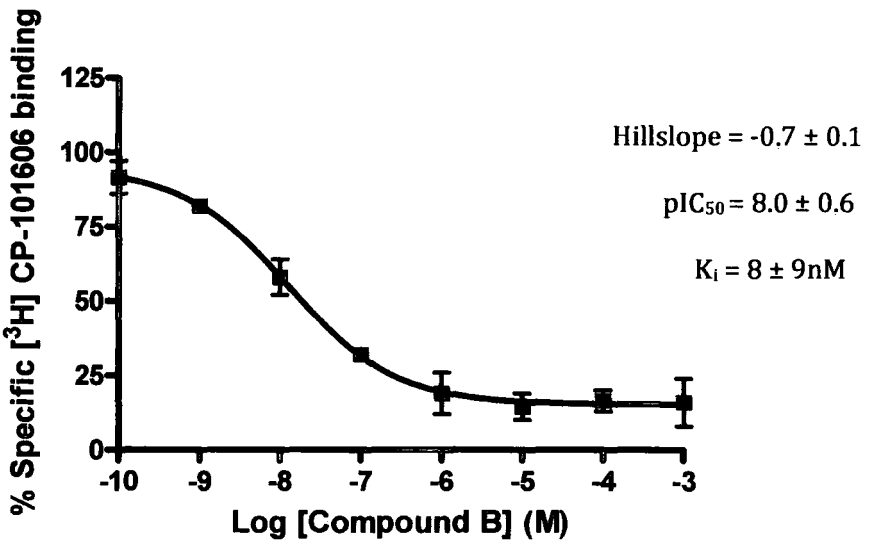


**Figure 3.5 Competition binding experiment showing COMPOUND B displacement of [$^3$H] CP-101,606 in adult rat forebrain tissue fitted to a one-site binding model. Non-specific binding was defined with ifenprodil (1mM).**

In order to further characterise the binding affinity and selectivity of COMPOUND A and COMPOUND B, competition binding assays were carried out using recombinant rNR1/NR2B receptors, in order to compare binding pharmacological properties with native tissue.

Before binding assays were undertaken, the expression of NR1/NR2B receptors was confirmed.

### 3.2.6 Confirmation of recombinant NMDA receptor subunit expression

The recombinant NR1/NR2B NMDA receptors were expressed in HEK293 cells, following transient transfection using Lipofectamine reagent (2.2.15-18), and harvested 48 hours post-transfection.

To confirm NMDA receptor subunit expression, SDS-PAGE and immunoblotting was undertaken using cell homogenate. Immunoreactivity at ~120 and 170KDa shows successful co-expression of both NR1 and NR2B subunits, respectively.

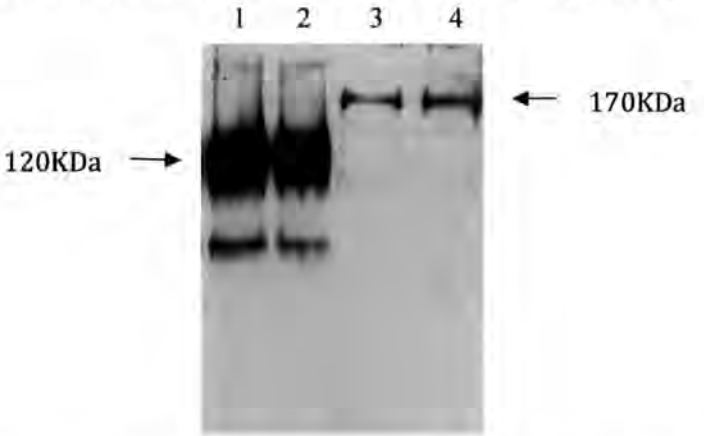


**Figure 3.6 Immunoblot confirming the expression of NR1 and NR2B subunits in HEK293 cells for use in radioligand binding experiments. Lanes 1+2 HEK 293 cells expressing NR1/NR2B receptors and probed with anti-NR1 (2μg/ml). Lanes 3+4 HEK 293 cells expressing NR1/NR2B receptors probed with anti-NR2B (2μg/ml). Representative blot from n=3 experiments.**

### 3.2.7 Competition binding assay to investigate the displacement of [$^3$H] Ro-256981 by COMPOUND A in recombinant NR1/NR2B receptor complexes.

NR1/NR2B receptors were transiently expressed in HEK 293 cells and harvested 48 hours post-transfection for use in radioligand binding studies.

This competition assay shows two-site displacement of [$^3$H] Ro-256981 binding by COMPOUND A [$10^{-3}$M-$10^{-10}$M] and therefore affinity for two receptor populations. A small proportion (24%) of binding to a high affinity site ($K_i$ = 10 ± 10nM) was evident, but the largest proportion (76%) of binding was to a second lower affinity site ($K_i$ = 26 ± 3μM). The high affinity binding is likely to be towards the recombinant NR1/NR2B receptors, whereas the lower affinity site may be another non-specific site endogenously expressed in HEK 293 cells.

The data analysed are an average ± SD of three individual experiments, each performed in triplicate.

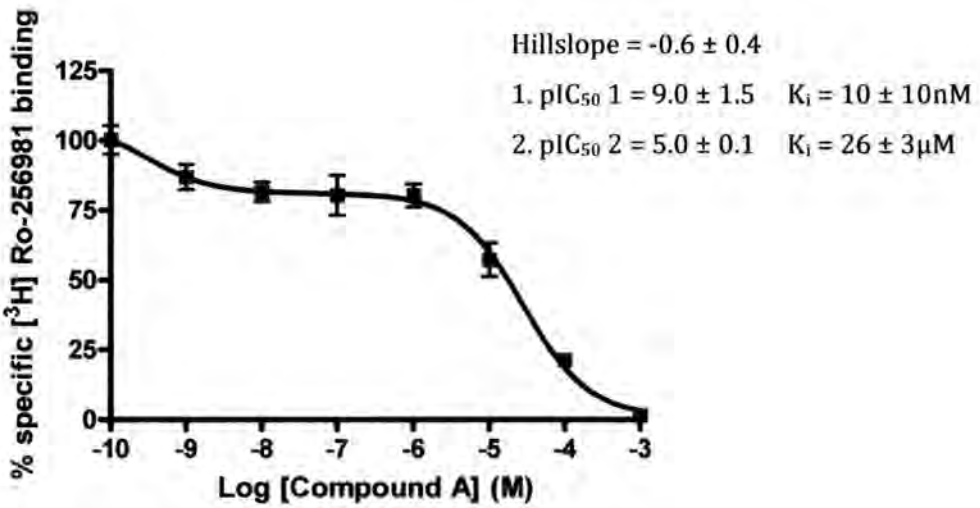


**Figure 3.7 Competition binding showing two-site displacement of [$^3$H] Ro-256981 by COMPOUND A in recombinant NMDA NR1/NR2B receptors expressed in HEK293 cells. Non-specific binding was defined with ifenprodil (1mM).**

### 3.2.8 Competition assay investigating the displacement of [$^3$H] Ro-256981 by COMPOUND B in recombinant NR1/NR2B receptors.

NR1/NR2B receptor subunits were transiently expressed in HEK 293 cells and used as the source of NMDA receptors for this competition assay.

Displacement of [$^3$H] Ro-256981 binding by COMPOUND B [$10^{-3}$-$10^{-10}$M] was fitted to a two-site model showing binding affinity to potentially two populations of receptors (binding ratio 33:67%). COMPOUND B displays high affinity binding ($K_i$ = 5 ± 3nM) probably to NR1/NR2B receptors, with lower affinity ($K_i$ = 19 ± 12μM) binding towards another population of receptors present in the HEK 293 cells. The data shown are an average ± SD of four individual experiments, each performed in triplicate.

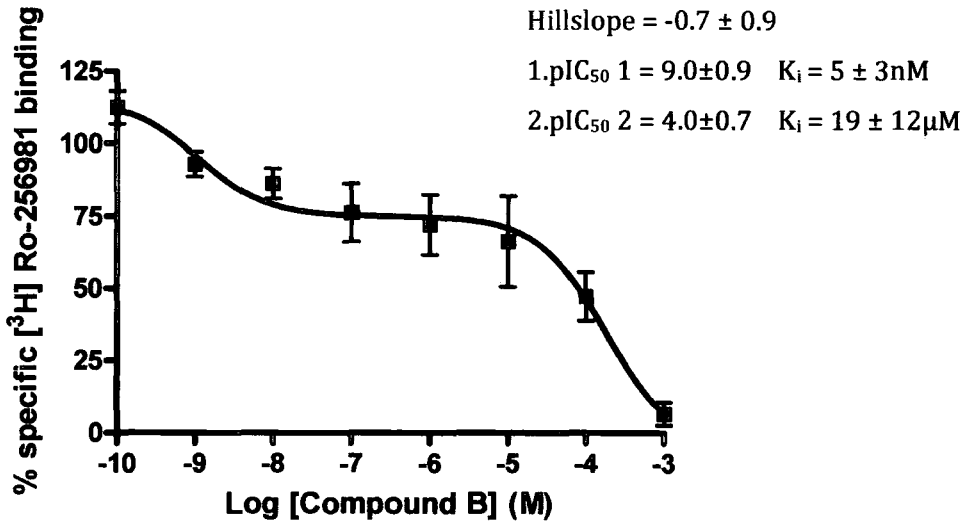


**Figure 3.8 Competition binding experiment showing two-site displacement of [$^3$H] Ro-256981 by COMPOUND B in recombinant NR1/NR2B receptors expressed in HEK293 cells. Non-specific binding was defined with ifenprodil (1mM).**

### 3.2.9 Competition binding assay to investigate the influence of COMPOUND A upon the binding of [$^3$H] CP-101606 in recombinant NR1/NR2B receptors.

NR1/NR2B recombinant receptors were transiently expressed in HEK 293 cells and used as the source of NMDA receptors in this assay.

COMPOUND A displayed two-site displacement of [$^3$H] CP-101,606 showing high affinity binding ($K_i$ = 5 ± 6nM) to NR1/NR2B populations (binding ratio 82:18%). A small proportion of binding to a low affinity site at higher concentrations of COMPOUND A possibly results from non-specific binding to other receptor sites present endogenously in HEK 293 cells.

The data plotted are an average ± SD of three individual experiments, each carried out in triplicate.

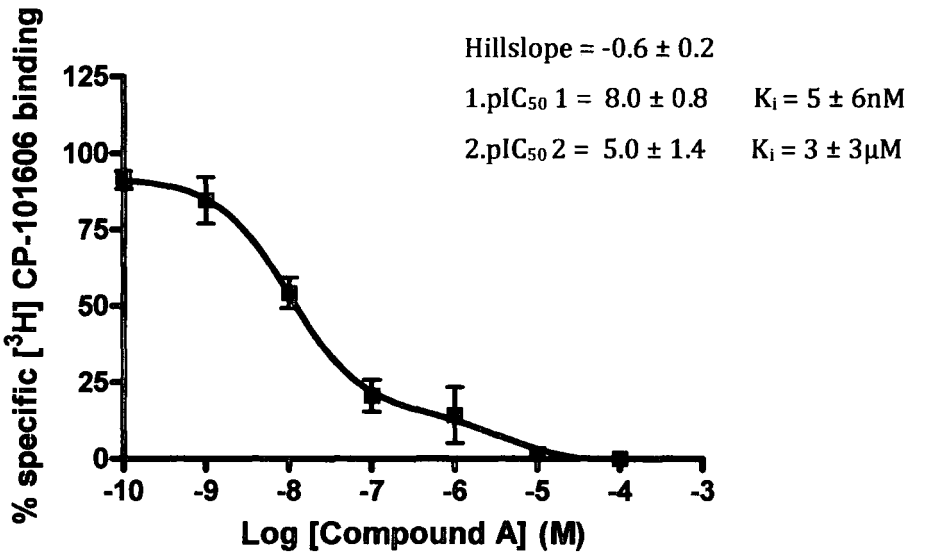


**Figure 3.9 Competition binding showing the two-site displacement of [$^3$H] CP-101,606 by COMPOUND A in recombinant NR1/NR2B receptors expressed in HEK 293 cells. Non-specific binding was defined with ifenprodil (1mM).**

### 3.2.10 Competition assay to show the influence of COMPOUND B upon the binding of [$^3$H] CP-101606 towards recombinant NR1/NR2B receptors.

NR1/NR2B recombinant receptors were transiently expressed in HEK 293 cells and harvested 48 hours post-transfection for use as the source of NMDA receptors in this assay.

COMPOUND B displayed high affinity one-site displacement of [$^3$H] CP-101606. A steep hillslope and high affinity binding ($K_i$ = 9 ± 10nM) of COMPOUND B towards NR1/NR2B containing receptors is evident. COMPOUND B completely displaces the CP-101606 radioligand, showing that the two compounds display equivalent pharmacology in HEK293 cells, and also highlighting potentially different binding interactions between COMPOUND B and COMPOUND A.

The data presented are an average ± SD of three individual experiments, each performed in triplicate.

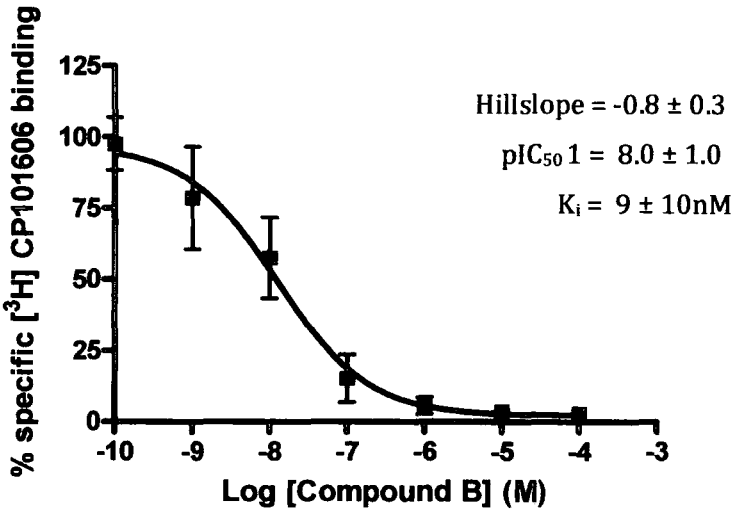


**Figure 3.10 Competition binding experiment showing one-site high affinity displacement of [$^3$H] CP-101,606 by COMPOUND B in recombinant NR1/NR2B receptors expressed in HEK293 cells. Non-specific binding was defined using ifenprodil (1mM).**

To further characterise the binding site of the two novel compounds COMPOUND A and COMPOUND B and investigate their interactions, competition binding was carried out with [$^3$H] MK-801. MK-801 is a non-selective NMDA channel antagonist and enabled any allosteric interactions of the novel compounds with the channel pore to be investigated.

### 3.2.11 Competition curve to investigate the competitive binding between [$^3$H] MK-801 and ifenprodil in adult rat forebrain tissue.

Following a 90 minute incubation period ifenprodil ($10^{-3}$-$10^{-9}$M) displacement of [$^3$H] MK-801 binding was fitted to a one-site competition model in this assay using adult rat forebrain membranes as the source of NMDA receptors with a $K_i$ = 120 ± 10μM. Reducing the incubation times to sub-equilibrium (30 and 60 minutes) shifted the binding curve to the left indicating a reduction in open channel probability reducing the ability of [$^3$H] MK-801 binding and/or an allosteric linkage with the channel pore binding site, consistent with previous findings (data provided by Chazot, unpublished). The data presented for 90minute incubation are an average ± SD for three individual experiments carried out in triplicate.

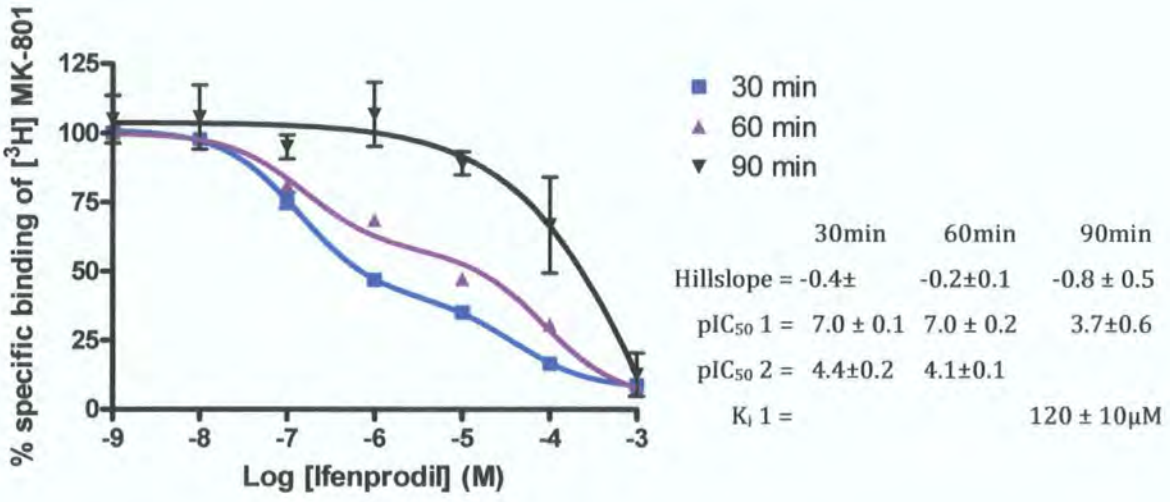


| | 30min | 60min | 90min |
|---|---|---|---|
| Hillslope = | -0.4± | -0.2±0.1 | -0.8 ± 0.5 |
| $pIC_{50}$ 1 = | 7.0 ± 0.1 | 7.0 ± 0.2 | 3.7±0.6 |
| $pIC_{50}$ 2 = | 4.4±0.2 | 4.1±0.1 | |
| $K_i$ 1 = | | | 120 ± 10μM |

**Figure 3.11 Competition binding experiment showing low affinity ifenprodil displacement of [$^3$H] MK-801 binding in adult rat forebrain membranes. Non-specific binding was defined with ketamine (1mM) and the reaction terminated after 30, 60 and 90 minutes.**

### 3.2.12 Competition assay to investigate the influence of COMPOUND A upon the binding of [$^3$H] MK-801 to adult rat forebrain tissue.

Adult Sprague-Dawley rat forebrain membranes (100µg protein/tube) were used as the source of NMDA receptors in this assay. The experiment was carried out on ice and terminated after either 30, 60 or 90 minutes to investigate time-dependent binding affinities. The data was fitted to a one-site competition model with similar low affinity binding of COMPOUND A at all three time-points ($K_i$ = 14 ± 0µM, 18 ± 9µM, 15 ± 10µM, respectively. This evidence suggests that binding of COMPOUND A has minimal allosteric linkage with the receptor channel and therefore MK-801 binding remains unaffected until high concentrations.

The data shown are an average ± SD of two individual experiments, each carried out in triplicate.

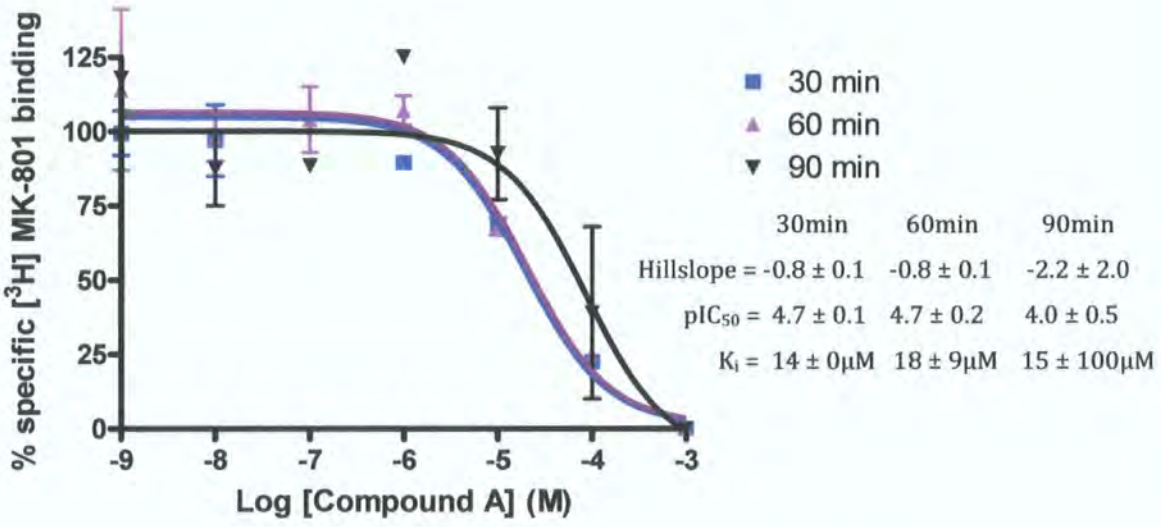


**Figure 3.12 Competition binding experiments showing the COMPOUND A displacement of [$^3$H] MK-801 binding in adult rat forebrain, terminating the reaction after 30, 60 and 90minutes. Non-specific binding was defined with ketamine (1mM).**

### 3.2.13 Competition binding assay investigating the influence of COMPOUND B on the specific binding of [$^3$H] MK-801 in adult rat forebrain tissue.

Adult Sprague-Dawley rat forebrain membranes (100µg protein/tube) were utilised as the source of NMDA receptors for this assay. Again, the reaction was terminated after 30, 60 and 90 minutes before and after equilibrium was achieved to assess time-dependent responses. Following 90 minute incubation period COMPOUND B displacement of [$^3$H] MK-801 was best fitted to a one-site model with a $K_i$ = 13 ± 15µM. A shift to the left of the curves sub-equilibrium at 30 and 60 minutes showed two-site binding with a high affinity $pIC_{50}$ = 8 and $K_i$ = 4nM after 30 minutes. These results may be indicative of potential differences in the binding interactions and kinetics of the two compounds, as COMPOUND B shows greater allosteric interaction with the MK-801 binding site particularly sub-equilibrium than COMPOUND A. Data shown are an average ± SD of between one-five experiments, each carried out in triplicate.

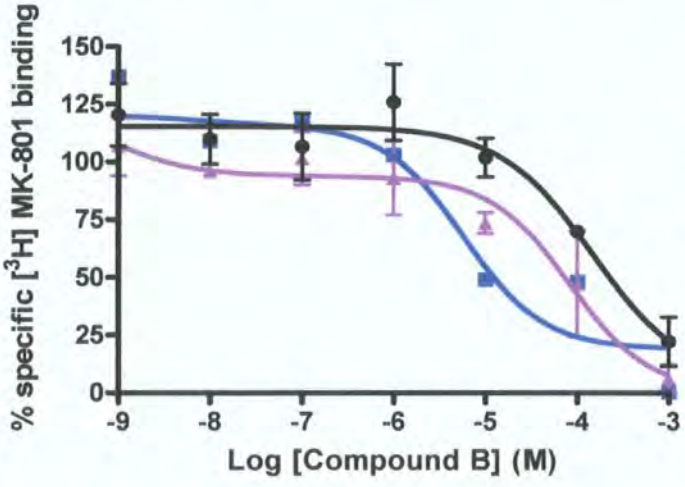


| | 30 | 60 | 90 |
|---|---|---|---|
| Hillslope = -0.4 | | -0.5 ± 0.1 | -0.7 ± 0.5 |
| $pIC_{50}$ 1 = 8.0 | | 8.0 ± 1.8 | 4.0 ± 0.0 |
| $pIC_{50}$ 2 = 5.0 | | 3.0 ± 2.0 | |
| $K_i$ 1= 4nM | | 57 ± 7nM | 13 ± 15µM |
| $K_i$ 2 = 4µM | | 5 ± 6mM | |

**Figure 3.13 Competition binding experiments showing the COMPOUND B displacement of [$^3$H] MK-801 binding in adult rat forebrain, terminating the reaction after 30, 60 and 90minutes. Non-specific binding was defined with ketamine (1mM).**

| Receptors | | Competitive-displacement with novel compounds | |
|---|---|---|---|
| | | **COMPOUND A** | **COMPOUND B** |
| **[$^3$H] Ro-256981** | Native | Low affinity<br>$K_i$ = 158μM | Low affinity<br>$K_i$ = 180μM |
| | Recombinant | Proportion of high Affinity (24%)<br>$K_i$ = 10nM | Proportion of high affinity (33%)<br>$K_i$ = 5nM |
| **[$^3$H] CP-101606** | Native | High affinity<br>Ki = 6nM | High affinity<br>Ki = 8nM |
| | Recombinant | High affinity<br>Ki = 5nM | High affinity<br>Ki = 9nM |
| **[$^3$H] MK-801** | Native | Low affinity<br>Ki = 14, 18, 15μM | Proportion of high affinity sub-equilibrium<br>Ki = 4, 57nM, 13μM |
| **Comment** | | High affinity antagonism NR1/NR2B populations Minimal influence on channel pore binding sites. | High affinity antagonism NR1/NR2B populations Potentially some inter-action with channel pore. |

**Table 3.1 Summary of the competitive binding data obtained for the novel compounds COMPOUND A and COMPOUND B.**

### 3.3 Discussion

NR2B subunit-selective NMDA antagonists are some of the most clinically advanced compounds targeting this excitatory receptor family, with the potential clinical benefits of pharmaceutical intervention evident from animal models and *in vitro* systems. Continuing the generation and development of high-affinity, subunit-selective compounds is therefore very important to ensure specific, effective targeting with minimal adverse side-effects.

This study focuses on the characterisation of two novel anti-NR2B antagonists developed by GlaxoSmithKline COMPOUND A and COMPOUND B, using competitive radioligand binding experiments.

The NR2B selective antagonist ifenprodil and its analogues Ro-256981 and CP-101606, and the channel blocker MK-801, were utilised in this series of experiments to characterise the binding properties and kinetics of the two novel compounds.

To confirm assay protocol and validate the action of the test compounds, initial competition experiments were carried out with ifenprodil ($10^{-4}$-$10^{-9}$M) and tritiated Ro-256981. Ifenprodil displayed high affinity binding towards NR2B-containing receptors in native tissue, with a $K_i$ of 52nM, similar to previous findings of 37nM (Bradford and Chazot, unpublished), 20nM (Mutel *et al.*, 1998) and 33nM (Grimwood *et al.*, 2000). Ifenprodil has been the prototypical NR2B-selective antagonist since it was shown to have a significantly higher affinity for NR2B-containing NMDA receptors than those containing alternative NR2 subunits (Williams, 1993; Williams, 2001) in both native (Tovar *et al.*, 2000) and recombinant receptors (Williams, 1993). Originally developed as a vasodilating agent, as it binds to adrenergic-α1 receptors, it was found to have

selectivity for NR2B-containing NMDA receptors, providing neuroprotection with more limited side-effects than the broad spectrum, non-selective channel blockers.

Effective, high affinity displacement of [$^3$H] Ro-256981 binding by ifenprodil shows both compounds are actively competing for the same receptor binding sites.

Ifenprodil and its analogues bind to a distinct site (LIVBP-like domain) on the NR2B subunit (see section 1.7.3) and act via increasing proton inhibiton at these receptors (Perin-Dureau *et al.*, 2002). Sequence variation of the LIVBP-like domain between NR2 subunit family members enables the selective targeting of the NR2B subunit (Malherbe *et al.*, 2003).

The NR2B-selectivity of ifenprodil and its analogues therefore arises from specific modulation and interaction with this binding domain. Chemically, ifenprodil-like compounds contain a common motif thought to be important for NR2B selectivity, where a tertiary basic amine is attached via linkers to an aryl ring (Nikam and Meltzer, 2002) in an optimum spatial orientation (Williams, 2002).

The number of bonds between the acidic groups appears to be important for subunit selectivity with Feng *et al.*, (2005) showing that longer chain antagonists (containing seven instead of five bond lengths) displayed greater subunit selectivity aiding the design of new analogues. Of these analogues, Ro-256981 developed by Roche (Fischer *et al.*, 1997) and CP-101606 developed by Pfizer (Menniti *et al.*, 1997) showed advanced affinity and selectivity for NR2B-containing receptors via addition of a linker bearing a hydroxyl group and a hydroxyl group in the aryl-ring, which reduced compound non-specific affinity for adrenergic, sodium and potassium channels (Williams, 2002).

In animal models Ro-256981 has been shown to effectively attenuate glutamate induced NMDA currents (Malherbe *et al.*, 2003) showing success in disease models (Loschmann *et al.*, 2004). Ro-256981 binds to NR2B-containing receptors with high affinity despite the presence of alternative NR2 subunits (Chazot *et al.*, 2002) highlighting the different populations of receptors which would be targeted by this compound.

Like ifenprodil and Ro-256981, CP-101606 acts to inhibit NMDA receptor channel activity by potentiating proton inhibition (Chazot, 2000) and is able to distinguish between sub-populations of receptor, binding with significantly greater potency to NR1/NR2B populations (Chazot *et al.*, 2002).

Competition binding using these NR2B-selective tools was performed to characterise and assess the binding properties and affinities of the two novel compounds.

Competition binding assays using unlabelled COMPOUND A and COMPOUND B($10^{-3}$-$10^{-10}$M) and [$^3$H] Ro-256981 showed low affinity binding to NMDA receptors within the native adult rat forebrain tissue, with inhibition of [$^3$H] Ro-256981 binding at relatively high concentrations only ($K_i$ = 158 ± 14 and 180 ± 7μM, respectively). This low affinity binding may result from the presence of heterogeneous NMDA receptor populations within the forebrain to which Ro-256981 binds but COMPOUND A and COMPOUND B do not, preventing high affinity binding. It could also be an indication that COMPOUND A and COMPOUND B bind to distinct sites or interact differently with the Ro-256981 binding pocket on the receptor complex. It is also possible that assay conditions were unfavourable for effective compound binding, for example if high concentrations of magnesium were present blocking receptor activity, or if receptor

expression levels were different between tissue homogenates, however parallel experiments with the control compound ifenprodil showed competitive displacement. The lack of apparent effect by COMPOUND A and minimal high affinity displacement by COMPOUND B of [$^3$H] Ro-256981 binding in the brain is surprising, yet consistent (observed with three separate batches of radioligand which were all displaced as expected with the control compound ifenprodil). These data are in contrast to previous data, where this low affinity inhibition of [$^3$H] Ro-256981 is not seen with other NR2B antagonists such as ifenprodil, CP-101606 and RGH-896 (Chazot *et al*, 2002 and Bradford, unpublished) (data not shown), which support confidence in the assay.

In the second set of competition experiments, [$^3$H] CP-101606, a compound which binds primarily to NR1/NR2B receptors, was used to assess the binding properties of the two novel compounds in adult rat forebrain. Experiments with unlabelled COMPOUND A ($10^{-3}$-$10^{-10}$M) showed a steep, sigmoidal displacement curve indicative of high affinity competitive binding ($K_i$ = 6 ± 2nM) to populations of receptor containing only NR1/NR2B subunits. Under the same assay conditions, COMPOUND B ($10^{-3}$-$10^{-10}$M) again displayed high affinity binding ($K_i$ = 8 ± 9nM), with a single-site displacement of [$^3$H] CP-101606. COMPOUND A and COMPOUND B ($K_i$ = 6 and 8nM, respectively) therefore show a greater binding affinity than ifenprodil (20nM), haloperidol (600nM) and eliprodil (200nM) (Mutel *et al.*, 1998) and display comparable selectivity and potency with other NR2B antagonists such as Ro-256981 and CP-101606. The competitive antagonism of [$^3$H] CP-101606 binding in particular is comparable with published $K_i$ values for unlabelled CP-101606 (8nM) (Mutel *et al.*, 1998) and tritiated

CP-101606 (12nM) (Chazot *et al.*, 2002), (13nM) (Menniti *et al.*, 1997) showing that both COMPOUND A and COMPOUND B are potent NR2B-selective antagonists. Interestingly, even at high concentrations complete inhibition and displacement of [$^3$H] CP-101606 by COMPOUND B was not achieved. This provides evidence suggesting that CP-101,606 may bind to an alternative site/receptor population within the native tissue to which COMPOUND A but not COMPOUND B binds.

To further assess the binding properties and selectivity of the novel compounds, the assays were repeated using recombinant NR1/NR2B receptors expressed in HEK 293 cells.

COMPOUND A ($10^{-3}$-$10^{-10}$M) displayed biphasic displacement of [$^3$H] Ro-256981, showing a site of high affinity binding, presumed to be NR1/NR2B receptors ($K_i$ = 10 ± 10nM) and a lower affinity site ($K_i$ = 26 ± 3μM) possibly non-specific binding to other non-sigma receptor sites endogenously expressed in HEK 293 cells. The inhibition of [$^3$H] Ro-256981 binding by COMPOUND B ($10^{-3}$-$10^{-10}$M) shows a comparable biphasic two-site binding curve with recombinant NR1/NR2B receptors as was seen with COMPOUND A, with a high affinity NR1/NR2B binding site ($K_i$ = 5 ± 3nM) and a low affinity at the second binding site ($K_i$ = 19 ± 12μM, ratio 33:67%).

This low affinity site has previously been detected using other NR2B-ligands in HEK 293 cells (Bradford and Chazot, unpublished) and reported in L (tk-) cells (Grimwood *et al.*, 2000). To minimize the effects of this endogenous element in HEK293 cells and maximize NR1/NR2B receptor binding, immunopurification of the recombinant receptors could be carried out prior to the assay. It should also be noted that *in vitro*

modelling in HEK 293 cells also presents potential changes in the cell membrane, receptor trafficking and expression mechanisms in comparison to the host neurons in native tissue, which may affect pharmacology.

Comparing this data with that obtained from adult rat forebrain tissue, the high affinity site seen in the recombinant NR1/NR2B receptors may be masked in the native tissue due to the presence of alternative receptor subunit combinations or receptor conformations.

Competitive antagonism of COMPOUND A ($10^{-3}$-$10^{-10}$M) towards [$^3$H] CP-101,606 in recombinant NR1/NR2B receptors displayed a biphasic distribution with high affinity binding ($K_i$ = 5 ± 6nM) to NR1/NR2B receptors comparable to that obtained in the native tissue ($K_i$ = 6 ± 2nM).

Displacement of [$^3$H] CP-101606 with COMPOUND B ($10^{-3}$-$10^{-10}$M) also showed comparable high affinity binding in recombinant NR1/NR2B receptors ($K_i$ = 9 ± 10nM) and native tissue ($K_i$ = 8 ± 9nM). Again these high affinity binding values are comparable with published values for [$^3$H] CP-101606 binding to NR1/NR2B recombinant receptors expressed in HEK 293 cells ($K_D$ = 6nM) (Chazot *et al.*, 2002) demonstrating high affinity novel compounds. The discrimination between two receptor populations shown by COMPOUND A in this assay provides further evidence for distinct binding interactions to receptor populations between the two novel compounds.

In the recombinant NR1/NR2B receptors, both COMPOUND A and COMPOUND B display high affinity inhibition of [$^3$H] Ro-256981 and [$^3$H] CP-101606 binding, which may indicate that HEK 293 cells lack components which prevent high affinity inhibition

of [$^3$H] Ro-256981 binding by COMPOUND A and COMPOUND B in the brain. Both COMPOUND A and COMPOUND B appear to have a high affinity for NR1/NR2B receptors and are potentially more sensitive to receptors containing alternative NR2 subunits as is evident from their competitive antagonism of [$^3$H] CP-101606 binding. The data may also suggest evidence for distinct, but possibly overlapping binding sites between the novel compounds and Ro-256981.

To further investigate the binding site characteristics and any allosteric modulations of the receptor channel inferred by the two novel compounds, competition studies with [$^3$H] MK-801 were undertaken, terminating the reaction after 30 minutes, 60 minutes and 90 minutes to observe any time-dependent changes. Competitive binding with ifenprodil ($10^{-3}$-$10^{-9}$M) and [$^3$H] MK-801 showed evidence for allosteric coupling between the ifenprodil binding site and the channel pore binding site.

Displacement curves with both COMPOUND A and COMPOUND B were fitted to one-site binding models at equilibrium, with indication of differential allosteric coupling to the channel pore site using sub-equilibrium conditions.

COMPOUND A displays very little competitive antagonism of [$^3$H] MK-801, with similar binding affinities at all three time-points (14, 18 and 15μM, respectively).

In contrast, COMPOUND B shows increased binding affinity, with a curve shift to the left and shallowing of the curves following 60 and 30 minute incubation times, respectively.

These apparent differences in the modulatory effects on the channel pore binding sites, shows that COMPOUND A and COMPOUND B may have overlapping binding sites or

distinctive interactions with their binding sites which mediate different open channel probabilities or different allosteric effects on the MK-801 binding site.

From the evidence collected both COMPOUND A and COMPOUND B display high affinity antagonism towards NR1/NR2B-containing receptors and could be classified along with CP-101606 in terms of NMDA receptor selectivity as both compounds appear to be sensitive to the presence of alternative NR2 or NR3 subunits in the receptor complex.

Furthermore, the data indicates that COMPOUND B and COMPOUND A may have distinct pharmacological interactions with the receptor complex, which differentially effect channel open probability and allosteric coupling.

In order to increase the efficacy and selectivity of NR2B-selective antagonists as well as understand the implications of targeting this population, the heterogeneous nature of the NMDA receptor and the subunit co-assemblies need to be considered.

# Chapter 4

# Investigating NR3B co-expression and co-assembly in rat and human spinal cord using subunit-selective antibodies

## 4.0 Introduction

Immunological probes are an essential, extremely useful tool within molecular biology. Since Paul Erhlich first proposed the antibody formation theory in 1900 huge advances in the field of immunology have led to the development of commercial antibodies which are utilised in research to provide an effective means of identifying, locating, targeting and characterising proteins both *in vivo* and *in vitro*. Antibody molecules are a large family of glycoproteins, produced by B-lymphocytes in response to the presence of foreign molecules in the body (Janeway *et al.*, 2001). Structurally, immunoglobulins are composed of three protein domains, forming a bivalent Y-shaped molecule (Fig.4.1), composed of two heavy chain polypeptides (approximately 55KDa) and two light chain polypeptides (approximately 25kDa) held together by disulphide bonds. The amino terminals of the heavy and light chains associate to construct an Fab fragment with an antigen-binding domain specific to a particular epitope on an antigen molecule. The carboxy-terminals of the heavy chains associate to form the Fc fragment, which binds to specific proteins within the immune system.

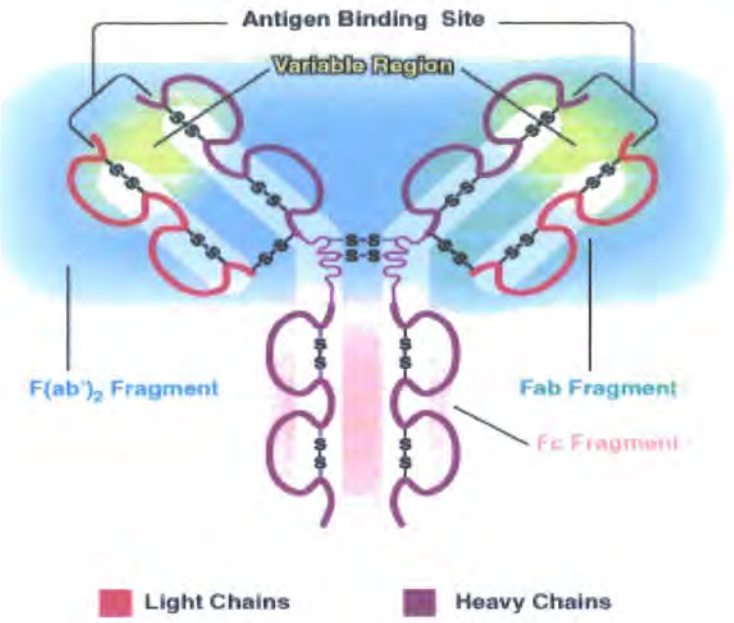


**Figure 4.1 Schematic diagram of immunoglobulin structure**

Cloning of NMDA receptor subunits has allowed the design and production of epitope-specific antibodies, which have been used to study expression and to characterise the component parts of the receptor using immunohistochemistry and western blotting. The antibodies have also been used to affinity purify receptor complexes, allowing subunit compositions to be determined (e.g., Chazot and Stephenson, 1997; Blahos and Wenthold, 1996). The generation of polyclonal antibodies relies upon the humoral response of laboratory animals following immunisation with a specific peptide. In order to elicit a strong host response against the peptide molecule, the immunogenicity of the peptide may be increased via conjugation to a larger carrier protein such as thyroglobulin. Development of the immune response takes several weeks, after which blood samples are collected, from which the antibody may be purified.

In this study the heterogeneity of the NMDA receptor complex was investigated utilising a panel of previously validated subunit specific polyclonal antibodies; anti-rNR1-1a (929-938) (Chazot *et al.*, 1992), anti-rNR2A (1435-1445) (Cik *et al.*, 1993) and anti-rNR2B (46-60) (Chazot and Stephenson, 1997). In addition, two further antibodies were generated, purified and characterised; anti-rodent NR3B (885-899) (Based on a sequence previously published by Matsuda *et al.*, 2002 and a novel anti-human NR3B (885-899) (sequence selected in house). This chapter presents novel data that collectively maps the protein expression of the NR1, NR2A, NR2B and particularly the NR3B subunit in rat spinal cord at the cervical, thoracic and lumbar level and human spinal cord at the cervical level using immunohistochemistry. Previously research has focussed on mRNA and/or protein expression of NR1, NR2A, NR2B, NR2C/D in the adult rat brain and lumbar cord regions (Nagy *et al.*, 2004; Tolle *et al.*, 1993) and adult human lumbar-sacral regions (Sundstrom *et al.*, 1997), showing widespread NR1 expression with more specific localisation of the NR2 subunits. One study mapped expression in a range of cord levels, investigating NMDA NR1 and NR2 expression in cervical, thoracic and lumbar regions of the human spinal cord during first trimester development (Akesson *et al.*, 2000). mRNA (Nishi *et al.*, 2001; Fukaya *et al.*, 2005) and protein (Matsuda *et al.*, 2003) expression studies of the NR3B subunit in the adult mouse brain and spinal cord show motor neuron-specific expression, though a recent study provided evidence for a more widespread expression in the cortex, cerebellum, hippocampus and spinal cord of the adult rat (Wee *et al.*, 2007).

This chapter also describes the optimisation of NMDA receptor solubilisation and immunoaffinity purification to investigate the native co-associations of the NR3B

subunit within the rat spinal cord. Immunopurification studies to date describe the co-associations of NR1 and NR2 subunits in the adult rat brain (Dunah *et al.*, 1998; Chazot and Stephenson, 1997) and human lumbar-sacral spinal cord (Sundstrom *et al.*, 1997), though native spinal cord complexes containing NR3B remain unknown.

## 4.1 Results

### 4.1.1 Rodent anti-NR3B characterization.

### 4.1.2 Immunopurification of polyclonal rodent anti-NR3B

The peptide corresponding to residues 885-899 in the C-terminus of the mouse NR3B subunit (ISL, Paignton, UK) was conjugated to thyroglobulin (section 2.2.1) and emulsified with Freund's adjuvant and injected into New Zealand rabbits (section 2.2.3). The induction of a secondary immune response in the rabbits generates polyclonal antibodies raised against both the peptide and its affiliated conjugated protein thyroglobulin. The production of non peptide-specific antibodies therefore necessitated purification of selective anti-NR3B antibodies via an NR3B peptide immunoaffinity column, which utilizes specific antigen-antibody interaction to pull down the peptide specific antibodies (see section 2.2.1).

Following collection and preparation of the antiserum, immunoaffinity purification of 5mls yielded the following concentrations of anti-mNR3B polyclonal antibody from each bleed, as determined by Lowry protein assays (section 2.2.7).

| Bleed | anti-rodent NR3B antibody yield (µg/ml) |
|---|---|
| 1 | 57 |
| 2 | 170 |
| 3 | 190 |

**Table 4.1 Anti-rodent NR3B antibody yield (µg/ml) from each collection of antisera.**

### 4.1.3 Characterisation of anti-rodent NR3B antibody via western blotting with recombinant NMDA receptor subunits.

To confirm the subunit specificity and characterization of the purified rodent anti-NR3B antibody previously published by Matsuda *et al.*, 2002, western blotting was carried out on both native and recombinant receptors.

HEK 293 cells recombinantly expressing the single subunits of rNR3B, rNR3A or rNR1-1a were harvested 48hours post-transfection and utilized as the source of recombinant NMDA receptor subunits for this analysis. SDS-PAGE was followed by overnight incubation of the nitrocellulose with anti-rodent NR3B (2μg/ml) and resulted in evidence for selective NR3B recognition with an immunoreactive band at approximately 100KDa. The lack of immunoreactivity with the NR3A subunit (which shares close sequence homology with NR3B) and NR1, shows no non-specific cross-reactivity of the antibody, verifying the anti-rodent NR3B selectivity and displaying consistency with results published by Matsuda *et al.*, 2002.

The non-specific bands of approximately 90 and 80KDa are likely to be cross-reacting irrelevant proteins endogenously expressed in the HEK 293 cells.

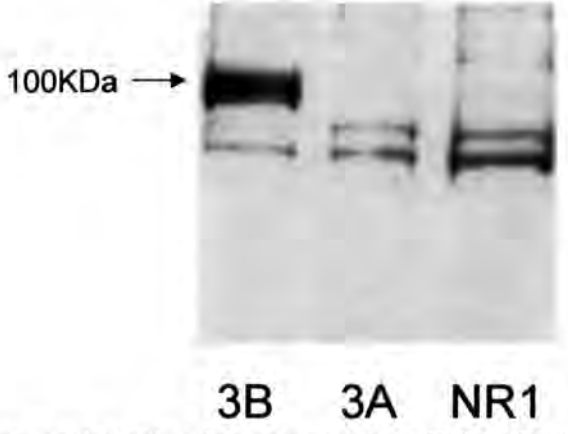


**Figure 4.2 Immunoblot showing recombinant NR3B, NR3A and NR1 subunits expressed in HEK 293 cells. Probed with anti-rodent NR3B (2μg/ml). Representative from n=3 experiments.**

### 4.1.4 Characterisation of anti-rodent NR3B using western blotting with native and recombinant NMDA receptors.

To analyse the binding selectivity of the anti-rodent NR3B antibody in native tissue, adult Sprague-Dawley rat forebrain and spinal cord membranes were prepared and utilized in immunoblotting experiments. 20µg/lane forebrain and spinal cord membranes were loaded for SDS-PAGE together with samples of transiently transfected cells expressing NR3B as a positive control. The immunoblot was then probed overnight with anti-rNR3B, bleed 2 (2µg/ml).

Immunoreactivity was detected in both the forebrain and spinal cord membranes showing the detection of NR3B in both tissues. In the forebrain homogenate, an immunoreactive band was detected at ~110KDa, a molecular weight similar to that detected in the HEK 293 cells expressing NR3B (100KDa) and consistent with previously published data (Nishi *et al.*, 2001; Matsuda *et al.*, 2002), though interestingly in both forebrain and spinal cord homogenates an immunoreactive band ~30KDa was also detected. This species may be due to NR3B subunit proteolysis and/or post-translational modifications, but to ensure specificity a peptide block was performed.

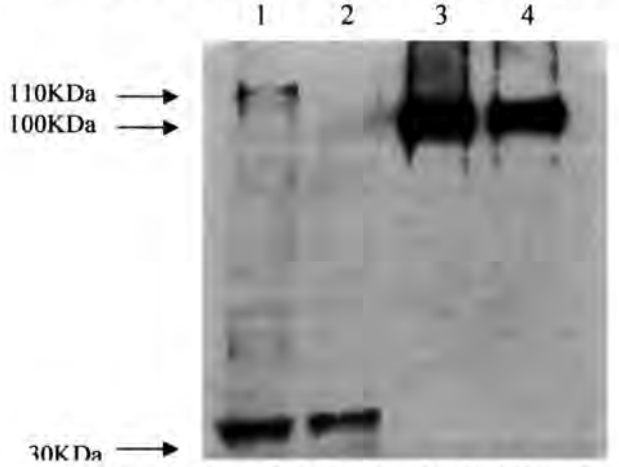


**Figure 4.3 Immunoblot showing adult rat forebrain (1) and spinal cord (2) membranes (30µg) and recombinant NR3B expressed in HEK 293 cells (3+4), probed with anti-rodent NR3B (2µg/ml). Representative from n=3 experiments.**

### 4.1.5 Characterisation of the specificity of the anti-rodent NR3B with antigenic peptide blockade.

To confirm the selectivity of the anti-rodent NR3B antibody for the antigenic peptide and thus for the NR3B subunit, immunoblotting was carried out on both native and recombinant rNR3B sources using anti-rodent NR3B antibody which was pre-incubated with the peptide used to generate the antiserum.

Pre-absorption of the anti-NR3B antibody with the respective antigenic peptide completely inhibited immunoreactive signaling confirming antibody selectivity for the peptide antigen. Detection of smaller molecular weight proteins may therefore be an indication of proteolysis of the NR3B subunit within native tissue which isn't replicated in recombinant models probably due to the absence of endogenous neuronal processing and transporting machinery.

This antibody was utilized for immunohistochemical investigations detailed in chapter 6.

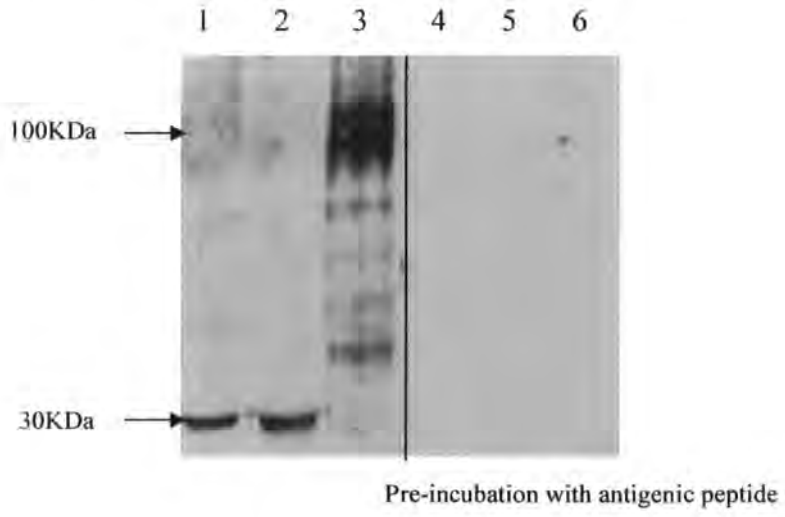


**Figure 4.4 Immunoblot showing adult rat forebrain (1+4) and spinal cord (2+5) (30µg, respectively), and recombinant NR3B (3+6) subunits expressed in HEK 293 cells probed overnight with anti-rodent NR3B (2µg/ml). Representative from n=2 experiments.**

## 4.2 Anti-human NR3B characterization

### 4.2.1 Immunoaffinity purification of polyclonal anti-human NR3B

An anti-human NR3B antibody was generated from the antigenic peptide C T G P P E G S K E E T A E A E corresponding to amino acids 885-899 in the C-terminal region of the NR3B protein.

As previously stated, following the generation of an immune response in the host rabbit, resulting antisera was collected and purified using a newly generated human NR3B peptide immunoaffinity column (see section 2.2.2).

Following the collection and preparation of antisera, 5mls from each bleed generated the following antibody yields.

| Bleed | Anti-human NR3B stock concentration (µg/ml) |
|---|---|
| 1 | 323 |
| 2 | 350 |
| 3 | 439 |

**Table 4.2 Anti-human NR3B antibody yield (µg/ml) from each collection of antisera.**

### 4.2.2 Characterisation of the anti-human NR3B antibody using western blotting on native NMDA receptors.

To investigate the binding selectivity of the anti-human NR3B antibody, western blotting analyses were performed using adult human putamen membranes (50µg protein) (obtained as a gift from Dr Margaret Piggott, Newcastle University) and adult Sprague-Dawley rat forebrain membranes (30µg) to detect any cross-reactivity between species. Following SDS-PAGE, the nitrocellulose was probed overnight with anti-hNR3B (2µg/ml, bleed 3), with resulting immunoreactivity in both species. A large molecular weight species (174KDa) was detected in the human putamen, together with smaller fractions around 110KDa (the expected molecular weight for NR3B) and ~50KDa, similar to species detected by the anti-rodent NR3B antibody. Some cross-reactivity is also evident from detection of NR3B at 110KDa and 50KDa in the rat forebrain. To confirm specificity, an antigenic peptide block was performed.

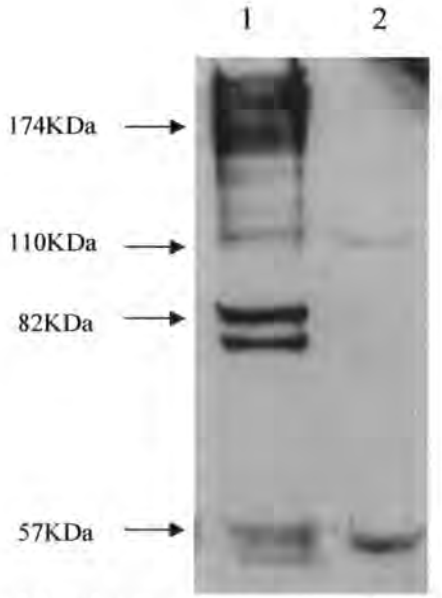


**Figure 4.5 Immunoblot showing post-mortem human putamen membranes (1) (50µg) and adult rat forebrain membranes (2) (30µg) probed with anti-human NR3B (2µg/ml). representative from n=3 experiments.**

### 4.2.3 Characterisation of anti-human NR3B in both human and rat native tissue with antigenic peptide blockade.

Immunoblotting was performed on adult Sprague-Dawley rat forebrain and spinal cord membranes (30μg, respectively) and human putamen membranes (50μg) and probed with either anti-hNR3B (2μg/ml, bleed 2) or anti-hNR3B which had been pre-incubated overnight with the antigenic peptide to which it was derived.

Pre-absorption of the anti-hNR3B antibody with the antigenic peptide blocked specific antibody-protein interactions. The resulting blockade of all immunoreactive bands demonstrates the selectivity of the anti-hNR3B and shows that the high molecular weight species (174KDa) in the human tissue is NR3B, possibly in a dimeric form, and that this antibody cross-reacts with rat NR3B.

A human NR3B recombinant clone was not available for further characterization.

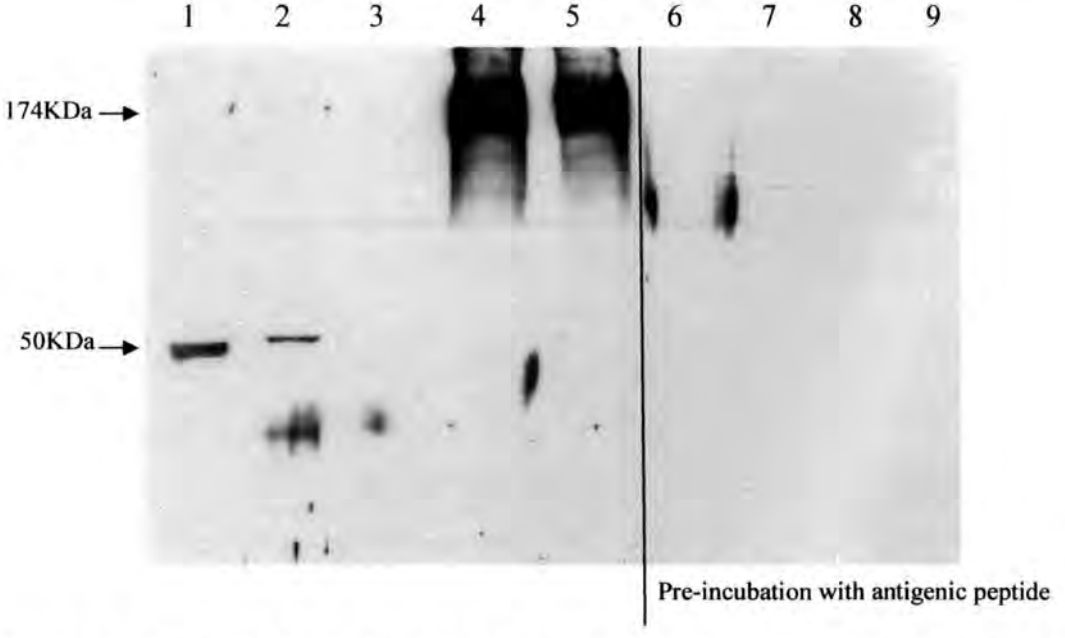


**Figure 4.6 Immunoblot (n=1) showing adult rat forebrain membranes (1+6), adult rat spinal cord membranes (2+7) (30μg) and human putamen membranes (4, 5, 8+9) (50μg) probed with anti-human NR3B (2μg/ml). Lane 3 was loaded with sample buffer.**

### 4.3 Characterisation of the commercial anti-rat NR3B Upstate®

A commercial anti-NR3B antibody generated against amino acids 916-928 in the C-terminal domain, with a peptide sequence R R V R R A V V E R E R R was purchased for experimental use during generation and characterization of our antibodies.

To characterize and verify the selectivity of this commercial antibody, immunoblotting was carried out with native NMDA receptors from rat forebrain and spinal cord membranes (30µg/lane) and with recombinant NR3B expressed in HEK 293 cells, probing with commercial anti-NR3B (1:1000).

The commercial anti-NR3B displayed immunoreactivity in the native tissue, detecting species at ~110KDa in both rat forebrain and spinal cord, where expression of NR3B may be reduced. Other smaller species are detectable, including the species ~30KDa, which may be the result of post-translational modifications. No clear band of immunoreactivity can be detected in the recombinant NR3B, in contrast to the in house anti-rNR3B, which may be due to ineffective transfection and subunit expression, or due to a lack of specific reactivity in *in vitro* models.

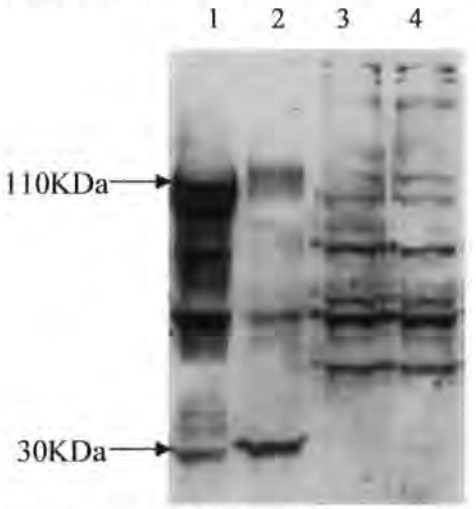


**Figure 4.7Representative immunoblot (n=2) showing adult rat forebrain membranes (1) and adult rat spinal cord membranes (2) (30µg) and recombinant NR3B expressed in HEK 293 cells (3+4) probed with commercial anti-NR3B (1:1000).**

## 4.4 Co-expression of the NMDA receptor subunits NR1, NR2A, NR2B and NR3B in the adult rat and adult human spinal cord.

In order to map subunit expression within the rat and human spinal cord tissue, purification of anti-NR1, anti-NR2A and anti-NR2B antibodies was also carried out to produce a panel of subunit selective antibodies which were used for immunohistochemical and immunopurification investigations.

### 4.4.1 Purification of subunit selective anti-NMDA antibodies

New batches of anti-rNR1, anti-rNR2A and anti-rNR2B antisera (previously published Chazot *et al.*, 1992; Cik *et al.*, 1993; Chazot and Stephenson, 1997) were purified using selective peptide affinity columns to generate a panel of subunit selective antibodies to define NMDA receptor subunit localisation. Immunoblotting was performed with adult rat forebrain and spinal cord membranes (25μg), and probed with the respective antibody overnight (2μg/ml).

The immunoblots show clear immunoreactivity towards each NMDA subunit species. Anti-rNR1, anti-rNR2A and anti-rNR2B display distinct immunoreactive bands at ~120KDa, 180KDa and 180KDa, respectively, in both forebrain and spinal cord, concurring with previously published sizes for each subunit (Hawkins *et al.*, 1999).

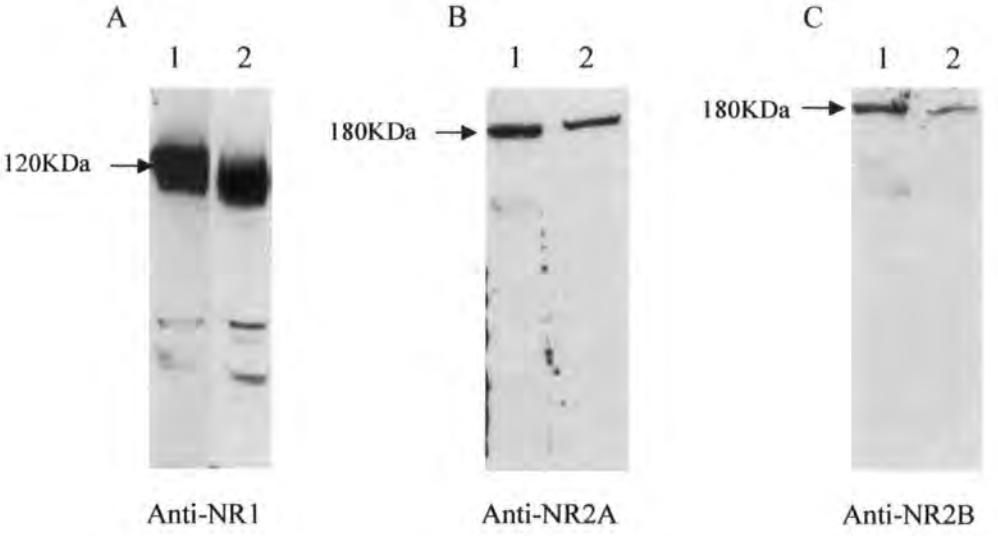


**Figure 4.8 Representative immunoblots (n=3) showing adult rat forebrain membranes (25µg) (Lane 1) and adult rat spinal cord membranes (25µg) (Lane 2), probed overnight with anti-rNR1 (2µg/ml) (A), anti-rNR2A (2µg/ml) and anti-rNR2B (2µg/ml).**

### 4.4.2 Immunohistochemical investigations of NMDA subunit co-expression in the rat spinal cord.

All animal and human studies were performed with full ethical and Home Office approval (Project licence PPL-6003437).

Adult male Sprague-Dawley rat spinal cords were dissected and rapidly frozen, before cryostat sectioning (see 2.2.9). Immunohistochemical analysis (see 2.2.10) was then performed on the cervical, thoracic and lumbar regions of rat spinal cord using the panel of subunit selective antibodies previously generated. Controls were carried out in the absence of primary antibodies (see figure 4.10). Both the dorsal (sensory) and the ventral (motor) areas of the cord were investigated and NMDA subunit expression mapped for each antibody according to the immunoreactivity in the spinal laminae shown below.

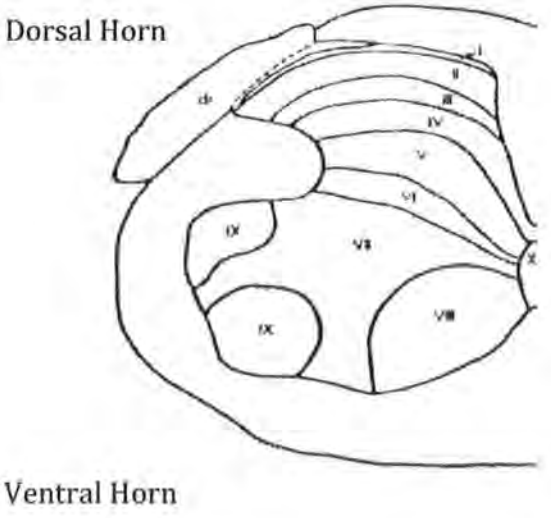


**Figure 4.9 Schematic diagram showing the laminae in the dorsal and ventral regions of the rodent lumbar spinal cord (Tolle *et al.*, 1993).**

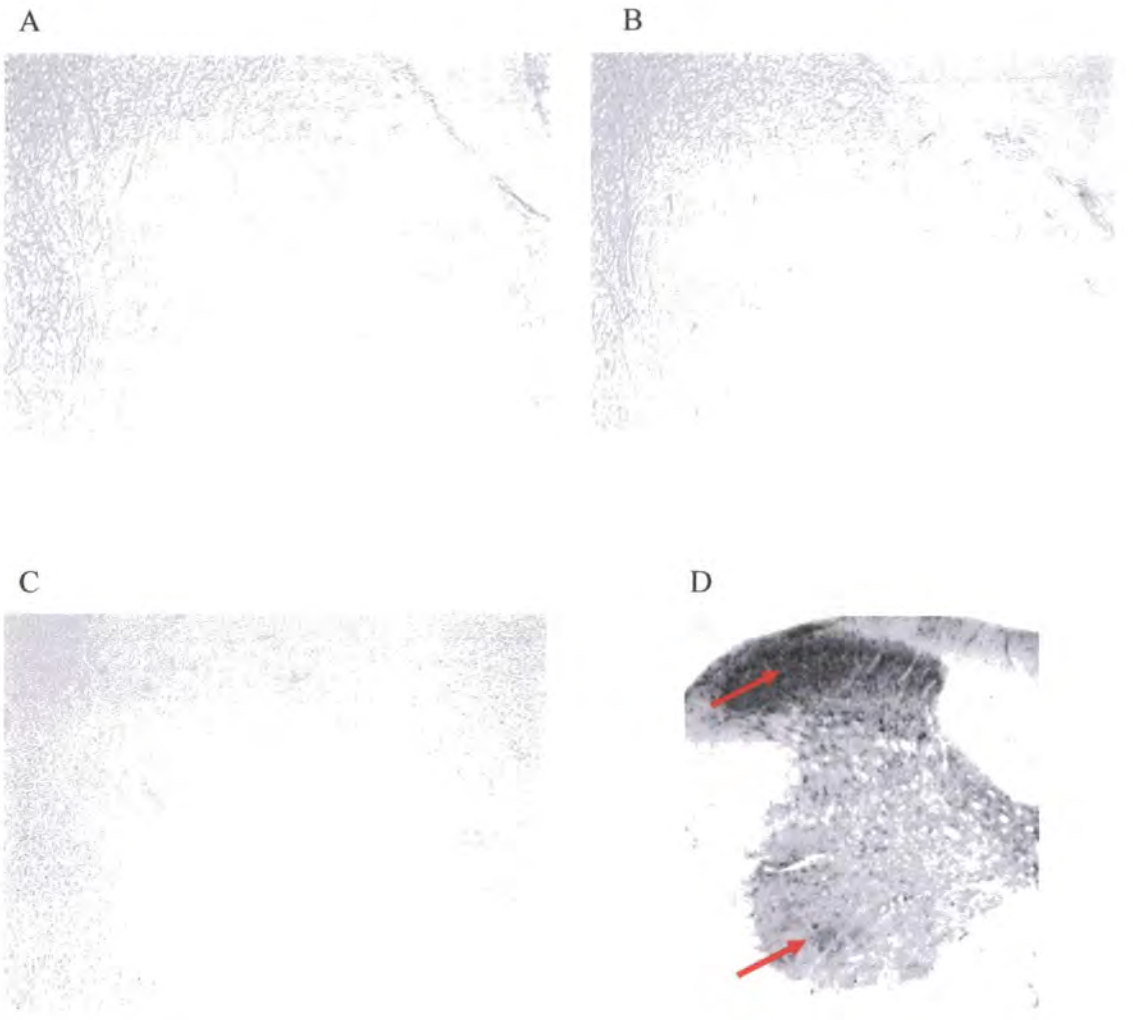


**Figure 4.10 Control sections showing the immunoreactivity in tissue in the absence of primary antibodies in the cervical dorsal horn (A), the lumbar dorsal horn (B) and the thoracic ventral horn (C). Low resolution image of the cervical cord showing NR1 immunostaining (Bigini *et al.*, 2006) with red arrows highlighting the dorsal and ventral areas of the cord focused upon in this study.**

#### 4.4.2.1 Expression of NR1, NR3B, NR2A and NR2B in adult rat cervical spinal cord

Immunohistochemical analysis in the cervical region of the adult rat spinal cord revealed differential expression of the four subunits between motor and sensory areas confirming distinct cellular localization and likely modulatory functioning of the subunits.

NR1 is ubiquitously expressed throughout the spinal cord layers, with its abundant expression confirming that previously published for mRNA (Tolle *et al.*, 1993; Furuyama *et al.*, 1993) and protein (Nagy *et al.*, 2004) studies in the lumbar region.

NR3B expression is predominantly confined to the motor neuron cell bodies and dendrites within the ventral horn, with modest immunoreactivity in the dorsal sensory regions consistent with previous mRNA expression studies (Nishi *et al.*, 2001).

Immunoreactivity to both NR2A and NR2B was detected in dorsal and ventral horns, particularly in motor neuron cell bodies and outer laminae I, II and III, concurring with previous studies in cervical (Watanabe *et al.*, 1994) and lumbar (Nagy *et al.*, 2004) tissue and suggesting a role in motor and sensory transmissions.

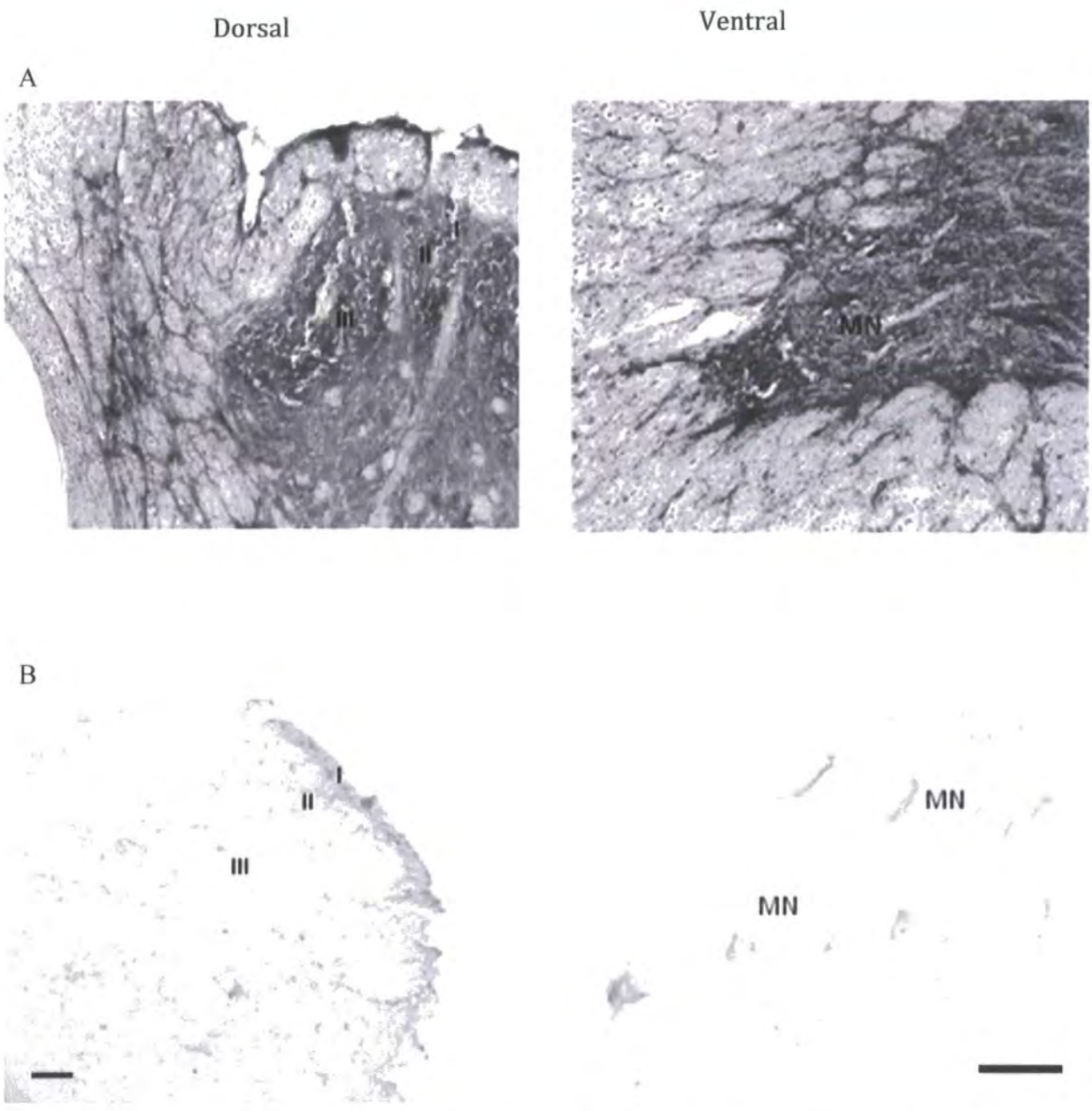


**Figure 4.11 Expression of NR1 (probed anti-rNR1 2μg/ml) (A), NR3B (commercial anti-rNR3B 1:1000) (B) in the dorsal horns laminae I, II, III and ventral horns showing the motor neurons (MN) of the cervical rat spinal cord (n=2). Scale bars represent 100μm.**

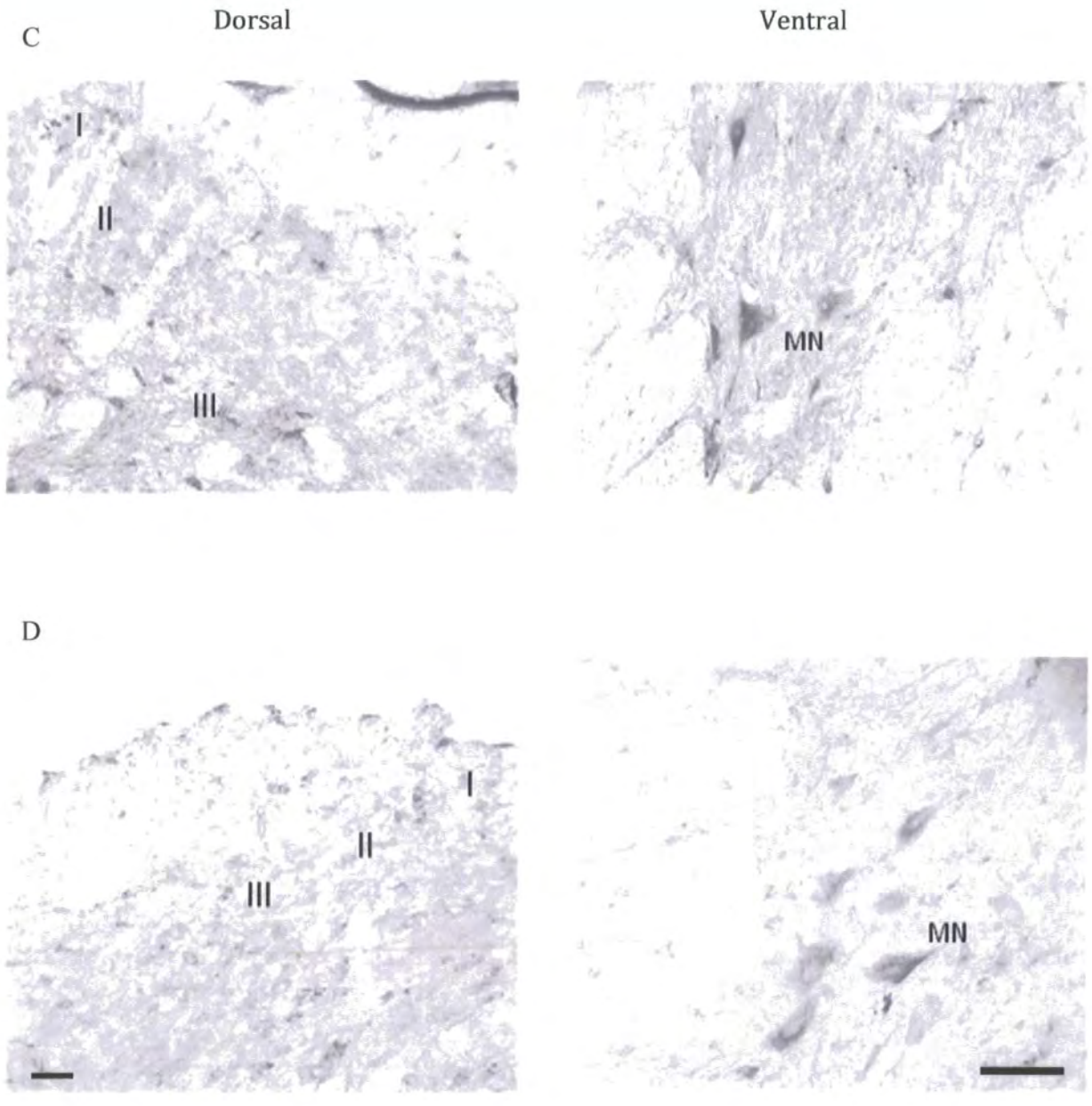


**Figure 4.12 Expression of NR2A (anti-rNR2A 2µg/ml) (C) and NR2B (anti-rNR2B 2µg/ml) (D) in the dorsal horns laminae I, II, III and ventral horns showing the motor neurons (MN) of the cervical rat spinal cord (n=2). Scale bars represent 100µm.**

**4.4.2.2 Expression of NR1, NR2A, NR2B and NR3B in adult rat thoracic spinal cord.**

Immunohistochemical analysis was then performed using the same panel of subunit selective antibodies on adult rat thoracic spinal cord sections. The tissue was probed overnight with anti-rNR1 (1μg/ml), anti-rNR2A (2μg/ml), anti-rNR2B (2μg/ml) and the commercial anti-rNR3B (1:1000) and analysed using a Nikon Eclipse E300 light microscope with a Coolpix MDC lens Nikon Camera (Japan) (x400 magnification).

Distinct patterns of subunit expression were detected in the thoracic region of the adult rat spinal cord, showing prominent changes and potential evidence for varying NMDA subunit modulation and function in different cord regions.

NR1 expression is again abundant with immunoreactivity evident in the ventral horn and the dorsal horn. A prominent band of immunoreactivity was detected in laminae II of the dorsal horn, possibly implying increased NMDA receptor presence in this puncta of sensory neurons. The concentration of anti-NR1 was reduced in order to reduce the high level of background staining seen in the cervical region.

NR3B expression remains comparatively low and concentrated mainly within the motor neuron cell bodies of the ventral horn.

NR2A expression appears to have shifted predominantly from the dorsal to the ventral horn with concentrated immunoreactivity within the motor neuron cell bodies within laminae IX, consistent with previous mRNA studies on human spinal cord (Samarasinghe *et al.*, 1996). The predominant immunoreactivity of the NR2B subunit appears to shift from more wide-spread expression to the dorsal horn and in particular laminae I and II, consistent with published data (Nagy *et al.*, 2004; Mutel *et al.*, 1998).

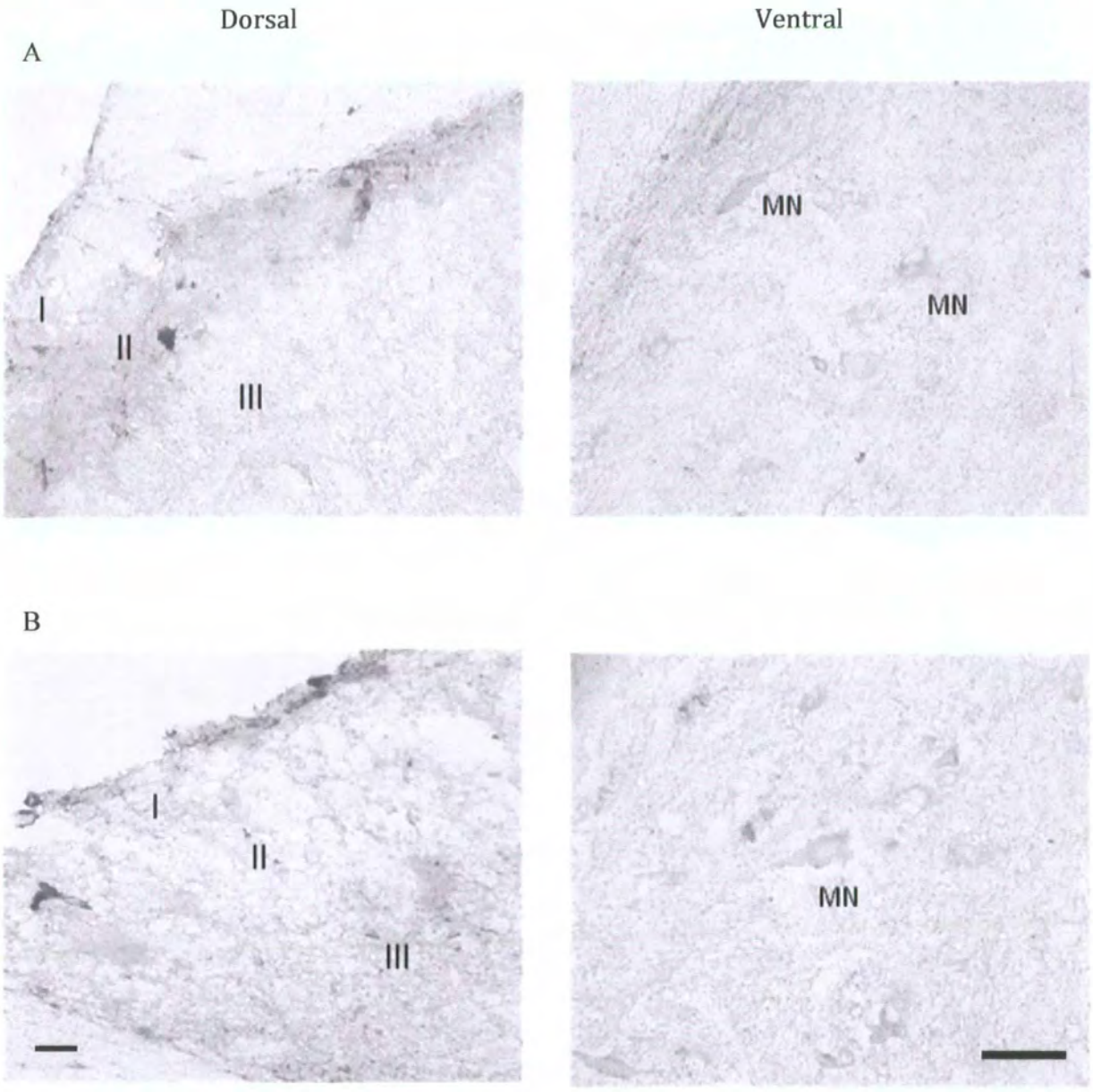


**Figure 4.13 Expression of NR1 (probed anti-rNR1 1μg/ml) (A), NR3B (commercial anti-rNR3B 1:1000) (B) in the dorsal horn laminae I, II, III and ventral horns showing the motor neurons (MN) of the thoracic rat spinal cord (n=2). Scale bars represent 100μm.**

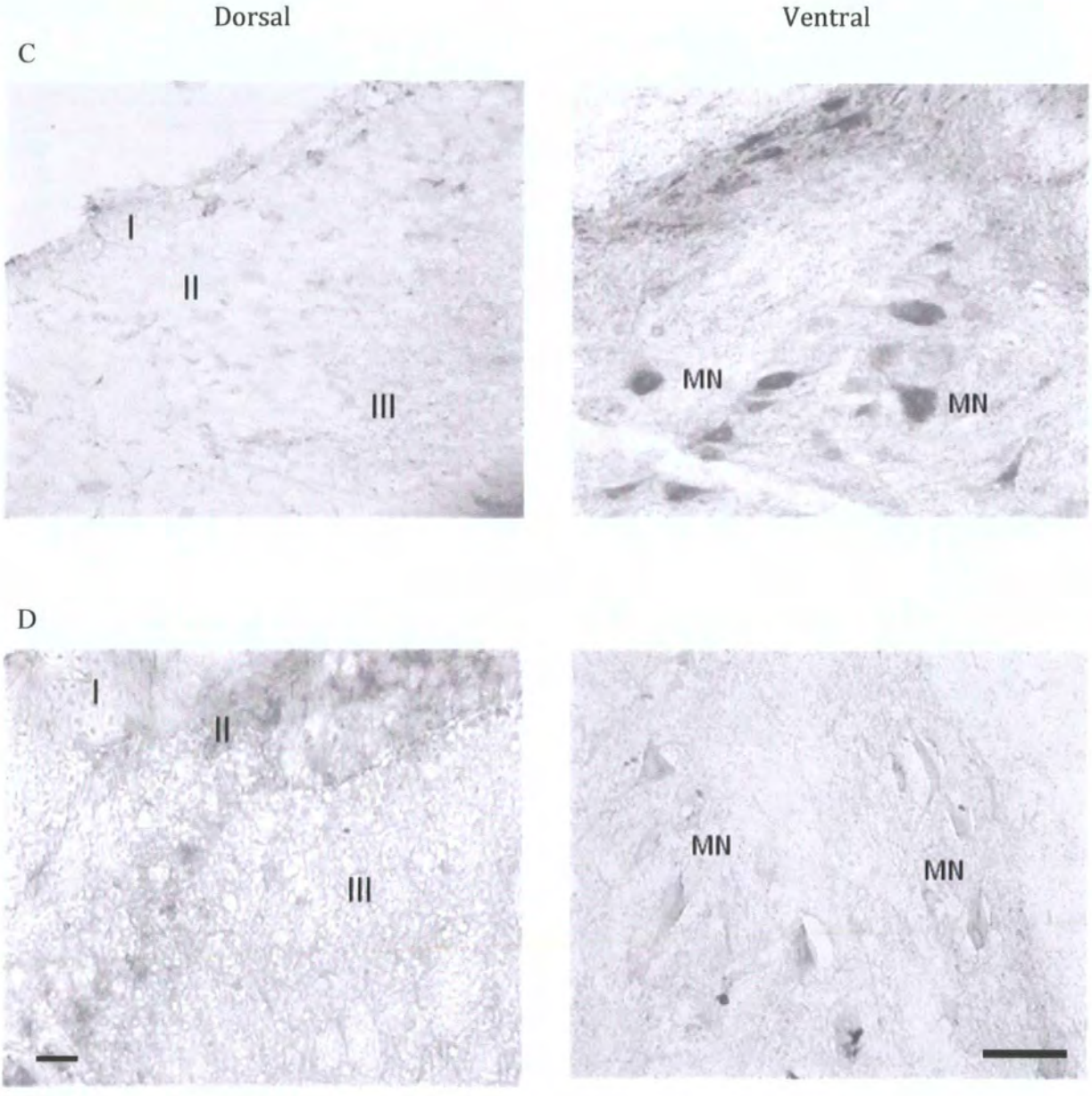


**Figure 4.14 Expression of NR2A (anti-rNR2A 2µg/ml) (C) and NR2B (anti-rNR2B 2µg/ml) (D) in the dorsal horn laminae I, II, III and ventral horns showing the motor neurons (MN) of the thoracic rat spinal cord (n=2). Scale bars represent 100µm.**

#### 4.4.2.3 Expression of NR1, NR2A, NR2B and NR3B in the adult rat lumbar spinal cord

Immunohistochemistry was carried out on adult rat lumbar spinal cord using the panel of subunit selective antibodies previously used. The tissue was probed overnight with anti-rNR1 (1μg/ml), anti-rNR2A (2μg/ml), anti-rNR2B (2μg/ml) and the commercial anti-rNR3B (1:1000).

The immunoreactivity of the four NMDA receptor subunits in lumbar tissue shows a similar pattern to expression in the thoracic tissue. NR1 shows abundant expression in both the ventral horns and the dorsal horns, again with particularly concentrated immunoreactivity in laminae II.

NR3B immunoreactivity is concentrated within the cell bodies of the motor neurons with minimal expression in the sensory dorsal horn.

NR2A immunoreactivity remains predominantly in the ventral regions, in the cell bodies of the motor neurons.

The NR2B subunit remains predominantly located in the dorsal regions, again particularly in the outer laminae, with some immunoreactivity within the motor neurons of the ventral horn.

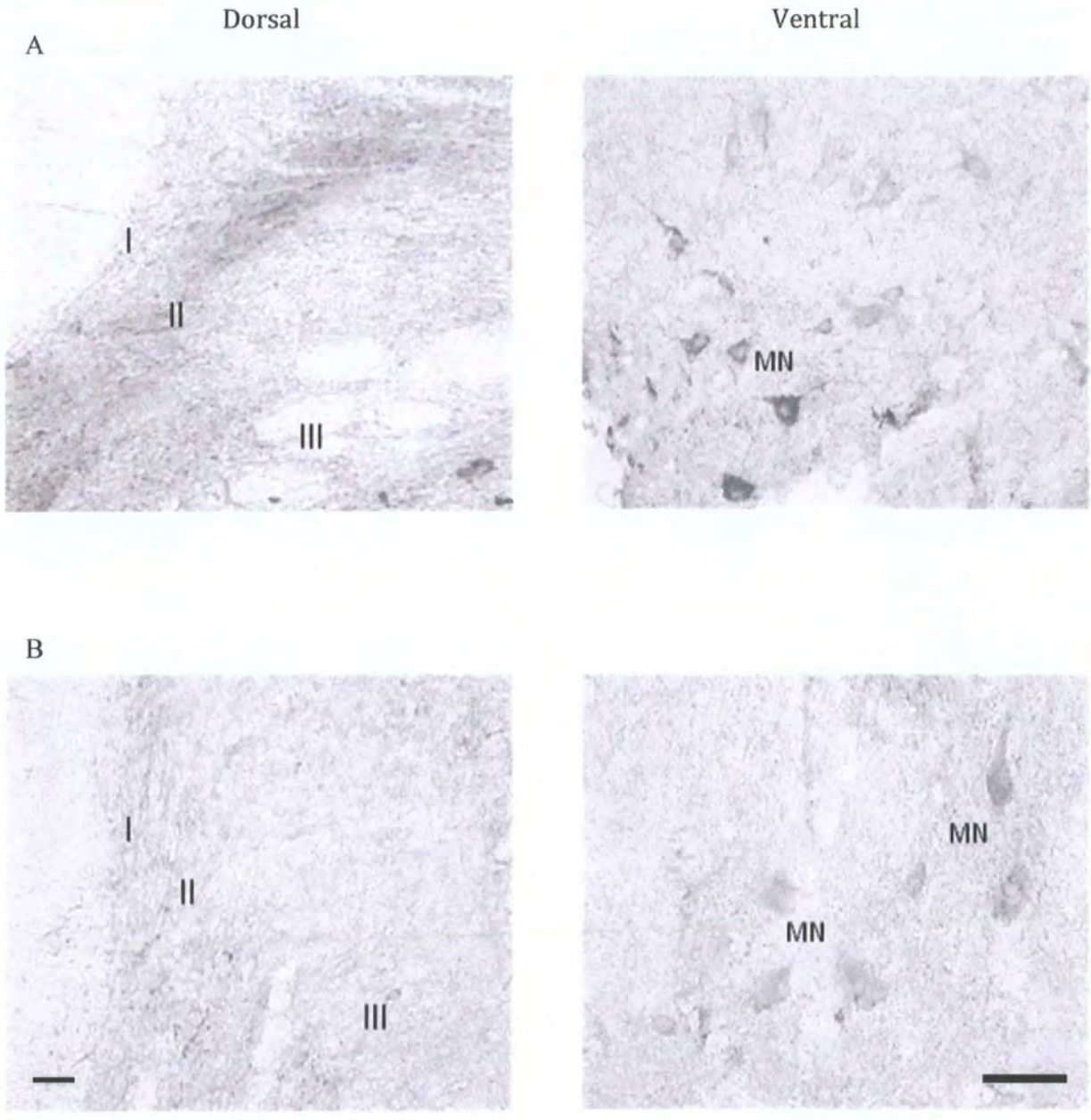


**Figure 4.15 Expression of NR1 (probed anti-rNR1 1µg/ml) (A), NR3B (commercial anti-rNR3B 1:1000) (B) in the dorsal horn laminae I, II, III and ventral horns showing the motor neurons (MN) of the lumbar rat spinal cord (n=2). Scale bars represent 100µm.**

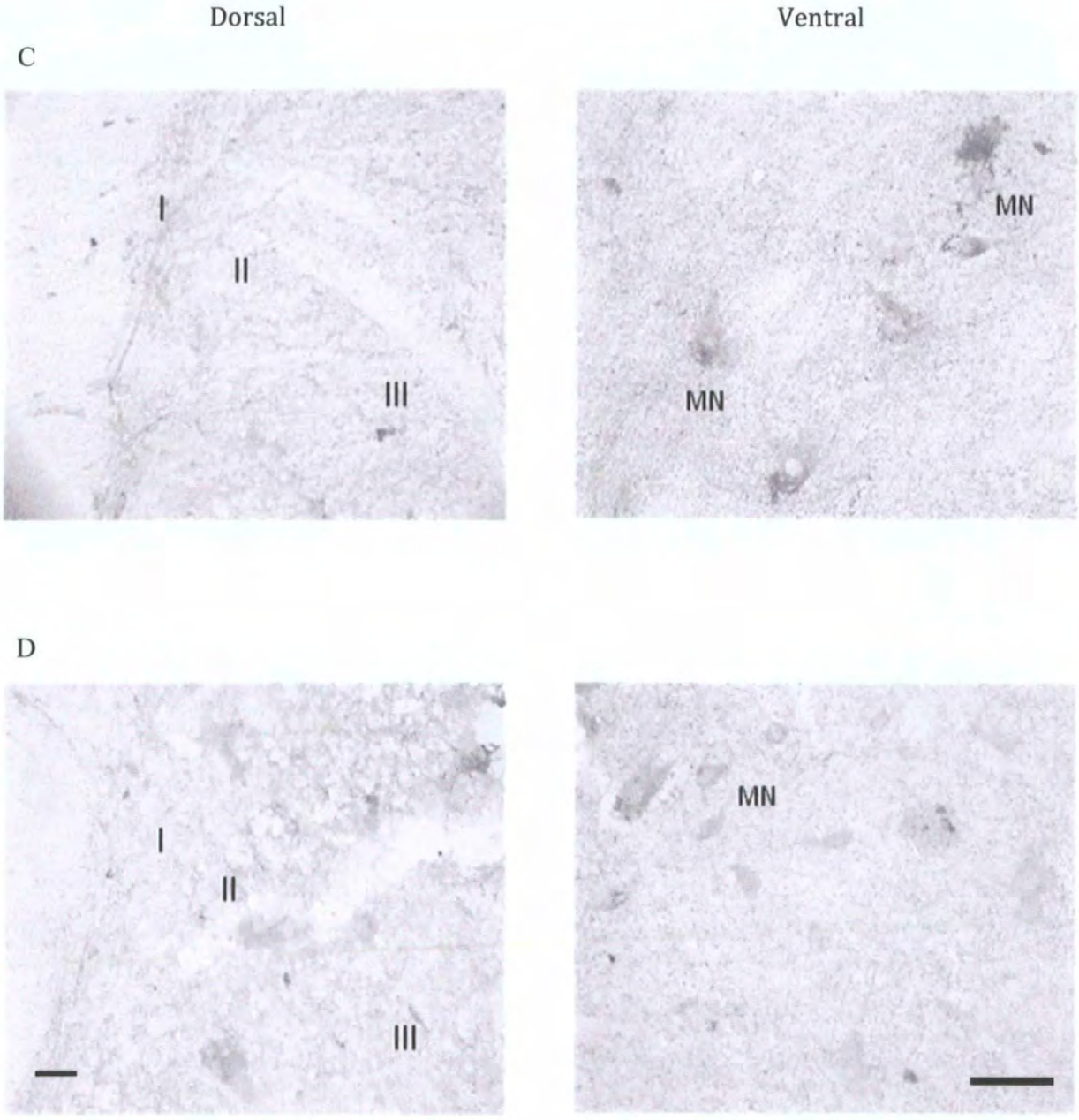


**Figure 4.16 Expression of NR2A (anti-rNR2A 2µg/ml) (C) and NR2B (anti-rNR2B 2µg/ml) (D) in the dorsal horn laminae I, II, III and ventral horns showing the motor neurons (MN) of the lumbar rat spinal cord (n=2). Scale bars represent 100µm.**

**4.4.2.4 Qualitative summary of NMDA subunit expression in the dorsal and ventral horns spanning the three different upper regions of the adult rat spinal cord.**

From the immunohistochemical investigations on rat spinal cord, the four NMDA subunits appear to be differentially expressed both between the sensory and motor areas of the cord and between the different regions of the cord. The NR1 subunit is ubiquitous and essential for all functional NMDA receptors with expression subsequently prominent throughout all regions. The modulatory NR2 subunits appear to be differentially expressed, with NR2A immunoreactivity predominant in the motor neurons in the ventral horns of the cord, whereas the NR2B subunit appears to be more concentrated in the dorsal sensory horns, particularly in the thoracic regions. The NR3B subunit shows modest expression in the sensory areas of the cord, but in all regions shows predominant expression within the ventral horns. This data provide the first comparative study of the major NMDA receptor subunits in the dorsal and ventral horns of the upper levels of the rat spinal cord. Generally NR2A appears to be the major subunit in the ventral horn, whereas NR2B appears to be the major subunit in the dorsal horn.

| Spinal cord level | Region | Intensity of immunoreactivity | | | |
|---|---|---|---|---|---|
| | | **NR1** | **NR2A** | **NR2B** | **NR3B** |
| | **Dorsal horn** | ++++ | ++ | +++ | (+) |
| **Cervical** | **Ventral horn** | +++ | +++ | ++ | +++ |
| | **Dorsal horn** | ++++ | ++ | +++ | + |
| **Thoracic** | **Ventral horn** | ++++ | +++ | + | +++ |
| | **Dorsal horn** | ++++ | + | ++ | (+) |
| **Lumbar** | **Ventral horn** | ++++ | +++ | ++ | ++ |

**Table 4.3 Qualitative summary of the average intensity of immunoreactivity for each subunit in the cervical, thoracic and lumbar regions of adult rat spinal cord.**
**(+) = Very weak expression, + = Weak expression, ++ = Moderate expression, +++ = Strong expression, ++++ = Very strong expression.**

### 4.4.3 NMDA subunit expression in human cervical spinal cord

Expression profiles of the NMDA subunits NR1, NR2A, NR2B and NR3B were mapped in the adult male human cervical spinal cord (obtained ethically under project licence PPL-6003437) using immunohistochemistry (see 2.2.10). The anti-hNR3B antibody (2μg/ml) was utilized along with the anti-rNR1 (1μg/ml), anti-rNR2A (2μg/ml) and anti-rNR2B (2μg/ml).

As in the rat tissue, NR1 expression is abundant throughout the dorsal and ventral regions of the human cervical spinal cord showing consistency with previous studies of mRNA expression (Samarasinghe *et al.*, 1996) and protein expression in lumbar regions of human spinal cord (Sundstrom *et al.*, 1997).

The NR3B subunit displays discrete expression in the motor neuron cell bodies and dendrites of the ventral horn, displaying a similar distribution pattern to that in the rat and consistent with mRNA studies in the mouse (Fukaya *et al.*, 2005; Nishi *et al.*, 2001; Matsuda *et al.*, 2002).

Consistent with published literature, NR2A showed wide-spread distribution, similar to that of NR1 (Samarasinghe *et al.*, 1996) with expression in the dorsal laminae, particularly II and III and in the cell bodies of the motor neurons in the ventral horn.

NR2B expression is predominantly concentrated in laminae I and II of the dorsal horn consistent with previous primate studies (Rigby *et al.*, 2002) and immunoreactivity seen in the rat. Evidence for prominent expression in the motor neurons in the ventral horn shows initial evidence for species difference in NR2B protein expression between the rat and human.

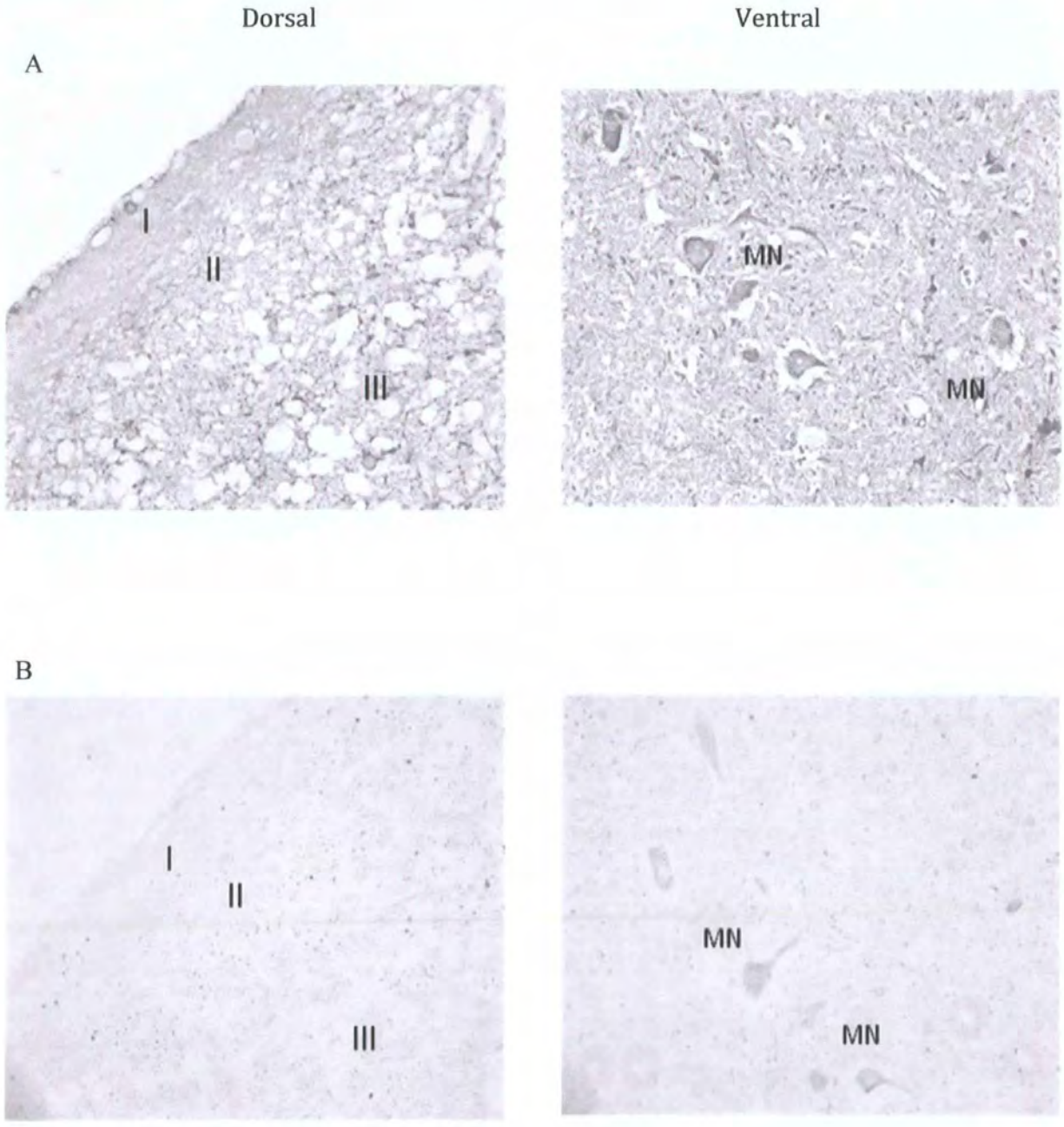


**Figure 4.17 Expression of NR1 (probed anti-hNR1 1µg/ml) (A), NR3B (commercial anti-rNR3B 1:1000) (B) in the dorsal horn laminae I, II, III and ventral horns showing the motor neurons (MN) of the cervical human spinal cord (n=1). Scale bars represent 100µm.**

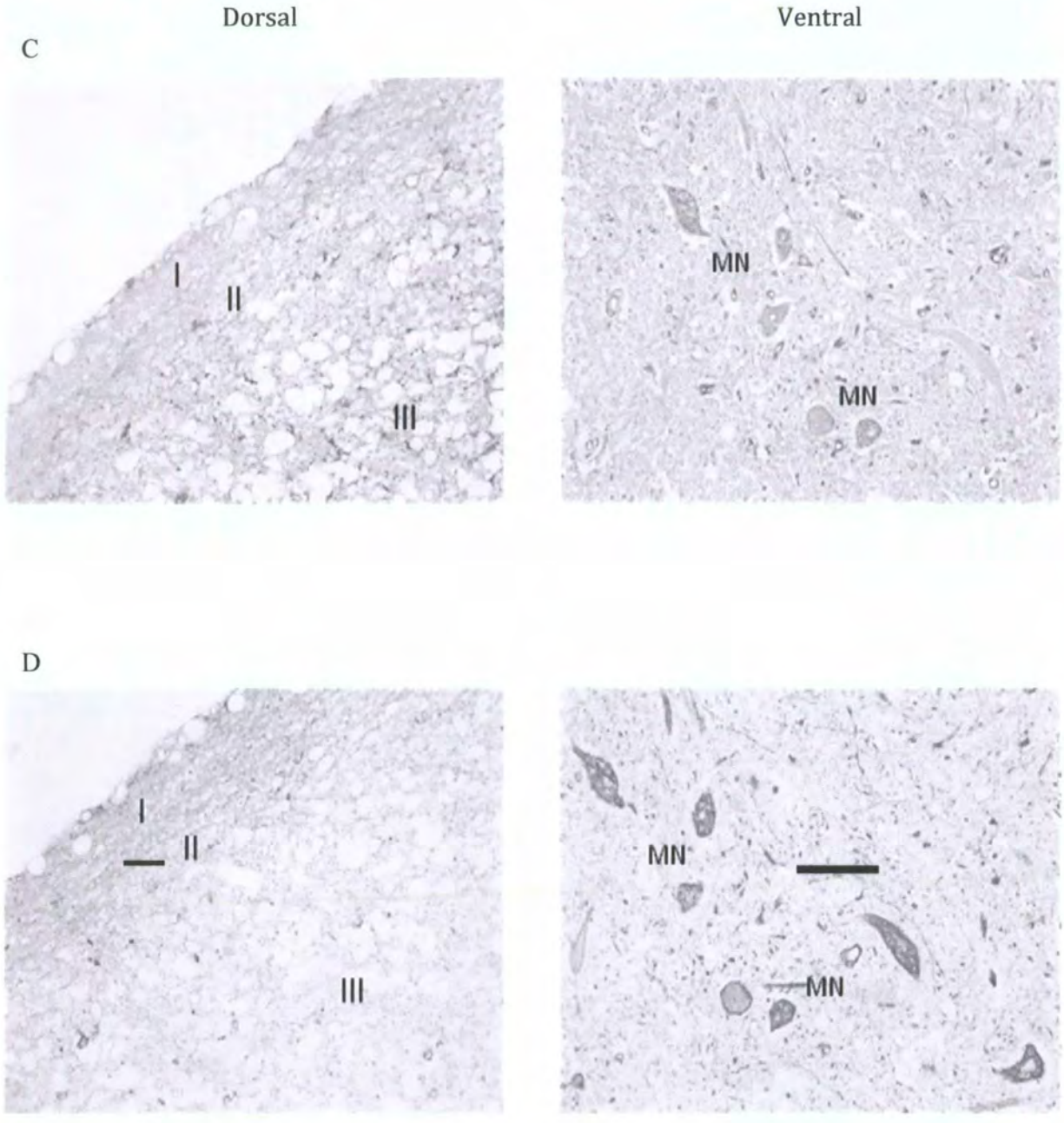


**Figure 4.18 Expression of NR2A (anti-rNR2A 2µg/ml) (C) and NR2B (anti-rNR2B 2µg/ml) (D) in the dorsal horn laminae I, II, III and ventral horns showing the motor neurons (MN) of the cervical human spinal cord (n=1). Scale bars represent 100µm.**

### 4.4.4 Qualitative summary of NMDA receptor subunit expression in the dorsal and ventral horns of the adult human cervical spinal cord

Immunohistochemical investigations into the subunit expression in adult human cervical spinal cord have revealed some initial evidence for NMDA receptor subunit localization differences between the rat and human.

Both species show abundant NR1 expression throughout cervical regions in both the dorsal and ventral horns, consistent with previous findings (Samarasinghe *et al.*, 1996; Sundstrom *et al.*, 1997).

In the human tissue, NR2A shows strong immunoreactivity in the dorsal and ventral horns, showing a similar distribution pattern to NR1, however in the rat spinal cord; more prominent expression was evident in the ventral horn, suggesting more widespread inclusion and prominent role for NR2A in receptor complexes in the human.

NR2B showed prominent immunoreactivity specifically in the superficial laminae of the dorsal horn and in the ventral horn of the adult human cervical cord, whereas in the rat, NR2B was more prominent in the dorsal horn and showed more limited expression in the ventral areas. This evidence suggests that NR2B may have a greater role in motor neuronal transmissions in the human than in the rat.

| Spinal cord level | Region | Intensity of immunoreactivity | | | |
|---|---|---|---|---|---|
| | | NR1 | NR2A | NR2B | NR3B |
| | Dorsal horn | ++++ | +++ | ++ | (+) |
| Cervical | Ventral horn | ++++ | +++ | ++++ | ++ |

**Table 4.4 Qualitative summary of the average intensity of immunoreactivity for each subunit in the cervical region of adult human spinal cord.**
**(+) = Very weak expression, + = Weak expression, ++ = Moderate expression,**
**+++ = Strong expression, ++++ = Very strong expression.**

## 4.5 Co-associations of NMDA subunits in the rat spinal cord

Co-expression of specific NMDA subunits within particular cells and regions of the spinal cord has been established, however, the specific co-associations, particularly of the NR3B subunit, which combine to form functional NMDA receptors within these neurons is a characterisation needed to further understand the pharmacology and function of these channels and for therapeutic receptor targeting.

Optimisation of solubilisation conditions to isolate these membrane bound receptors was undertaken followed by generation of NR1, NR2A immunoaffinity columns to pull down and isolate specific NMDA receptor subunits and their co-associations from native receptors in adult rat cervical spinal cord.

### 4.5.1 Solubilisation and immunopurification of adult rat spinal cord receptors using 1% SDS.

The cervical region of adult rat spinal cord (3-4mg/ml protein) was homogenized and solubilised using 1% SDS, a technique utilized by Lau *et al.*, 1996 and Chung *et al.*, 2004 to purify NMDA receptors from adult rat forebrain.

Immunoblotting was carried out following solubilisation with 1% SDS (2.2.12.2), loading the solubilised and unsolubilised fractions for analysis. The nitrocellulose was probed overnight with anti-rNR1 (2μg/ml), anti-rNR2A (2μg/ml), anti-rNR2B (2μg/ml) and the commercial anti-rNR3B (1:1000), with the resulting detection of NR1 (120KDa), NR2A (180KDa), NR2B (180KDa) and NR3B (100KDa) and therefore efficient solubilisation of all four subunits from the rat spinal cord.

This solubilised material was then applied to an anti-NR1 immunoaffinity column to investigate the co-associations of the NR1 subunit within this tissue.

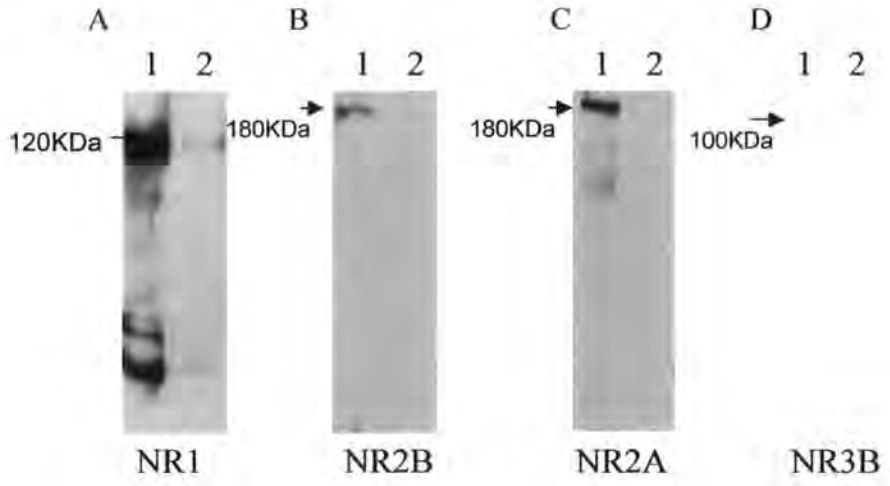


**Figure 4.19 Representative immunoblots (n=2) showing solubilised membranes (lane 1) and unsolubilised membranes (lane 2) probed overnight with anti-rNR1 (2µg/ml) (A), anti-rNR2B (2µg/ml) (B), anti-rNR2A (2µg/ml) (C) and anti-rNR3B (1:1000) (D).**

#### 4.5.1.1 Immunopurification of 1% SDS solubilised adult rat spinal cord homogenate using an anti-NR1 immunoaffinity column

Following the solubilisation of the cervical spinal cord homogenate in 1% SDS and dialysis of the solubilised material, the solubilised fraction was applied to an anti-NR1 immunoaffinity column overnight at $4^0$C to investigate co-associations with the NR1 subunit. Following washing steps, the bound fraction was eluted with glycine pH 2.3, immediately neutralized with 2M Tris pH 7.4 and analysed using immunoblotting.

The NR1 subunit has been successfully solubilised, purified and eluted in elutions 2-4, confirming the functioning of the column. Both the NR2A and the NR2B subunits have also been solubilised, though show no co-associations with NR1 under these conditions as there is no evidence of these subunits in the column elutions implying disruption of the native receptor complex and protein instability. In these assays, NR3B solubilisation was inconsistent, likely to be due to such low expression levels in the spinal cord.

To reduce the denaturing conditions of solubilising in 1% SDS, optimization of detergent concentrations was investigated.

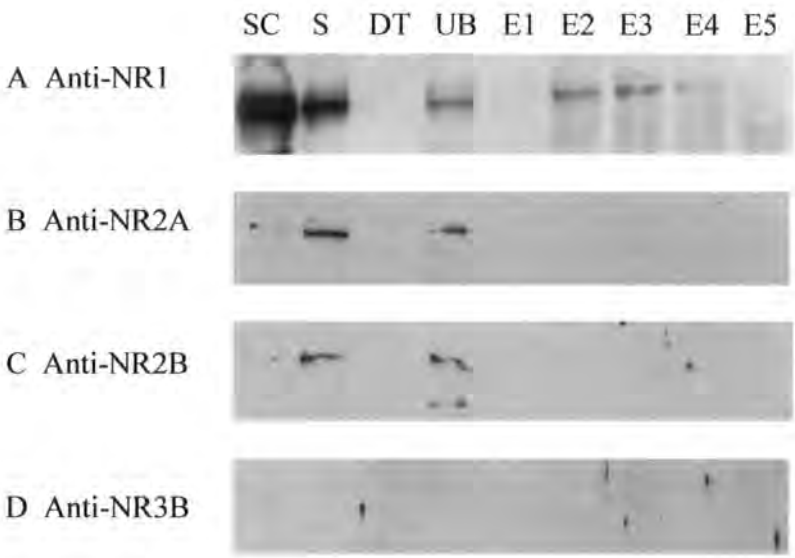


**Figure 4.20 Immunoblot showing adult rat spinal cord homogenate (25µg/ml) (SC), solubilised membranes (S), unsolubilised membranes (DT), unbound material (UB) and elutions 1-5 (E1-5), probed overnight with anti-NR1 (2µg/ml), anti-NR2A (2µg/ml), anti-NR2B (2µg/ml) and anti-NR3B (1:1000). Representative immunoblots from n=3 experiments.**

#### 4.5.1.2 Optimisation of SDS solubilisation between 0.75 and 0.05%.

To investigate the optimal SDS concentrations for effective solubilisation and co-association, the concentration of the detergent SDS was reduced in increments between 0.75% and 0.05%. Following solubilisation, the material was analysed using immunoblotting, probing overnight with anti-rNR1 (2µg/ml), anti-rNR2A (2µg/ml), anti-rNR2B (2µg/ml) and commercial anti-NR3B (2µg/ml). The first set of immunoblots showed that the abundant NR1 subunit solubilised effectively down to 0.05% [SDS], possibly due to large intracellular pools which are easy to solubilise. Both NR2A and NR2B were solubilised at 0.5% [SDS], with lower concentrations seemingly unsuccessful at removing these subunits from the cell membrane. NR3B was solubilised effectively to 0.1% [SDS], suggesting it may be more readily removable from the cell membrane than the NR2 subunits.

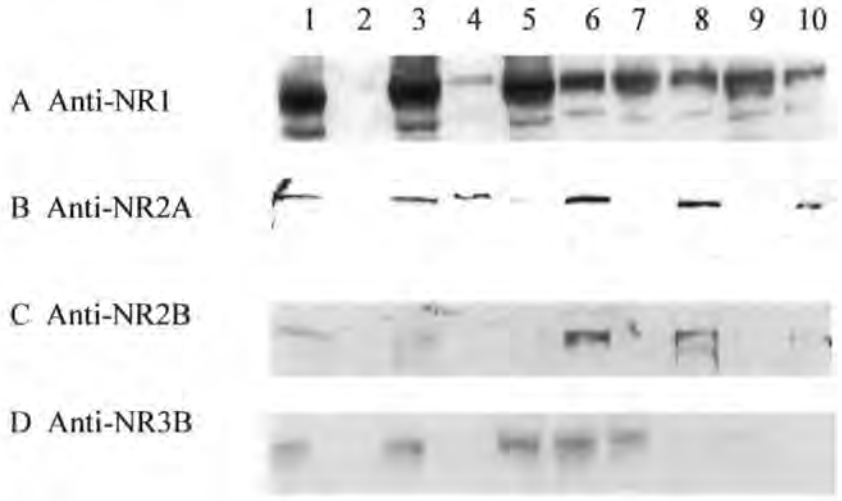


**Figure 4.21 Immunoblots (n=1) showing solubilised and unsolubilised membranes at 0.75% [SDS] (1+2), solubilised and unsolubilised membranes at 0.5% [SDS] (3+4), solubilised and unsolubilised membranes at 0.25% [SDS] (5+6), solubilised and unsolubilised membranes at 0.1% [SDS] and solubilised and unsolubilised membranes at 0.05% [SDS]. Probed with anti-NR1 (2µg/ml) (A), anti-NR2A (2µg/ml) (B), anti-NR2B (2µg/ml) and anti-NR3B (1:1000).**

#### 4.5.1.3 Optimisation of SDS solubilisation between 0.5 and 0.2%.

The variable extents to which the four subunits were solubilised between 0.5 and 0.1% required further optimization; therefore concentrations between 0.5 and 0.2% SDS were also investigated using the same immunoblotting procedure.

Again, NR1 was effectively solubilised down to 0.2% SDS. NR2A was effectively solubilised at concentrations down to 0.3% before the levels of NR2A in unsolubilised material were greater. NR2B and NR3B were also effectively solubilised at 0.2% SDS in a similar manner to NR1. From these concentration ranges of SDS, all four subunits were solubilised effectively at 0.3% SDS and therefore it was decided to proceed to immunopurification using this detergent concentration, applying the solubilised material firstly to an anti-NR1 column and secondly to an anti-NR2A column.

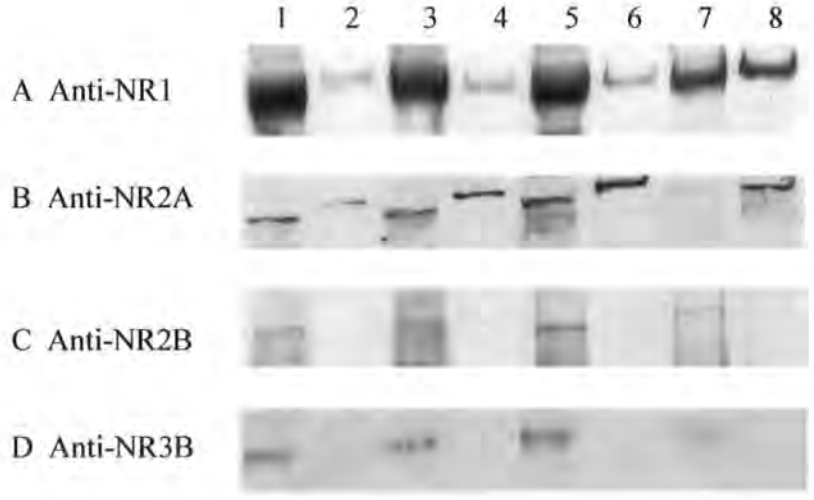


**Figure 4.22 Immunoblots (n=1) showing solubilised and unsolubilised membranes at 0.5% [SDS] (1+2), solubilised and unsolubilised membranes at 0.4% [SDS] (3+4), solubilised and unsolubilised membranes at 0.3% [SDS] (5+6), solubilised and unsolubilised membranes at 0.2% [SDS]. Probed with anti-NR1 (2µg/ml) (A), anti-NR2A (2µg/ml) (B), anti-NR2B (2µg/ml) and anti-NR3B (1:1000).**

#### 4.5.1.4 Immunopurification of 0.3% SDS solubilised material from adult rat cervical spinal cord using anti-NR1 and anti-NR2A immunoaffinity columns

Using the optimized concentration of 0.3% SDS to effectively solubilise the NMDA receptor subunits, immunopurification was carried out to determine whether the native receptor complex associations could be elucidated.

Solubilised material was applied to either an anti-NR1 immunoaffinity column or an anti-NR2A immunoaffinity column as described previously (2.2.12.3) and following overnight incubation, the bound fractions were eluted and analysed with immunoblotting. The nitrocellulose was probed with anti-rNR1 (2μg/ml), anti-rNR2A (2μg/ml), anti-rNR2B (2μg/ml) and commercial anti-NR3B (2μg/ml).

#### 4.5.1.5 Immunopurification using an anti-NR1 affinity column.

NR1 has been successfully solubilised, purified and eluted from the column. NR2A has also been effectively solubilised, bound to the column (demonstrated by lack of protein in the unbound lane) and possibly eluted in fractions 4 and 5. Faint immunoreactivity shows minimal solubilisation of NR2B with an indication, but no clear elution. NR3B has also been solubilised, with seemingly specific immunoreactive bands in elutions 2 and 3, which are of a higher molecular weight possibly due to dimerisation of associated subunits. This experiment gives potential evidence of NR1, NR2A and NR3B co-association from native adult rat spinal cord preparations.

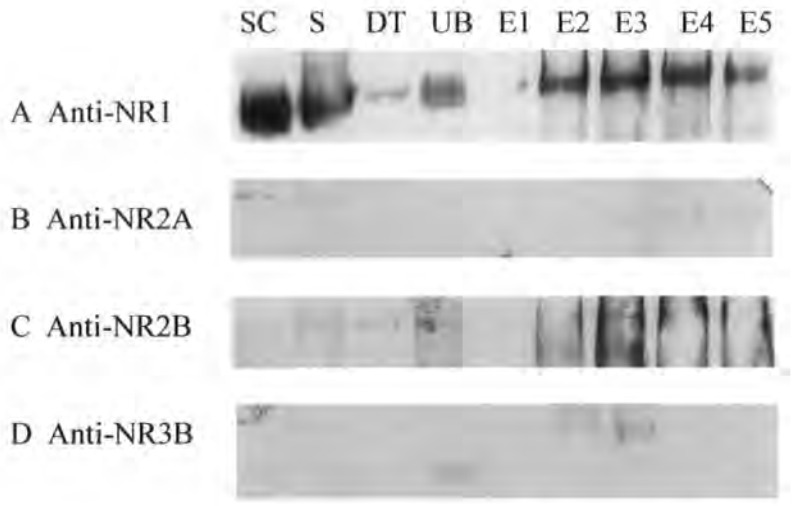


**Figure 4.23 Representative immunoblots (n=2) showing purified fractions from an anti-NR1 affinity column. Spinal cord homogenate (25µg/ml) (SC), solubilised membranes (S), unsolubilised membranes (DT), unbound material (UB) and elutions 1-5 (E1-5). Probed with anti-NR1 (2µg/ml) (A), anti-NR2A (2µg/ml) (B), anti-NR2B (2µg/ml) and anti-NR3B (1:1000).**

### 4.5.1.6 Immunopurification using an anti-NR2A affinity column

Applying the 0.3% SDS solubilised material to an anti-NR2A immunoaffinity column resulted in NR2A uptake onto the column but minimal immunoreactivity in the elutions. NR1 has been solubilised and purified in elutions 1 and 2 via co-association with the NR2A subunit. Low level expression of NR3B in the cervical spinal cord is evident from weak immunoreactivity, though the subunit has been solubilised. The majority of the solubilised NR3B remains unbound to the column, though immunoreactivity in elution 2 may be evidence for co-association of NR3B with NR2A. Therefore, again there is possible evidence for co-association of NR1, NR2A and NR3B in native adult rat cervical spinal cord. It has previously been suggested that NR3A has weak interactions with anchoring proteins and possibly other subunits (Perez-Otano *et al.*,

2006) and therefore NR3B may behave similarly, solubilising effectively but loosing interactions, reducing purification efficiencies. The difficulty in solubilising and eluting NR2B and in maintaining receptor complex co-assembly is likely to be the result of low expression levels in the cervical cord and possibly protein instability and sensitivity towards the strongly ionic detergent SDS.

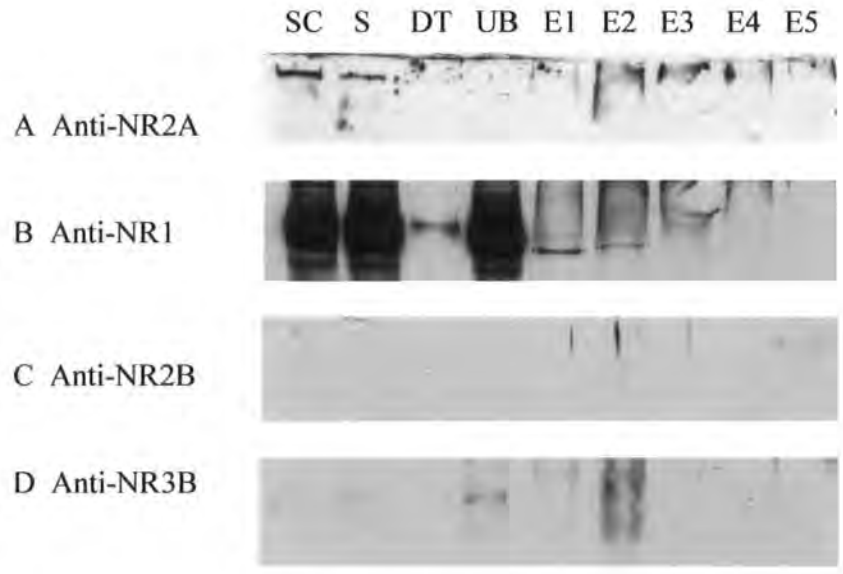


**Figure 4.24 Representative immunoblots (n=2) showing purified fractions from an anti-NR2A affinity column. Spinal cord homogenate (25µg/ml) (SC), solubilised membranes (S), unsolubilised membranes (DT), unbound material (UB) and elutions 1-5 (E1-5). Probed with anti-NR1 (2µg/ml) (A), anti-NR2A (2µg/ml) (B), anti-NR2B (2µg/ml) and anti-NR3B (1:1000).**

**4.6 NR2A, NR2B and NR3B protein expression levels in different spinal cord regions**

To further optimize the likelihood of effective solubilisations, different regions of the adult rat spinal cord were analysed using immunoblotting to investigate expression levels of NR2A, NR2B and NR3B.

SDS-PAGE was carried out with adult rat forebrain membranes (20μg), cervical spinal cord membranes (20μg) and thoracic/lumbar spinal cord membranes (20μg) and the nitrocellulose probed overnight with anti-rNR2A (2μg/ml), anti-rNR2B (2μg/ml) and commercial anti-rNR3B (2μg/ml). Re-probing the nitrocellulose with β-actin (an endogenous 'house-keeping' protein) enabled quantitative comparisons of lane loading. The immunoblot shows that NR2A appears to be the most prominent subunit expressed both in the forebrain and spinal cord across the regions. NR3B is particularly expressed within the lower regions of the spinal cord which are more associated with motor systems. The NR2B subunit is more prominently expressed in forebrain regions, with some expression mainly in the lower spinal cord regions. NR2A, NR2B and NR3B therefore have higher expression levels in the lower regions of the spinal cord and it may be important for future investigations to isolate receptors from this region of the cord, or for whole cord preparations to be used, as one of the main difficulties in successful purifications appears to be the low abundance of expression.

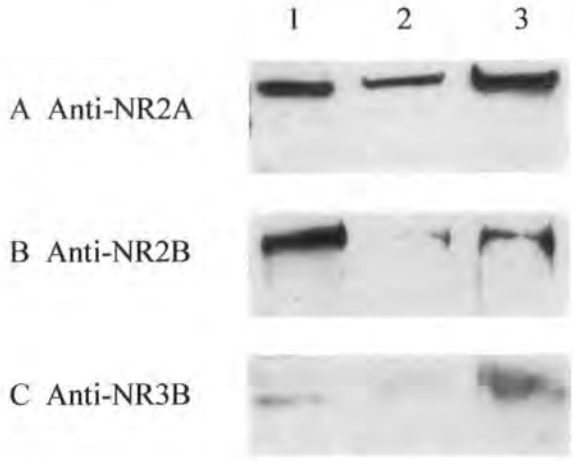


**Figure 4.25 Representative immunoblots (n=3) showing adult rat forebrain membranes (20µg) (1), adult rat cervical cord membranes (20µg) (2) and adult rat thoracic/lumbar cord membranes (20µg) (3). Probed with anti-rNR2A (2µg/ml), anti-rNR2B (2µg/ml) and anti-rNR3B (1:1000).**

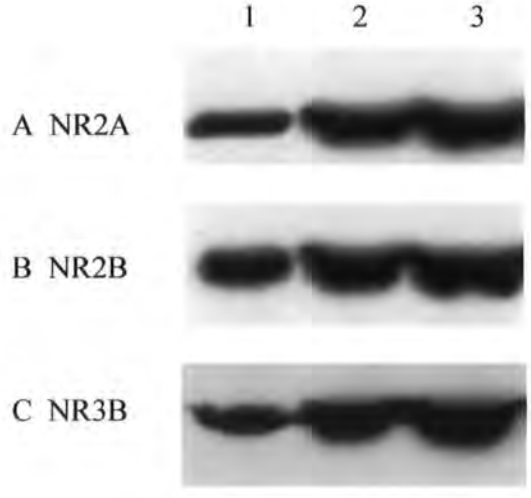


**Figure 4.26 Re-probing the immunoblots in figure 4.22 with anti-mouse β-actin (1:1000). Immunoblot showing adult rat forebrain membranes (20µg) (1), adult rat cervical cord membranes (20µg) (2) and adult rat thoracic/lumbar cord membranes (20µg) (3).**

## 4.7 Discussion

The importance of unravelling the heterogeneity of the NMDA receptor complex and understanding the impact of different subunit combinations on receptor signaling is evident when considering pharmaceutical intervention.

Antibodies remain one of the most useful, diverse molecular tools for investigating these factors and have been widely used for NMDA receptor characterization since the molecular cloning of the respective subunits. In this chapter a panel of subunit-selective polyclonal antibodies was used to investigate NMDA subunit expression in the adult rat and human spinal cord, and to decipher native NMDA receptor subunit co-associations in the adult rat spinal cord.

The panel of selective anti-NR1 (929-938), anti-NR2A (1435-1445) and anti-NR2B (46-60) polyclonal antibodies utilized throughout this thesis for western blotting, immunohistochemsitry and immunopurification have previously been characterized and validated in our laboratory (Chazot *et al.*, 1992; Cik *et al.*, 1993; Chazot and Stephenson, 1997). In order to investigate the expression patterns and associations of the NR3B subunit, an anti-rodent NR3B (885-899) polyclonal C-terminal antibody previously published and characterized by Matsuda *et al.*, 2002 was generated and affinity purified via coupling specifically to a newly generated antigenic peptide sepharose column. The synthetic peptide TGPPEGQQERAEQEC corresponding to amino acids 885-899 in the mouse NR3B C-terminal region is identical to the rat NR3B sequence except for one amino acid change substituting at the end of the sequence from cysteine to arginine. To confirm the characterisation and specificity noted by Matsuda and colleagues, the anti-NR3B (885-899) was tested against native adult rat forebrain

and spinal cord tissue and recombinant rat NR3B clones (pCISNR3B, pCISNR1-1a, pCISNR3A cDNA transfection into HEK 293cells) and the peptide specificity confirmed using peptide blockade. Immunoreactivity towards the recombinant NR3B cDNA identifying a species approximately 100KDa and a lack of cross-immunoreactivity with the NR3A cDNA was in agreement with results published by Matsuda *et al.*, who also confirmed specificity with recombinant NR3B expression in HEK293 cells (Matsuda *et al.*, 2002). Immunoreactivity in the native tissue identified molecular weight species at approximately 100KDa, but also a more prominent smaller molecular weight species at approximately 30KDa. This protein species was confirmed as antigenic peptide specific, upon pre-absorption of anti-NR3B with the antigenic peptide, therefore this smaller species is likely to be a proteolytic fragment or due to post-translational modifications of the subunit present in native neurons.

During the development and characterization of the anti-NR3B (885-899) antibody, an Upstate® commercial polyclonal rat anti-NR3B antibody was purchased for expression studies. The commercial anti-rNR3B was raised in rabbits against the C-terminal amino acids 915-927 RRVRRAVVERERR and showed immunoreactivity towards a diffuse species of ~110KDa in adult rat forebrain and spinal cord homogenate and towards a smaller species ~30KDa likely to result from post-translational modifications, consistent with that of the in house anti-rodent NR3B (885-899).

A novel anti-human NR3B (885-889) raised against the synthetic peptide sequence CTGPPEGSKEETAEAE in the C-terminal of the human NR3B sequence, was also generated and affinity purified via a novel antigenic peptide sepharose affinity column. The anti-hNR3B (885-899) antibody was characterized using western blotting with post-

mortem human putamen homogenate (obtained as a gift from Dr Margaret Piggott, Newcastle University) where immunoreactivity identified a large peptide specific species ~174KDa which may be due to NR3B subunit dimerisation. A prominent doublet species evident at ~82KDa may be a proteolytic fragment of this larger NR3B species caused by post mortem delay. The human anti-NR3B (885-899) also showed immunoreactivity towards adult rat forebrain and spinal cord membranes, identifying the same small molecular weight species ~30KDa despite eight amino acid changes in the sequence. This evidence for cross-reactivity with the rat NR3B protein was also confirmed using ELISA data and was again shown to be specific with antigenic peptide blockade. ELISA assays (data not shown) were performed on each bleed of the anti-human NR3B antibody and showed that it has a high titer (1 in 30000) and cross-reacts with the rat antigenic peptide due to sequence homology with the first 6 amino acids of the peptide, which may form the primary epitope.

The expression pattern of the various NMDA receptor subunits has been the focus of many studies particularly within the rodent brain and spinal cord, though many focus on single subunit expression (e.g. Samarasinghe *et al.*, 1996) or expression of multiple subunits in one particular region of tissue (e.g. Nagy *et al.*, 2004). This study enhances current knowledge by directly analysing NR1, NR2A, NR2B and NR3B subunit expression in human cervical tissue and within rat cervical, thoracic and lumbar tissue, providing the first parallel data set on NR3B protein expression in different spinal levels. Immunohistochemical analysis probing adult rat tissue with anti-NR1 (929-938) shows abundant expression throughout the cervical, thoracic and lumbar regions

confirming the presence of NMDA receptors on glutamatergic synapses (Nagy *et al.*, 2004) throughout the spinal cord adding to previously published mRNA (Tolle *et al.*, 1993; Furuyama *et al.*, 1993; Goebel *et al.*, 1999) and protein (Nagy *et al.*, 2004) expression studies in rat lumbar cord. NR1 protein expression was evident in both the dorsal and ventral horns, showing NMDA receptor involvement in both sensory and motor system transmissions. High levels of immunoreactivity may also result from the large intracellular pools of monomeric NR1 subunits, associated with endoplasmic reticulum, which may serve as a reserve for receptor up-regulation (Chazot and Stephenson, 1997).

Expression of the NR2A subunit followed a similar abundant pattern to that of the NR1 subunit showing that NMDA receptors in the spinal cord may be predominantly composed of receptors containing NR1/NR2A subtypes. This data is consistent with previous findings detailing prominent NR2A mRNA expression in adult rat (Nagy *et al.*, 2004) and human spinal cord (Samarasinghe *et al.*, 1996), but in contrast to Tolle *et al.*, 1993 who report undetectable levels of NR2A mRNA in rat lumbar spinal cord.

Interestingly, Nagy *et al.*, 2004 and Watanabe *et al.*, 1994 report a distinctly increased level of NR2A mRNA expression in laminae III of the dorsal horn in comparison with laminae I and II, thought to be particularly located within post-synaptic areas, however no such clear distinction in protein expression is apparent in this study which may be accounted for by post-translational protein transportation within the cell to processes located in other regions. The distribution of low-threshold cutaneous primary afferent terminals within laminae III and the presence of NR2A immunoreactivity on synapses

opposed to primary afferent terminals suggest a role for NR2A-containing receptors in low threshold sensory transmission (Nagy *et al.*, 2004).

In this study prominent expression of NR2A is apparent within the cell bodies of motor neurons consistent with previous results showing protein expression of NR2A in lamina IX and NR2A presence on synapses in the ventral horn (Nagy *et al.*, 2004) and suggesting a role for NR2A-containing receptors in motor systems.

Expression patterns of the NR2B subunit show some distinction from the NR2A subunit, implying a different functional role within distinct loci. NR2B protein expression was concentrated in the superficial laminae I and predominantly II in the dorsal horn throughout each region of the spinal cord particularly evident in the thoracic and lumbar regions. These findings are consistent with previous research showing NR2B mRNA concentrated in lamina II (Watanabe *et al.*, 1994) and NR2B protein expression in rat lumbar cord (Shibata *et al.*, 1999; Nagy *et al.*, 2004), though in contrast to a study showing undetectable levels of NR2B mRNA in adult rat lumbar cord (Tolle *et al.*, 1993). Implications of NR2B subunit involvement in nociceptive transmission resulted from the detection of prominent expression in the superficial laminae of the spinal cord where most nociceptive primary afferents terminate and has since been proven with many studies where NR2B gene knockdown attenuates formalin-induced nociception in the rat (Tan *et al.*, 2005) and NR2B-selective antagonists induce antinociception (e.g., Boyce *et al.*, 1999). Current data contributes to the evidence for NR2B involvement in windup of spinal neurons with both synaptic (Nagy *et al.*, 2004) and extrasynaptic (Momiyama, 2000) NR2B-containing receptors in this region. It is

this combined evidence that is driving forward the search for effective NR2B antagonists.

NR2B protein expression was also detected in the large cell bodies of motor neurons in the ventral horn, particularly within the cervical region, suggesting a role for the NR2B subunit in motor neurons as well as sensory neurons. These results confirm previous findings showing NR2B mRNA (Shibata *et al.*, 1999) and protein (Nagy *et al.*, 2004) expression in somatic motor neurons and therefore pharmaceutical targeting of NR2B-containing receptors is likely to additionally affect motor systems. This modulation could therefore present adverse side effects, when targeting sensory areas; however it could potentially be advantageous and therapeutically useful for diseases such as motor neuron disease where antagonists may be able to reduce motor neuronal cell death due to glutamate toxicity, as well as targeting the sensory areas to combat conditions such as chronic pain.

NR3B expression was predominantly located within the large cell bodies of motor neurons and their dendrites in all three regions of the rat spinal cord consistent with previous mouse mRNA data (Nishi *et al.*, 2001; Matsuda *et al.*, 2002; Fukaya *et al.*, 2005). The immunoreactivity of NR3B within the motor neuron cell bodies may result from the presence of large intracellular pools of monomeric subunit or extrasynaptic receptors (Matsuda *et al.*, 2003), activated following synaptic stimulation (Clark and Cull-Candy, 2002). It is possible that NR3B is transported from internal stores and incorporated into the receptor complex upon up-regulation of synaptic input in order to regulate calcium entry into the cell.

There was also evidence for some minimal immunoreactivity of NR3B within the dorsal horn particularly within the thoracic and lumbar regions suggesting that NR3B may additionally be involved in modulation of sensory pathways. A previous study identified rat NR3B mRNA in the hippocampus (Andersson *et al.*, 2001) and recent research suggests more wide-spread localization with NR3B protein expression in the cortex, striatum and hippocampus (Wee *et al.*, 2007), evidence to suggest NR3B-containing NMDA receptor modulation of sensory signaling.

In the human cervical spinal cord, NR1 protein was abundantly expressed in both dorsal and ventral horns and again predominantly in neuronal cell bodies, consistent with previous studies examining mRNA expression (Samarasinghe *et al.*, 1996) and protein expression in lumbar regions of human spinal cord (Sundstrom *et al.*, 1997).

Expression of NR2A protein in the human cervical cord, showed a similar wide-spread distribution to that detected in the rat tissue, but with seemingly increased expression in the dorsal regions. Prominent immunoreactivity was evident in the superficial laminae I, II and III of the dorsal horn and in the motor neuronal cell bodies of the ventral horn consistent with mRNA studies in human spinal cord (Samarasinghe *et al.*, 1996), lumbar-sacral (Sundstrom *et al.*, 1997) and cervical regions (Luque *et al.*, 1994).

In the human cervical tissue, NR2B protein expression is predominantly located in the superficial laminae I and II contrasting with a previous study which showed undetectable levels of NR2B protein in human lumbar-sacral cord (Sundstrom *et al.*, 1997). The expression pattern of NR2B implies a similar involvement of NR2B-containing receptors in nociceptive afferent signaling in the human and the rat. There is also prominent immunoreactivity of NR2B in the motor neurons of the ventral horn,

greater than that observed in the rat cervical tissue, possibly implying a greater role for NR2B in motor transmissions in the human.

Interestingly, expression levels of the NMDA NR2 subunits between rodent species varies considerably. The immunoblot below carried out using adult mouse tissue, shows that the predominant subunit expressed in the forebrain and spinal cord is the NR2B subunit, however in adult rat tissue, the predominant NR2 subunit appears to be NR2A showing an expression pattern more closely related to the human. These important species differences have yet to be fully characterized but this initial evidence could have important implications for the design of subunit specific drugs and the use of animal models when relating data to human NMDA targets.

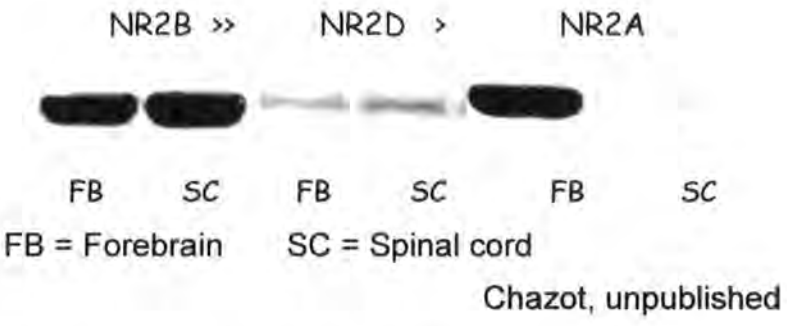


Expression of the NR3B protein in the human cervical tissue showed a similar distribution to that of the rat with predominant localization in the motor neurons of the ventral horn consistent with expression in rodent studies (Matsuda *et al*, 2003; Fukaya *et al*., 2005; Wee *et al*., 2007). Undetectable expression of NR3B in the dorsal horn of the human cervical cord may be initial evidence for either a species difference or for expression changes between the cervical, thoracic and lumbar regions, as in the rat NR3B expression in the dorsal horn appeared to increase as the spinal cord was descended.

These data provide evidence for protein expression and co-localisation of NR1, NR2A, NR2B and NR3B in adult rat spinal cord in both dorsal and ventral horns and for the co-localisation of NR1/NR2A/NR2B in human dorsal horn and NR1/NR2A/NR2B/NR3B co-localisation in adult human ventral horn of the cervical spinal cord.

Co-localisation of NR1, NR2A, NR2B and NR3B within the same cell type (and even the same cell) does not necessarily translate into the co-assembly of all four subunits to form functional NMDA receptors expressed on the cell surface. Therefore it was important to investigate the native spinal cord NR3B-containing receptor co-assemblies, via immunopurification.

In order to carry out immunopurification, the NMDA receptors present in the rat spinal cord homogenate must be available in a stable, detergent-solubilised preparation although previous research has found that the NMDA receptor is notoriously resistant to detergent extraction (Chazot and Stephenson, 1997).

The detergent most widely used for extraction of NMDA receptors from rodent brain tissue is 1% (wt/vol) sodium deoxycholate (pH9.0) (Chazot and Stephenson, 1997; Blahos and Wenthold, 1996; Sundstrom *et al.*, 1997) though inconsistent levels of subunit solubilisation were achieved from spinal cord preparations in this study (data not shown) possibly due to the lower expression levels of the subunits in the spinal cord. Temperature optimization was attempted to increase solubilisation efficiencies (Blahos and Wenthold, 1996) though immunoblotting analysis of the solubilised receptors showed minimal differences in the efficiency of solubilisation of the NR1, NR2A, NR2B and NR3B subunits between 4 and $37^0$C. The inconsistencies in solubilisation

efficiency with 1% DOC between experiments may be due to reduced receptor abundance in the spinal cord or possible differences in the stability of the complexes between the forebrain and spinal cord. Blahos and Wenthold, 1996 stated that 'the NMDA receptor complex is dissociated more readily than it is solubilised' causing inherent problems when trying to extract in-tact native complexes for analysis.

To achieve increased efficiency of solubilisation, particularly of the NR2 and NR3 subunits, detergent extraction using SDS (pH7.4) was attempted, following a protocol published by Richard Huganir's group in 2004 (Chung *et al.*, 2004). As expected, this strongly ionic detergent successfully solubilised high yields of all four subunits NR1, NR2A, NR2B and NR3B, though immunoaffinity purification demonstrated that the NMDA complex had been dissociated by the stringent conditions. The concentration of SDS required for effective solubilisation but maintenance of complex association was therefore optimized. 0.3% (wt/vol) SDS was the lowest concentration that successfully achieved good solubilisation and provided some limited initial purification data. Immunopurification using the anti-NR1 column showed potential evidence for co-association of NR1/NR2A/NR3B and possibly NR2B subunits, with a high molecular weight species in the elutions possibly suggesting subunit dimerisation of NR3B. Immunopurification using an anti-NR2A column yielded clear association of NR1/NR2A, though solubilisation of NR2B remained problematic. The association between the NR1 and NR2A subunit reflects the abundant expression of these two subunits in the spinal cord seen in the immunohistochemical analysis, and it may be the reduced expression of NR2B and NR3B in this region of the spinal cord which made effective solubilisation and detection very difficult. It is also possible that associations

between the NR1, NR2 and NR3 subunits differs in strength between the brain and the spinal cord, with weaker associations being disrupted in the spinal cord preventing successful purifications.

The NR1/NR2A and possible NR1/NR2B, NR1/NR2A/NR2B associations observed are consistent with previous co-immunoprecipitation data of NMDA subunits from adult rat forebrain (Blahos and Wenthold, 1996), immunopurification data from adult mouse forebrain using an anti-NR1 column (Chazot and Stephenson, 1997) and immunoprecipitation from adult human lumbar-sacral cord (Sundstrom *et al.*, 1997).

Initial evidence for the co-association of NR3B with NR1 or NR1/NR2A and possibly NR1/NR2B or NR1/NR2A/NR2B from adult rat spinal cord supports previous data showing NR1/NR2A/NR3B association in recombinant HEK293 cell *in vitro* models (Nishi *et al.*, 2001; Matsuda *et al.*, 2003). It has also been shown that the NR3A subunit (shares 62% homology with NR3B) associates with NR1/NR2A/NR2B in adult rat brain preparations (Al-Hallaq *et al.*, 2002) and adult human brain and spinal cord (Nilsson *et al.*, 2007).

In order to maximize the likelihood of effective solubilisation and purification of NR3B-containing NMDA receptors whole spinal cords, or preparations containing thoracic and lumbar sections should be used to ensure the greatest abundance of subunit expression, as it is evident from the immunoblotting studies that subunit expression is increased in lower regions of the cord.

The data in this chapter provides novel evidence for co-localisation of the NR3B protein and NR1, NR2A and NR2B throughout the cervical, thoracic and lumbar regions of rat spinal cord and human cervical cord. It also presents initial data to suggest variable

expression patterns of the NR3B subunit between spinal cord regions and co-association of NR3B with NR1 and NR2A in native receptors from adult rat cervical spinal cord. Further characterization of native NMDA receptor complexes within the spinal cord is required, particularly of the little known NR3B subunit to fully understand the mechanisms of NMDA receptor signalling and the consequences of pharmaceutical targeting.

# Chapter 5

# The influence of NR3 subunits on NMDA receptor cytotoxicity, physiology and pharmacology

## 5.1 Introduction

### 5.1.1 Effect of NR3 subunits upon NMDA-mediated cytotoxicity

Influx of calcium, mediated in part by NMDA receptors plays a vital role in normal neurological functions. However, over-activation of NMDA receptors leading to calcium toxicity has been implicated in various neuropathologies, for example dementias and neurodegenerative disorders such as motor neuron disease.

NR2B-containing receptors in particular have been implicated in the aetiology of disease states due to hyperexcitability of NMDA receptors (Fuller *et al.*, 2006) and have therefore been a target for novel NMDA antagonists with selective subunit specificity.

Interestingly, in contrast to the NR1 and NR2 subunits, previous research suggests that NR3A and NR3B reduce $Ca^{2+}$ permeability when part of the receptor complex (Nishi *et al.*, 2001; Matsuda *et al.*, 2002), potentially reducing intracellular calcium levels and reducing associated adverse effects.

This chapter explores the possibility that this reduction in $Ca^{2+}$ permeability induced by the NR3A and NR3B subunits would be reflected *in vitro* as reduced calcium toxicity and cytoprotection.

The immunohistochemical data in the previous chapter provides initial evidence for NR3B co-localisation with NR1, NR2A and NR2B in both rat and human spinal cords.

The cytotoxicity experiments therefore investigated the potential influences of the NR3 subunits upon both NR2A and NR2B-containing receptors.

### 5.1.2 Effect of NR3 upon the functional and biophysical characteristics of the NR1/NR2B receptor channel

In addition to the cytotoxicity assay, whole-cell patch clamp electrophysiology (2.2.20) was used to investigate the influence of NR3B upon NR1/NR2B functional properties such as calcium permeability, current amplitude, magnesium blockade and reversal potential.

Ionic flux across the cell membrane mediated by NMDA receptor activity was measured using intracellular voltage clamp recordings. Here the cell membrane potential is controlled at -60mV and the ionic current crossing the membrane is measured via an electronic feedback system.

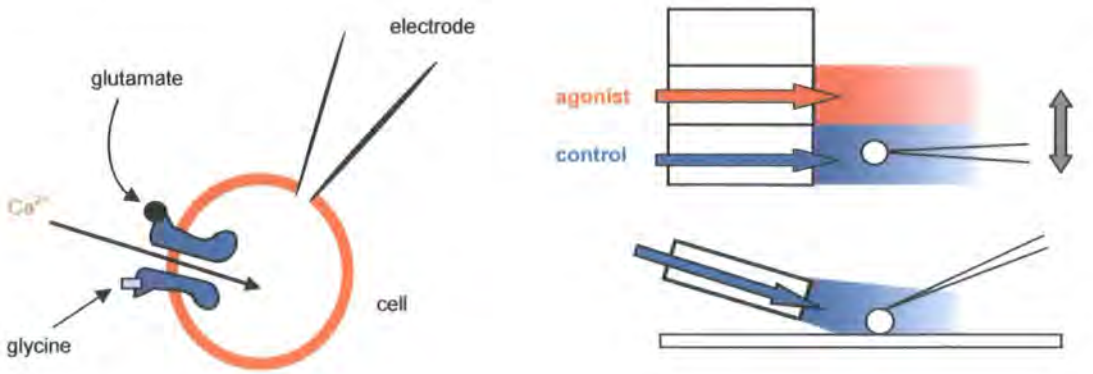


**Figure 5.1 Schematic diagram representing electrode position and cell placement in the microscope bath beneath the barrels used for rapid agonist and antagonist application (From Jon Spencer, GSK).**

Previous research suggests that the NR3 subunits have a modulatory role within the receptor complex. Recombinant expression of NR3A with NR1/NR2A and NR1/NR2B (Al-Hallaq *et al.*, 2002) and NR3B with NR1/NR2A (Nishi *et al.*, 2001; Matsuda *et al.*, 2002) suggest reduced $Ca^{2+}$ permeability of the receptor in addition to lowered magnesium sensitivity of the complex. This novel study reports the effect of NR3B upon NR1/NR2B and NR1/NR2A receptors and therefore provides important information regarding putative motor neuron NMDA receptor complexes.

### 5.1.3 Pharmacological influences of the NR3B subunit upon NR1/NR2B receptors

Some of the most promising NMDA antagonists generated to date are NR2B subunit selective compounds. In order to understand the pharmacological interactions between these compounds and to develop new higher affinity, potentially more selective antagonists, the associations of NR2B-containing receptors and the influence of the NR3B subunit upon compound pharmacology is vital.

Research to date has shown evidence for two classes of NR2B subunit selective compounds, one which binds only to NR2B-containing receptors and one which binds to NR2B-containing receptors in the presence of other NR2 subunits (Chazot *et al.*, 2002). There is currently no data regarding the influence of the NR3 subunits upon NR2B receptor pharmacology or NR2B-subunit selective compounds. Using the cytotoxicity assay (2.2.19), whole-cell patch clamp electrophysiology (2.2.20) and radioligand binding (2.2.14), this study therefore provides the first novel data investigating the effect of NR3B upon the NR2B-selective compounds Ro-256981, CP-101606, ifenprodil and the novel antagonists COMPOUND A and COMPOUND B.

## 5.2 Results

### 5.2.1 Differential cytoprotective effects of NR3A and NR3B upon cell death mediated by NR1/NR2A and NR1/NR2B receptors expressed in HEK 293 cells.

The Promega CytoTox 96™ cytotoxicity assay can be used as a measure of cell lysis in mammalian cells. The assay allows quantitative measurements of lactate dehydrogenase (LDH), a stable cytosolic enzyme which is released upon cell lysis. LDH from the cultured supernatants is measured with a 30 minute coupled enzymatic reaction that results in conversion of a tetrazolium salt into a red formazan product which can be quantified through measuring absorbance at 490nm.

**5.2.1.1 Differential cytotoxicity of various recombinant NMDA receptors.**

Recombinant NMDA receptor complexes; NR1/NR2A, NR1/NR2A/NR3A, NR1/NR2A/NR3B, NR1/NR2B, NR1/NR2B/NR3A and NR1/NR2B/NR3B were expressed in HEK 293 cells. Following 48hr incubation in the absence of an NMDA antagonist, the cytotoxicity assay was performed (n=6-10 individual experiments).

Co-expression of NR1/NR2B receptor subunits resulted in the highest incidence of cell mortality (50 ± 11%), in comparison to no DNA and NR1 controls. Co-expression of NR1/NR2A receptor subunits resulted in a significantly lower level of cell death (19 ± 2%). The inclusion of the NR3 subunits with NR1/NR2B receptors significantly reduced cell death in comparison to NR1/NR2B receptors alone; NR1/NR2B/NR3A and NR1/NR2B/NR3B co-assemblies showed 29 ± 3% and 23 ± 3% cell mortality, respectively, reflecting significant levels of cytoprotection (figure 5.2). However, co-expression of NR3 subunits with NR1/NR2A receptors showed no significant influence on cell mortality. NR1/NR2A/NR3A and NR1/NR2A/NR3B resulted in 17 ± 3% and 23 ± 2% cytotoxicity with no significant cytoprotection (figure 5.2). These data provide evidence for a differential influence of NR3A and NR3B upon cytotoxicity mediated by NR1/NR2B and NR1/NR2A receptors.

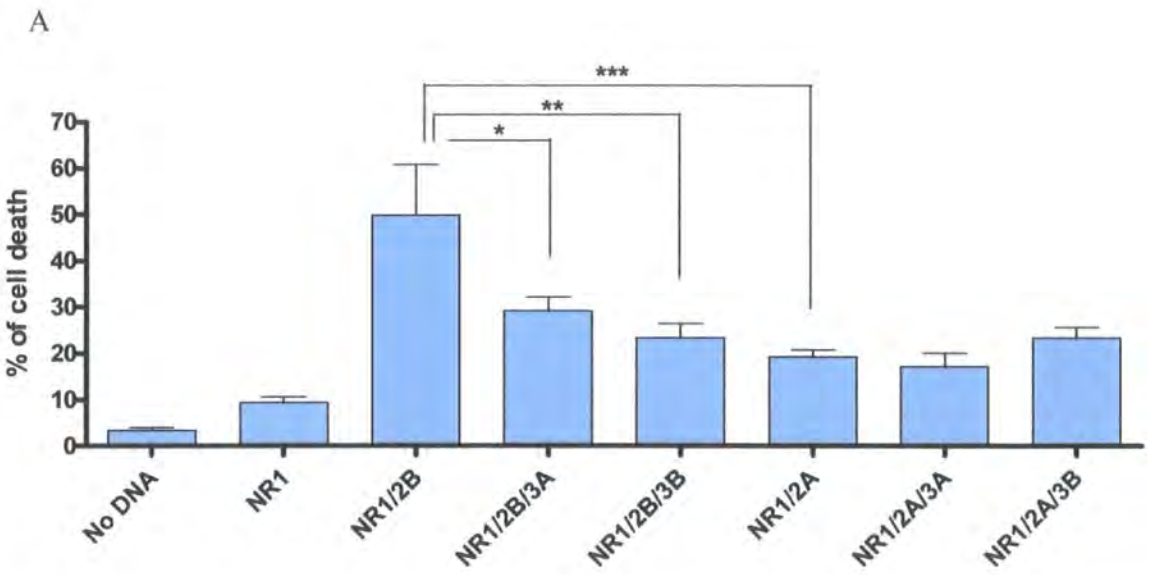


| Receptor combination | Mean ± SEM |
|---|---|
| No DNA | 3 ± 0.6 |
| NR1 | 9 ± 1 |
| NR1/2B | 50 ± 11 |
| NR1/2B/3A | 29 ± 3 |
| NR1/2B/3B | 23 ± 3 |
| NR1/2A | 19 ± 2 |
| NR1/2A/3A | 17 ± 3 |
| NR1/2A/3B | 23 ± 2 |

**Figure 5.2 The percentage cytotoxicity of HEK 293 cells expressing various combinations of NMDA receptor subunits *p<0.05, **p<0.01, ***p<0.001 one way ANOVA.**

### 5.2.2 Functional influence of NR3B upon NR1/NR2B receptor physiology

In order to investigate the functional effects of the NR3B subunit on the NR1/NR2B receptor complex, patch clamp electrophysiology was carried out on recombinant receptors transiently expressed in HEK 293 cells. The parameters measured were current amplitude, reversal potential, calcium permeability and magnesium sensitivity.

### 5.2.2.1 Peak NMDA current amplitude of cells transfected with NR1/NR2B and NR1/NR2B/NR3B receptors.

Whole-cell patch clamp recordings were made from cells transfected with NR1, NR1/NR2B and NR1/NR2B/NR3B receptors (n=25, respectively). GFP-positive cells were taken as a marker of successful transfection. The peak amplitude resulting from receptor channel activation with 10 second application of co-agonists glutamate (100μM) and glycine (10μM) was measured. Pooled data show minimal channel activity (18 ± 5pA) for control NR1 expressed as a single subunit (C). Functional activity in cells expressing NR1/NR2B and NR1/NR2B/NR3B showed peak amplitudes averaging 675 ± 146pA and 592 ± 130pA, respectively; however, there was no statistically relevant reduction in peak amplitude in the presence of NR3B (D and E).

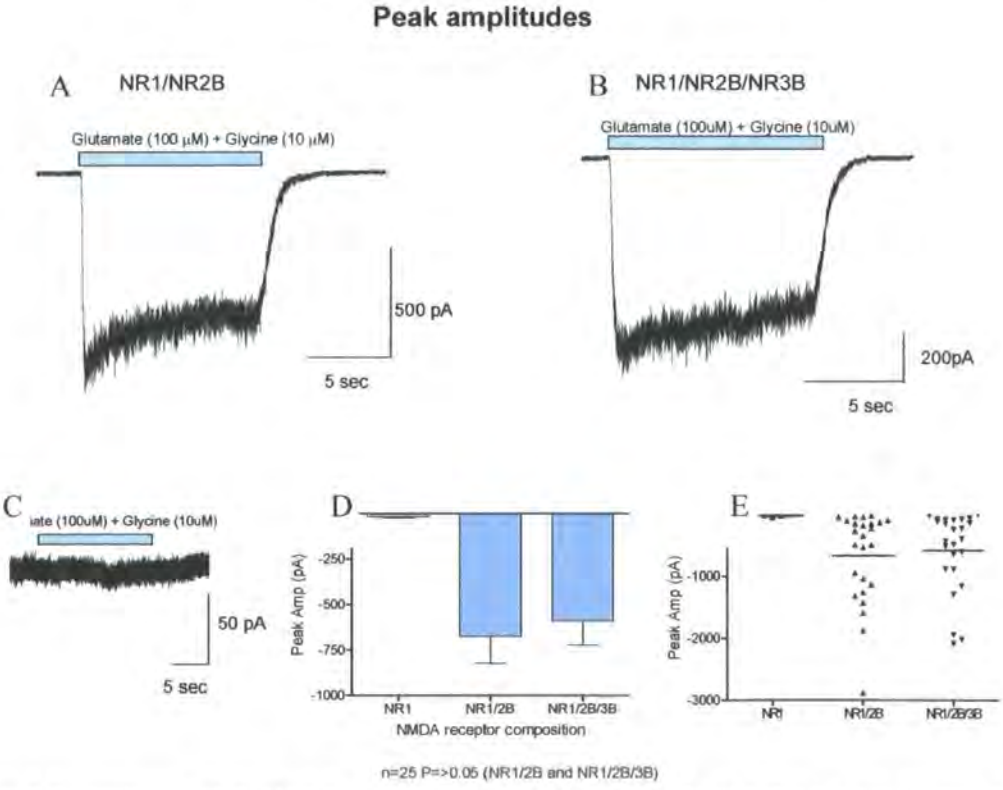


**Figure 5.3 Electrophysiological traces of peak amplitudes (pA) obtained from recombinant NR1/NR2B (A), NR1/NR2B/NR3B (B) and NR1 (C) receptors. Histogram (D) and data range charts (E) show the mean ± SD for 25 individual experiments.**

### 5.2.2.2 Reversal potentials of cells transfected with NR1/NR2B and NR1/NR2B/NR3B receptors.

The current/voltage (I/V) relationship was measured in cells transfected with NR1/NR2B (A) and NR1/NR2B/NR3B (B) receptors (n=21, n=15, respectively). Taking into account the junction potential (potential between two salt solutions, i.e. different concentrations of ions) the reversal potential ($E_{rev}$) for NR1/NR2B was -3.9 ± 1.6mV and for NR1/NR2B/NR3B -3.6 ± 1.6mV. Therefore the characteristics of each channel were very similar, again the presence of NR3B had no statistical effect on reversal potential.

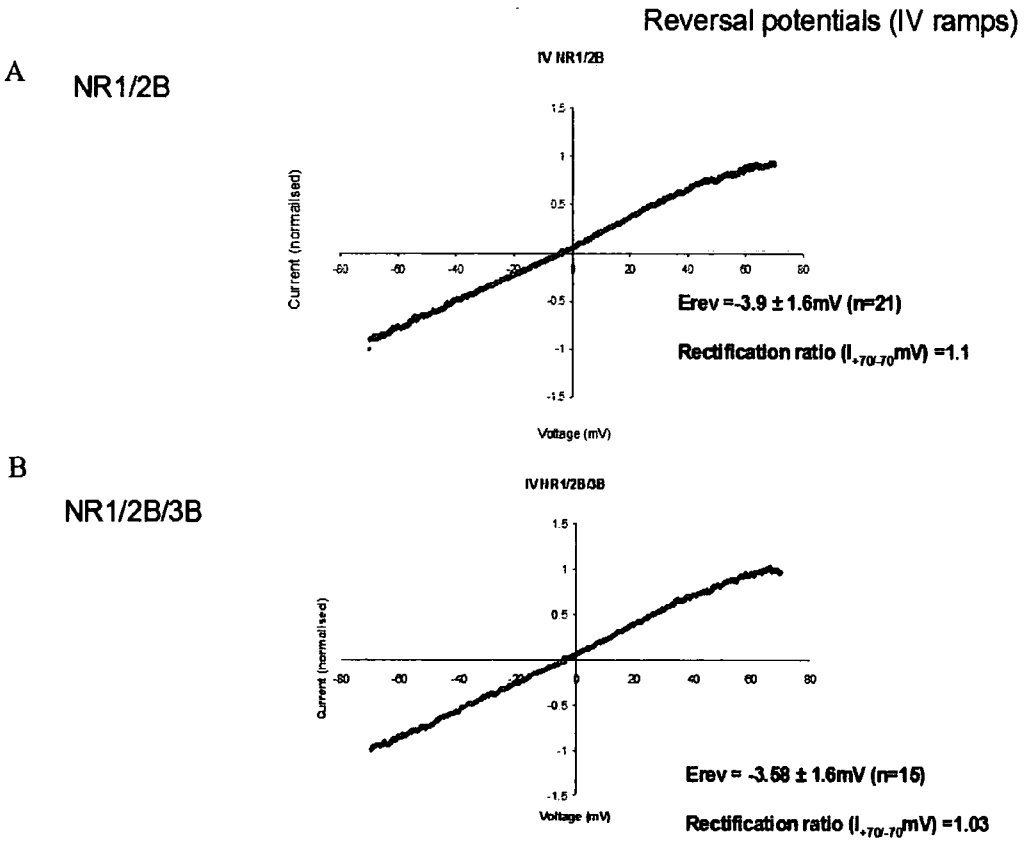


**Figure 5.4 Current/voltage (IV) relationships for NR1/NR2B (A) and NR1/NR2B/NR3B (B) receptors expressed in HEK 293 cells, showing no statistical differences between channel characteristics.**

### 5.2.2.3 Calcium permeability experiments investigating the shift in reversal potentials of HEK 293 cells transfected with NR1/NR2B and NR1/NR2B/NR3B receptors.

The I/V relationship for each receptor complex was used to investigate calcium permeability of the two receptor complexes. GFP-positive NR1/NR2B (n=10) (A) and NR1/NR2B/NR3B (n=9) (B) cells were exposed to 0.3mM and 30mM extracellular calcium concentrations in succession. The subsequent shift in reversal potentials between the two solutions was calculated for each receptor complex. Taking into account the junction potential the shift in reversal potential was measured (15.9 ± 10mV and 21 ± 9mV for NR1/NR2B and NR1/NR2B/NR3B, respectively), no statistical differences were detected, contrasting previous research (Matsuda *et al.*, 2002) and showing no differences in calcium permeability in this assay.

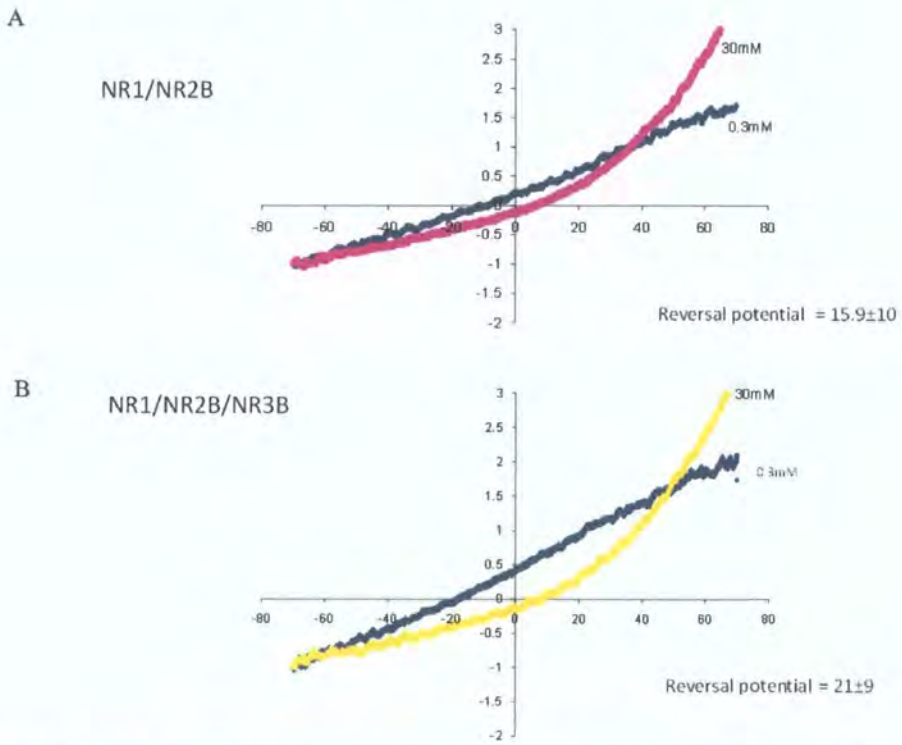


**Figure 5.5 Calcium permeability experiments, measuring the shift in reversal potential of the receptor channel between 0.3 and 30mM extracellular calcium.**

### 5.2.2.4 Sensitivity of NR1/NR2B and NR1/NR2B/NR3B receptor complexes to magnesium blockade using current/voltage (I/V) relationship.

The I/V relationship for each receptor complex was used to investigate the voltage-dependency of the magnesium blockade at both 100μM and 20μM concentrations. The magnesium blockade is almost maximal at hyperpolarised potentials (-70mV) and is released when the membrane potential becomes more positive. 100 and 20μM $Mg^{2+}$ block of NR1/NR2B receptors remains at almost 100% until the membrane potential reaches approximately -35mV, whereas both concentrations of $Mg^{2+}$ blockade are relieved at membrane potentials of ~ -50-60mV in NR1/NR2B/NR3B receptors providing evidence for reduced sensitivity of NR3B-containing receptors towards magnesium.

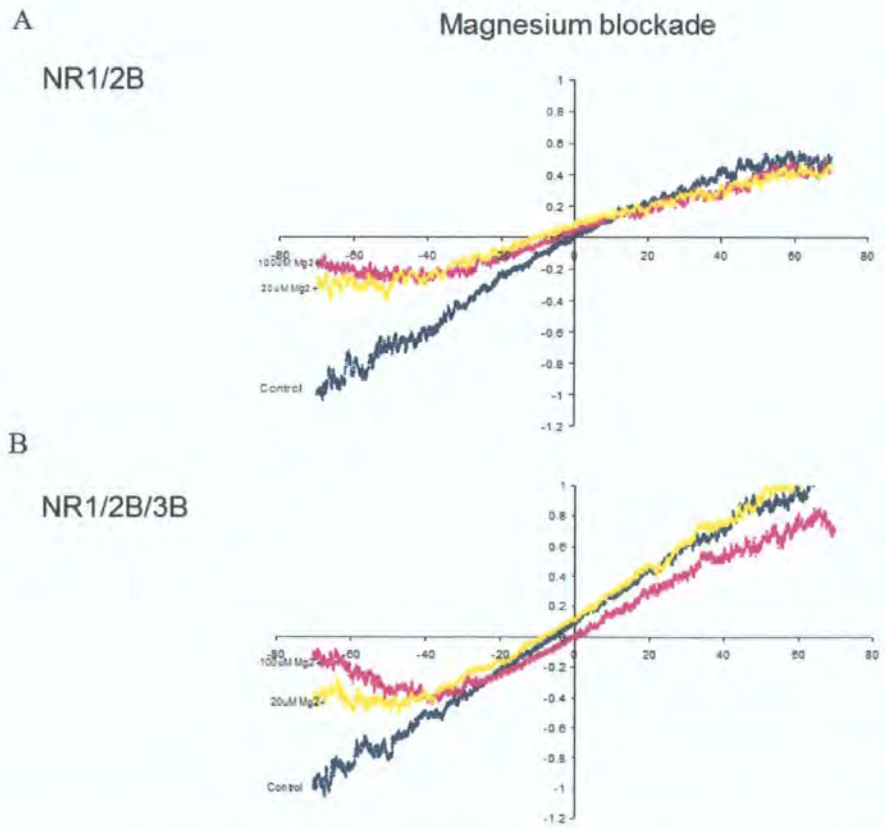


**Figure 5.6 Characterisation of magnesium sensitivity of recombinant NR1/NR2B (A) (n=8) and NR1/NR2B/NR3B (B) (n=6) receptors using current/voltage (I/V) relationships.**

### 5.2.2.5 Investigating the sensitivity of NR1/NR2B and NR1/NR2B/NR3B receptor complexes towards 100μM magnesium blockade.

GFP-positive NR1/NR2B (n=8) and NR1/NR2B/NR3B (n=6) cells were selected for patching. 100μM $MgCl_2$ was applied for 10 seconds following activation of the receptors using 100μM glutamate and 10μM glycine. 83 ± 5% inhibition resulted from 100μM $MgCl_2$ application to NR1/NR2B receptors whereas 69 ± 3% (mean ± SD) inhibition of NR1/NR2B/NR3B receptors showed a slightly reduced level of sensitivity towards the magnesium blockade (previously suggested in the literature to be due to amino acid alteration in TM2 region, Matsuda *et al.*, 2002). Kinetically 100μM $MgCl_2$ displayed both fast onset and rapid reversal of inhibition.

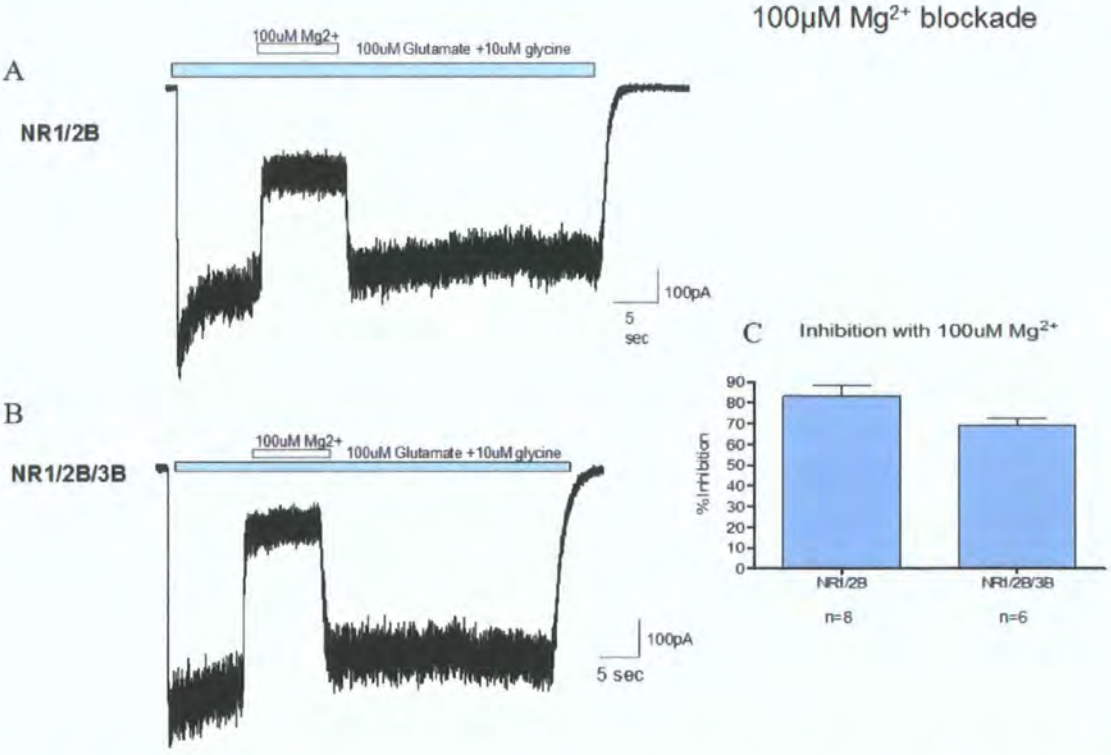


**Figure 5.7 Electrophysiological traces depicting the sensitivity of NR1/NR2B (A) and NR1/NR2B/NR3B (B) receptors towards 100uM concentrations of magnesium and a histogram (C) representing the mean ± SD of data from all experiments.**

### 5.2.2.6 Investigation the sensitivity of NR1/NR2B and NR1/NR2B/NR3B receptors towards 20μM magnesium blockade.

Again, GFP-positive NR1/2B (n=8) and NR1/2B/3B (n=6) cells were selected and exposed to 20μM $MgCl_2$ following activation of the receptor channels with 100μM glutamate and 10μM glycine. The application of 20μM $MgCl_2$ resulted in 49 ± 5% and 44 ± 3% (mean ± SD) inhibition of both NR1/NR2B and NR1/NR2B/NR3B receptor combinations, respectively. Once again, there is a slightly lower sensitivity with the inclusion of the NR3B subunit; however, there is no significant difference between the data sets.

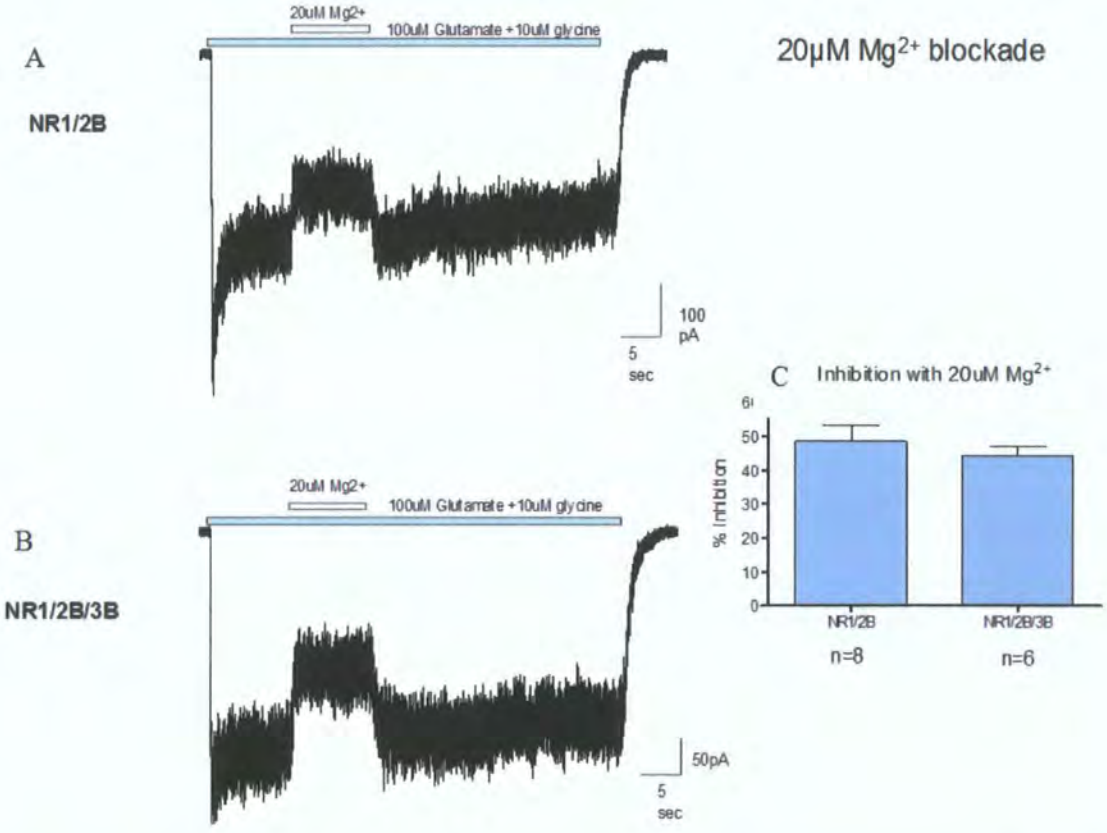


**Figure 5.8 Electrohysiological traces representing the signals measured from NR1/NR2B (A) and NR1/NR2B/NR3B (B) receptor complexes when exposed to 20μM magnesium chloride, and a histogram (C) showing the mean± SD of all data sets.**

### 5.2.3 Pharmacological influence of NR3B upon NR2B subtype selective antagonists

In order to investigate the pharmacological influences of NR3B, cytotoxicity assays, whole cell patch-clamp electrophysiology and radioligand binding were carried out using NR2B subunit-selective antagonists.

#### 5.2.3.1 Cytoprotective effect of NR2B-selective antagonists upon NR1/NR2B and NR1/NR2B/NR3B receptors expressed in HEK293 cells.

Cytotoxicity assays were performed in parallel on recombinant NR1/NR2B and NR1/NR2B/NR3B receptors expressed in HEK 293 cells in the presence of the NR2B-subunit selective antagonists ifenprodil (100nM, 1μM, 10μM), COMPOUND A (10nM, 100nM, 1μM) and COMPOUND B (10nM, 100nM, 1μM) (n=4 respectively) and with no antagonist as a control. The level of cell death with no antagonist present was significantly reduced from 41±4% to 23±5% in the presence of NR3B.

All three compounds effectively antagonized NR1/NR2B receptor activity in this functional assay, particularly 10μM ifenprodil and 1μM COMPOUND A which significantly reduced cytotoxicity to 17 ± 6 % and 16 ± 4% respectively.

The presence of NR3B appears to slightly increase the binding of ifenprodil towards the receptor complex, reducing cytotoxicity at 100nM, 1μM and 10μM to 16 ± 6%, 18 ± 5% and 9 ± 5%, respectively. The binding affinity and effective cytoprotection of COMPOUND B is similar in the presence and absence of NR3B. Binding affinity of COMPOUND A appears to have been reduced by the presence of NR3B, with no

significant reduction in cytotoxicity, showing that inclusion of this subunit may modify the binding site or allosteric interactions of the two novel compounds.

A

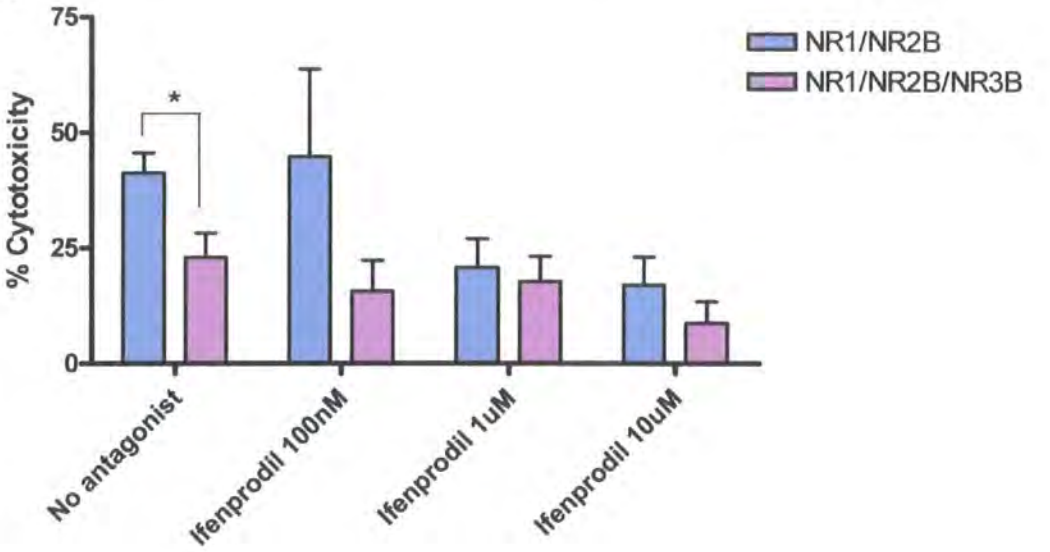


B

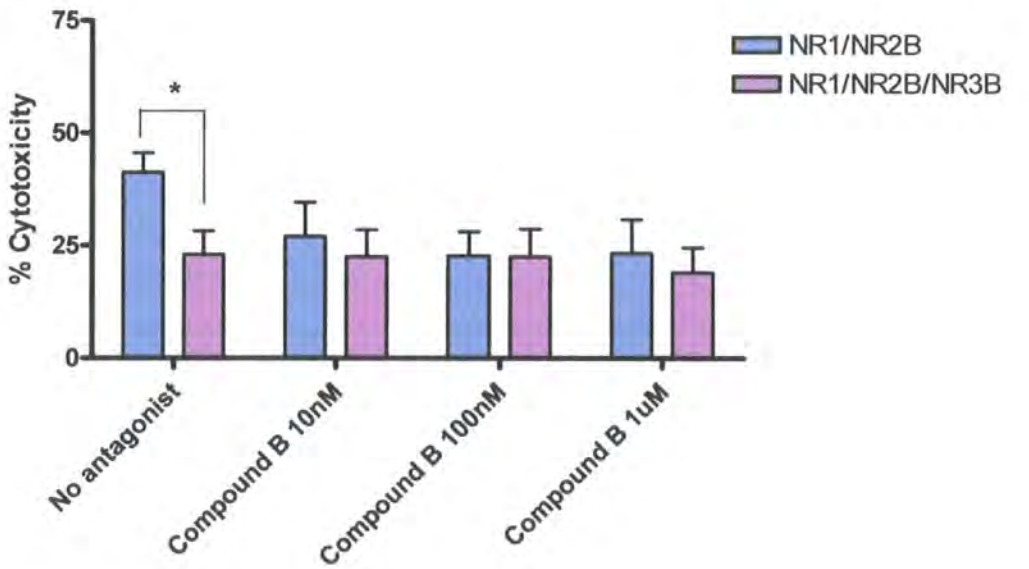

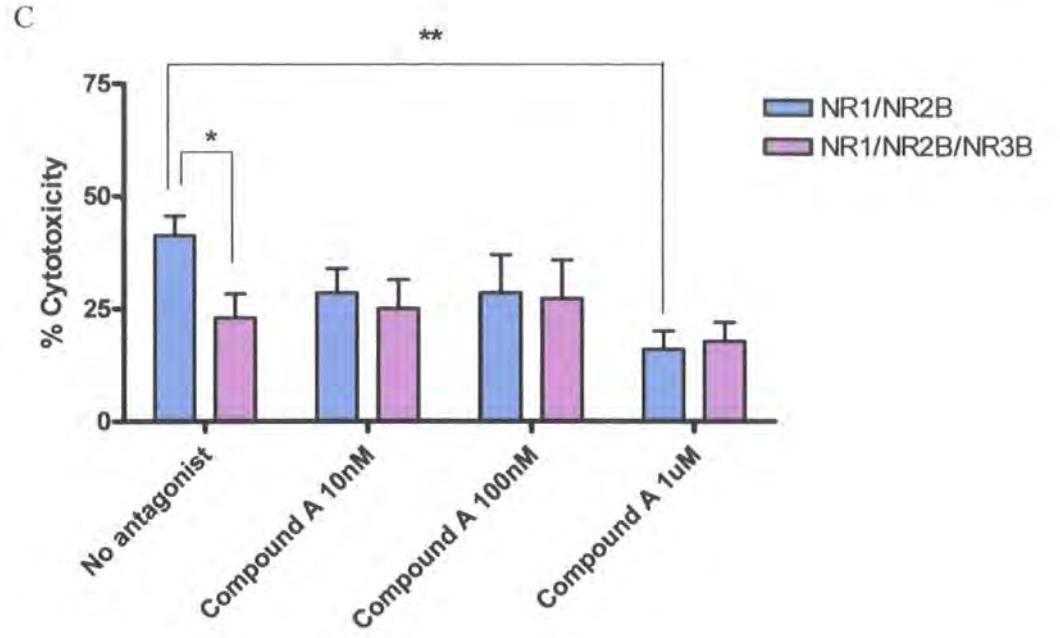


**Figure 5.9 Differential cytoprotective effects of the NR2B-selective antagonists ifenprodil (A), COMPOUND B (B) and COMPOUND A (C) upon NR1/NR2B and NR1/NR2B/NR3B receptor complexes * p=<0.05, **p=<0.01 Two-tailed T-Tests.**

### 5.2.3.2 Investigating the influence of the NR3B subunit upon the NR2B subtype-selective antagonist CP-101,606 (10 μM) in recombinant NR1/NR2B and NR1/NR2B/NR3B receptors.

Cells transfected with NR1/NR2B (n=9) and NR1/NR2B/NR3B (n=11) were exposed to co-agonists (glutamate (100μM) and glycine (10μM)) and the NR2B-subtype selective antagonist CP-101606 for 10 seconds. A fast onset of blockade and minimal wash-out after several minutes demonstrated high affinity binding of the antagonist to the complex. Pooled data showed no significant effect of the NR3B subunit with 84 ± 2% and 83 ± 3% (mean ± SD) inhibition of NR1/NR2B and NR1/NR2B/NR3B receptor complexes, respectively.

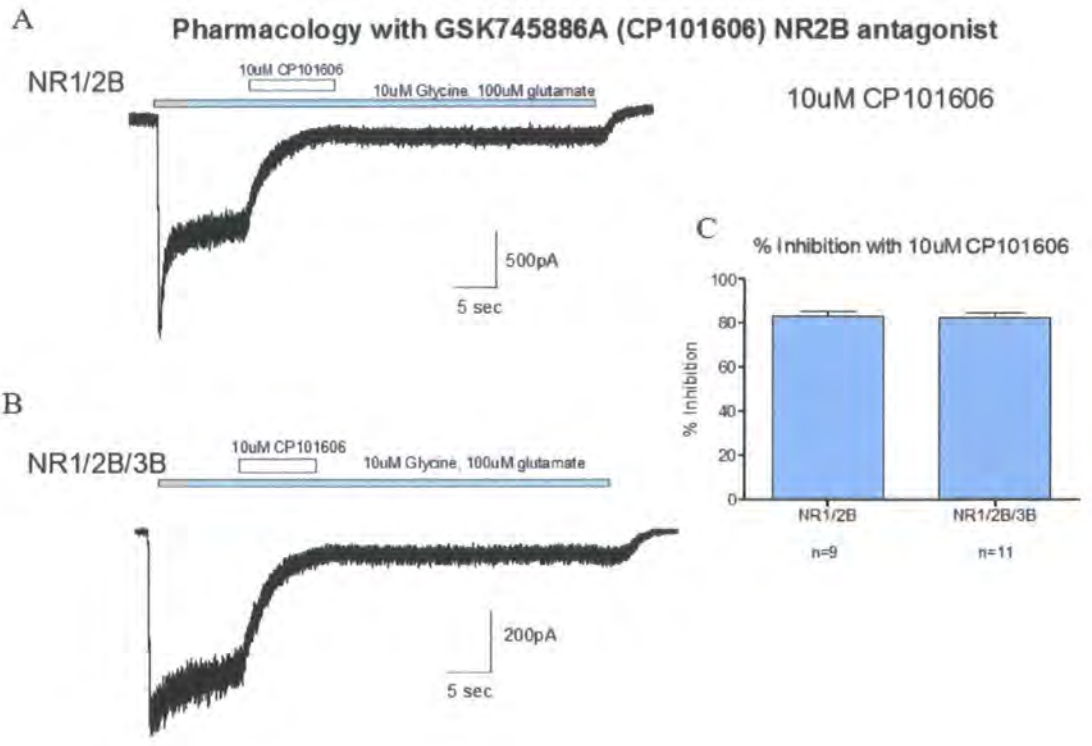


**Figure 5.10 Electrophysiological traces representing inhibition of signals from recombinant NR1/NR2B (A) and NR1/NR2B/NR3B (B) receptors. Figure C represents the mean ± SD of percentage inhibition from all data sets.**

**5.2.3.3 Investigating the influence of the NR3B subunit upon the activity of the selective NR2B antagonist CP-101,606 (300nM, 10 seconds) in recombinant NR1/NR2B and NR1/NR2B/NR3B receptors.**

Cells transfected with NR1/NR2B (n=12) and NR1/NR2B/NR3B (n=10) receptors were exposed to co-agonists (glutamate (100μM) and glycine (10μM)) and the NR2B subtype selective antagonist CP-101606 (300nM) for 10 seconds. Inhibition was calculated to be 28 ± 6% and 20 ± 3% (mean ± SD) for NR1/NR2B and NR1/NR2B/NR3B receptor complexes respectively, with no significant reduction in sensitivity of CP-101,606 in the presence of NR3B. In order to maximize inhibition and investigate time-dependent blockade at 300nM, application time of CP-101606 was increased to 60seconds.

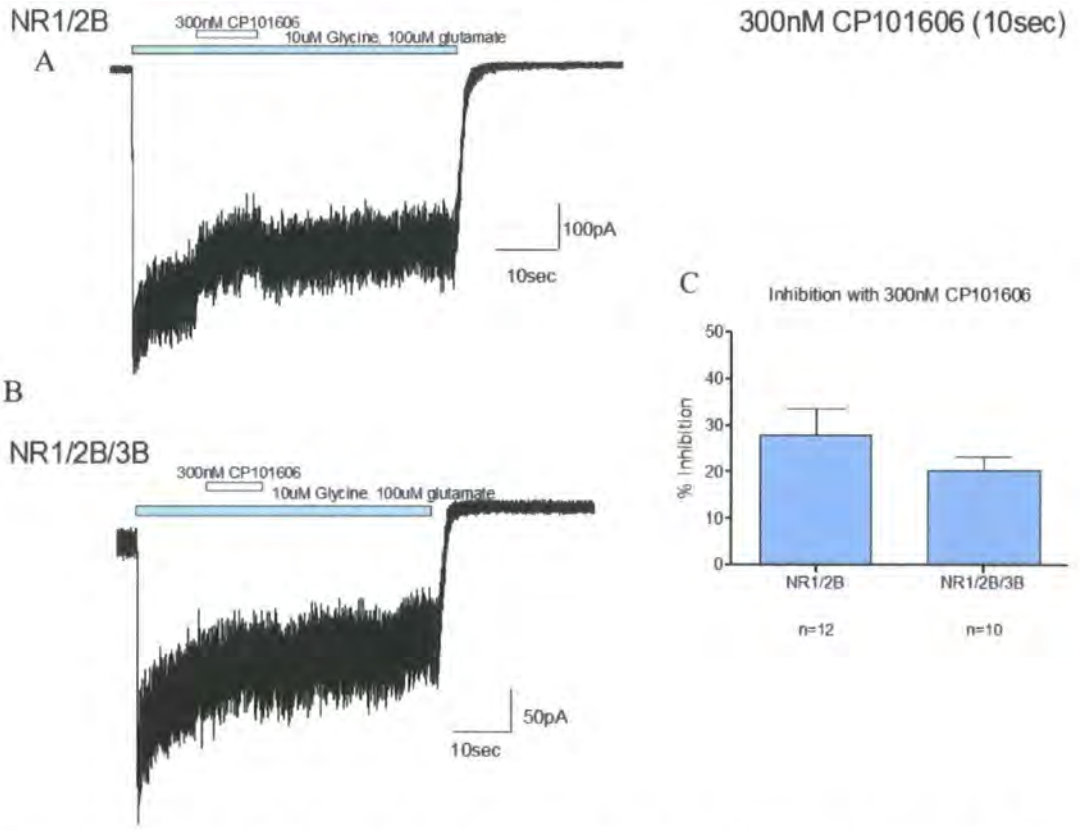


**Figure 5.11 Electrophysiological traces representing the inhibition of NR1/NR2B (A) and NR1/NR2B/NR3B (B) receptor activity by 300nM CP-101606. Figure C shows the mean ± SD of percentage inhibition from all data sets.**

### 5.2.3.4 Investigating the influence of the NR3B subunit upon the activity of the selective NR2B antagonist CP-101,606 (300nM, 60 seconds) in recombinant NR1/NR2B and NR1/NR2B/NR3B receptors.

300nM CP-101606 was applied to cells transfected with receptor complexes NR1/NR2B (n=4) and NR1/NR2B/NR3B (n=4) for 60 seconds. A slower, gradual onset of time-dependent inhibition was observed, which was maintained after antagonist application, indicating potent high-affinity binding to both receptor complexes and no significant modulation induced by the NR3B subunit.

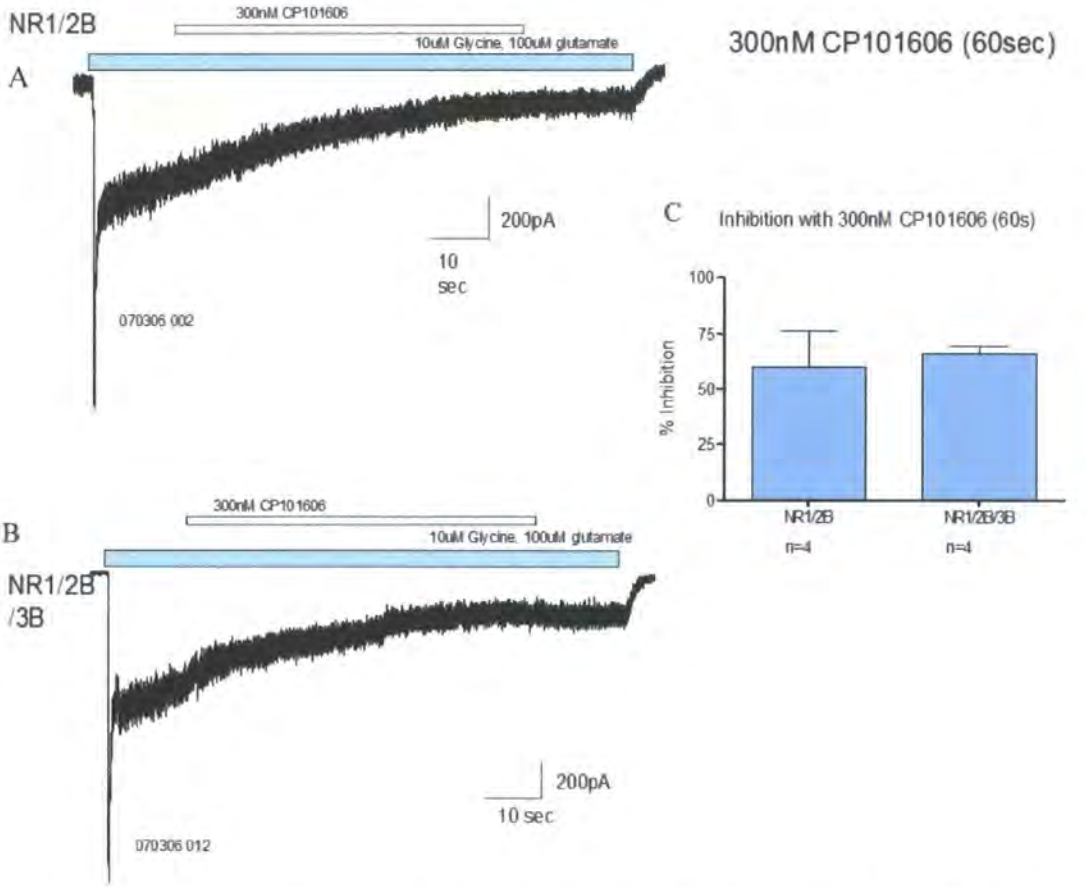


**Figure 5.12 Electrophysiological traces representing the inhibition of NR1/NR2B (A) and NR1/NR2B/NR3B (B) receptor activity by 300nM CP-101606. Figure C shows the mean ± SD of percentage inhibition from all data sets.**

**5.2.3.5 Investigating the influence of the NR3B subunit upon the activity of the selective NR2B antagonist CP-101,606 (30nM, 60 seconds) in recombinant NR1/NR2B and NR1/NR2B/NR3B receptors.**

Antagonism of GFP-positive cells NR1/NR2B (n=5) and NR1/NR2B/NR3B (n=5) using CP-101606 (30nM), applied for 60seconds was then investigated. No significant alterations in binding affinities were observed between the two receptor populations although inhibition of NR1/NR2B receptors was greater (40 ± 9%) than inhibition of NR1/NR2B/NR3B complexes (29 ± 14%), again suggesting possible reduced sensitivity of the compound in the presence of NR3B.

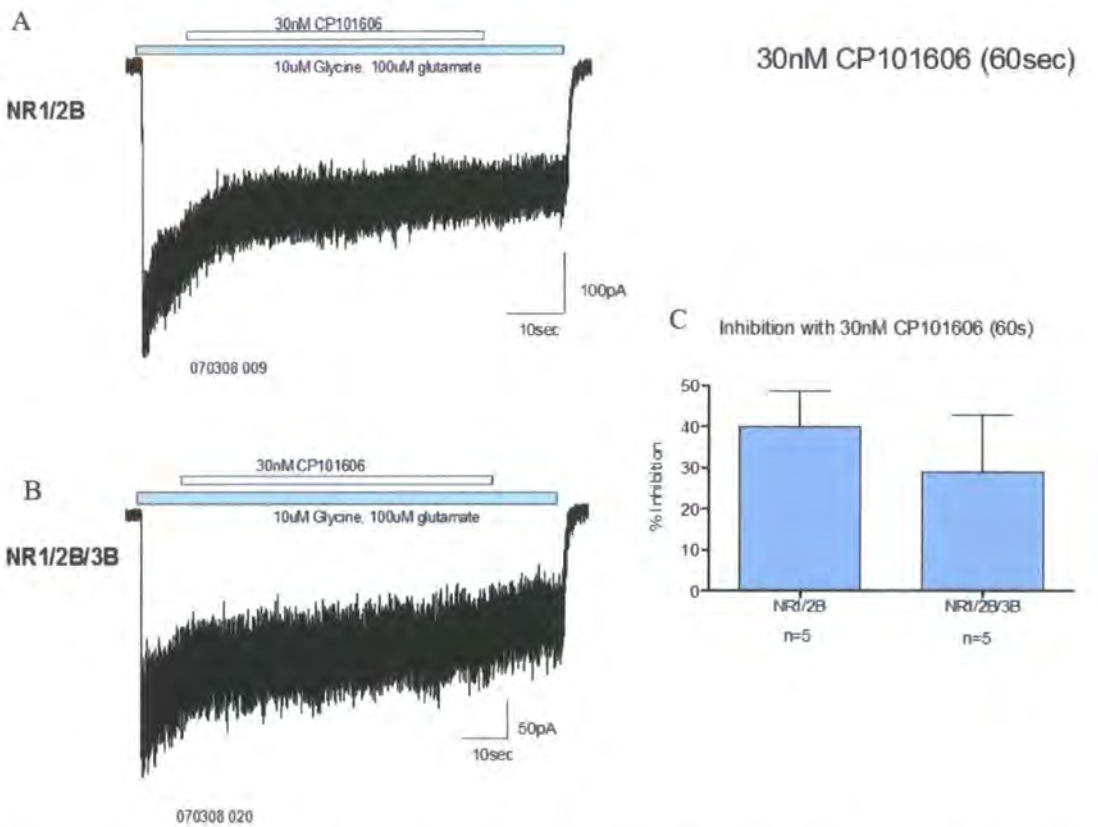


**Figure 5.13 Electrophysiological traces representing the inhibition of NR1/NR2B (A) and NR1/NR2B/NR3B (B) receptor activity by 30nM CP-101606. Figure C shows the mean ± SD of percentage inhibition from all data sets.**

**5.2.3.6 Investigating the influence of the NR3B subunit upon the activity of the selective NR2B antagonist Ro-256981 (10μM, 10 seconds) in recombinant NR1/NR2B and NR1/NR2B/NR3B receptors.**

10μM of the selective NR2B antagonist Ro-256981 was applied to GFP-positive cells NR1/NR2B (n=6) and NR1/NR2B/NR3B (n=6) for 10 seconds following activation of NMDA currents with co-agonists. Ro-256981 showed high-affinity interaction with percentage inhibition of 100 ± 14% and 93 ±2% (mean ± SD) for NR1/NR2B and NR1/NR2B/NR3B complexes respectively, with fast-onset of action and minimal wash-out towards both receptor complexes.

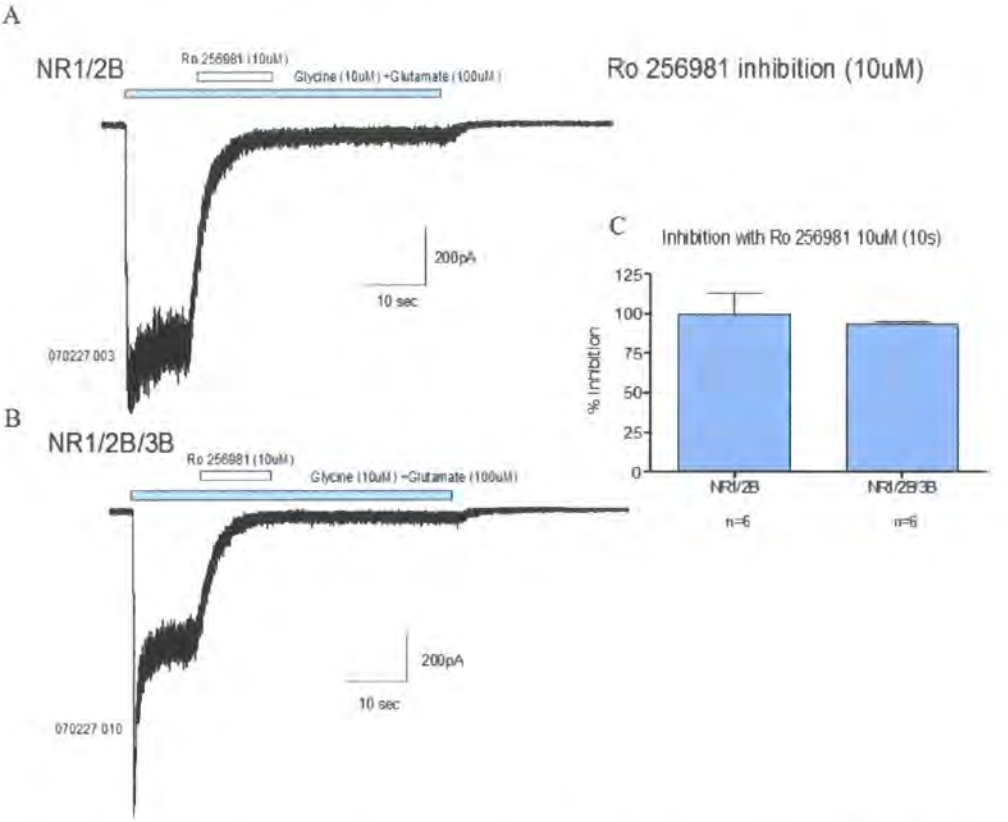


**Figure 5.14 Electrophysiological traces showing the inhibition of NR1/NR2B (A) and NR1/NR2B/NR3B (B) receptor activity by the NR2B-selective antagonist Ro 256981 (10μM 10 seconds). Figure C shows the mean ± SD of percentage inhibition from all data sets.**

**5.2.3.7 Investigating the influence of the NR3B subunit upon the activity of the selective NR2B antagonist Ro-256981 (30nM, 60 seconds) in recombinant NR1/NR2B and NR1/NR2B/NR3B receptors.**

Ro-256981 (30nM) was applied to GFP-positive NR1/NR2B (n=5) and NR1/NR2B/NR3B (n=4) cells for 60 seconds to investigate time-dependent inhibition. At 30nM, the presence of the NR3B subunit in the receptor complex significantly reduced the percentage inhibition from 41 ± 12% (NR1/NR2B) to 10 ± 7% (NR1/NR2B/NR3B) implying potential alterations in binding affinity, the complexes reaching the cell surface or allosteric modulations of the antagonist binding site.

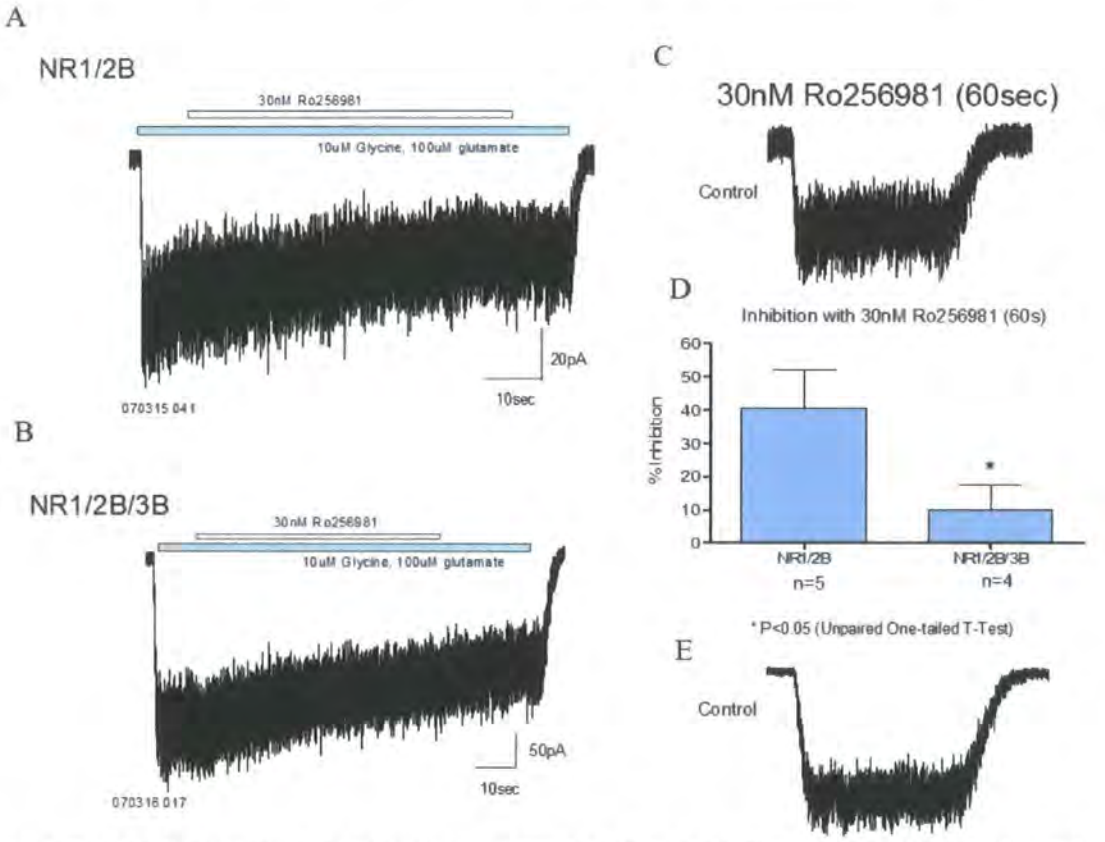


**Figure 5.15 Electrophysiological traces showing the inhibition of NR1/NR2B (A) and NR1/NR2B/NR3B (B), by recombinant receptor activity by Ro-256981 (30nM, 60seconds). Figure C, shows signal from NR1/NR2B receptors before antagonist application, Figure E, shows signal from NR1/NR2B/NR3B receptors before antagonist application. Figure D, shows the mean ± SD of percentage inhibition from all data sets.**

**5.2.3.8 Competition binding to investigate the pharmacological influence of NR3B expression upon the displacement of [$^3$H] CP-101606 by COMPOUND A.**

Competition binding was carried out on recombinant NR1/NR2B and NR1/NR2B/NR3B receptors expressed in HEK 293 cells. The two-site displacement of [$^3$H] CP-101606 by COMPOUND A showed high affinity binding (82% in NR1/NR2B cells, 53% in NR1/NR2B/NR3B cells). Therefore, NR3B reduced the number of high affinity sites (by 29%), and therefore appeared to reduce the affinity of COMPOUND A for the NR1/NR2B receptors ($K_i$ = 14 ± 22nM in the presence of NR3B). The increase in lower affinity sites ($K_i$ = 12 ± 15μM in the presence of NR3B) may be the result of reduced receptor numbers reaching the cell surface and/or modulation of the compound binding site by inclusion of NR3B in the receptor complex. The data displayed are mean ± SD taken from three individual experiments performed in triplicate.

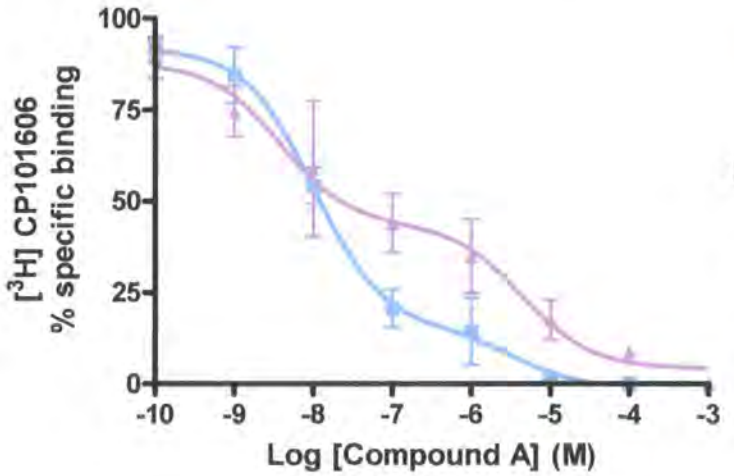


| | NR1/2B | NR1/2B/3B |
|---|---|---|
| Hillslope | -0.6 ± 0.2 | -0.3 ± 0.2 |
| 1.$pIC_{50}$ | 8.0 ± 0.8 | 8.0 ± 1.1 |
| 2.$pIC_{50}$ | 5.0 ± 1.4 | 5.1 ± 0.5 |
| 1.$K_i$ | 5 ± 6nM | 14 ± 22nM |
| 2.$K_i$ | 3 ± 3μM | 12 ± 15μM |

**Figure 5.16 Competition binding showing two-site displacement of [$^3$H] CP-101606 by COMPOUND A in recombinant NR1/NR2B and NR1/NR2B/NR3B receptors. The results displayed are mean ± SD of three individual experiments and non-specific binding was defined using 1mM ifenprodil.**

### 5.2.3.9 Competition binding to investigate the pharmacological influence of NR3B upon the displacement of [$^3$H] CP-101606 by COMPOUND B.

Competition binding was carried out to investigate the displacement of [$^3$H] CP-101606 by COMPOUND B in recombinant NR1/NR2B and NR1/NR2B/NR3B receptors expressed in HEK 293 cells. In cells expressing NR1/NR2B receptors, COMPOUND B displacement of [$^3$H] CP-101606 was fitted to a one-site curve, showing high affinity binding ($K_i$=14 ± 11nM) to this receptor population. However, co-expression of NR3B with NR1/NR2B receptors results in the binding of COMPOUND B to two receptor populations, one with high affinity ($K_i$ = 0.4nM, 54%), likely to be NR1/NR2B receptors and one with a lower affinity ($K_i$ = 1μM, 46%). Therefore the presence of NR3B in the receptor complex introduces low affinity binding sites and thus appears to reduce the affinity of COMPOUND B for the NR1/NR2B populations. The data displayed are mean ± SD taken from two individual experiments performed in triplicate.

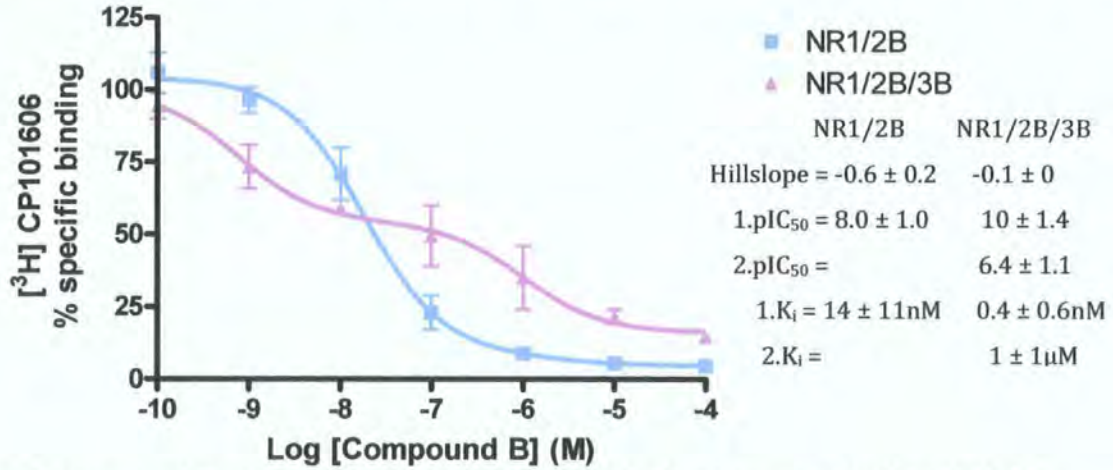


**Figure 5.17 Competition binding experiments showing the displacement of [$^3$H] CP-101606 by COMPOUND B in recombinant NR1/NR2B and NR1/NR2B/NR3B receptors. Data shown are mean ± SD for two individual experiments and non-specific binding was defined using 1mM ifenprodil.**

**5.2.3.10 Radioligand binding assay investigating the specific binding of [$^3$H] Ro-256981 in recombinant NR1/NR2B and NR1/NR2B/NR3B receptors.**

NR1/NR2B and NR1/NR2B/NR3B receptors were transiently expressed in HEK293 cells and harvested for parallel binding experiments with [$^3$H] Ro-256981. This histogram represents the specific binding of [$^3$H] Ro-256981 at 16 and 25nM and shows a reduced, but not significantly reduced level of binding in the presence of the NR3B subunit at both concentrations of radioligand. This data shows that the binding of this NR2B-selective antagonist may be affected by the presence of NR3B in the receptor complex due to modulation of the Ro-256981 binding site, or a reduction in the number of NR1/NR2B receptors at the cell surface.

The data presented are generated from the mean ± SD for two individual experiments performed in triplicate.

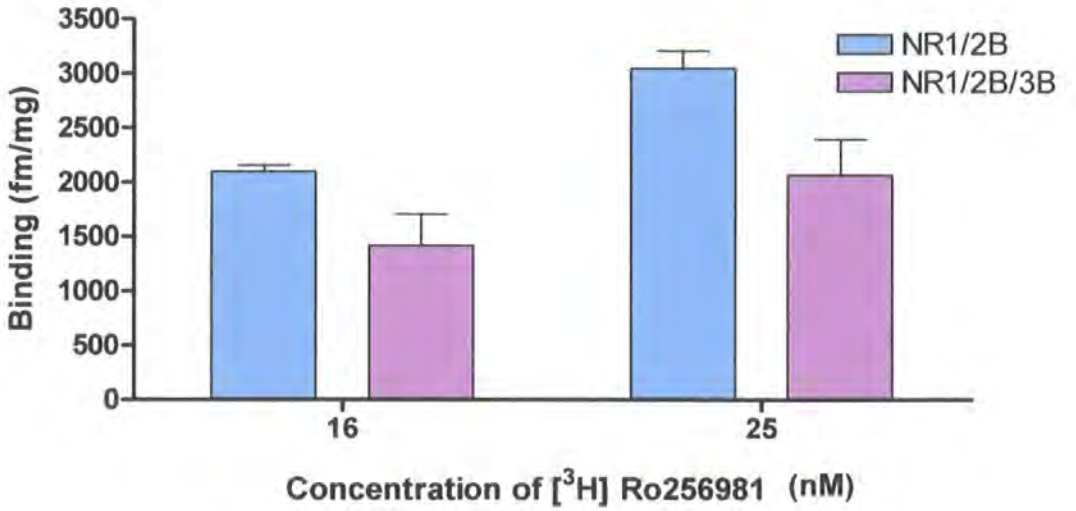


**Figure 5.18 Histogram representing specific binding data for [$^3$H] Ro-256981 in recombinant NR1/NR2B and NR1/NR2B/NR3B receptors. The data shown are mean ± SD for two individual experiments. Non-specific binding was defined using 1mM ifenprodil.**

**5.2.3.11 Radioligand binding assay investigating the specific binding of [$^3$H] CP-101606 in recombinant NR1/NR2B and NR1/NR2B/NR3B receptors.**

Parallel binding experiments were carried out with [$^3$H] CP-101606 on NR1/NR2B and NR1/NR2B/NR3B receptor populations expressed in HEK 293 cells. This histogram represents specific binding of [$^3$H] CP-101606 at 4 and 9nM and shows a reduction in the level of binding in the presence of the NR3B subunit, however the data are not significant. This preliminary data may provide further evidence for a modulatory effect of the NR3B subunit upon the pharmacology of the receptor complex by altering the binding site of CP-101606 or reducing the number of NR1/NR2B receptor sites available.

The results displayed are mean ± SD from two individual experiments carried out in triplicate.

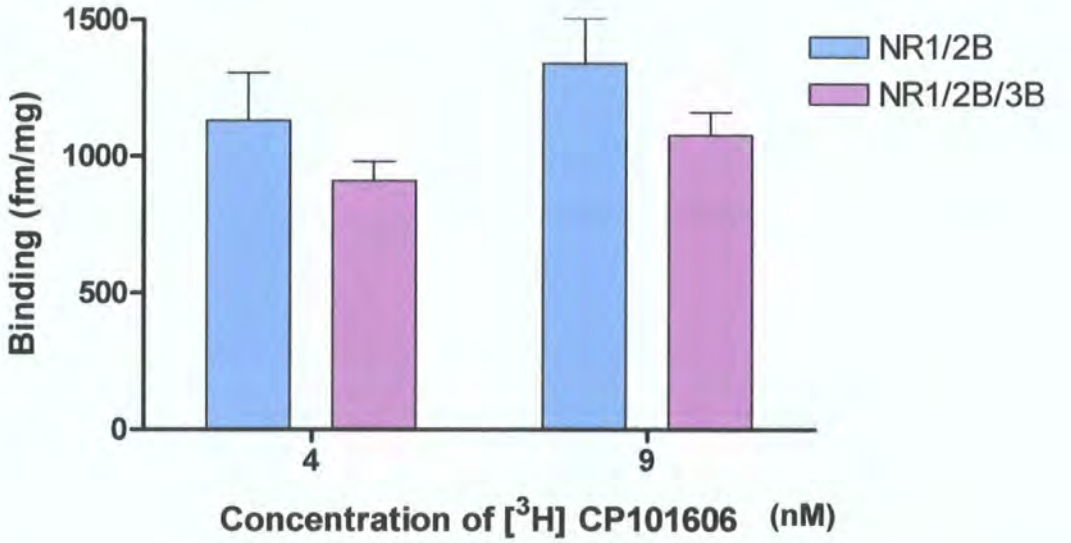


**Figure 5.19 Histogram to represent the specific binding data for [$^3$H] CP-101606 in recombinant NR1/NR2B and NR1/NR2B/NR3B receptors. The data shows the mean ± SD for two individual experiments. Non-specific binding was defined with 1mM ifenprodil.**

| Assay | Compound | Effect of NR3B |
|---|---|---|
| Cytotoxicity Assays % cytoprotection | Ifenprodil | Trend to Increase |
| | COMPOUND B | No effect/trend to decrease |
| | COMPOUND A | Decrease |
| Electrophysiology % current inhibition | CP-101606 | Trend to Decrease |
| | Ro-256981 | Trend to Decrease |
| Radioligand Binding | COMPOUND B Competition | Decrease binding affinity |
| | COMPOUND A Competition | Decrease binding affinity |
| | CP-101606 Specific Binding | Decrease binding affinity |
| | Ro-256981 Specific Binding | Decrease binding affinity |

**Table 5.1 Summarising the pharmacological influence of the NR3B subunit upon NR2B-selective antagonists ifenprodil, Ro-256981, CP-101606, COMPOUND A and COMPOUND B.**

## 5.3 Discussion

The heteromeric nature of the NMDA receptor complex gives rise to large variations in channel characteristics which need to be elucidated before the functional implications of such receptors in native tissue can be fully understood. The most recently discovered and most poorly characterised NR3 subunits were the focus of investigation in this chapter investigating their functional and pharmacological modulation of NR1/NR2A and NR1/NR2B receptor complexes.

The percentage of cell death in HEK 293 cells co-expressing various NMDA receptor subunit combinations was measured using the promega non-radioactive cytotoxicity assay, as previously described by Cik *et al.*, 1995. The membrane potential of the HEK293 cells is approximately -10 to -20mV (Chazot, unpublished) and therefore depolarised enough to relieve blockade by magnesium in the culture medium and activate the receptors. In the absence of an NMDA antagonist the l-glutamate and glycine present in the culture medium were sufficient to activate the receptors allowing excessive calcium influx and cell mortality. It has previously been shown that calcium influx is a major cause of toxicity in HEK 293 cells expressing recombinant NMDA receptors in studies using calcium chelators such as EDTA (Cik *et al.*, 1995; Chazot *et al.*, 1999) and expression of the mutant NMDAR1-1a (N598Q)/NMDAR2A which reduces calcium permeability of the receptors (Cik *et al.*, 1994).

HEK293 cells transfected without plasmid DNA acted as a negative control and resulted in a low background cell toxicity of 3 ± 0.6%. HEK293 cells transfected with the NR1 subunit alone acted as a positive single-subunit control and showed 9

± 1% cell death. Co-transfection of NR1/NR2B receptor subunits resulted in the highest incidence of cell death (50 ± 11%) due to calcium toxicity mediated by l-glutamate activated NMDA receptor $Ca^{2+}$ influx. Co-transfection of NR1/NR2A subunits to form another diheteromeric complex commonly found in native adult tissue (Chazot *et al.*, 1997; Stephenson, 2001) resulted in significantly lower levels of cytotoxicity (19 ± 2%) compared to that resulting from NR1/NR2B co-expression. This differential degree of cell death may be the result of variations in transfection efficiencies within the model system; however, this result is consistent with previous work associating NR2B-containing receptors with NMDA-mediated excitotoxicity (Fuller *et al.*, 2006; Loftis and Janowsky, 2003; Liu *et al.*, 2007). In comparison to the NR2A subunit, NR2B confers increased duration of channel opening, increased permeability to calcium and a higher sensitivity to glutamate (Fuller *et al*, 2006; Cull-Candy *et al.*, 2001). These factors are likely to enhance NR2B-containing NMDA receptor activity and therefore result in increased levels of cell death.

Triheteromeric complexes generated from co-transfection of NR3A with NR1/NR2B and NR3B with NR1/NR2B receptor complexes resulted in significant reductions in the levels of cell death (29% and 23% cytotoxicity, equating to 42% and 54% cytoprotection respectively) in comparison to NR1/NR2B alone. The differential level of cytoprotection between the NR3A and NR3B subunit may imply that NR3B reduces calcium permeability to a greater extent than NR3A therefore potentially having a greater impact in our model.

These novel results provide possible evidence that the proposed reduction in $Ca^{2+}$ influx mediated by the NR3 subunits (Nishi *et al.*, 2001; Matsuda *et al.*, 2002, Al-Hallaq *et al.*, 2002) is sufficient to significantly reduce cytotoxicity and have a profound cytoprotective effect *in vitro*. In these studies despite the likely formation of both diheteromeric (NR1/NR2B and NR1/NR3B) and triheteromeric (NR1/NR2B/NR3B) complexes from the co-transfection of three subunits (Brimcombe *et al.*, 1997), the presence of the NR3 subunits had a significant effect, consistent with the findings of Nishi *et al.*, 2001.

Interestingly, no significant cytoprotection was seen when NR3A and NR3B were co-transfected with NR1/NR2A receptors. This result opposes that which would have been expected from previous work by Nishi *et al*, 2001 and Matsuda *et al.*, 2002 who found reduced calcium permeability in recombinant NR1/NR2A/NR3B receptors in comparison to NR1/NR2A receptors alone. It is possible that in this system, the NR3 subunits are not associating with NR1/NR2A receptors and are therefore not being expressed at the receptor surface. It is also possible that any cytoprotective effect of the NR3 subunits is beyond detection limits when compared with the level of cell death resulting from NR1/NR2A receptors which is comparatively lower than NR1/NR2B.

The cytoprotection seen with inclusion of NR3A and NR3B in NR1/NR2B receptors may be initial evidence to suggest a mechanism of NR3 retention of NR2B-containing receptors within the ER reducing protein trafficking and expression at the cell surface which would reduce $Ca^{2+}$ influx. There may also be specific interactions between the NR2B/NR3B-containing receptors and

intracellular signalling cascades which alter the internal processing of calcium, neutralising excess concentrations with uptake into stores or disrupting CaMKII kinase stability, an enzyme linked with NR2B and important for promoting $Ca^{2+}$ influx (Bayer *et al.*, 2001; Lisman *et al.*, 2002).

The stoichiometry of the heteromeric complex may also play a role in NR3 subunit modulation. For example, inclusion of NR3B in the receptor complex may substitute for one NR2B subunit, forming a tetramer composed of two NR1 subunits, one NR2B subunit and one NR3B subunit. This formation would reduce the number of NR2B glutamate binding sites, potentially reducing the influence of the NR2B subunit and attenuating receptor activation however this hypothesis is not supported by the electrophysiological peak current amplitude data. It has also been suggested that the NR3A subunit doesn't undergo extensive molecular re-arrangement upon channel activation, and with NR1 forms a narrow vestibule, modulating the influx of cations (Wada *et al.*, 2006). The NR3B subunit may therefore act similarly, when part of the receptor complex.

Electrophysiological experiments were then undertaken to further characterise the effects of the NR3 subunits on NMDA receptor biophysical properties and function. NR3B and its influence on NR1/NR2B receptors was the focus for these experiments to reflect receptors present in adult rat tissue and because this receptor combination showed the highest degree of cytoprotection.

The peak amplitudes resulting from NMDA-mediated currents in HEK 293 cells co-transfected with NR1/NR2B and those with NR1/NR2B/NR3B were measured upon application of co-agonists glutamate (100μM) and glycine (10μM).

Experiments were carried out in the absence of magnesium to ensure no voltage-dependent blockade of the receptor channel. Both populations of cells showed functional activity with similar fast onset activation and deactivation kinetics though no significant difference in peak amplitude was observed between cells co-transfected with NR1/NR2B/NR3B and those with NR1/NR2B. Previous electrophysiological studies showed reduced glutamate induced whole-cell current in NR1/NR2A/NR3A (Ciabarra *et al.*, 1995; Sucher *et al.*, 1995) and NR1/NR2A/NR3B (Nishi *et al.*, 2001) recombinant receptors, however, in contrast Matsuda *et al.*, 2002 found no significant reduction in current amplitudes in cells co-expressing NR1/NR2A/NR3B when compared to NR1/NR2A receptors. These conflicting results provide evidence to support the theory that NR3 subunits have a modulatory rather than a dominant negative (Nishi *et al.*, 2001) role when part of the receptor complex and may have diverse interactions with different NR2 subunits, also evident from the cytotoxicity data. A recent study has highlighted the potential for different effects of NR1 splice variants when investigating *in vitro* interactions. Interestingly, it was noted that co-expression of NR1-1a and NR3B with either NR2B or NR2D in *Xenopus laevis* oocytes resulted in potentiated currents, though co-expression of NR1 (regardless of variant) and NR3B with either NR2A or NR2C showed the dominant attenuation of currents previously seen (Cavara and Hollmann, 2007) suggesting important differential modulation depending upon receptor composition. The electrophysiological studies carried out in this chapter were carried out on cells co-expressing the NR1-1a splice variant with NR3B and NR2B and therefore the data supports these previous findings as no

dominant attenuation of current was observed. These differences in modulatory properties conveyed by alternative receptor co-assemblies may explain the discrepancies between the data presented in this chapter and the literature.

It must also be remembered that expression efficiencies will vary between systems and cell labelling with GFP was taken as a marker for successful expression of potentially all three cDNA plasmids, but may not be absolute. In future experiments, it may be advantageous to tag the NR3B subunit or all three subunits with fluorophores, so that cells co-expressing all subunits could be identified.

The current/voltage (I/V) relationship of both receptor populations revealed no significant alteration to the reversal potential of the receptor channel being -3.9 and -3.6mV for NR1/NR2B and NR1/NR2B/NR3B respectively, a novel finding showing that the species of ion permeant to the receptor is the same in the presence and absence of NR3B. The I/V relationship was then used to measure $Ca^{2+}$ permeability between the two receptor populations. Measuring the reversal potential of glutamate induced currents in 3mM and 30mM external calcium resulted in a shift in potential of 15.9 ± 10.0mV for NR1/NR2B and 21.9 ± 9.0mV for NR1/NR2B/NR3B and therefore no significant reduction in calcium permeability of the receptor in the presence of NR3B. The large variability in these measurements may be an indication of variable transfection efficiencies and therefore must be considered when drawing conclusions. These findings further suggest a differential modulatory effect of NR3B upon NR2B subunits in comparison to NR2A as previous research by Matsuda *et al.*, 2002 reported a

reduced shift in reversal potential from 16.6 ± 0.6mV for NR1/NR2A and 9.3 ± 0.8mV for NR1/NR2A/NR3B equating with attenuated $Ca^{2+}$ permeability.

The conflicting data between the cytotoxicity and electrophysiological experiments may be evidence for a different, non-NMDA interaction of the NR3 subunits, such as with internal calcium stores, which may reduce intracellular calcium concentrations, seen as a cytoprotective effect in whole cell functional assays, which would not be detected in NMDA channel physiology. Calcium imaging via fluorescence imaging plate reader (FLIPR) was attempted to investigate intracellular calcium concentrations in large cell populations, with and without NR3B, however the data obtained was inconclusive and is therefore not shown.

The sensitivity of NR1/NR2B and NR1/NR2B/NR3B receptors towards magnesium blockade was characterised by I/V relationships and percentage inhibition of current amplitude in 100μM and 20μM external magnesium. At both concentrations of magnesium, blockade of NR1/NR2B receptors remains maximal until the membrane potential reaches ~ -35mV, however, both 100μM and 20μM $Mg^{2+}$ blockade are relieved at much lower membrane potentials of ~ -50-60mV in receptors containing the NR3B subunit. This data is consistent with previous data suggesting the NR3 subunits confer reduced magnesium sensitivity towards the receptor complex due to a key amino acid change (asparagine to glycine) within the M2 domain (Matsuda *et al.*, 2002). The percentage inhibition of 100μM magnesium was reduced from 83 ± 5% in NR1/NR2B receptors to 69 ± 3% in the

presence of NR3B and with 20μM $Mg^{2+}$ from 49 ± 5% to 44 ± 3% though there is no statistical difference between receptor populations.

Implication of NR2B-containing receptor involvement in hyperexcitability of NMDA receptors has led to the development of novel subunit selective antagonists for therapeutic targeting. The subunit composition of the receptor complex has proved to be an important factor for pharmacological affinity of compounds for the receptor and for targeting specific sub-populations of receptor in different CNS regions. The interactions and influence mediated by the NR3B subunit upon NR2B receptor pharmacology is therefore potentially very important particularly for regulation and assessment of the impact of receptor targeting in motor neurons, where NR3B is predominantly expressed.

The cytotoxicity assay was performed with HEK293 cells co-transfected with NR1/NR2B and NR1/NR2B/NR3B receptors in the presence of three NR2B specific antagonists and using no antagonist as a control.

When no NMDA antagonist was present, NR1/NR2B/NR3B receptors showed a significant reduction in cell death compared to NR1/NR2B receptors again confirming a cytoprotective property of the NR3B subunit. The addition of ifenprodil to cells co-expressing NR1/NR2B receptors resulted in a reduction in cell death to 21% and 17% at 1μM and 10μM concentrations, showing effective antagonism of NR2B-containing receptors. Interestingly, the co-expression of NR3B with NR1/NR2B seemingly increased the sensitivity of ifenprodil, reducing cytotoxicity to 16 ± 7%, 18 ± 5% and 9 ± 5% at 100nM, 1μM and 10μM,

respectively. This apparently enhanced binding affinity of ifenprodil for receptors containing NR3B may be the result of conformational and/or allosteric changes of the ligand binding domain or an impact on the activation state of the NMDA receptors as it has been reported that ifenprodil binds with higher affinity towards receptors in the activated state (Mutel *et al.*, 1998). Ifenprodil is also reported to bind to other non-NMDA receptors such as voltage-gated $Ca^{2+}$ channels (Church *et al.*, 1994) which may be modulated by NR3B and up-regulated, increasing binding and reducing intracellular $Ca^{2+}$ in HEK 293 cells.

Antagonism with the novel compounds COMPOUND B and COMPOUND A resulted in significant reduction in cell death to 23 ± 7% and 16 ± 4%, respectively at 1μM in cells co-expressing NR1/NR2B receptors. The addition of NR3B into the receptor complex slightly reduced the sensitivity to COMPOUND B although overall the protective effect remained similar to that observed in NR1/NR2B cells. In the presence of NR3B, antagonism with COMPOUND A showed reduced sensitivity and binding affinity as no significant reduction in cytotoxicity was observed. This may be due to an allosteric effect of the inclusion of NR3B in the receptor complex, altering the binding site of COMPOUND A and reducing its affinity, or it could be due to a reduction in the numbers of NR2B subunit expressing on the cell surface, thereby reducing the number of available binding sites.

This data provides initial evidence for differential cytoprotective effects of the two novel compounds COMPOUND B and COMPOUND A upon recombinant NMDA receptor-mediated cytotoxicity *in vitro* and potentially shows that COMPOUND A

is more sensitive to the presence of alternative subunits, a finding also highlighted in chapter 3. The sources of variability seen in these assays should be taken into consideration and are likely to result from the natural variability in the health and age of the cell cultures. Also, due to physical limitations in the number of assays which could be performed at one time, experiments were repeated over a number of weeks, increasing the likelihood of variability occurring.

Whole-cell patch clamp electrophysiology was then used in order to investigate the pharmacological effect of NR3B inclusion in NR1/NR2B receptor complexes upon Ro-256981 and CP-101606. Both Ro-256981 and CP-101606 are highly selective NR2B-containing receptor antagonists commonly used as tools for receptor characterisation. Following agonist activation of receptor currents, application of CP-101606 (10μM, 300nM and 30nM) displayed fast onset of blockade, but very slow, minimal wash-out after several minutes, demonstrating high affinity binding to both NR1/NR2B and NR1/NR2B/NR3B complexes. A trend towards reduced inhibition in the presence of NR3B with short 10 second application of 300nM CP101606 supports previous findings that this compound binds with higher affinity towards only NR2B-containing receptors (Chazot *et al.*, 2002) over receptors containing NR2B plus other subunits. Overall however, no significant differences in the percentage inhibition were observed implying a distinction between the allosteric modulatory effects of the NR2 and NR3B subunits on ligand binding domains.

Application of Ro-256981 (10μM) also showed high functional potency towards both receptor complexes inhibiting NMDA receptor mediated currents by

approximately 100%, with fast onset of action and minimal wash-out. At 30nM, 60 second application of Ro-256981 showed a time-dependent response with apparently reduced inhibition of NR1/NR2B/NR3B receptor-mediated currents (10 ± 7%) in comparison to NR1/NR2B (41 ± 12%). These data show that the sensitivity of Ro-256981 may be reduced in the presence of NR3B implying that NR3B confers distinct pharmacological changes to the receptor complex in comparison to alternative NR2 subunits, although due to the small replicate number, further characterisation would be required to confirm results.

Parallel radioligand binding assays also enabled pharmacological characterisation of the influence of NR3B upon NR2B-selective compounds. COMPOUND A and COMPOUND B both show high affinity [$^3$H] CP-101606 displacement curves with NR1/NR2B receptors ($K_i$ = 5 ± 6nM and 14 ± 11nM respectively) which are shifted to the right in the presence of NR3B. In cells co-expressing NR1, NR2B and NR3B, COMPOUND A and COMPOUND B displayed low affinity binding sites (12 and 1μM, respectively), providing further evidence for reduced sensitivity of these compounds toward triheteromeric NR1/NR2B/NR3B complexes.

Interestingly, the presence of the NR3B subunit may also be reducing receptor numbers or NR2B subunits at the cell surface, or affecting antagonist binding sites. Herein, it is shown that in comparison with NR1/NR2B receptors, co-expression of NR1/NR2B/NR3B reduced the specific binding of both [$^3$H] Ro-256981 (3000 to 2000 fmoles/mg at 25nM) and [$^3$H] CP-101606 (1300 to 1000fmoles/mg at 9nM).

The pharmacological modifications of antagonist sensitivities in the presence of NR3B are likely to be due to physical alteration of the compound binding sites, reduced numbers of NR2B subunit expression at the cell surface or alterations in functional receptor expression levels. Compound binding sensitivities would be reduced if the number of functional receptors reaching the cell surface was lowered by changes in receptor trafficking mechanisms or increases in the number of receptors undergoing endocytosis. Previous research suggests that receptors containing NR3A (sharing large sequence homology with NR3B) undergo rapid endocytosis from dendritic plasma membranes during post-natal development. Specific removal is regulated by PACSIN1/syndapin which binds selectively to NPF motifs in the carboxyl terminal of the 3A subunit. (Perez-Otano *et al*, 2006). It is possible that NR3B shares this binding motif and is similarly internalised rapidly, reducing the number of receptors and thus binding sites available, however, the protein complexes required for this internalisation are likely to be different in our model from those of native dendritic membranes.

This potential reduction in receptor numbers reaching the cell surface or the reduced expression of the NR2B subunit supports the cytotoxicity data as a reduction in the number of NR2B subunits would probably lower $Ca^{2+}$ influx into the cell thereby reducing toxicity. However, this potential reduction of NR2B at the cell surface was not reflected in the channel conductance as no significant changes were apparent between the NR1/NR2B and NR1/NR2B/NR3B populations, therefore further investigation is required.

It is evident from the data presented that both NR3A and NR3B have distinct modulatory influences on the NMDA receptor complex which may alter receptor physiology, pharmacology, subunit expression, transportation and signalling. Elucidating these modulations conferred by the NR3 subunits is therefore very important for understanding the full extent of NMDA receptor heterogeneity and its implications for receptor function and pharmacological development of new drug candidates.

# Chapter 6

# NMDA subunit expression in a chronic pain model

## 6.1 Introduction

The hyper-excitation of the NMDA receptors within the central nervous system has been implicated as a pathogenic mechanism in a wide-range of disease states including neurodegenerative conditions, stroke, head trauma, schizophrenia and chronic pain.

Increasing understanding of the molecular mechanisms behind chronic nociceptive signalling via prolonged activation of excitatory neurotransmitters and their receptors led to the focus of research upon NMDA receptors, their function and pharmacology. Persistence of the nociceptive response is mediated, in part, by synaptic changes and long-term potentiation of NMDA receptor signalling, resulting in central sensitisation, an enhanced responsiveness of neurons within the spinal cord and brain stem. Pharmacological intervention of these signalling pathways may therefore provide potentially novel, effective analgesic treatments for chronic pain. As discussed previously in chapters 1, 4 and 5 the undesirable side-effect profile of broad-range NMDA receptor antagonists necessitates the selective targeting of specific receptor populations within nociceptive signalling and processing pathways. NR2B-containing receptors have since become the focus for NMDA receptor targeting, due to their expression patterns and proven involvement in nociceptive transmission (eg, Wei *et al.*, 2001; Zhuo., 2002; Nishimura *et al.*, 2004; Wu *et al.*, 2005).

The development of novel pharmaceutical compounds requires effective animal modelling to closely reproduce clinically relevant symptoms and phenotypes of disease.

The development of NR2B-selective compounds has been reliant upon animal models of peripheral nerve lesion and inflammation (Karlsson *et al.*, 2002; Wu *et al.*, 2005), nerve injury (Dickenson *et al.*, 1997) or subcutaneous injection of an inflammatory mediator into the rat hind paw with measurements of inflammation and pain recorded within several hours of the insult (Chaplan *et al.*, 1994). These models therefore display predominantly acute nociceptive phenotypes and show limited success as bases for developing chronic therapies in the clinic. A requirement therefore exists for improved animal modelling of chronic pain which mimics the more persistent responses displayed in the clinic.

This chapter will discuss and utilise tissue from a novel animal model of chronic inflammatory pain, developed by Alex Wilson and colleagues at GlaxoSmithKline (Wilson *et al.*, 2005). The model was developed for therapeutic advancement of analgesic compounds including NR2B-selective antagonists and aimed to induce the peripheral and central sensitisation seen in chronic pain states. Inflammatory pain is induced by injection of the inflammatory mediator Freund's Complete Adjuvant (FCA) into the left knee joint of adult male Random-Hooded rats with weight bearing and joint diameter measurements made daily for up to 90 days post-FCA.

Previous research has shown changes in NMDA receptor expression including up-regulation of NR2B-containing receptors (Wu *et al.*, 2005), down-regulation of NR2A-containing receptors (Karlsson *et al.*, 2002) and increased phosphorylation of NR1, NR2A and NR2B subunits in dorsal horn neurons (Zou *et al.*, 2000; Gou *et al.*, 2002) during inflammatory pain states. This chapter presents novel data investigating NMDA receptor subunit expression and phosphorylation states in rat brain and spinal cord tissue

from this pain model. NR1, NR2A, NR2B, NR3B and PSD-95 protein expression and phosphorylation of NR2A (pY1325, pY1387) and NR2B (p1252, p1336, p1472) was investigated using immunohistochemical analysis (2.2.11). Functional NR2B-containing receptors were mapped using autoradiographical analysis (2.2.22) with the NR2B-selective compound [$^3$H] Ro-256981, to provide a data set detailing modulation of NMDA receptor complexes during chronic pain states.

## 6.2 Results

Inflammatory hyperalgesia of the left knee joint was induced in adult male Random Hooded rats via injection of 150µl Freund's Complete Adjuvant (containing 1mg/ml *Mycobacterium tuberculosis*). Sham control animals were injected with a saline solution. 16 days post-injection the rats were sacrificed and whole brains (n=8 sham, n=8 FCA) and spinal cords (n=8 sham, n=8 FCA) dissected and either snap frozen on dry ice or fixed in 4% paraformaldehyde until processing.

### 6.2.1 Immunohistochemical characterisation of subunit expression in the spinal cord of adult male rats subjected to a novel chronic pain model

Immunohistochemical analysis was carried out on the lumbar and thoracic regions of the fixed spinal cord tissue (n=4 sham, n=4 FCA) as detailed in 2.2.11.

Following cryostat sectioning of the spinal cords (2.2.9.2) and blockade of endogenous peroxidase activity, the tissue was probed overnight with primary antibodies from the panel previously described in chapter 4; anti-NR1 (1µg/ml), anti-NR2A (2µg/ml), anti-NR2B (2µg/ml), anti-NR3B(885-899) (2µg/ml) and also anti-PSD-95 (1:1000) and phosphorylation antibodies anti-NR2A (py1325, py1387) (1:1000) and anti-NR2B (p1252, p1336, p1472) (1:1000) provided as a gift from Professor Seth Grant, Sanger Institute. Sections probed without primary antibodies acted as controls (figure 6.1).

Both the sensory (dorsal) and motor (ventral) regions of the lumbar and thoracic spinal cord were analysed and immunoreactivity of each antibody compared between the sham and model (FCA) tissue for changes in expression.

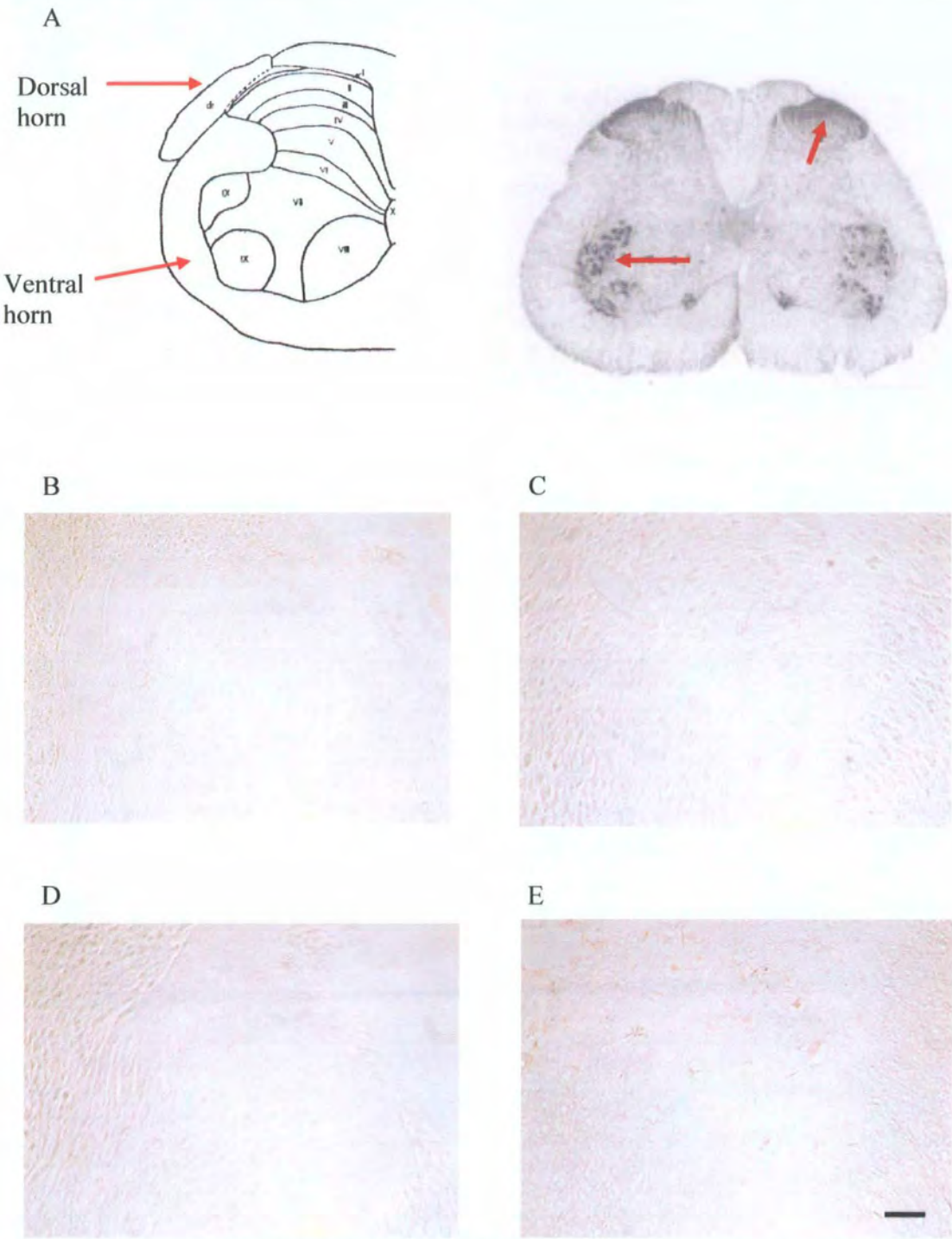


**Figure 6.1 Schematic (Tolle *et al.*, 1993) and low resolution images (Liu *et al.*, 1994) of the cord highlighting the dorsal (outer lamina) and ventral regions (motor neurons) investigated in this study (A) and control sections showing the immunoreactivity in tissue in the absence of primary antibodies in the lumbar dorsal horn (B), the lumbar ventral horn (C), the thoracic dorsal horn (D) and the thoracic ventral horn (E).**

### 6.2.1.1 NR1 expression

The ubiquitously expressed NR1 subunit showed abundant expression throughout the outer laminae of the dorsal horn and large cell bodies of the motor neurons in laminae IX in both the thoracic and lumbar regions of the spinal cords. An example of NR1 immunoreactivity in thoracic spinal cord is shown in figure 6.1. No detectable change in immunoreactivity between the sham and model tissue perhaps indicates that there is minimal modulation of the total numbers of NMDA receptors in an inflammatory state compared to control tissue, an observation supported by previous results showing no change in the number of neurons between control and nerve lesioned animals (Ultenius *et al.*, 2006).

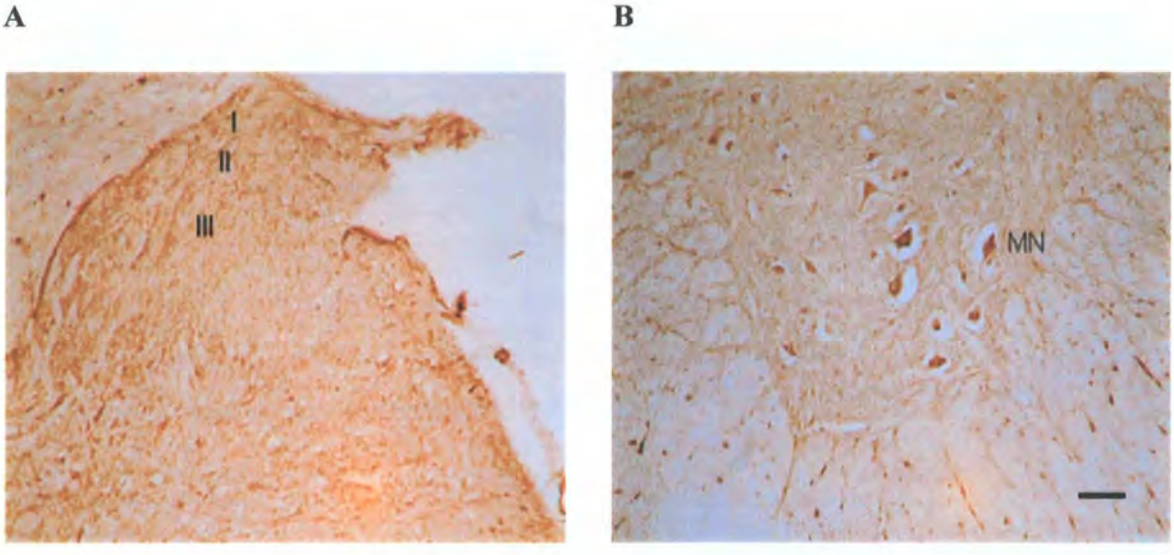


**Figure 6.2 Expression of NR1 protein in the dorsal (A) and ventral (B) horns of the thoracic cord in a sham animal probed with anti-NR1 (1µg/ml). The outer laminae I, II, III are labelled in the dorsal horn (A) and cell bodies of motor neurons (MN) in lamina IX in the ventral horn (B). Scale bar represents 100µm.**

### 6.2.1.2 NR2A expression

Immunohistochemical analysis of NR2A protein showed immunoreactivity in the ventral horns of lumbar cord in both sham and FCA animals. NR2A expression showed no apparent changes in immunoreactivity between the sham and FCA tissue, consistent with previous research that detected no differences in immunoreactivity of non-phosphorylated NR2A in a rat model of peripheral nerve injury (Ultenius *et al.*, 2006) but contradicting a study which detected reduced NR2A mRNA expression after peripheral nerve lesion (Karlsson *et al.*, 2002). Prominent NR2A protein expression was detected in the motor neuronal cell bodies of lamina IX in the ventral horn with more limited expression in the dorsal horns showing that NR2A plays a role in sensory and motor modulation consistent with previous research (Nagy *et al.*, 2004).

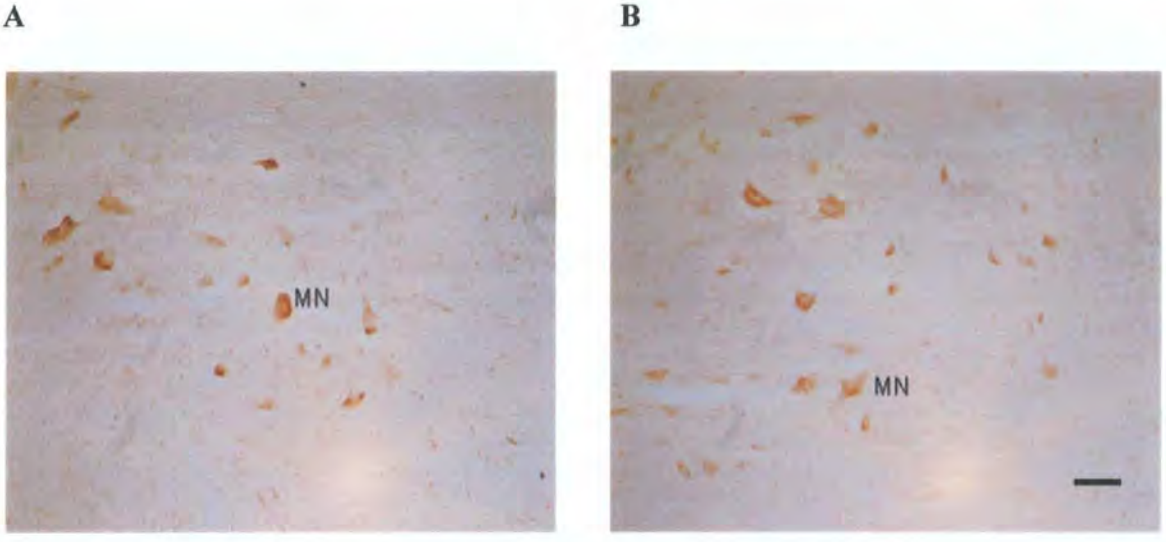


**Figure 6.3 Expression of NR2A protein in the ventral horns of lumbar spinal cord in sham (A) and FCA model (B) animals, probed with anti-NR2A (2µg/ml). The cell bodies of the motor neurons (MN) within laminae IX show high levels of NR2A protein expression. Scale bar represents 100µm.**

### 6.2.1.3 NR2A phosphorylation

Changes in the phosphorylation of the NR2A subunit between the sham and FCA animals was analysed using two antibodies; one which recognised single phosphorylation at tyrosine 1325 (p1325) and one which recognised single phosphorylation at tyrosine 1387 (p1387). Both tyrosine residues are located in the C-terminus of the NR2A protein and can be phosphorylated by the Src family of protein tyrosine kinases (Lee, 2006). It has been proposed that Src-mediated tyrosine phosphorylation of the NR2A subunit potentiates NMDA receptor function by reducing tonic $Zn^{2+}$ inhibition (Zheng *et al.*, 1998).

Phosphorylation of the NR2A subunit was evident in both the dorsal and ventral horns of lumbar and thoracic spinal regions. Immunoreactivity with the anti-py1325 antibody showed no detectable changes in NR2A phosphorylation at this residue between the sham and FCA animals (figure 6.3). Analysis with the anti-py1387 antibody showed initial evidence for enhanced phosphorylation of NR2A at this residue during an inflammatory response with increased immunoreactivity of the dorsal and ventral horns in the FCA lumbar tissue in comparison with the sham tissue (figure 6.4). However, immunoreactivity in the thoracic tissue was unchanged possibly indicating that phosphorylation may be confined to the lumbar region at the site of tibial and fibular nerve entry into the cord. The over-all immunoreactivity of the phosphorylated subunit was reduced possibly because it is detecting only NR2A as part of functional receptors at the cell surface which are phosphorylated and at synapses which are not as prominently labelled as cell bodies with this technique.

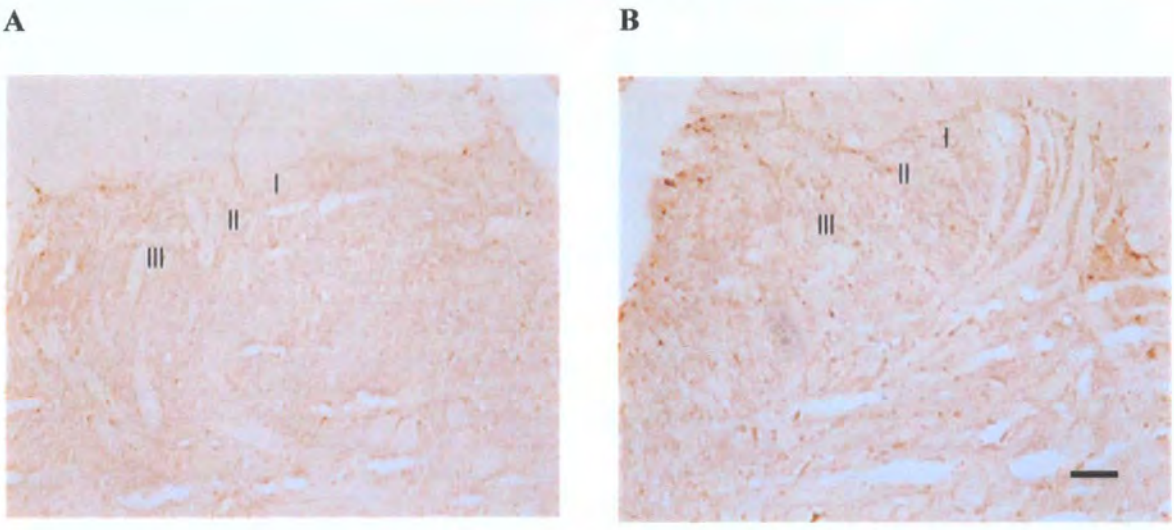


**Figure 6.4 Expression of phosphorylated NR2A subunit at tyrosine residue 1325 in the dorsal horn of sham (A) and FCA (B) lumbar cord tissue. Weak immunoreactivity is present particularly in the outer laminae (I, II and III) of the dorsal horn. Scale bar represents 100μm.**

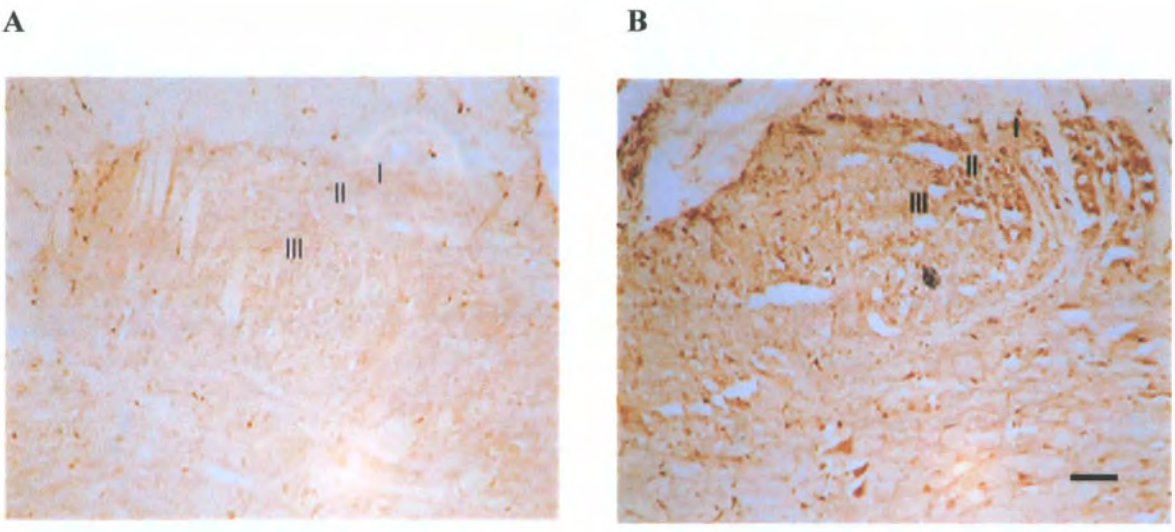


**Figure 6.5 Expression of phosphorylated NR2A subunit at tyrosine 1387 in the dorsal horn of sham (A) and FCA (B) lumbar cord tissue. Initial evidence for increased phosphorylation of NR2A at tyrosine 1387 in the outer laminae (I, II and III) during the inflammatory response. Scale bar represents 100μm.**

### 6.2.1.4 NR2B expression

NR2B protein expression was concentrated in the outer laminae I, II and III of the dorsal horn and motor neuronal somata in the ventral horn, consistent with previous studies (Boyce *et al.*, 1999; Nagy *et al.*, 2004; O'Donnell *et al.*, 2004). No detectable differences in immunoreactivity between the sham and FCA tissue suggest that NR2B expression is unchanged in the spinal cord under these inflammatory conditions. Previous studies have shown up-regulation of forebrain NR2B receptors after inflammation (Wu *et al.*, 2005) and up-regulation of NR2B mRNA in the rat dorsal horn following nerve lesion (Karlsson *et al.*, 2002). Figure 6.5 shows NR2B immunoreactivity within the dorsal horn of the lumbar cord of both sham and FCA animals.

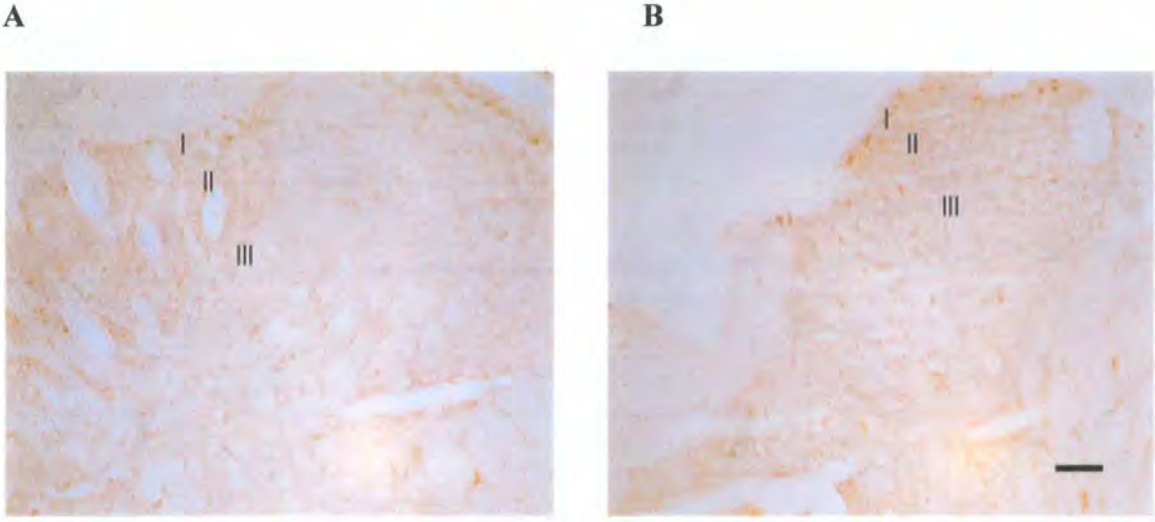


**Figure 6.6 Expression of NR2B protein within the dorsal horns of lumbar spinal cord in sham (A) and FCA (B) tissue. NR2B shows expression in the outer laminae (I, II and III) in both sham and model tissue showing involvement in sensory inputs to the cord. Scale bar represents 100μm.**

### 6.2.1.5 NR2B phosphorylation

Phosphorylation of the NR2B subunit was investigated using three antibodies which recognised tyrosine residues Y1252, Y1336 and Y1472 respectively, again located in the C-terminal of the protein, which are phosphorylated via the Fyn family of kinases (Nakazawa *et al.*, 2001). Analysis with all three antibodies revealed phosphorylated NR2B subunits in the dorsal and ventral horns throughout the spinal cord. Immunoreactivity with anti-pY1252 showed no detectable changes in phosphorylation between the sham and FCA tissue (figure 6.6). Immunoreactivity with anti-pY1336 and anti-pY1472 showed initial evidence for increased phosphorylation of the NR2B subunit at these residues in both the dorsal and ventral horns of the lumbar cord of FCA animals compared to sham tissue (figure 6.7 and figure 6.8). These findings are consistent with previous research which shows increased phosphorylation of NR2B with induction of LTP (Nakazawa ***et al.***, 2001) and blockade of NR2B receptor internalisation via phosphorylation at Y1472 potentiating receptor activity (Prybylowski *et al.*, 2005).

**A** **B**

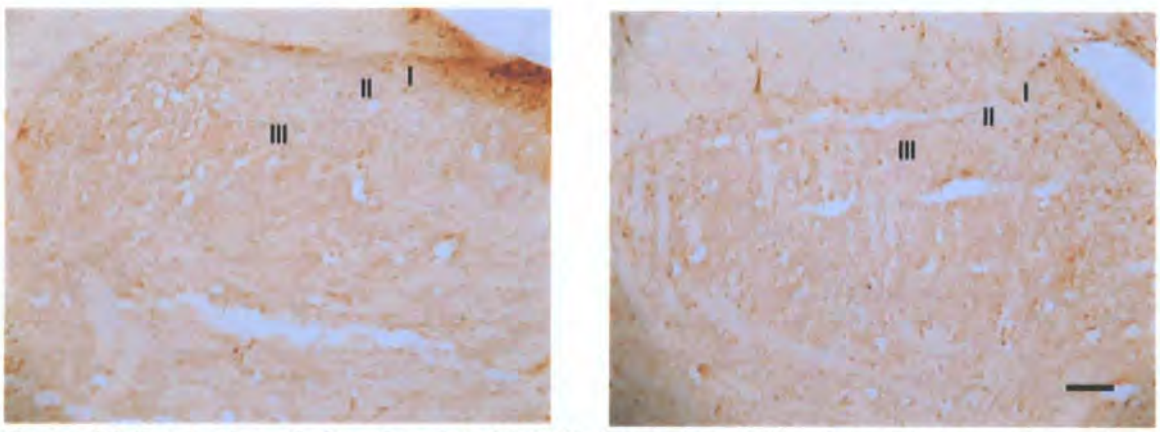


**Figure 6.7 Expression of phosphorylated NR2B at tyrosine 1252 within the dorsal horn of lumbar sham (A) and FCA (B) tissue. Similar levels of immunoreactivity suggest no alteration in phosphorylation of Nr2B at this residue in the outer laminae I, II and III of the dorsal horns. Scale bar represents 100μm.**

A B

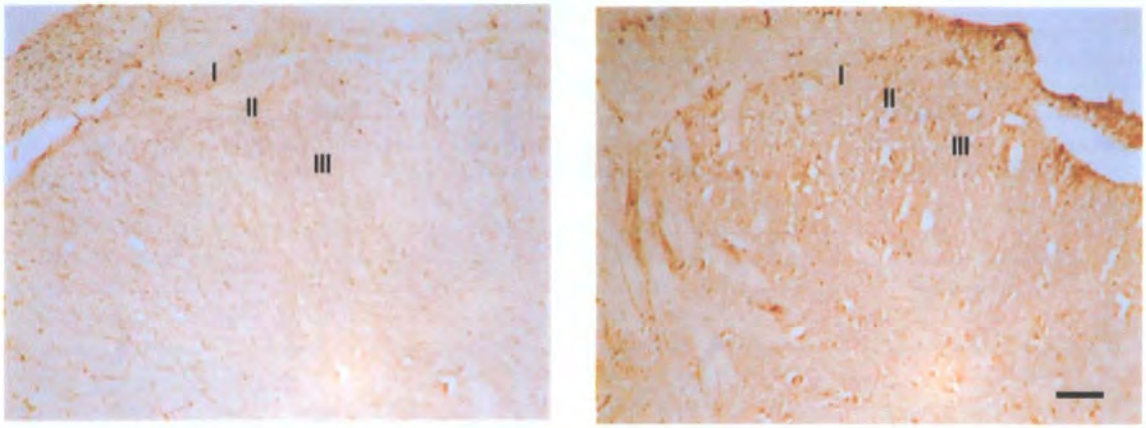


**Figure 6.8 Expression of phosphorylated NR2B at residue y1336 within the dorsal horn of lumbar sham (A) and FCA (B) tissue. Initial evidence for increased phosphorylation of NR2B at this residue in the outer laminae I, II and III, suggesting potentiation of sensory NR2B-mediated transmission. Scale bar represents 100μm.**

A B

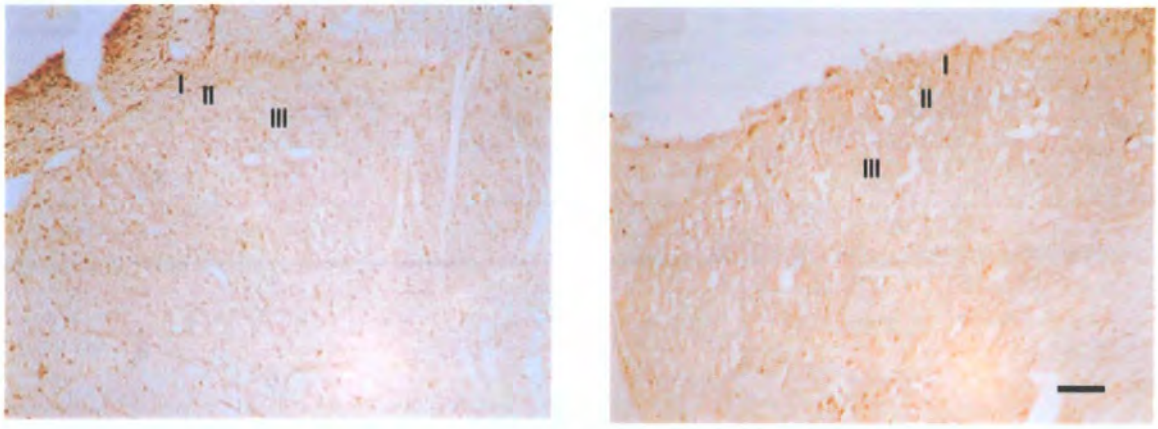


**Figure 6.9 Expression of phosphorylated NR2B at residue y1472 within the dorsal horn of lumbar sham (A) and FCA (B) tissue. Initial evidence for enhanced phosphorylation of the NR2B subunit at residue 1472, in outer laminae I, II and III, important for blockade of receptor internalisation. Scale bar represents 100μm.**

### 6.2.1.6 NR3B expression

NR3B protein expression was prominent in the motor neuronal cell bodies in lamina IX of the ventral horn in all regions of the spinal cord of both sham and FCA animals. Somatic motor neuronal expression of NR3B is consistent with previous research mapping NR3B protein (Matsuda *et al.*, 2002) and mRNA (Nishi *et al.*, 2001). Moderately high levels of immunoreactivity in the dorsal horns were detected, with potentially initial evidence for an increase in NR3B protein expression in the FCA animal dorsal horn in laminae I, II and III (figure 6.9). This provides novel data suggesting that inflammatory conditions may up-regulate NR3B expression in sensory areas.

A B

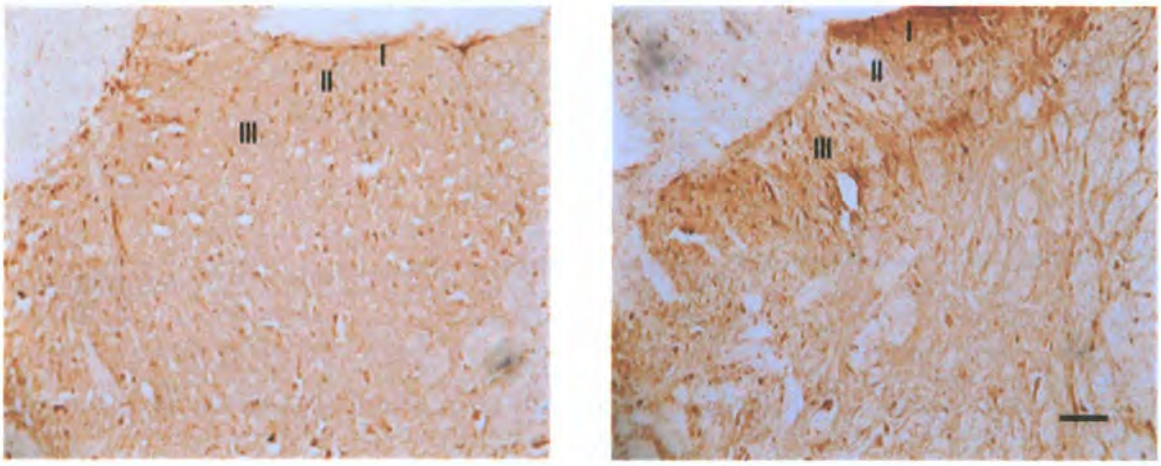


**Figure 6.10 Expression of NR3B protein within the dorsal horns of the lumbar spinal cord in sham (A) and FCA (B) tissue. Initial evidence for increased NR3B expression in outer laminae I, II and III following onset of the inflammatory response. Scale bar represents 100μm.**

### 6.2.1.7 Post-synaptic density 95 (PSD-95) expression

Analysis of the post-synaptic density using an anti-PSD-95 antibody revealed very weak immunoreactivity, particularly in the dorsal horns, where it may be difficult to detect due to its predominantly synaptic localisation. In the ventral horn, the large motor neuronal soma show immunoreactivity (figure 6.10), supporting previous data suggesting that intracellular pools of PSD-95 exist and can exhibit plastic changes and movement between synapses.

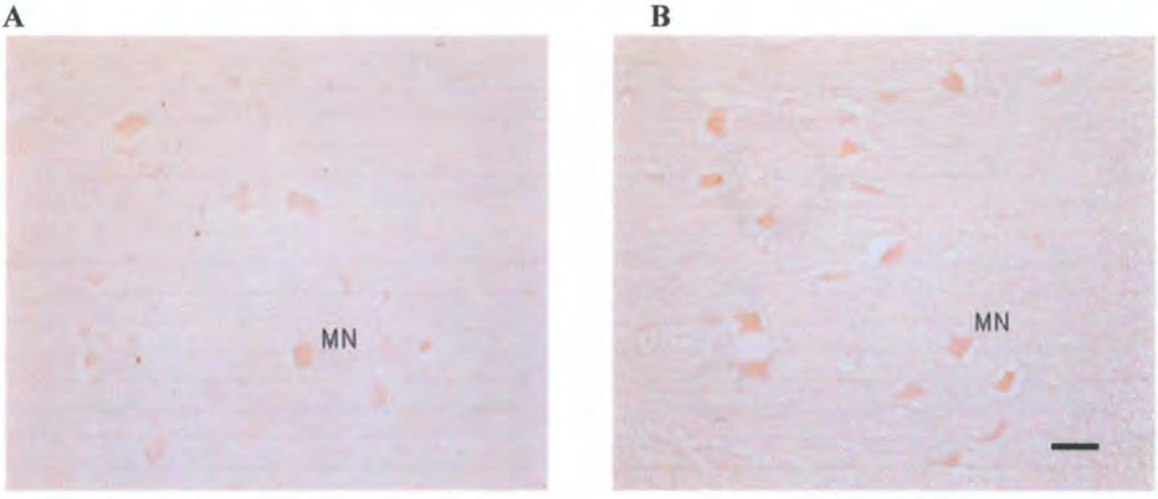


**Figure 6.11 Expression of PSD-95 within the ventral horns of the lumbar cord in sham (A) and FCA (B) tissue. Initial evidence for increased expression of PSD-95 in the motor neuronal soma (MN) of FCA model tissue (B) in comparison with sham tissue (A). Scale bar represents 100μm.**

**6.2.1.8 Qualitative summary of NMDA receptor subunit expression and phosphorylation state in the lumbar and thoracic regions of spinal cord from control and model tissue.**

The data are semi-quantified and shown as the average intensity of immunoreactivity detected from parallel experiments in spinal cords from 2-4 sham animals and 2-4 FCA treated animals.

| | Lumbar cord | | | | Thoracic cord | | | |
|---|---|---|---|---|---|---|---|---|
| | Sham | | Model | | Sham | | Model | |
| | VH | DH | VH | DH | VH | DH | VH | DH |
| Anti-NR1 | +++ | +++ | +++ | +++ | +++ | +++ | +++ | +++ |
| Anti-NR2A | +++ | ++ | +++ | ++ | ++++ | ++ | ++++ | ++ |
| Anti-py1387 | ++ | ++ | +++ | +++ | ++ | ++ | ++ | ++ |
| Anti-py1325 | ++ | ++ | ++ | ++ | ++ | +++ | ++ | ++ |
| Anti-NR2B | ++ | ++ | ++ | ++ | (+) | (+) | (+) | (+) |
| Anti-p1252 | +++ | ++ | +++ | ++ | ++ | ++ | ++ | ++ |
| Anti-p1336 | + | + | ++ | ++ | ++ | ++ | ++ | ++ |
| Anti-p1472 | ++ | + | ++ | ++ | ++ | ++ | ++ | ++ |
| Anti-NR3B | +++ | ++ | +++ | +++ | +++ | +++ | +++ | +++ |
| Anti-PSD-95 | + | (+) | + | (+) | + | (+) | + | (+) |

**Table 6.1 Qualitative summary of the average intensity of immunoreactivity detected with each of the antibodies, in the lumbar and thoracic regions of the spinal cord.**
**(+) = Very weak expression, + = Weak expression, ++ = Moderate expression, +++ = Strong expression, ++++ = Very strong expression.**

### 6.2.2 Autoradiographical analysis of the distribution and density of NR2B-containing receptors in the CNS of adult male rats exposed to a chronic pain model.

Following dissection and rapid freezing of the tissue, autoradiography was carried out on lumbar and thoracic spinal cord regions and whole brains of FCA treated animals compared with sham animals (2.2.22). The NR2B-subtype selective compound [$^3$H] Ro-256981 was used to map NR2B expression in these tissues, defining non-specific binding with ifenprodil (1mM). Following autoradiography, the tissue sections were exposed to tritium-sensitive film together with slide-mounted tritium standards, used during analysis to calculate optical density values, and thus the concentration of bound radioligand (Bq/mg). The autoradiographs were exposed for 5-6 weeks at room temperature and developed for 5 minutes

#### 6.2.2.1 Analysis of autoradiography on the adult rat spinal cord

Autoradiographical analysis on the adult rat spinal cord showed a high level of specific binding within the dorsal and ventral horns of the sham and FCA treated animals (Figure 6.11). Effective displacement of [$^3$H] Ro-256981 using 1mM ifenprodil (figure 6.11) showed specific binding towards NR2B-containing receptors and is consistent with previous findings (Sheahan and Chazot, unpublished).

The outer laminae of the dorsal horn and lamina IX of the ventral horn were regions of the spinal cord selected for analysis due to the high level of NR2B expression in these areas and their involvement in sensory and motor pathways.

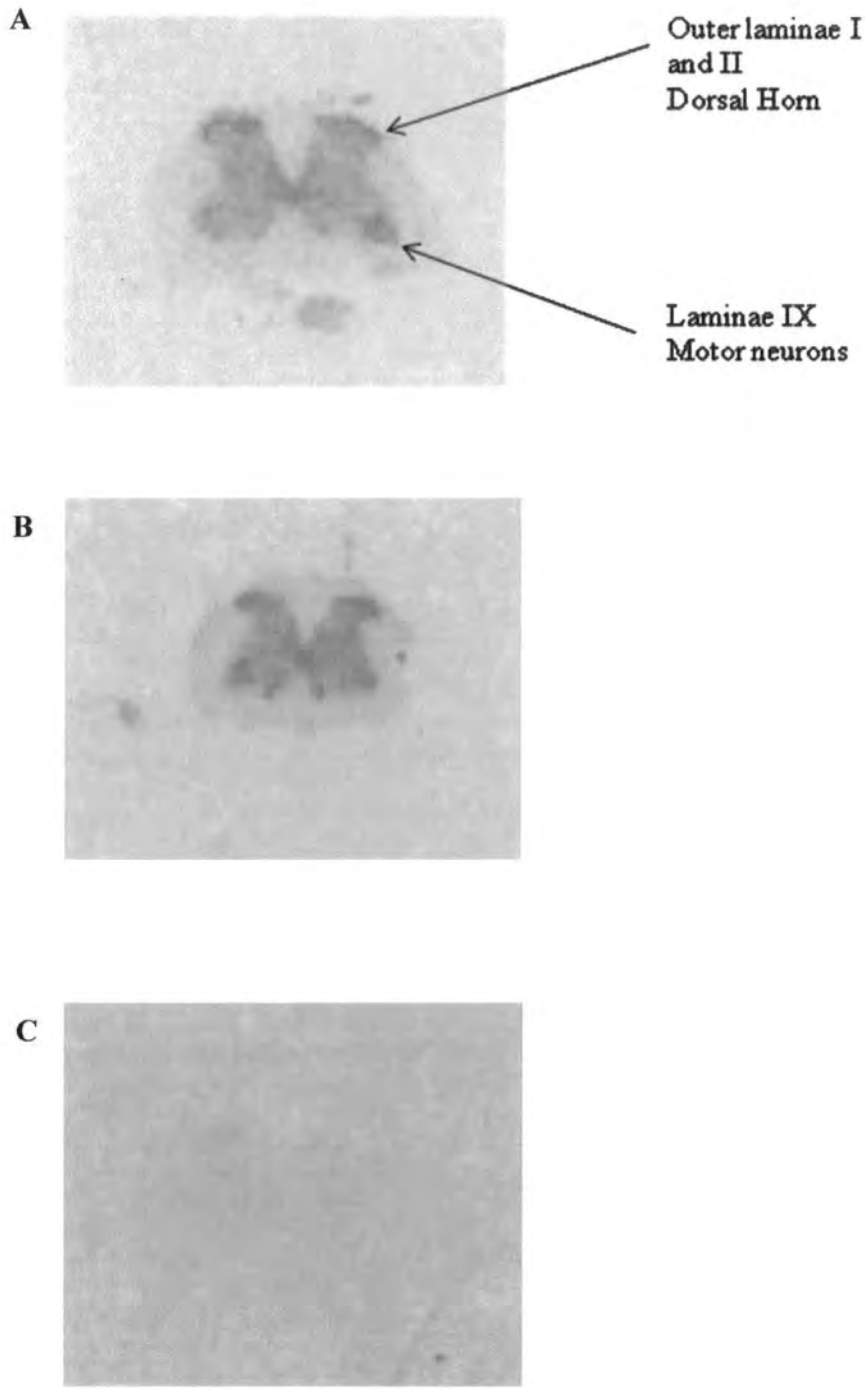


**Figure 6.12 Representative autoradiograms of adult rat lumbar spinal cord using [$^3$H] Ro-256981 in sham (A) and FCA treated (B) animals. Representative image showing non-specific binding defined using ifenprodil (1mM) (C).**

**6.2.2.1.1 Mapping the expression of functional NR2B-containing receptors in the spinal cord of sham and FCA treated adult rats using [$^3$H] Ro-256981.**

Binding of [$^3$H] Ro-256981 within each region of the sham and FCA-treated spinal cord was compared using optical density measurements to calculate the concentration of bound radioligand (Bq/mg).

[$^3$H] Ro-256981 binding in the outer lamina (I and II) of the dorsal horn showed prominent distribution of NR2B-containing receptors in this region of the cord consistent with previous immunohistochemical findings. Comparing the two regions of cord analysed, overall more [$^3$H] Ro-256981 binding was evident in the lumbar cord, likely to be due to a greater proportion of grey matter, though the density changes between the sham and FCA tissue were most evident in the thoracic cord.

In the lumbar region enhanced NR2B expression was evident in the dorsal horn with increased [$^3$H] Ro-256981 binding, however, not to a significant level, possibly showing that induction of inflammation in this model results in up-regulation of NR2B-containing receptors. These data are consistent with previous findings in forebrain (Wei *et al.*, 2001; Wu *et al.*, 2005) but contradict previous IHC findings, likely either to be due to the comparative insensitivity of IHC method or that IHC can't distinguish between an individual subunit and those in a functional complex. In the thoracic cord, both the dorsal and ventral horns showed increased binding of [$^3$H] Ro-256981 in the FCA-treated animals in comparison to sham animals. This provides evidence for up-regulation of NR2B-containing receptor expression or activity in a region other than where the initial insult enters the spinal cord.

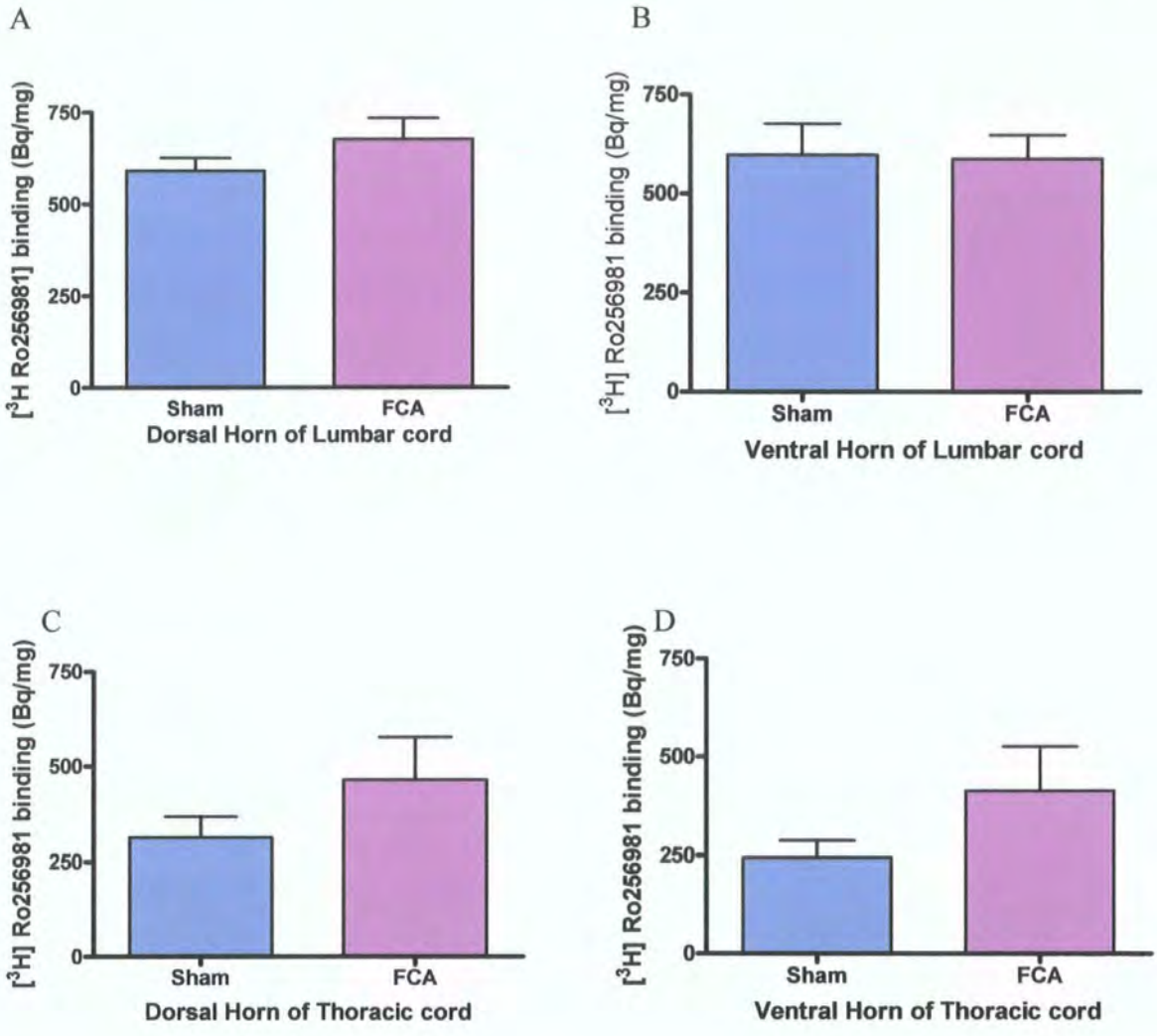


**Figure 6.13 Autoradiographical data showing [$^3$H] Ro-256981 binding within the dorsal and ventral horns of sham and FCA spinal cord.**

**Data shown are the mean values ± standard deviation for n=4 sham and n=4 FCA spinal cords. Sham and FCA tissue is compared in the dorsal horn of the lumbar cord (A), the ventral horn of the lumbar cord (B), the dorsal horn of the thoracic cord (C) and the ventral horn of the thoracic cord (D). Levels of [$^3$H] Ro-256981 binding are higher in the lumbar region than the thoracic region, consistent with NR2B immunoreactivities in IHC experiments.**

### 6.2.2.2 Analysis of autoradiography on the adult rat brain

[$^3$H] Ro-256981 autoradiography on sham and FCA-treated rat brain revealed specific binding confined to forebrain regions, consistent with data showing minimal NR2B subunit expression in the cerebellum (Bradford and Chazot, unpublished, Thompson *et al.*, 2000).

The structures important for nociceptive signalling and processing were selected for analysis to determine any up-regulation in NR2B expression as a result of the inflammatory response. These structures were the somatosensory cortices, the anterior cingulate cortex, the periaqueductal grey, the thalamus and the hippocampal regions (CA1, CA2, CA3 and dentate gyrus) and were analysed from horizontal and coronal brain slices.

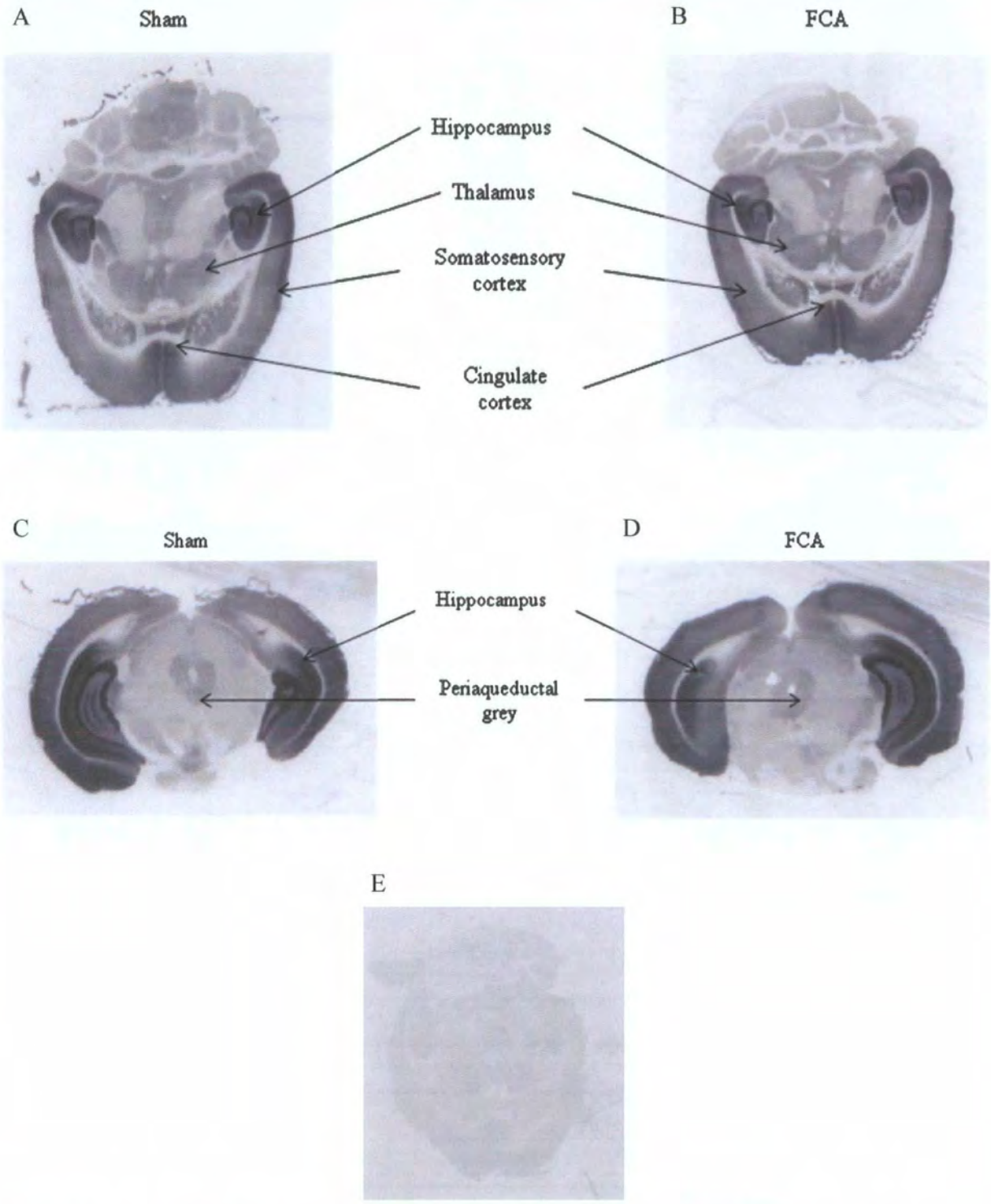


**Figure 6.14 Representative horizontal (A+B) and coronal (C+D) autoradiograms showing [$^3$H] Ro-256981 binding within sham and FCA-treated rat brains. Non-specific binding was defined using 1mM ifenprodil (E).**

**6.2.2.2.1 Mapping the expression of functional NR2B-containing receptors in the brain of sham and FCA treated adult rats using [$^3$H] Ro-256981.**

Binding of [$^3$H] Ro-256981 within each region of the sham and FCA-treated whole brains was compared using optical density measurements to calculate the concentration of bound radioligand (Bq/mg).

Overall, the level of [$^3$H] Ro-256981 binding in the FCA-treated animals was enhanced in comparison to sham tissue showing that this chronic pain model stimulates up-regulation of NR2B-containing receptors. The somatosensory cortices, the cingulate cortex and the periaqueductal grey showed minimal increases in [$^3$H] Ro-256981 binding levels in both the left and right hemispheres. The cingulate cortex and periaqueductal grey are components of the descending modulatory pathway of pain transmission which act to induce 'endogenous analgesia' and attenuate responses, therefore no significant up-regulation of excitatory NR2B-containing receptors may imply a reduced role for this subunit in descending transmission. The brain regions showing significant increases in [$^3$H] Ro-256981 binding were the thalamus, the hippocampal regions CA1, CA3 and the dentate gyrus showing differential, rather than universal up-regulation. Interestingly, in CA3 and dentate gyrus, significant changes were only detected in the right hemisphere where information from the left knee would be processed. Increases in NR2B expression in the hippocampal regions may be indicative of the onset of stress-induced plastic changes of pain transmission and would thus be more evidence for the induction of chronic conditions in this model.

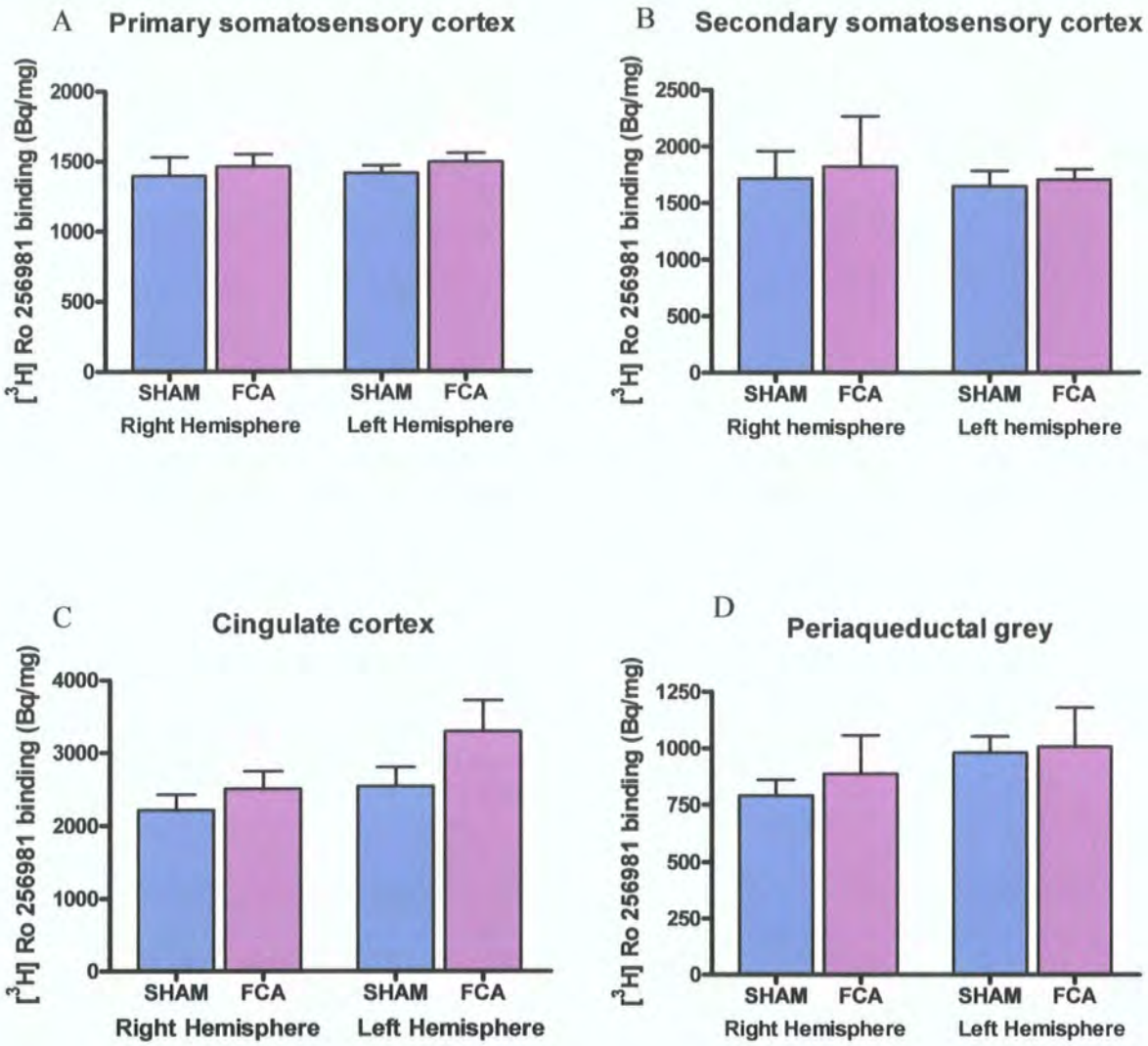


**Figure 6.15 Autoradiographical data showing [$^3$H] Ro-256981 binding within the whole brain of sham and FCA-treated animals.**

**Data shown are the means ± standard deviation of between n=3/4 sham and n=3/4 FCA whole brains. Sham and FCA tissue is compared in 1$^0$ somatosensory cortex (A), the 2$^0$ somatosensory cortex (B), the cingulate cortex (C), the periaqueductal grey (D).**

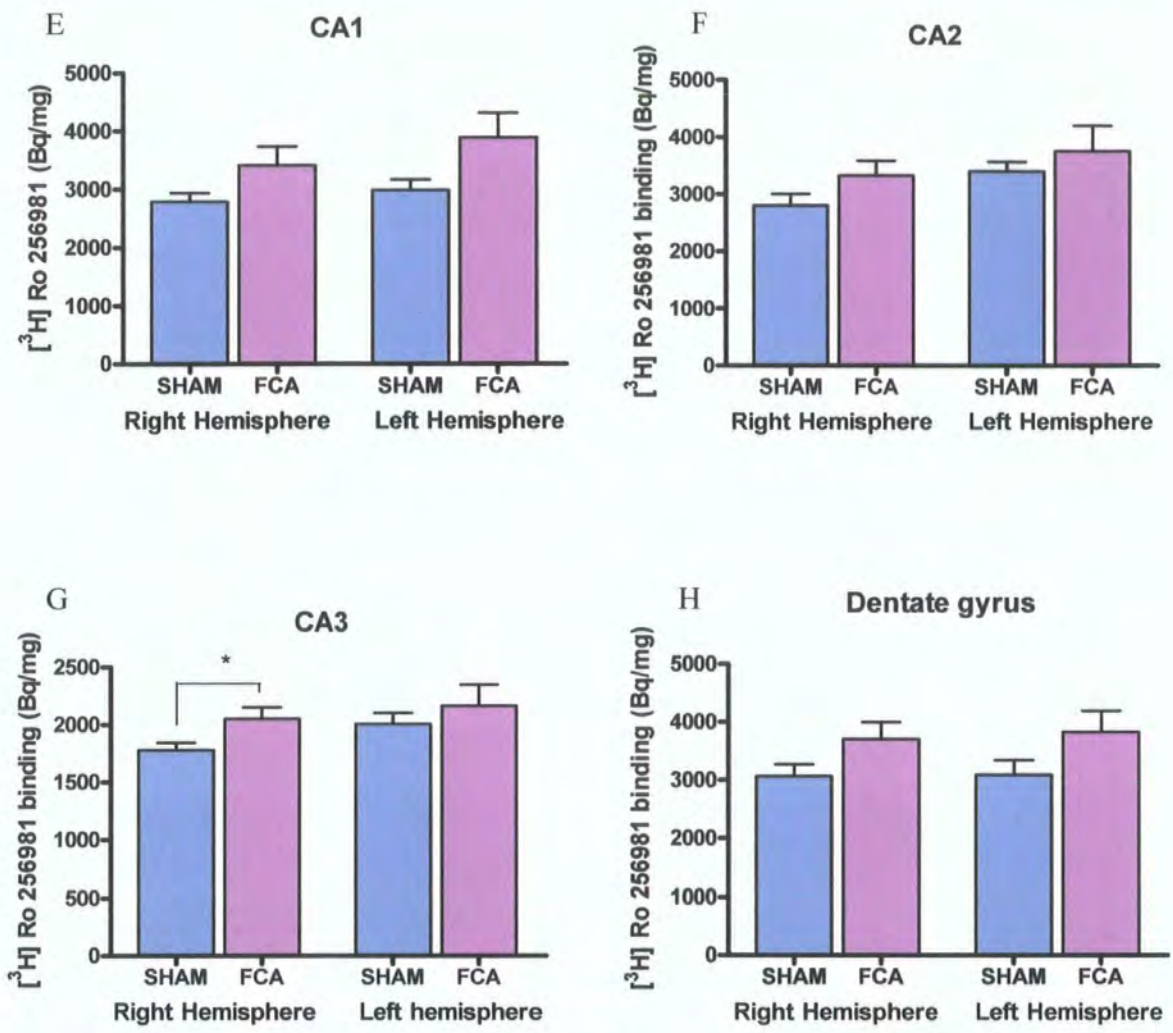


**Figure 6.16 Autoradiographical data showing [³H] Ro-256981 binding within the whole brains of sham and FCA treated animals.**

**Data shown are the means ± standard deviation of between n=3/4 sham and n=3/4 FCA whole brains. Sham and FCA tissue is compared in hippocampal regions CA1 (E), CA2 (F), CA3 (G), the dentate gyrus (H).* p=< 0.05 Unpaired Two-tailed T-Test.**

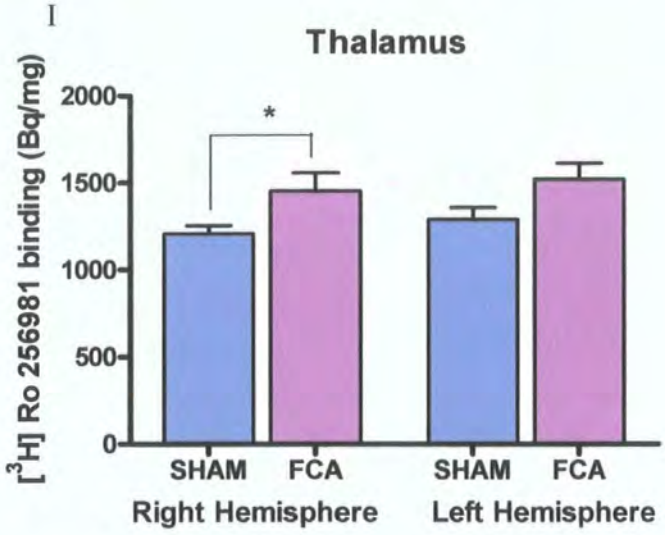


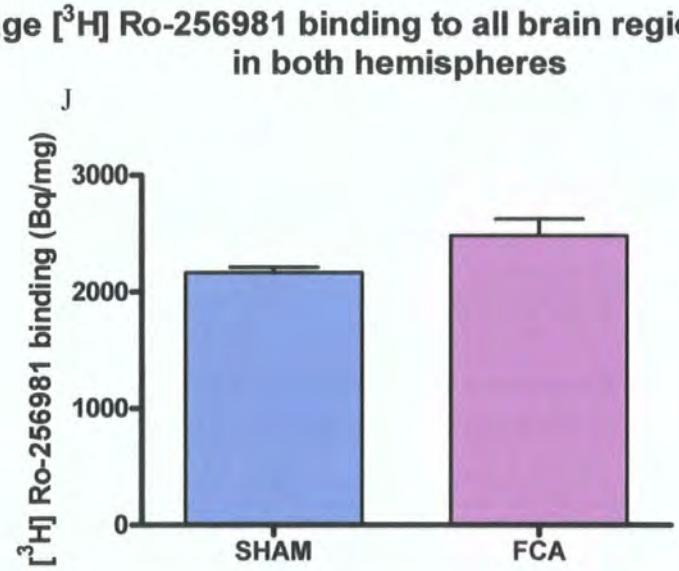


**Figure 6.17 Autoradiographical data showing [³H] Ro-256981 binding within the whole brains of sham and FCA-treated animals.**

**Data shown are the means ± standard deviation of between n=3/4 sham and n=3/4 FCA whole brains. Sham and FCA tissue is compared in the thalamus (I) and all brain regions in both hemispheres combined (p=0.05) (J). * p=<0.05 Unpaired Two tailed T-Test.**

### 6.3 Discussion

The involvement of NMDA receptors in nociceptive transmissions has been widely researched (e.g., Fisher *et al.*, 2000, Wei *et al.*, 2001, Wu *et al.*, 2005, Wilson *et al.*, 2005) with strong evidence to suggest involvement in plastic neuronal changes and chronification of the response.

As discussed previously, the pharmacological development of effective analgesics relies heavily upon accurate, representative animal models which mimic clinical symptoms. This chapter presents novel data showing modulation of NMDA receptor subunit expression in an animal model of chronic inflammatory pain (Wilson *et al.*, 2005). The model seeks to stimulate onset of peripheral sensitisation as a result of knee joint insult and to allow this primary afferent discharge to stimulate centrally mediated changes in the spinal cord (central sensitisation), a marker of chronification. This activity-dependent facilitated transmission of dorsal horn nociceptive neurons occurs due to glutamate and neuromodulator activation of multiple intracellular signalling pathways via ionotropic and metabotropic glutamate receptors and protein kinases. Synaptic efficacy is increased by changes in ion channel activity, such as increased phosphorylation, increasing channel open-time, removing magnesium blockade of NMDA receptors and promoting receptor trafficking to the membrane (Woolf and Salter, 2000). The onset of NMDA receptor modulation, particularly the increased phosphorylation and up-regulation of NR2B-containing receptors, shown in this chapter provides some evidence supporting the attainment of chronicity in this model. This is consistent with data presented in the initial study where hypersensitivity of the animal was maintained over 90 days, despite significant reductions in inflammation, and

effective NR2B-selective antagonism was observed suggesting central plastic changes had occurred (Wilson *et al.*, 2005).

In this study, analysis of the lumbar and thoracic regions of the spinal cord and the brain was carried out to record ascending and descending modulation of the nociceptive response.

The immunohistochemical data showed abundant NR1 expression throughout sensory and motor regions of sham and FCA-treated tissue, consistent with previous data showing no apparent difference in NR1 protein or mRNA expression after nerve crush injury (Virgo *et al.*, 2000). This data provided evidence to suggest that the overall number of NMDA receptors remains unchanged during chronic responses, but that receptor composition is altered by the enhancement of activity showing the NMDA complex to be a flexible assembly. There were also no apparent bilateral differences between the ipsilateral and contralateral sides of the cord. An interesting addition to the current data would be to investigate the time at which NMDA modulation begins, to gain a more accurate insight into the onset of chronification.

Expression of NR2A and NR2B protein remained unaltered in FCA treated animals in comparison to sham animals providing possible evidence to suggest that the NR2A subunit is not replaced by NR2B under such circumstances to enhance receptor activation. However, these findings are in contrast to previous work which showed reduced NR2A mRNA following peripheral nerve injury and previous research showing up-regulation of NR2B mRNA after nerve injury (Virgo *et al.*, 2000), up-regulation of forebrain NR2B receptors after inflammation (Wu *et al.*, 2005) and a

specific 28% increase in NR2B protein expression following colitis (Li *et al.*, 2006). Also, the autoradiographical data in this chapter shows increased [$^3$H]-Ro256981 binding towards NR2B-containing receptors possibly indicating up-regulation of NR2B-containing receptors in the spinal cord and brain, and therefore sensitivity of the immunohistochemical assay must be considered.

NMDA receptor phosphorylation is a critical mechanism for protein regulation, function and involvement in intracellular signal transduction. Initial evidence for enhanced phosphorylation of both the NR2A and the NR2B subunit shows that the activation/function of the existing subunits may be enhanced in addition to or instead of up-regulating the subunit protein. Src-mediated tyrosine phosphorylation of the NR2A subunit potentiates NMDA receptor function by reducing tonic $Zn^{2+}$ inhibition (Zheng *et al.*, 1998) therefore phosphorylation at residue y1387 in both the lumbar dorsal and ventral horns in FCA-treated tissues suggests enhanced receptor activity in both sensory and motor systems. However, immunoreactivity in the thoracic tissue was unchanged possibly indicating that NR2A phosphorylation-mediated receptor enhancement is confined to the lumbar region at the site of nerve fibre entry into the L4 cord region. Fyn-mediated tyrosine phosphorylation of the NR2B subunit at residues y1336 and y1472 was enhanced again in the lumbar cord in the dorsal and ventral horns, showing enhanced receptor activity at the site of afferent entry into the cord, where nociceptive afferents from the injured knee synapse with the dorsal horn neurons. Repeating low frequency stimulations, causing slow synaptic potentials gradually produce a cumulative summation of responses, a phenomenon known as windup. A resulting cumulative depolarisation occurs, releasing the voltage-dependent magnesium block on NMDA

receptors, inducing increased activation and phosphorylation of receptors increasing the action potential response (Thompson *et al.*, 1990; Ji *et al.*, 2003) and leading to early onset central sensitisation within the cord.

These findings are consistent with previous research showing increased phosphorylation of NR2B with induction of LTP (Rosenblum *et al.*, 1996; Nakazawa *et al.*, 2001) and imply enhanced receptor activity on sensory and motor neurons and potential onset of hyperalgesia (demonstrated by animals in the model upon mechanical stimulation). Phosphorylation of the tyrosine residue 1472 is thought to inhibit NR2B-containing receptor internalisation thereby potentiating receptor presence at the cell surface and augmenting transmissions. Phosphorylation at this residue prevents AP-2 adaptors from binding to the critical internalisation sequence YEKL in the C-terminal of NR2B, blocking endocytosis and potentiating surface expression (Lee, 2006). This may again be evidence to suggest that the NR2B protein itself is not up-regulated, just the phosphorylation, holding the receptor at the cell surface for longer, increasing binding. Expression of NR3B showed initial evidence of up-regulation in the lumbar cord posterior dorsal horn in the FCA-treated animals in comparison to the sham tissue suggesting that inflammatory conditions may up-regulate NR3B expression in sensory areas. It is possible that this up-regulation of NR3B may have a protective role, to counteract and regulate $Ca^{2+}$ entry into the cells in the event of NR2B-mediated hyper-activation. Prominent expression in the outer laminae also suggests NR3B involvement in afferent terminal transmissions, providing further evidence for a more extensive role than previously considered and consistent with recent data (Wee *et al.*, 2007).

Expression in the motor neurons in lumbar and thoracic regions (lamina IX) remained prominent throughout both the FCA and sham tissues and again no observable differences were detected between the ipsilateral and contralateral sides of the cord.

Expression levels of PSD-95 were low in both the FCA-treated and sham cords, with no detectable differences between the comparable sections of tissue. Immunoreactivity was most prominent in the soma of motor neurons in lamina IX, likely to be due to the large area for staining in these cells and lack of sensitivity in smaller neuronal processes or possibly intracellular storage pools of protein. It would be expected that PSD-95 would have abundant expression throughout the spinal cord, over-lapping with that of the NMDA receptor subunits, in both the posterior and anterior horn due to its vital role as a multivalent adaptor and anchoring protein (Garry *et al.*, 2003). A previous study showed PSD-95 expression restricted to lamina II of the dorsal horn (Garry *et al.*, 2003), therefore these contrasting results may be indicative of detection sensitivity issues as the PSD-95 complex is constantly changing and re-locating within the cell according to requirement.

Autoradiographical analysis of sham and FCA-treated spinal cords and whole brains enabled detailed, quantifiable mapping of the expression and modulation of NR2B-containing receptors via the specific binding of the NR2B-selective antagonist [$^3$H] Ro-256981. Transverse sectioning of thoracic and lumbar spinal cords and horizontal and coronal sectioning of the brains facilitated specific binding to NR2B-containing

receptors in the spinothalamic tracts and higher brain centres important in nociceptive processing.

The spinal cord autoradiograms showed prominent specific radioligand binding in the superficial laminae of the dorsal horns and lamina IX of the ventral horns (figure 6.12), which displayed a similar bilateral distribution, reflecting previously published patterns of NR2B expression (Nagy *et al.*, 2004). This specific binding in the sensory and motor regions was analysed to investigate the potential up-regulation of NR2B expression and its involvement in both afferent and efferent pathways following nociceptive stimulation.

Comparing the two regions of spinal cord tissue, the overall level of specific [$^3$H] Ro 256981 binding was greater in the lumbar cord than in the thoracic cord probably due to the increased grey matter proportions in this region containing a larger quantity of neuronal cell bodies and dendrites, but also because this is the site of entry to the cord of the afferent neurons from the knee insult.

In the thoracic cord, [$^3$H] Ro-256981 binding was increased in similar proportions in both the dorsal and ventral horns, potentially implying an increase in NR2B-containing receptors as a result of enhanced transduction, possibly descending as both sensory and motor transmissions from higher brain centres to different areas of the cord.

This data may provide initial evidence for an increase in [$^3$H] Ro-256981 binding in diseased tissue as a result of either up-regulation of the NR2B subunit, or increased NMDA phosphorylation maintaining NR2B-containing receptor expression at the cell surface, though further work to increase the number of samples would be required for more accurate conclusions. This data is consistent with previously published results

detailing increased expression of NR2B in lumbar-sacral spinal cord regions after colitis (Li *et al.*, 2006) and the genetic enhancement of inflammatory pain by over expression of forebrain NR2B receptors (Wei *et al.*, 2001).

Autoradiographical analysis of sham and FCA-treated rat whole brains revealed NR2B expression confined to forebrain regions consistent with previous data (Sheahan and Chazot, unpublished; Stephenson, 2001). Minimal background binding in the cerebellum is consistent with previous findings in the laboratory (Sheahan and Chazot, unpublished; Bradford and Chazot, unpublished) and may result from an additional binding site of [$^3$H] Ro-256981. A previous study also showed some NR2B immunoreactivity in cell bodies and dendritic arbors of Purkinje cells (Thompson *et al.*, 2000).

Analysis of the forebrain areas was concentrated on the structures important for nociceptive processing and comprising the sensory-discriminative and emotional-affective areas of pain perception (Tracey *et al.*, 2002). Structures involved in the ascending spinothalamic tract were investigated, with cortical sensory areas, and the descending pathway thought to modulate endogenous analgesia.

To detect any bilateral changes, the left and right hemispheres were analysed separately, with a greater proportion of significant modifications being evident in the right hemisphere. This observation shows that despite overall increases in [$^3$H] Ro-256981 binding throughout the brain ($p=0.05$), the resultant modifications occur primarily in the contralateral hemisphere directly processing information from the insult on the left knee. It would be interesting to see if this hemispheric separation remained throughout a

longer time-course to distinguish any patterns of hyper-sensitisation and observe any masking of bilateral differences.

Radioligand binding in the primary and secondary somatosensory cortices was slightly increased in the FCA-treated tissue in comparison with the sham brains in both the left and right hemispheres, though no significant increase was observed. To perceive acute rapid pain in the somatosensory cortex fast conducting, first order neurons enter the spinal cord synapsing in the dorsal horn, with second order neurons crossing to the contralateral side and forming the axons of the spinothalamic tract. The spinothalamic tract ascends to the thalamus terminating in the ventral posterolateral thalamic nucleus (VPL) where third order neurons then ascend and pass into the sensory cortex and sensations are perceived (Young and Young, 1997). However, in chronic pain, spinal cord reorganisation modifies pathways and slower, more chronic pain is transmitted via a more diffuse pathway called the spinoreticulothalamic tract which is located more medially in the brain stem, synapses in the reticulothalamic system, which projects to medial parts of the thalamus and consequently to more widespread regions of the cortex, particularly those responsible for an emotional response to pain, such as the limbic system, rather than the somatosensory cortex. Therefore the small changes in the sensory cortex seen in this model, but the significant changes seen in the hippocampus may again provide more evidence for the onset of slower, chronic nociceptive transmissions.

[$^3$H] Ro256981 binding in the thalamus was significantly increased in FCA-treated tissue in comparison to sham brains providing evidence for increased NR2B expression and/or NR2B-containing receptor activation in this model, consistent with up-regulation

of forebrain receptors following inflammation (Wu *et al.*, 2005). The thalamus is a large nuclear mass forming 80% of the diencephalon (Tortora and Grabowski, 2003), an area of the forebrain vital for the integration and dissemination of ascending and descending sensory impulses from the spinal cord and brain stem to the cortices (Young and Young, 1997) and back again. As previously described, nociceptive transmissions ascending the spinal cord arrive in the medial thalamus for processing and dispersal to cortical areas responsible for emotional and motor responses. Increased NMDA receptor activity in the thalamus therefore provides evidence for the onset of centrally mediated enhanced activity and persistent responses in this model.

[$^3$H] Ro-256981 binding to the hippocampal formation showed prominent NR2B expression in the neuronal cell bodies of the CA1, CA2 and CA3 fields, and in the granular cell layer of the dentate gyrus consistent with previously published data (Thompson *et al.*, 2002). Significant increases in [$^3$H] Ro-256981 binding were apparent in FCA-treated tissue in comparison with sham tissue in the CA3 region where some hemispheric differences were again evident. NMDA receptors and their involvement in neuronal plasticity, LTP and LTD have been well characterised in the hippocampus which is critical for learning and formation of new memories (Bliss and Lømo, 1973; Bliss and Collingridge, 1993; Kim *et al.*, 1996; Yang *et al.*, 2005, Toyoda *et al.*, 2006.). The increase in hippocampal NR2B-containing receptor activity in this model may be the result of increases in synaptic strength and possibly the onset of LTP induced by the summation of excitatory post-synaptic potentials (EPSP), excessive membrane depolarisation and enhanced NMDA receptor activation enabling increased calcium influx. The calcium signal within the cell is thought to contribute to the

plasticity of a synapse inducing either LTP or LTD to increase or reduce synaptic strength accordingly (Bienenstock *et al.*,, 1982).

Hippocampal connections with the cingulum and the cortex may transmit perceptions of pain and thus form stress responses and fear memories in animals experiencing hyperalgesia and mechanical allodynia from external stimuli. Previous findings have demonstrated that behavioural stress induced by repeated tail shock in adult rats, facilitated LTD in hippocampal CA1 regions (Yang *et al.*, 2005) possibly as a mechanism to regulate neuronal activity (Zhuo 2002). It is proposed that the stress-induced increase in corticosterone levels activates glucocorticoid receptors and inhibits uptake of synaptically released glutamate, enabling glutamate spill over from the synaptic cleft and subsequent activation of extrasynaptic NR2B-containing NMDA receptors. It is therefore possible that a similar mechanism of plasticity could arise from stress induced by FCA treatment in this model, facilitating increased NR2B-receptor activation.

Small increases in [$^3$H] Ro-256981 binding were observed in FCA-treated tissue in comparison with sham tissue in the cingulate cortex and periaqueductal grey, possibly indicating the onset of descending modulatory inhibition, though no statistically significant increases were measured. Overall, the level of radioligand binding was much lower in the periaqueductal grey possibly showing a lower expression level of NR2B-containing receptors in this region. Supraspinal structures such as the cingulate cortex and the periaqueductal grey–rostroventral medulla are part of a descending pathway involved with endogenous analgesic control and transmit descending facilitatory modulation to the dorsal horn neurons in the spinal cord via glutamate, inhibitory

transmitters GABA and glycine, and with the release of endogenous opioids (Zhuo 2002, Tracey *et al.*, 2002). Connections with reticular formation nuclei inhibit the transmission of ascending nociceptive signals via secondary neurons (Young and Young, 1997) and peripheral nociceptive signals from descending higher cortical pathways can also be controlled. It has been shown that direct electrical stimulation of the PAG in humans and in rats can inhibit reflex responses to noxious stimulation (Tracey *et al.*, 2002) and therefore this descending pathway may provide potential targets for pharmaceutical intervention to stimulate the internal analgesic mechanisms in chronic conditions.

In conclusion, the novel data presented in this chapter provides evidence to suggest the attainment of chronic pain in this model, which could therefore be used to provide more clinically significant representations of persistent pain.

Immunohistochemical analysis showing an up-regulation of phosphorylated NR2A and NR2B proteins and autoradiographical data detailing the up-regulation and/or increased expression of NR2B-containing receptors in both the spinal cord and forebrain in this model confirm the critical involvement of NMDA receptor modulation in nociceptive transmissions and therefore support the pharmacological targeting of NR2B-containing receptors for analgesia.

# Chapter 7

# Overall discussion and further work

This thesis has investigated the physiological flexibility of the NMDA receptor, analysing subunit expression and assessing changes in receptor physiology and pharmacology conveyed by the distinct modulatory properties of its component subunits.

The work contained herein was focused on investigation of three main hypotheses: to investigate the potential of selective pharmacological targeting of NR2B-containing receptors and to characterise two novel NR2B-selective antagonists, to investigate the influence of the NR3 subunits upon receptor physiology and NR2B-selective antagonist function, and to investigate changes in NMDA receptor physiology during chronic pain states.

## 7.1 Characterisation of COMPOUND A and COMPOUND B

In chapter 3, characterisation of the two novel NR2B-selective antagonists COMPOUND A and COMPOUND B, revealed that both compounds displayed a high affinity for native and recombinant receptors composed exclusively of NR1/NR2B subunits. Low affinity displacement of [$^3$H] Ro-256981 suggests that the novel compounds are sensitive to the presence of alternative NR2 or NR3 subunits or interacting proteins in the receptor complex, or that they have possibly distinct but overlapping binding sites to that of the Roche compound.

High affinity competitive antagonism with [$^3$H] CP-101606 showed that COMPOUND A and COMPOUND B compete for the same NR1/NR2B receptor populations and are likely to compete for the same binding sites on the receptor complex. Incomplete displacement with COMPOUND B suggests that CP-101606

binds to an alternative receptor population or non-NMDA receptor component in the native tissue to which COMPOUND A also binds, but COMPOUND B does not, implying different interactions between the two novel compounds. These data provide evidence that these novel antagonists potentially show an advanced selectivity profile in comparison to the most effective NR2B antagonists currently in the public domain, sharing properties with the Pfizer compound CP-101606 and showing higher selectivity than the Roche antagonist Ro-256981 (Represented in figure 7.1).

Distinct displacement patterns of [$^3$H] MK-801 demonstrated the potential for differential modulation of the channel pore between the two compounds, showing that COMPOUND B binding effects open-channel probability and may have some allosteric interaction with the channel pore MK-801 binding site. Therefore COMPOUND B may have a distinct mode of action and possibly site of action to COMPOUND A.

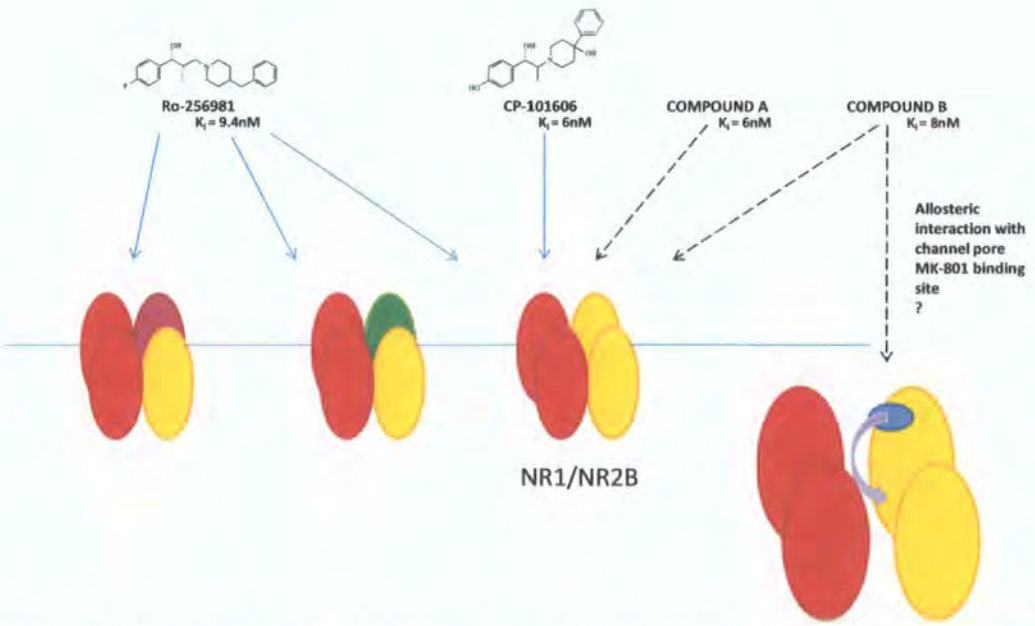


**Figure 7.1 Schematic diagram showing the binding affinities and selectivity towards NR2B-containing receptors of Ro-256981, CP-101606, COMPOUND A and COMPOUND B, and the potential allosteric interaction of COMPOUND B with the channel pore.**

Investigating the functional effects of the two novel compounds with cytotoxicity assays revealed differential antagonistic effects of COMPOUND A and COMPOUND B in recombinant NR1/NR2B receptors. Effective cytoprotection was evident for both compounds at 1μM concentration. To further characterize these novel NR2B antagonists, whole-cell patch clamp electrophysiology could be carried out as a functional assay to look at binding efficacy, effectiveness of current inhibition and reversible inhibition. Site-directed mutagenesis studies could also be carried out to analyse the binding sites of each compound in detail.

### 7.2 Expression and differential cytoprotective effects of NR3 subunits

To further enhance the understanding of the impact of alternative subunits upon NR2B receptor populations and NR2B-selective antagonists, interactions with the NR3 subunits were investigated. It has been shown that the NR3 subunits are expressed predominantly in motor neurons but more recent studies suggest a wider distribution throughout the brain (Wee *et al.*, 2007, Nilsson *et al.*, 2007), particularly in the human and therefore their impact upon NMDA receptor physiology and pharmacology is important to understand.

This thesis presents novel data, showing the co-expression of the NR3B subunit with NR1, NR2A and NR2B protein in adult rat and human spinal cord, in the motor and possibly sensory regions and provides putative evidence for their co-assembly in these structures. Further work in this area would be fundamental to understand the native interactions of the NR3B subunit in the spinal cord and the brain. In future experiments lumbar/thoracic spinal cord homogenate should be used for solubilisation to maximize receptor subunit expression, particularly of NR2B and

NR3B. Direct immunoprecipitation with the anti-NR3B antibody may be a more effective tool than immunopurification, though it would be important to confirm antibody specificity using tissue from knock-out mice (Neimann *et al.*, 2007). It would also be very interesting to investigate any potential changes in native NR3B co-assemblies in human tissue both from normal patients and from patients who have suffered a neurodegenerative illness.

Chapter 5 presents novel evidence for a differential cytoprotective effect of the NR3 subunits upon NR1/NR2A and NR1/NR2B receptors *in vitro*, highlighting the potential for different interactions and effects within native receptor populations.

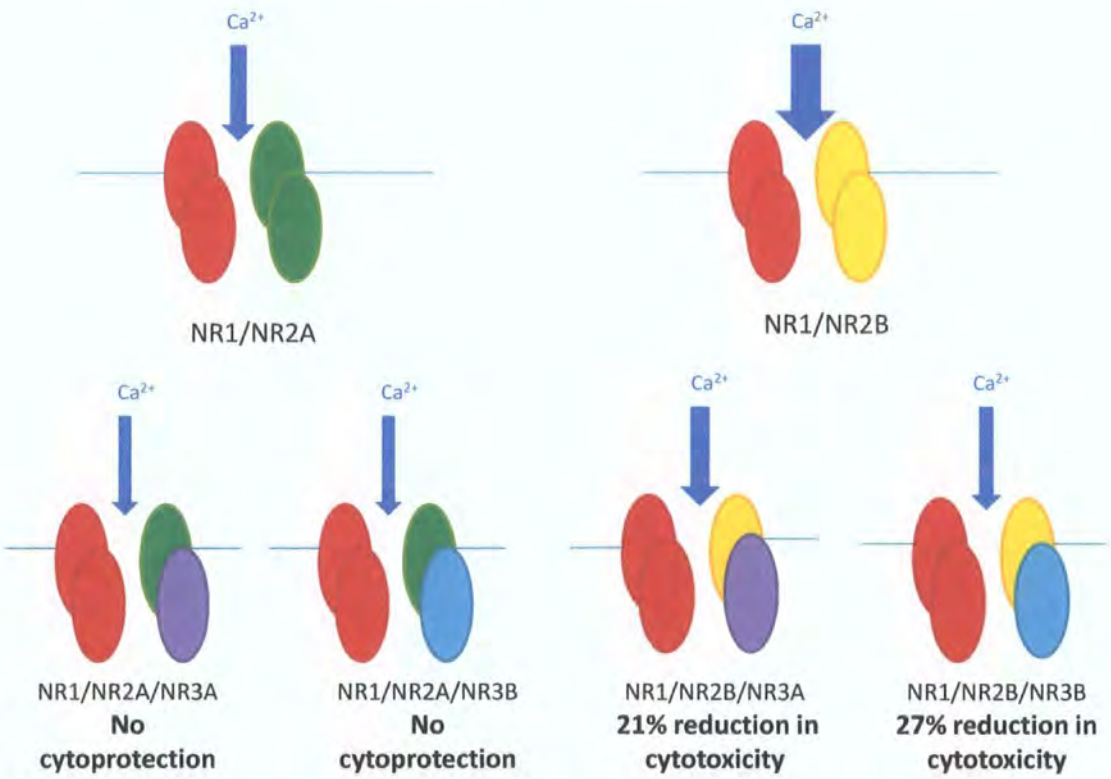


**Figure 7.2 A schematic diagram showing the differential protective effect of the NR3 subunits upon the proposed NMDA-mediated calcium toxicity in NR1/NR2A and NR1/NR2B receptors.**

A significant reduction in cell death when both NR3A and NR3B are co-expressed with NR1/NR2B receptors may indicate an endogenous mechanism triggered to counteract the hyper-excitation of the NR2B-containing NMDA receptors and reduce cytotoxicity in native systems. Indeed, initial evidence for an increase in NR3B expression throughout the spinal cord presented in the rat model of chronic pain, shows that this endogenous protective mechanism may be induced in pathological conditions.

From this work, it was possible to hypothesise that neurodegenerative conditions mediated in part by NMDA calcium toxicity may develop from defective NR3 expression. Recently a study was published suggesting that 10% of the normal European-American population lacks NR3B due to a homozygous occurrence of a null allele in the gene (Niemann *et al.*, 2007). The question arising about the phenotypic consequences of this genetic loss was partly answered in the same study which looked specifically at ALS (motor neuron disease). The researchers reported no obvious impairment of motor neuronal function or increased susceptibility for ALS in the absence of NR3B suggesting that 'NR3B is functionally redundant' (Niemann *et al.*, 2007) in humans. However, species differences are clearly apparent as animal models have shown that NR3B knockout mice develop progressive paresis and die at P5 with loss of motor neurons in the spinal cord (Qu *et al.*, 2004) and genetic ablation of NR3B in mice showed a moderate but significant impairment of motor co-ordination and enhanced anxiety-like behaviour consistent with effects of NR3B loss in higher brain centers such as the hippocampus and amygdala (Niemann *et al.*, 2007).

These apparent variations between species therefore require further investigation to confirm the role of NR3B in the receptor complex. It would be interesting to

investigate the cytoprotective effects of human recombinant receptor combinations in the presence and absence of NR3B and compare them with the rodent studies. Also more expression and purification studies are required to map NR3B expression in rodents, monkeys and humans to see if there is an evolutionary stage at which NR3B became redundant, confirming or refuting the recent publication. It would also be interesting to see if expression levels of NR3A are increased as a compensatory mechanism in individuals lacking the NR3B subunit as recent studies showed NR3A expression in the adult human (Eriksson *et al.*, 2002; Niemann *et al.*, 2007) whereas only minimal expression in the adult rodent is evident (Sucher *et al.*, 1995).

To further investigate the cytoprotective properties of the NR3A and NR3B subunits it would be interesting to repeat the cytotoxicity assays co-transfecting both NR3A and NR3B with NR1/NR2B receptors, to see if a combination of both NR3 subunits enhances the cytoprotective effect. The recent studies showing NR3A expression in the adult human (Eriksson *et al.*, 2002; Niemann *et al.*, 2007), suggest that potentially both NR3A and NR3B could be expressed together in the same receptor complex.

### 7.3 Physiological impact of NR3B in NR1/NR2B receptors

In chapter 5, electrophysiological analysis of the physiological impact of NR3B upon NR1/NR2B receptors showed that current amplitudes and calcium permeabilities remained unchanged in this system, contrasting with literature previously published on co-expression of NR1/NR2A/NR3B (Nishi *et al.*, 2001; Matsuda *et al.*, 2002). However, recent work, published only in abstract form, suggests that receptor currents are significantly altered depending on co-expression

of NR1 splice variant, suggesting that NR1-1a expression with NR2B/NR3B potentiates currents, whilst expression with NR2A/NR3B attenuates currents (Cavara and Hollmann, 2007). Whilst this study supports the electrophysiological data presented in this thesis, it contradicts the cytotoxicity data which suggests suppression of receptor activity. It is therefore apparent that further research is required to explain these contradictions in the current data set and it may become evident that NR3B interacts with other protein complexes in the cell to reduce internal calcium concentrations. Repetition of these studies using single channel electrophysiology could enable more detailed study of the differences in receptor channel activity imposed by NR3B and may reduce the potential for subtle changes in whole receptor populations measured with whole-cell assays. Further experiments using FLIPR analysis could also be used to measure intracellular calcium concentrations in large cell populations expressing various combinations of rodent and human NR3 subunits. Effective subunit tagging before transfection could also ensure that measurements were taken from cells co-expressing all three subunits and transfection with different NR1 splice variants should be investigated. Tracking the movement of NR3B within a cell or neuron may indicate whether it interacts with alternative intracellular complexes, and purification of NR3B from the cell surface, may indicate any non-NMDA associations.

### 7.4 Pharmacological impact of NR3B in NR1/NR2B receptors

Novel pharmacological interactions of the NR3B subunit with NR1/NR2B containing receptors were also presented in this thesis, providing evidence for potentially important modifications of compound interaction. Co-expression of NR3B in the receptor complex appeared to enhance the apparent affinity of the

NR2B-antagonist ifenprodil for the receptor complex, increasing the level of cytoprotection conveyed by this compound. Furthermore, in the cytotoxicity assay COMPOUND A sensitivity appeared reduced in the presence of NR3B, with no significant reduction in cytotoxicity measured. Interestingly, in binding assays, the inclusion of NR3B in the receptor complex appeared to reduce binding affinities of COMPOUND A, COMPOUND B, CP-101606 and Ro-256981 to the receptor. These data provide initial evidence to suggest a potentially important pharmacological impact of the NR3B subunit upon NR2B-selective antagonists.

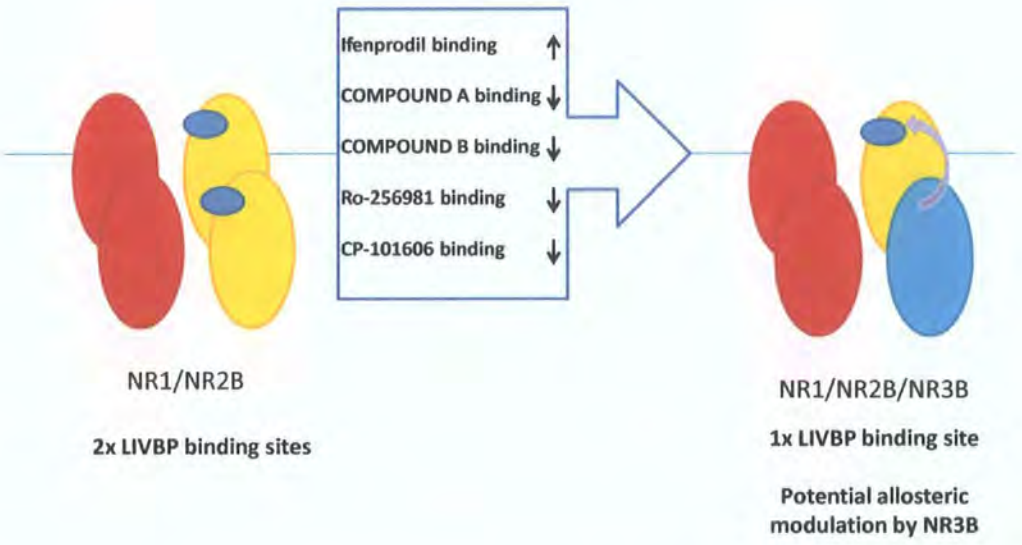


**Figure 7.3 A schematic diagram showing that the inclusion of an NR3B subunit into the receptor complex may have an allosteric effect upon the LIVBP binding domain of the NR2B-selective antagonists.**

To expand upon these findings it would be important to repeat the binding experiments and the cytotoxicity assays with wider concentration ranges of the five compounds and to repeat the binding assays with ifenprodil for direct comparison. Surface binding experiments, using cross-linking reagents could show if the

expression of NR2B at the cell surface is reduced upon inclusion of NR3B. Whole-cell electrophysiology could be carried out to analyse the effects of all five compounds towards recombinant receptors and site-directed mutagenesis studies could be used to investigate and compare the binding sites of each antagonist.

It may also be possible to culture motor neurons and sensory neurons *in vitro* and see if they respond differently to the antagonists thereby investigating whether the NR3B subunit has similar effects in native neurons as in receptors expressed in HEK 293cells. It would also be interesting to see if co-expression of NR3A with NR1/NR2B affected the antagonists in a similar manner to NR3B.

### 7.5 NMDA receptor modulation in a chronic pain model

Autoradiographical and immunohistochemical analysis of rat spinal cord and whole brain from a chronic pain model showed initial evidence for increased NR3B expression and NR2A phosphorylation in comparison to controls, suggesting increased NMDA receptor activity and up-regulation of NR3B as an endogenous cytoprotective mechanism. Increased binding of [$^3$H] Ro-256981 and increased phosphorylation of NR2B in comparison to control tissue also provides evidence for increased expression of NR2B and/or potentiation of NR2B-containing receptor activity via inhibition of endocytosis. These modulations to NMDA receptor activity, induced by persistent nociceptive inputs, suggest attainment of a level of central sensitization and chronicity in this model.

This work provides evidence for a simultaneous increase in NR2B receptor activity in both the dorsal and the ventral horns of the spinal cord, particularly in the thoracic region showing hyperactivity and increased sensitivity in both sensory and motor

systems. Also, significant increases in [$^3$H] Ro-256981 binding in the thalamus and hippocampus show the onset of increased receptor activity in supraspinal structures and the recruitment of emotional brain centers during chronic pain states, possibly effecting memory formation in these animals and relaying the onset of stress and fear.

These physiological changes in receptor properties and the up-regulation of NR2B-receptors at the cell surface in chronic pain states are consistent with previous publications and provide further evidence to support the targeting of NR2B-containing receptors for analgesia.

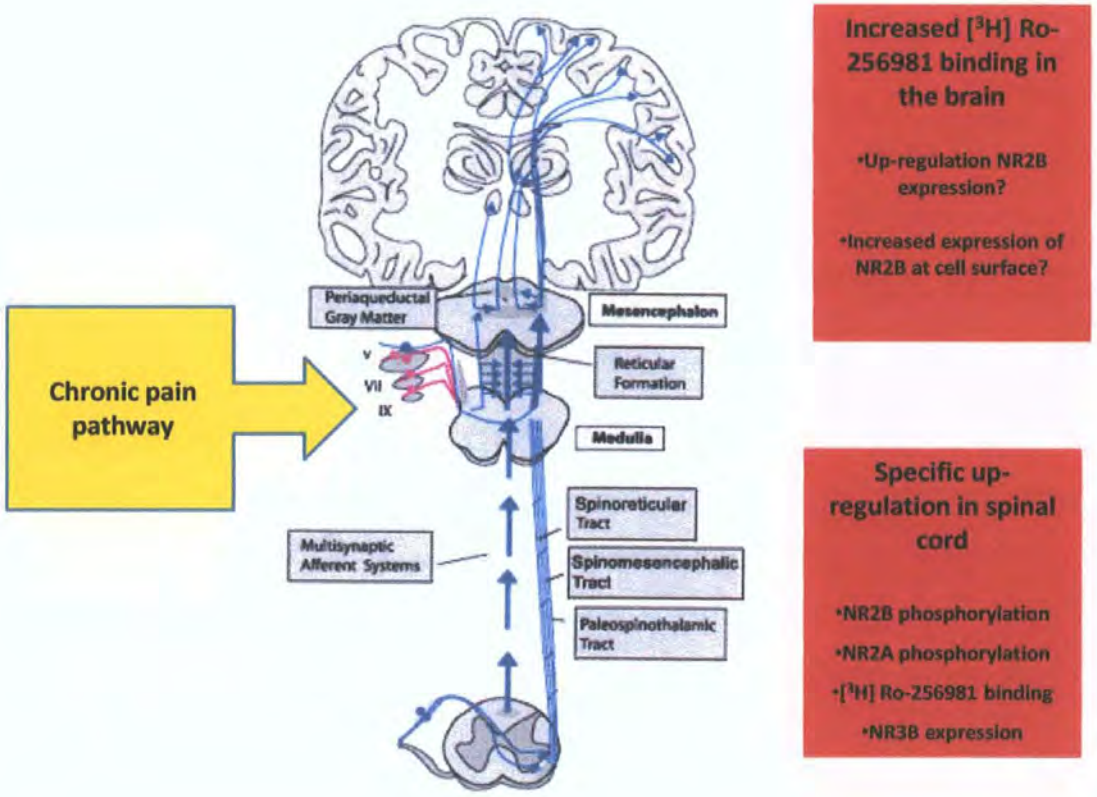


**Figure 7.4 A schematic diagram showing the pathway of chronic pain transmission from the spinal cord, through the brainstem and into the cortex (Anaesthesia, UK www.frca.co.uk) and the changes in the NMDA receptor which may contribute to the persistent response.**

To confirm the results presented in this thesis, the assays could be repeated using a larger number of animals and replicates for each study. Perfusion fixation may increase the quality of the tissue for immunohistochemistry, the whole brains should be analysed and the immunoreactivity in the tissue could be quantified using a slice densitometer (Ultenius *et al.*, 2006) to avoid subjective conclusions. It would also be interesting to compare tissue from this model with that from an acute model, and analyse different time-points during the experiment to determine the stage at which persistent pain occurs and where NMDA involvement is enhanced. It would also be interesting to perform high resolution studies to see if up-regulation of receptor activity is concentrated synaptically or extrasynaptically.

### 7.6 Overall findings

- The novel compounds presented in this thesis are high affinity, selective NR2B antagonists, which have potential to be developed as clinical analgesics following further investigations into their side effect profile and effectiveness *in vivo*.
- The NR3 subunits show differential cytoprotective properties when co-expressed within recombinant NMDA receptor complexes, providing significant cytoprotection towards NR1/NR2B receptors but not to NR1/NR2A receptors, though the mechanism by which this reduction in cytotoxicity is mediated requires further investigation.
- The inclusion of NR3B in NR1/NR2B receptor complexes appears to modulate the binding affinities of some NR2B-selective antagonists, possibly by allosterically altering their binding sites.

- The up-regulation of NR3B and NR2B subunit expression and increased phosphorylation of NR2B and NR2A provides evidence for NMDA receptor subtype involvement in the onset of persistent pain and further supports NR2B-subunit targeting for analgesic development. From the evidence published (Wilson *et al.*, 2005) and the work presented in this thesis, this chronic pain model appears to provide an effective mimic of clinical symptoms of long-term inflammatory pain, and therefore would provide an essential tool for assessing future drug candidates.

# References

Abe T, Matsumura S, Katano T, Mabuchi T, Takagi K, Xu L, Yamamoto A, Hattori K, Yagi T, Watanabe, Sakimura K, 2005, Fyn kinase-mediated phosphorylation of NMDA receptor NR2B subunit at Tyr1472 is essential for maintenance of neuropathic pain, *European Journal of Neuroscience*, 22: 1445-1454.

Akesson E, Kjaeldgaard A, Samuelsson EB, Seiger A, Sundstrom E, 2000, Ionotropic glutamate receptor expression in human spinal cord during first trimester development, *Developmental Brain Research*, 119, 55-63.

Akazawa C, Shigemoto R, Bessho Y, Nakonishi S, Mizuno N, 1994, Differential expression of five N-methyl-D-aspartate receptor subunit mRNA's in the cerebellum of developing and adult rats, *Journal of Computational Neurology*, 347 (1): 150-60.

Albensi BC, Igoechi C, Janigro D, Ilkanich E, 2004, Why do many NMDA antagonists fail, while others are safe and effective at blocking excitotoxicity associated with dementia and acute injury?, *American Journal Alzheimers Disease and Other Dementias*.19 (5): 267-74.

Albin RL, Young AB, Penney JB, 1989, The functional anatomy of basal ganglia disorders, *Trends of Neuroscience*, 12 (10): 366-75.

Al-Hallaq RA, Jarabek BR, Fu Z, Vicini S, Wolfe BB, Yasuda RP, 2002, Association of NR3A with the N-Methyl-D-aspartate receptor NR1 and NR2 subunits, *Molecular Pharmacology* 62: 1119-1127.

Andersson O, Stenqvist A, Attersand A, Von Euler G, 2001, Nucleotide sequence, Genomic organisation and chromosomal localisation of genes encoding the human NMDA receptor subunits NR3A and NR3B, *Genomics*, 78: 178-184.

Antonov SM, Johnson JW, 1999, Permeant ion regulation of N-methyl-D-aspartate receptor channel block by $Mg^{2+}$, *PNAS*, 96: 14571-14576.

Armstrong N, Sun Y, Chen GQ, Gouaux E, 1998, Structure of a glutamate-receptor ligand-binding core in complex with kainite, *Nature*, 395: 913-917.

Arning L, Saft C, Wieczorek S, Andrich J, Kraus PH, Epplen JT, 2007, NR2A and NR2B receptor gene variations modify age at onset in Huntington disease in a sex-specific manner, *Human Genetics*, 122(2):175-82.

Arundine M, Tymianski M, 2003, Molecular mechanisms of calcium-dependent neurodegeneration in excitotoxicity, *Cell Calcium*, 34: 325-337.

Bayer KU, De Koninck P, Leonard AS, Hell JW, Schulman H, 2001, Interaction with the NMDA receptor locks CaM KII in an active conformation, *Nature*, 411: 801-834.

Beneyto M, Kristiansen LV, Oni-Orisan A, McCullumsmith RE, Meador-Woodruff JH, 2007, Abnormal glutamate receptor expression in the medial temporal lobe in schizophrenia and mood disorders, *Neuropsychopharmacology*, 32 (9): 1888-902.

Bennett DA, Lehmann J, Bernard PS, Leibman JM, Williams M, Wood PL, Boast CA, Hutchison AJ, 1990, CGS 19755: a novel competitive N-methyl-D-aspartate (NMDA) receptor antagonist with anticonvulsant, anxiolytic and anti-ischemic properties, *Progress in Clinical Biological Research,* 361: 519.

Bienenstock EL, Cooper LN, Munro PW, 1982, theory for the development of neuron selectivity: orientation specificity and binocular interaction in the visual cortex, *Journal of Neuroscience*, 2 (1): 32-48.

Bigini P, Gardoni F, Barbera S, Cagnotto A, Fumagalli A, Longhi A, Corsi M, Luca D, Mennini T, 2006, Expression of AMPA and NMDA receptor subunits in the cervical spinal cord of wobbler mice, *BMC Neuroscience*, 7: 71.

Blahos J, Wenthold RJ, 1996, Relationship between N-methyl-D-Aspartate receptor NR1 splice variants and NR2 subunits, *The Journal of Biological Chemistry*, 271: 15669-15674.

Bliss TV, Lomo T, 1973, Long-lasting potentiation of synaptic transmission in the dentate area of the anaesthetized rabbit following stimulation of the perforant path, *Journal of Physiology*, 232: 331-356.

Bliss TV, Collingridge GL, 1993, A synaptic model of memory: long-term potentiation in the hippocampus, *Nature*, 361: 31-39.

Boeckman FA, Aizenman E, 1994, Stable transfection of the NR1 subunit in Chinese hamster ovary cells fails to produce a functional N-methyl-D-aspartate receptor. *Neuroscience Letters*, 173:1291-1300.

Boyce S, Wyatt A, Webb JK, O'Donnell R, Mason G, Rigby M, Sirinathsianghi D, Hill RG, Rupniak NM, 1999, Selective NMDA NR2B antagonists induce antinociception without motor dysfunction: correlation with restricted localisation of NR2B subunit in dorsal horn, *Neuropharmacology* 38: 611-623.

Boyce S, Rupniak NMJ, 2002, Behavioural studies on the potential of NMDA receptor antagonists as analgesics, *NMDA Antagonists as Potential Analgesic Drugs*, Birkhauser Verlag Basel:147-164.

Brimcombe JC, Boeckmann FA, Aizenman E, 1997, Functional consequences of NR2 subunit composition in single recombinant N-methyl-D-Aspartate receptors, *PNAS*, 94: 11019-11024.

Brose N, Gasic G, Vetter DE, Sullivan JM, Heinemann SF, 1993, *Journal Biological Chemistry*, 268, 22663-22671.

Buller AL, Larson HC, Schneider BE, Beaton JA, Morrisett RA, Monaghan DT, 1994, The molecular basis of NMDA receptor subtypes: native receptor diversity is predicted by subunit composition, *Journal of Neuroscience*, 14 (9): 5471-84.

Bullock RM, Merchant RE, Carmack CA, Doppenberg E, Shah AK, Wilner KD, Ko G, Williams SA, 1999, An open-label study of CP-101,606 in subjects with a severe traumatic head injury or spontaneous intracerebral hemorrhage, Ann N.Y. Academy of Science, 890: 51-58.

Carlton SM, Hargett GL, 1995, Treatment with the NMDA antagonist memantine attenuates nociceptive responses to mechanical stimulation in neuropathic rats, *Neuroscience Letters*, 198:115-118.

Carter C, Benavides J, Legendre P, Vincent JD, Noel F, Thuret F, Lloyd KG, Arbilla S, Zivkovic B, Mackenzie ET, Scatton B, Langer SZ, 1988, Ifenprodil and SL 82.0715 as cerebral anti-ischemic agents. II:Evidence for N-methyl-D-aspartate antagonist properties, *Journal Pharmacology and Experimental Therapeutics*, 247: 1222-1232.

Caudle RM, Perez FM, King C, Yu CG, Yezierski RP, 2003, N-methyl-D-aspartate receptor subunit expression and phosphorylation following excitotoxic spinal cord injury in rats, *Neuroscience Letters*, 349: 37-40.

Cavara NA, Hollman M, 2007, NR3 differentially influences NMDAR function, SfN Abstract, November 2007.

Chaplan SR, Bach FW, Pogrel JW, Chung JM, Yaksh TL, 1994, Quantitative assessment of tactile allodynia in the rat paw, *Journal of Neuroscience Methods*, 53: 55-63.

Chan WY, Soloviev MM, Ciruela F, McIlhinney RA, 2001, Molecular determinants of metabotropic glutamate receptor 1B trafficking, *Molecular and Cellular Neuroscience*, 17: 577-588.

Chatterton JE, Awobuluyi M, Premkumar LS, Takahasi H, Talantova M, Shin Y, Cui J, 2002, Excitatory glycine receptors containing the NR3 family of NMDA receptor subunits, *Nature*, 415, 793-798.

Chazot PL, Wilkins M, Strange PG, 1991, Site-specific antibodies as probes of the structure and function of the brain D2 dopamine receptor, *Biochemical Society Transactions*, 19 (2): 143S.

Chazot PL, Cik M, Stephenson, FA, 1992, Immunological detection of the NMDAR1 glutamate receptor subunit expressed in human embryonic kidney 293 cells and in rat brain, *Journal of Neurochemistry*, 59: 1176-1178.

Chazot PL, Fotherby A, Stephenson FA, 1993, Evidence for the involvement of a carboxyl group in the vicinity of the MK801 and magnesium ion binding site of the N-methyl-D-aspartate receptor, *Biochemical Pharmacology*, 45(3), 605-610.

Chazot PL, Coleman SK, Cik M, Stephenson FA, 1994, *Journal Biological Chemistry*, 269, 24403-24409.

Chazot PL, Stephenson FA, 1997, Biochemical evidence for the existence of a pool of unassembled C2 exon-containing NR1 subunits of the mammalian forebrain NMDA receptor, *Journal of Neurochemistry*, 68 (2): 507-516.

Chazot PL, Stephenson FA, 1997, Molecular dissection of native mammalian forebrain NMDA receptors containing the NR1 C2 exon: Direct demonstration of NMDA receptors comprising NR1, NR2A and NR2B subunits within the same complex, *Journal of Neurochemistry*, vol.69, 2138-2144.

Chazot PL, Cik M, Stephensohn FA, 1999, Transient expression of functional NMDA receptors in mammalian cells, *Methods in Molecular Biology*, 128: 33-42.

Chazot PL, Hawkins LM, 1999, NMDA receptor subtypes – Rationale for future CNS therapies, *Investigational Drugs*, 12: 1313.

Chazot PL, 2000, CP-101606 Pfizer Inc, *Current Opinion in Investigational Drugs*, 1(3), 370-374.

Chazot P.L, Lawrence.S, Thompson.C.L, 2002, Studies on the subtype selectivity of CP101606: evidence for two classes of NR2B-selective NMDA receptor antagonists, *Neuropharmacology* 42, 319-324.

Chazot P.L 2004, The NMDA Receptor NR2B Subunit: A valid Therapeutic Target for multiple CNS pathologies, *Current Medicinal Chemistry*,11, 389-396.

Chen N, Luo T, Wellington C, Metzler M, McCutcheon K, Hayden MR, Raymond LA, 1999, Subtype-specific enhancement of NMDA receptor currents by mutant hungtingtin, *Journal of Neurochemistry*, 72: 1890-1898.

Chen N, Luo T, Raymond LA, 1999, Subtype-dependence of NMDA receptor channel open probability, *Journal of Neuroscience*, 19: 6844-6854.

Chenard BL, Bordner J, Butler TW, 1995, (1S, 2S)-1-(4-hydroxyphenyl)-2-(4-hydroxy-4-phenylpiperidino)-1-propanol: a potent new neuroprotectant which blocks N-methyl-D-aspartate responses, *Journal of Medicial Chemistry*, 38: 3138-3145.

Chenard BL, Menniti FS, 1999, Antagonists selective for NMDA receptors containing the NR2B subunit, *Current Pharm. Des.*, 5: 381-404.

Cheng Y, Prusoff WH, 1973, Relationship between the inhibition constant ($K_i$) and the concentration of inhibitor which causes 50 per cent inhibition ($I_{50}$) of an enzymatic reaction, *Biochemical Pharmacology*, 22: 3099-3108.

Chizh BA, Headley PM, Tzschentke TM, 2001, NMDA receptor antagonists as analgesics: focus on the NR2B subtype, *Trends in Pharmacological Sciences,* 22 (12): 636-641.

Chizh BA, 2002, Novel approaches to targeting glutamate receptors for the treatment of chronic pain: Review article, *Amino Acids*, 23, 169-176

Chizh BA, Headley PM, 2005, NMDA antagonists and neuropathic pain-multiple drug targets and multiple uses, *Current Pharmaceutical Design*, 11: 2977-2994.

Choi DW, 1988, Glutamate neurotoxicity and disease and diseases of the nervous system, *Neuron*, 1: 623-634.

Choquet D, Triller A, 2003, The role of receptor diffusion in the organisation of the post-synaptic membrane, *Nature reviews Neuroscience*, 4: 251-265.

Chung HJ, Huang YH, Lau LF, Huganir RL, 2004, Regulation of the NMDA receptor complex and trafficking by activity-dependent phosphorylation of the NR2B subunit PDZ ligand, *The Journal of Neuroscience*, 24 (45): 10248-10259.

Church J, Fletcher EJ, Baxter K, MacDonald JF, 1994, Blockade by ifenprodil of high voltage-activated $Ca^{2+}$ channels in rat and mouse cultured hippocampal neurons: comparison with N-methyl-D-aspartate receptor antagonist actions, *British Journal of Pharmacology*, 113 (2): 499-507.

Ciabarra AM, Sullivan JM, Gahn LG, Pecht G, Heinemann S, Sevarino KA, 1995, Cloning and characterisation of chi-1: a developmentally regulated member of a novel class of the ionotropic glutamate receptor family, *Journal Neuroscience* 15: 6498-6508.

Cik M, Chazot PL, Stephenson FA, 1993, Optimal expression of cloned NMDAR1/NMDAR2A heteromeric glutamate receptors: a biochemical characterisation, *Biochemical Journal*, 296: 877-883.

Cik M, Chazot PL, Stephenson FA, 1994, Expression of NMDAR1-1a (N598Q)/NMDAR2A receptors results in decreased cell mortality, *European Journal of Pharmacology*, 266: R1-R3.

Cik M, Chazot PL, Coleman SK, Stephenson FA, 1995, Using Promega's Cytotox 96 non-radioactive cytotoxicity assay to measure cell death mediated by NMDA receptor subunits, *Promega Notes Magazine*, 51: 21-23.

Claiborne CF, McCauley JA, Libby BE, Curtis NR, Diggle HJ, Kulagowski JJ, Michelson SR, Anderson KD, Claremon DA, Freidinger RM, 2003, Orally efficacious NR2B-selective NMDA receptor antagonists, *Bioorg Med Chem Lett*, 13: 697-700.

Clark BA, Cull-Candy SG, 2002, Activity-dependent recruitment of extra-synaptic NMDA receptor activation at an AMPA receptor-only synapse, *Journal of Neuroscience*, 22: 4428-4436.

Colbran RJ, 2004, Targeting of calcium/calmodulin-dependent protein kinase II, *Journal of Biochemistry*, 378: 1-16.

Cook A, Woolf CJ, Wall PD, McMahon SB, 1987, Dynamic receptive field plasticity in rat spinal dorsal horn following C-primary afferent input, *Nature*, 325: 151-153.

Cottrell JR, Dube GR, Egles C, Liu G, 2000, Distribution, density and clustering of functional glutamate receptors before and after synaptogenesis in hippocampal neurons, Journal of Neurophysiology, 17: 1573-1587.

Cull-Candy S, Brickley S, Farrant M, 2001, NMDA receptor subunits: diversity, development and disease, *Current Opinion in Neurobiology*, 11, 327-335.

Dagert M, Ehrlich SD, 1979, Prolonged incubation in calcium chloride improves the competence of Escherichia coli cells, *Gene*, 23-8.

Das S, Sasaki YF, Rothe T, Premkumar LS, Takasu M, Crandall JE, Dikkes P, Conner DA, Rayudu PV, Cheung W, Chen HS, Lipton SA, Makanishi N, 1998, Increased NMDA current and spine density in mice lacking the NMDA receptor subunit NR3A, *Nature*, 393, 377-381.

Davies SN and Lodge D, 1987, Evidence for involvement of N-methylaspartate receptors in 'wind-up' of class 2 neurons in the dorsal horn of the rat. *Brain Research* 424:402-6.

Deupree JD, Bylund DB, Basic principles and techniques for receptor binding, Tocris Support, Tocris Cookson Inc., USA.

Di X, Bullock R, Watson J, Fatouros P, Chenard B, White F, Corwin F, 1997, Effect of CP-101606, a novel NR2B subunit antagonist of the N-methyl-D-aspartate receptor, on the volume of ischemic brain damage off cytotoxic brain oedema after middle cerebral artery occlusion in the feline brain, *Stroke*, 28 (11): 2244-2251.

Dickenson AH and Sullivan AF, 1987, Evidence for a role of the NMDA receptor in the frequency dependent potentiation of deep rat dorsal horn nociceptive neurons following C fibre stimulation, *Neuropharmacology* 26: 1235-8.

Dingledine R, Borges K, Bowie D, Traynelis SF, 1999, The glutamate receptor ion channels, *Pharmacology Reviews*, 51: 7-61.

Doraiswamy PM, 2003, Alzheimer's disease and the glutamate NMDA receptor, *Psychopharmacological Bulletin*, 37: 41-49.

Du Bois TM, Huang XF, 2007, Early brain development disruption from NMDA receptor hypofunction: relevance to schizophrenia, *Brains Research Reviews*, 53, 260-270.

Dunah AW, Luo J, Wang YH, Yasuda RP, Wolfe BB, 1998, Subunit composition of N-methyl-D-aspartate receptors in the central nervous system that contain the NR2D subunit, *Molecular Pharmacology*, 53: 429-437.

Eisenberg E, LaCross S, Strassman AM, 1995, The clinically tested N-methyl-D-aspartate receptor antagonist memantine blocks and reverses thermal hyperalgesia in a rat model of painful mononeuropathy, *Neuroscience Letters*, 187:17-20.

Eisenberg E, Kleiser A, Doertort A, Haim T, Yaritsky D, 1998, The NMDA receptor antagonist memantine in the treatment of postherpetic neuralgia: A double-blind, placebo-controlled study, *European Journal of Pain*, 2: 321-327.

Eriksson M, Nilsson A, Froelich-Fabre S, Akesson E, Dunker J, Seiger A, Filkesson R, Benedikz E, Sundstrom E, 2002, Cloning and expression of the human N-methyl-D-aspartate receptor subunit NR3A, *Neuroscience Letters*, 321, 177-181.

Erreger K, Traynelis SF, 2007, Zinc inhibition of NR1/NR2A N-methyl-D-aspartate receptors, *Journal of Physiology*.

Farkas S, Horvath C, Nagy J, 2003, RGH-896 is a novel potent and selective NR2B-NMDA antagonist with efficacy in neuropathic pain models, *Society for Neuroscience Abstract*, 382.8.

Feng B, Morley RM, Jane DE, Monaghan DT, 2005, The effect of competitive antagonist chain length on NMDA receptor subunit selectivity, *Neuropharmacology*, 48: 354-359.

Fisher K, Coderre TJ, Hagen NA, 2000, Targeting the N-methyl-D-aspartate receptor for chronic management. Preclinical animal studies, recent clinical experience and future research, *Journal of Pain Symptom Management*, 20 (5): 358-73.

Fischer G, Mutel V, Trube G, Malherbe P, Kew JN, Mohacsi E, Heitz MP, Kemp JA, 1997, Ro-25,6981, a highly potent and selective blocker of N-methyl-D-aspartate receptors containing the NR2B subunit. Characterisation in vitro, *Journal Pharmacology and Experimental Therapeutics*, 283: 1285-1292.

Fong DK, Rao A, Crump FT, Craig AM, 2002, Rapid synaptic remodelling by protein kinase C: reciprocal translocation of NMDA receptors and calcium/calmodulin-dependent kinase II, *Journal of Neuroscience*, 22: 2153-2164.

Fukaya M, Ueda H, yamauchi K, Inoue Y, Watanabe M, 1999, Distinct spatiotemporal expression of mRNAs for the PSD-95/SAP90 protein family in the mouse brain, *Neuroscience Research*, 33: 111-118.

Fukaya M, Kato A, Lovett C, Tonegawa S, Watanabe M, 2003, Retention of NMDA receptor NR2 subunits in the lumen of endoplasmic reticulum in targeted NR1 knockout mice, *PNAS*, 100 (8), 4855-4860.

Fukaya M, Hayashi Y, Watanabe M, 2005, NR2 to NR3B subunit switchover of NMDA receptors in early postnatal motoneurons, *European Journal Neuroscience*, 21: 1432-1436.

Fukaya M, Watanabe M, 2007, Selective localization of NR3A subunit at climbing fiber-interneuron synapses in the cerebellum, *SfN Abstract*, 349.12/E40

Fuller PI, Reddrop C, Rodger J, Bellingham MC, Phillips JK, 2006, Differential expression of the NMDA NR2B receptor subunit in motoneuron populations susceptible and resistant to amyotrophic lateral sclerosis, *Neuroscience Letters*, 399: 157-161.

Furuyama T, Kiyama H, Sato K, Park HT, Maeno H, Takagi H, Tohyama M, 1993, Region-specific expression of subunits of ionotropic glutamate receptors (AMPA-type, KA-type and NMDA receptors) in the rat spinal cord with special reference to nociception, *Brain Research and Molecular Brain Research*, 18 (1-2): 141-151.

Gao XM, Sakai K, Roberts RC, Conley RR, Dean B, Tamminga CA, 2000, Ionotropic glutamate receptors and expression of N-methyl-D-Aspartate receptor subunits in subregions of human hippocampus: Effects of schizophrenia, *American Journal Psychiatry*, 157: 1141-1149.

Gao X, Kim HK, Chung JM, Chung K, 2005, Enhancement of NMDA receptor phosphorylation of the spinal dorsal horn and nucleus gracilis neurons in neuropathic rats, *Pain*, 116: 62-72.

Gardoni F, DiLuca M, 2006, New targets for pharmacological intervention in the glutamatergic synapse, *European Journal of Pharmacology*, 545:2-10.

Garry EM, Moss A, Delaney A, O'Neill F, Blakemore J, Bowen J, Husi H, Mitchell R, Grant SGN, Fleetwood-Walker SM, 2003, Neuropathic sensitisation of behavioural reflexes and spinal NMDA receptor/CaM kinase II interactions are disrupted in PSD-95 mutant mice, *Current Biology*, 13: 321-328.

Gibb AJ, Colquhoun D, 1991, Glutamate activation of a single NMDA receptor channel produces a cluster of channel openings, *Proceedings of the Royal Society of London Biological Society*, 243:39-45.

Goebel DJ, Poosch MS, 1999, NMDA receptor subunit gene expression in the rat brain: A quantitative analysis of endogenous mRNA levels of NR1Com, NR2A, NR2B, NR2C, NR2D and NR3A, *Molecular Brain Research*, 69: 164-170.

Gogas KR, 2006, Glutamate-based therapeutic approaches: NR2B receptor antagonists, *Current Opinion in Pharmacology*, 6: 68-74.

Gorman AM, McGowan A, O'Neill C, Cotter T, 1996, Oxidative stress and apoptosis in neurodegeneration, *Journal of Neurological Science*, Suppl: 45-52.

Grimwood S, Slater P, Deakin JF, Hutson PH, 1999, NR2B-containing NMDA receptors are up-regulated in temporal cortex in schizophrenia, *Neuroreport*, 10: 461-465.

Grimwood S, Richards P, Murray F, Harrison N, Wingrove PB, Hutson PH, 2000, Characterisation of N-methyl-D-Aspartate receptor-specific [$^3$H] ifenprodil binding to recombinant human NR1a/NR2B receptors compared with native receptors in rodent brain membranes, *Journal of Neurochemistry*, 75 (6): 2455-2462.

Guillard L, Setou M, Hirokawa N, 2003, KIF17 dynamics and regulation of NR2B trafficking in hippocampal neurons, *Journal of Neuroscience*, 23: 131-140.

Haley JE, Sullivan AF, Dickenson AH, 1990, Evidence for spinal N-methyl-D-aspartate receptor involvement in prolonged chemical nociception in the rat, *Brain Research*, 518: 218-273.

Hallett PJ, Standaert DG, 2004, Rationale for and use of NMDA receptor antagonists in Parkinson's Disease, *Pharmacology and Therapeutics*, 102 (2): 155-174.

Hardingham GE, Fukunaga Y, Bading H, 2000, Extrasynaptic NMDARs oppose synaptic NMDARs by triggering CREB shut-off and cell death pathways, *Nature Neuroscience*, 5: 405-414.

Harris A, Petitt DL, 2007, The role of extrasynaptic NMDA receptors in plasticity, *Society for Neuroscience*, November 2007 abstract.

Hawkins LM, Chazot PL, Stephenson FA, 1999, Biochemical evidence for the co-association of three N-methyl-D-Aspartate (NMDA) R2 subunits in recombinant NMDA receptors, *The Journal of Biological Chemistry*, 274 (38):27211-27218.

Hawkins LM, Prybylowski K, Chang K, Moussan C, Stephenson FA, Wenthold RJ, 2004, Export from the endoplasmic reticulum of assembled N-methyl-D-aspartic

acid receptors is controlled by a motif in the C-terminus of the NR2 subunit, *The Journal of Biological Chemistry*, 279 (28): 28903-28910.

Heresco-Levy U, Javitt DC, 1998, The role of N-methyl-D-aspartate (NMDA) receptor-mediated neurotransmission in the pathophysiology and therapeutics of psychiatric syndromes, *European Neuropsychopharmacology*, 8: 141-152.

Hess SD, Daggett LP, Deal C, Lu CC, Johnson EC, Velicelebi G, 1998, Functional characterisation of human N-methyl-D-aspartate subtype 1A/2D receptors, *Journal of Neurochemistry*, 70: 1269-1279.

Hori N, Carpenter DO, 1994, Transient ischemia causes a reduction of Mg2+ blockade of NMDA receptors, *Neuroscience Letters*, 173: 75-78.

Ishii T, Moriyoshi K, Sugihara H, Sakurada K, Kadotani H, Yokoi M, Akazawa C, Shigemoto R, Mizuno N, Masu M, Nakanishi S, 1993, Molecular characterisation of the family of the N-methyl-D-aspartate receptor subunits, *Journal of Biological Chemistry* 268: 2836-2843.

Janeway CA, Travers P, Walport M, Shlomchik M, 2001, Immunobiology-The Immune System in Health and Disease, 5th Edition, garland Publishing and Churchill Livingstone:1-35.

Ji RR, Kohno T, Moore KA, Woolf CJ, 2003, Central sensitization and LTP: do pain and memory share similar mechanisms? *Trends in neuroscience*, vol.26 No.12: 696-705

Jones EG, Tighilet B, Tran BV, Huntsman MM, 1998, Nucleus and cell-specific expression of NMDA and non-NMDA receptor subunits in monkey thalamus, *Journal of Computational Neurology*, 397: 371-393.

Jordan BA, Devi LA, 1999, G-protein-coupled receptor heterodimerization modulates receptor function, *Nature*, 399: 697-700.

Khan AM, Curras MC, Dao J, Jamal FA, Turkowski CA, Goel RK, Gillard ER, Wolfsohn SD, Stanley BG, 1999, Lateral hypothalamic NMDA receptor subunits NR2A and/or NR2B mediate eating: immunochemical/behavioural evidence, *American Journal of Physiology*, 276: R880-891.

Karlsson U, Sjodin J, Moller A, Johansson S, Wikstrom L, Nasstrom J, 2002, Glutamate-induced currents reveal three functionally distinct NMDA receptor populations in rat dorsal horn-effects of peripheral nerve lesion and inflammation, *Neuroscience*, 112 No.4: 861-868.

Kemp JA, Foster AC, Wong EHF, 1987, Non-competitive antagonists of excitatory amino acid receptors, *Trends in Neuroscience*, 10: 294.

Kemp JA, McKernan RM, 2002, NMDA receptor pathways as drug targets, *Nature Neuroscience Supplement*, 5: 1039-1042.

Kew JN, Trube G, Kemp JA, 1996, A novel mechanism of activity-dependent NMDA receptor antagonism describes the effect if ifenprodil in rat cultured cortical neurones, *Journal of Physiology (London)*, 497: 761-772.

Kew JN, Kemp JA, 2005, Ionotropic and metabotropic glutamate receptor structure and pharmacology, *Psychopharmacology (Berl)*.179(1):4-29.

Kim JJ, Foy MR, Thompson RF, 1996, Behavioural stress modifies hippocampal plasticity through N-methyl-D-aspartate receptor activation, *PNAS*, 93: 4750-4753.

Kopke A, Bonk I, Sydow S, Menke H, Spiess, 2007, Characterisation of the NR1, NR2A and NR2C receptor proteins, *Protein Science*, 2: 2066-2076.

Kovacs G, Kocsis P, Tarnawa I, Horvath C, Szombathelyi Z, Farkas S, 2004, NR2B containing NMDA receptor dependent windup of single spinal neurons, *Neuropharmacology*, 46: 23-30.

Kuryatov A, Laube B, Betz H, Kuhse J, 1994, Mutational analysis of the glycine-binding site of the NMDA receptor: structural similarity with bacterial amino acid-binding proteins, *Neuron*, 12: 1291-1300.

Kutsuwada T, Kashiwabuchi N, Mori H, Sakimura K, Kushiya E, Araki K, Meguro H, Masaki H, Kumanishi T, Arakawa M et al, 1992, Molecular diversity of the NMDA receptor channel, *Nature*, 358: 36-41.

Kutsuwada T, Sakimura K, manabe T, Takayama C, Katakura N, Kushiya E, Natsune R, Watanabe M, Inoue Y, Yagi T, Aizawa S, Arakawa M, Takahashi T, Nakamura Y, Mori H, Mishina M, 1996, Impairment of suckling response, trigeminal neuronal pattern formation, and hippocampal LTD in NMDA receptor epsilon 2 subunit mutant mice, *Neuron*, 16: 333-344.

Lambe EK, Aghajanian GK, 2006, Hallucinogen-Induced UP states in the brain slice of rat prefrontal cortex: Role of glutamate spillover and NR2B-NMDA receptors, *Neuropsychopharmacology*, 31: 1682-1689.

Lau LF, mammen A, Ehlers MD, Kindler S, Chung WJ, Garner CC, Huganir RL, 1996, Interaction of the N-methyl-D-aspartate receptor complex with a novel synapse-associated protein, SAP102, *The Journal of Biological Chemistry*, 271 (35): 21622-21628.

Laube B, Kuhse J, Betz H, 1998, Evidence for a tetrameric structure of recombinant NMDA receptors, *Journal Neuroscience*, 18: 2954-2961.

Laurie DJ, Bartke I, Schoepfer R, Naujoks K, Seeburg PH, 1997, Regional, developmental and interspecies expression of the four NMDAR2 subunits, examined using monoclonal antibodies, *Brain Research and Molecular Brain Research*, 51: 23-32.

Lee HK, 2006, Synaptic plasticity and phosphorylation, *Pharmacology and Therapeutics*, 112: 810-832.

Leeson PD, Iverson LL, 1994, The glycine site on the NMDA receptor: structure-activity relationships and therapeutic potential, *Journal of Medicinal Chemistry*, 37: 4053-4067.

Levine ES, Kolb JE, 2000, Brain-derived neurotrophic factor increases activity of NR2B-containing N-methyl-D-aspartate receptors in excised patches from hippocampal neurons, *Journal of Neuroscience Research*, 62: 357-362.

Li L, Fan M, Icton CD, Chen N, Leavitt BR, Hayden MR, Murphy TH, Raymond LA, 2003, Role of NR2B-type NMDA receptors in selective neurodegeneration in Huntington Disease, *Neurobiology of Ageing*, 24: 1113-1121.

Li J, McRoberts JA, Ennes HS, Trevisani M, Nicoletti P, Mittal Y, Mayer EA, 2006, Experimental colitis modulates the functional properties of NMDA receptors in dorsal root ganglia neurons, *American Journal Physiology, Gastrointestinal Liver Physiology*, 291: G219-228.

Lin SY, Wu K, Levine ES, Mount HT, Suen PC, Black IB, 1998, BDNF acutely increases tyrosine phosphorylation of the NMDA receptor subunit NR2B in cortical and hippocampal postsynaptic densities, *Brain Research and Molecular Brain Research*, 55: 20-27.

Lim IA, Hall DD, Hell JW, 2002, Selectivity and promiscuity of the first and second PDZ domains of PSD-95 and synapse-associated protein 102, *Journal of Biological Chemistry*, 277: 21697-21711.

Lipton SA, 2007, Pathologically-activated therapeutics for neuroprotection: mechanism of NMDA receptor block by memantine and S-nitrosylation, *Current Drug Targets*, 8 (5): 621-632.

Lisman J, Schulman H, Cline H, 2002, The molecular basis of CaM KII function in synaptic and behavioural memory, *Nature Reviews Neuroscience*, 3: 175-190.

Liu H, Wang H, Sheng M, Jan LY, Jan LN, Basbaum AI, 1994, Evidence for presynaptic N-methyl-D-aspartate autoreceptors in the spinal cord dorsal horn, *Proceedings National Academy Sciences USA*, 91: 8383-8387.

Liu L, Wong TP, Pozza MF, Lingenhoehl K, Wang Y, Sheng M, Auberson YP, Wang YT, 2004, Role of NMDA receptor subtypes in governing the direction of hippocampal synaptic plasticity, *Science,* 304: 1021-1024.

Liu Y, Wong TP, Aarts M, Rooyakkers A, Liu L, Lai TW, Wu DC, Lu J, Tymianski M, Craig AM, Wang YT, 2007, NMDA receptor subunits have differential roles in mediating excitotoxic neuronal death both *in vitro* and *in vivo*, *The Journal of Neuroscience*, 27 (11): 2846-2857.

Loftis JM, Janowsky A, 2003, The N-methyl-D-aspartate receptor subunit NR2B:localisation, functional properties, regulation and clinical implications, *Pharmacology and Therapeutics*, 97: 55-85.

Loschmann PA, De Groote C, Smith L, Wullner U, Fischer G, Kemp JA, Jenner P, Klockgether T, 2004, Antiparkinsonian activity of Ro 25,6981, a NR2B subunit specific NMDA receptor antagonist, in animal models of Parkinson's disease, *Experimental Neurology*, 187: 86-93.

Luo J, Wang Y, Yasuda RP, Dunah AW, Wolfe BB, 1997, The majority of N-methyl-D-Aspartate receptor complexes in adult rat cerebral cortex at least three different subunits (NR1/NR2A/NR2B), *Molecular Pharmacology*, 51: 79-86.

Luque JM, Bleuel Z, Malherbe P, Richards JG, 1994, Alternatively spliced isoforms of the N-methyl-D-aspartate receptor subunit 1 are differentially distributed within the rat spinal cord, *Neuroscience*, 63(3): 629-35.

Lynch.D.R, Guttmann.R.P, 2001, NMDA receptor pharmacology:Perspectives from molecular biology, *Current Drug Targets*, 2: 215-231.

Ma QP, Hargreaves RJ, 2000, Localization of N-methyl-D-aspartate NR2B subunits on primary sensory neurons that give rise to small calibre sciatic nerve fibres in rats, *Neuroscience*, 101: 699-707.

Ma QP, Woolf CJ, 2002, The NMDA receptor, pain and central sensitization, *NMDA Antagonists as Potential Analgesic Drugs, Birkhauser Verlag Basel*: 83-103.

Malherbe P, Kratzeisen C, Lundstrom K, Richards JG, Faull RL, Mutel V, 1999, Cloning and functional expression of alternative spliced variants of the human metabotropic glutamate receptor 8, *Molecular Brain Research*, 67: 201-210.

Malherbe P, Mutel V, Broger C, Perin-Dureau F, Kemp JA, Neyton J, Paoletti P, Kew JNC, 2003, Identification of critical residues in the amino terminal domain of the human NR2B subunit involved in the Ro-256981 binding pocket, *The Journal of Pharmacology and Experimental Therapeutics*, 307: 897-905.

Markenson J.A 1996, Mechanisms of Chronic Pain, *The American Journal of Medicine*, vol 101 1A-7S.

Massey PV, Johnson BE, Moult PR, Auberson YP, Borwn MW, Molnar E, Collingridge GL, Bashir ZI, 2004, Differential roles of NR2A and NR2B-containing NMDA receptors in cortical long-term potentiation and long-term depression, *Journal of Neuroscience*, 24: 7821-7828.

Matsuda.K, Kamiya.Y, Matsuda.S, Yuzaki.M, 2002, Cloning and characterisation of a novel NMDA receptor subunit NR3B: a dominant subunit that reduces calcium permeability, *Molecular Brain Research* 100: 43-52.
Matsuda.K, Fletcher.M, Kamiya.Y, Yuzaki.M, 2003, Specific assembly with the NMDA Receptor 3B subunit controls surface expression and calcium permeability of NMDA receptors, *The Journal of Neuroscience*: 10064-10073.

McBain CJ, Mayer ML, 1994, N-methyl-D-aspartic acid receptor structure and function, *Physiological Review*, 74: 723-760.

McCauley JA, Theberge CR, Romano JJ, Billings SB, Anderson KD, Claremon DA, Freidinger RM, Bednar RA, Mosser SD, Gaul SL, Connolly TM, Condra CL, Xia M, Cunningham ME, Bednar B, Stump GL, Lynch JJ, Macaulay A, Wafford KA, Koblan KS, Liverton NJ, 2004, NR2B-selective N-methyl-D-aspartate antagonists: synthesis and evaluation of 5-substituted benzimidazoles, *Journal of Medicinal Chemistry*, 47 (8): 2089-2096.

McCauley JA, 2005, NR2B subtype-selective NMDA receptor antagonists: 2001-2004, *Expert Opinion Therapeutic Patents*, 15(4): 389-407.

Medvedev IO, Malyshkin AA, Belozertseva IV, Sukhotina IA, Sevostianova NY, Aliev K, Zvartau EE, Parsons CG, Danysz W, Bespalov AY, 2004, Effects of low-

affinity NMDA receptor channel blockers in two rat models of chronic pain, *Neuropharmacology*, 47: 175-183.

Menniti F, Chenard B, Collins M, Ducat M, Shalaby I, White F, 1997, CP-101,606, a potent neuroprotectant selective for forebrain neurons, *European Journal of Pharmacology*, 331: 117-126.

Menniti FS, Shah AK, Williams SA, Wilner KD, White WF, Chenard BL, 1998, CP-101606: An NR2B-selective NMDA receptor antagonist, *CNS Drug Reviews*, 4: 307-322.

Mercadante S, Lodi F, Sapio M, Calligara M, Serretta R, 1995, Long-term ketamine subcutaneous continuous infusion in neuropathic cancer pain, *Journal of Pain Symptom Management*, 10: 564-568.

Merchant RE, Bullock MR, Carmack CA, Shah AK, Wilner KD, Ko G, Williams SA, 1999, A double-blind, placebo-controlled study of the safety, tolerability and pharmacokinetics of CP-101, 606 in patients with a mild or moderate traumatic brain injury, *Ann NY Academy Science*, 890: 42-50.

Momiyama A, 2000, Distinct synaptic and extrasynaptic NMDA receptors identified in dorsal horn neurones of the adult rat spinal cord, *Journal of Physiology*, 523:621-628.

Mok H, Shin H, Kim S, Lee JR, Yoon J, Kim E, 2002, Association of the kinesin superfamily motor protein KIF1Balpha with postsynaptic density-95 (PSD-95), synapse-associated protein-97, and synaptic scaffolding molecule PSD-95/discs large/zona occludens-1 proteins, *Journal of Neuroscience*, 22: 5253-5258.

Monyer H, Sprengel R, Schoepfer R, Herb A, Higuchi M, Lomeli H, Burnashev N, Sakmann B, Seeburg PH, 1992, Heteromeric NMDA receptors: molecular and functional distinction of subtypes, *Science*, 256: 1217-1221.

Monyer H, Burnashev N, Laurie DJ, Sakmann B, Seeburg PH, 1994, Developmental and regional expression in the rat brain and functional properties of four NMDA receptors, *Neuron* 12: 529-540.

Motulsky H, 1995, Analyzing radioligand binding data, GraphPad Software Inc.

Moriyoshi K, Masu M, Ishii T, Shingemoto R, Mizuno N, Nakanishi S, 1991, Molecular cloning and characterisation of the rat NMDA receptor, *Nature*, 354: 31-37.

Mueller HT, Meador-Woodruff JH, 2004, NR3A NMDA receptor subunit mRNA expression in schizophrenia, depression and bipolar disorder, *Schizophrenia Research*, 71: 361-370.

Mueller HT, Meador-Woodruff JH, 2005, Distribution of the NMDA receptor NR3A subunit in the adult pig-tail macaque brain, *Journal Chemical Neuroanatomy*, 29: 157-172.

Murphy DE, Hutchison AJ, Hurt SD, Williams M, Sills MA, 1988, Characterisation of the binding of [$^3$H]-CGS 19755: a novel N-methyl-D-aspartate antagonist with nanomolar affinity in rat brain, *British Journal of Pharmacology*, 95: 932.

Mutel V, Buchy D, Klingelschmidt A, Messer J, Bleuel Z, Kemp JA, Richards JG, 1998, In vitro binding properties in the rat brain of [$^3$H] Ro-256981, a potent and selective antagonist of NMDA receptors containing NR2B subunits, *Journal of Neurochemistry*, 70: 2147-2155.

Nagy J, Boros A, Dezso P, Kolok S, Fodor L, 2003, Inducible expression and pharmacology of recombinant NMDA receptors, composed of rat NR1a/NR2B subunits, *Neurochemistry International*, 43:19-29.

Nagy GG, Watanabe M, Fukaya M, Todd AJ, 2004, Synaptic distribution of the NR1, NR2A and NR2B subunits of the N-methyl-D-aspartate receptor in the rat lumbar spinal cord revealed with an antigen-unmasking technique, *European Journal of Neuroscience*, 20: 3301-3312.

Nakanishi S, 1994, Metabotropic glutamate receptors: synaptic transmission, modulation and plasticity, Neuron, 13: 1031-7.

Nakazawa T, Komai S, tezuka T, Hisatsune C, Umemori H, Semba K, Mishina M, manabe T, Yamamoto T, 2001, Characterisation of Fyn-mediated tyrosine phosphorylation sites on GluRε2 (NR2B) subunit of the N-methyl-D-aspartate receptor, *Journal of Biological Chemistry*, 276: 693-699.

Nash JE, Ravenscroft P, McGuire S, Corssman AR, Menniti FS, Brotchie JM, 2004, The NR2B-selective NMDA receptor antagonist CP-101, 606 exacerbates L-DOPA-induced dyskinesia and provides mild potentiation of anti-parkinsonian effects of L-DOPA in the MPTP-lesioned marmoset model of Parkinson's disease, *Experimental Neurology*, 188: 471-479.

Niemann S, Kanki H, Fukui Y, Takao K, Fukaya M, Hynynen MN, Churchill MJ, Shefner JM, Bronson RT, Brown RH, Watanabe M, Miyakawa T, Itohara S, Hayashi Y, 2007, Genetic ablation of NMDA receptor subunit NR3B in mouse reveals

motoneuronal and nonmotoneuronal phenotypes, *European Journal of Neuroscience*, 26: 1407-1420.

Niethammer M, Kim E, Sheng M, 1996, Interaction between the C terminus of NMDA receptor subunits and multiple members of the PSD-95 family of membrane-associated guanylate kinases, *Journal of Neuroscience*, 16: 2157-2163.

Nikam SS, Meltzer LT, 2002, NR2B selective NMDA receptor antagonists, *Current Pharmaceutical Design*, 8: 845-855.

Nilsson A, Eriksson M, Chris Muly E, Akesson E, Samuelsson EB, Bogdanovic N, Benedikz E, Sundstrom E, 2007, Analysis of NR3A receptor subunits in human native NMDA receptors, *Brain Research*, 1186: 102-112.

Nishi M, Hinds H, Lu HP, Kawata M, Hayashi Y, 2001, Motoneuron-specific expression of NR3B, a novel NMDA-type glutamate receptor subunit that works in a dominant-negative manner, *Journal of Neuroscience*, 21, RC185.

Nishimura W, Muratani T, Tatsumi S, Sakimura K, Mishina M, Minami T, Ito S, 2004, Characterisation of N-methyl-D-aspartate receptor subunits responsible for postoperative pain, *European Journal of Pharmacology*, 503 (1-3): 71-5.

Nowak.LM, Wright.JM 1992, Slow voltage-dependent changes in channel open state probability underlie hysteresis of NMDA responses in $Mg^{2+}$-free solutions, *Neuron*,8: 181-187.

O'Donnell, Molon-Noblot S, Laroque P, Rigby M, Smith D, 2004, The ultrastructural localisation of the N-methyl-D-aspartate NR2B receptor subunit in rat lumbar spinal cord, *Neuroscience Letters*, 371: 24-29.

Paoletti P, Neyton J, 2006, NMDA receptor subunits: function and pharmacology, *Current Opinion in Pharmacology*, 6: 1-9.

Perin-Dureau F, Rachline J, Neyton J, Paoletti P, 2002, Mapping the binding site of the neuroprotectant ifenprodil on NMDA receptors, *Journal of Neuroscience*, 22: 5955-65.

Perez-Otano I, Schulteis CT, Contractor A, Lipton SA, Trimmer JS, Sucher NJ, Heinemann SF, 2001, Assembly with the NR1 subunit is required for surface expression of NR3A-containing NMDA receptors, *Journal of Neuroscience*, 21: 1228-1237.

Perez-Otano I, Lujan R, Tavalin SJ, Plomann M, Modregger J, Liu XB, Jones EG, Heinemann SF, Lo DC, Ehlers MD, 2006, Endocytosis and synaptic removal of NR3A-containing NMDA receptors by PACSIN1/syndapin1, *Nature Neuroscience*, 9: 611-621.

Petrenko AB, Yamakura T, Baba H, Shimoji K, 2003, The role of N-methyl-D-Aspartate (NMDA) receptors in pain: A review, *Anesthetics Analgesia*, 97: 1108-16.

Pina-Crespo JC, Heinemann SF, 2004, Physiological and pharmacological properties of recombinant NR3-type receptors expressed in mammalian cells, *Society Neuroscience Abstract*, 30:957.1

Priestley T, 2002, Pharmacology and electrophysiology of excitatory amino acid receptors, *NMDA Antagonists as potential analgesic drugs*, Birkhauser: 5-44.

Prybylowski K, Wenthold RJ, 2004, N-Methyl-D-aspartate receptors: subunit assembly and trafficking to the synapse, *Journal of Biological Chemistry*, 279 (11):9673-6.

Prybylowski K, Chang K, Sans N, Kan L, Vicini S, Wenthold RJ, 2005, The synaptic localisation of NR2B-containing NMDA receptors is controlled by interactions with PDZ proteins and AP-2, *Neuron*, 47: 845-857.

Qian J, Brown SD, Carlton SM, 1996, Systematic ketamine attenuates nociceptive behaviours in a rat model of peripheral neuropathy, *Brain Research*, 715: 271-278.

Qian A, Johnson JW, 2006, Permeant ion effects on external $Mg^{2+}$ block of NR1/2D NMDA receptors, *The Journal of Neuroscience*, 26(42): 10899-10910.

Qu, M., Chatterton, J.E., Wang, R., Huang, L., Millan, J., Lipton, S.A. & Zhang, D, (2004) Severe motor neuron loss in the spinal cord of NMDA receptor subunit, 3B (NR3B): null mice in the early postnatal period. *Society for Neuroscience Abstract*: 957.3.

Rao SD, Weiss JH, 2004, Excitotoxic and oxidative cross-talk between motor neurons and glia in ALS pathogenesis, *Trends in Neuroscience*, 27 (1): 17-23.

Rigby M, Heavens RP, Smith D, O'Donnell R, Hill RG, Sirinathsinghji DJS, 2002, Distribution of NMDA receptors in brain and spinal cord, *NMDA Antagonists as Potential Analgesic Drugs, Birkhauser Verlag-Basel*: 45-65.

Roche KW, Tu JC, Petralia RS, Xiao B, Wenthold RJ, Worley PF, 1999, Homer 1b regulates the trafficking of group 1 metabotropic glutamate receptors, *Journal of Biological Chemistry*, 274: 25953-25957.

Roesler R, Quevedo J, Schroder N, 2003, Is it time to conclude that NMDA antagonists have failed?, *The Lancet-Neurology*, 2: 13.

Robinson DA and Zhuo, 2002, Glutamatergic synapses serve as potential targets for controlling persistent pain, *Current Anaesthsia and Critical Care*, 13: 321-327.

Rodriguez FJ, Lluch M, Dot J, Blanco I, Rodriguez-Alvarez J, 1997, Histamine modulation of glutamate release from hippocampal synaptosomes, *European Journal of Pharmacology*, 323: 283-286.

Rosenblum K, Dudai Y, Richter-Levin G, 1996, Long-term potentiation increases tyrosine phosphorylation of the N-methyl-D-aspartate receptor subunit 2B in rat dentate gyrus *in vivo, PNAS*, 93: 10457-10460.

Rostas JA, Brent VA, Voss K, Errington ML, Bliss TV, Gurd JW, 1996, Enhanced tyrosine phosphorylation of the 2B subunit of the N-methyl-D-aspartate receptor in long-term potentiation, *PNAS*, 93: 10452-10456.

Samarasinghe S, Virgo L, De Belleroche J, 1996, Distribution of the N-methyl-D-aspartate glutamate receptor subunit NR2A in control and amyotrophic lateral sclerosis spinal cord, *Brain Research*, 727: 233-237.

Sang CN, Weaver JJ, Jinga L, Woulden J, Saltarelli MD, 2003, The NR2B subunit-selective NMDA receptor antagonist, CP-101,606, reduces spontaneous pain intensity in patients with central and peripheral neuropathic pain, *Abstract Society for Neuroscience, Washington* 2003: 814.9.

Sattler R, Xiong Z, Lu WY, Hafner M, MacDonald JF, Tymianski M, 1999, Specific coupling of NMDA receptor activation to nitric oxide neurotoxicity by PSD-95 protein, *Science,* 284: 1845-1848.

Sattler R, Tymianski M, 2000, Molecular mechanisms of calcium-dependent excitotoxicity, *Journal of Molecular Medicine*, 78: 3-13.

Scherzer CR, Landwehrmeyer GB, Kerner JA, Courihan TJ, Kosinski CM, Standaert DG, Daggett LP, Velicelebi G, penney JB, Young AB, 1998, expression of N-methyl-D-aspartate subunit mRNAs in the human brain: hippocampus and cortex, *Journal of Computational Neurology*, 1998: 390 (1): 75-90.

Shaw PJ, Ince PG, Matthews JNS, Johnson M, Candy JM, 1994, N-methyl-D-aspartate (NMDA) receptors in the spinal cord and motor cortex in motor neuron disease: a quantitative autoradiographic study using [$^3$H] MK-801, *Brain Research*, 637: 297-302.

Sheng M, Cummings J, Roldan LA, Jan Y, Jan LY, 1994, Changing subunit composition of heteromeric NMDA receptors during development of rat cortex, *Nature*, 368: 144-147.

Shibata T, Watanabe M, Ichikawa R, Inoue Y, Koyanagi T, 1999, Different expressions of alpha-amino-3-hydorxy-5-methyl-4-isoxazole propionic acid and N-methyl-D-aspartate receptor subunit mRNAs between visceromotor and somatomotor neurons of the rat lumbosacral spinal cord, *Journal of Computational Neurology*, 404: 172-182.

Smothers CT, Woodward JJ, 2007, Pharmacological characterisation of glycine-activated currents in HEK 293 cells expressing N-methyl-D-aspartate NR1 and NR3 subunits, *Journal of Pharmacology and Experimental Therapeutics*, 322 (2): 739-748.

Stanley BG, Willett VL Donias HW, Dee MG, Duva MA, 1996, Lateral hypothalamic NMDA receptors and glutamate as physiological mediators of eating and weight control, *American Journal of Physiology*, 270:R443-449.

Standley S, Roche KW, McCallum J, Sans N, Wenthold RJ, 2000, PDZ domain suppression of an ER retention signal in NMDA receptor NR1 splice variants, *Neuron*, 28: 887-898.

Stefani MR, Moghaddam B, 2005, Transient N-methyl-D-aspartate receptor blockade in early development causes lasting cognitive deficits relevant to schizophrenia, *Biological Psychiatry*, 57: 433-436.

Stephenson F A, 2001, Subunit characterisation of NMDA receptors, *Current Drug Targets*, 2: 233-239.

Stephenson FA, Duggan MJ, 1991, Molecular approaches to the structure and function of the $GABA_A$ receptors. In: Chad J, Wheal H editors. *Molecular Neurobiology: a practical approach.* Oxford, UK: IRL Press: 183-204.

Sucher NJ, Akbarian S, Chi CL, Leclerc CL, Awobuluyi M, Deitcher DL, Wu MK, Yuan JP, Jones EG, Lipton SA, 1995, Developmental and regional expression pattern of a novel NMDA receptor-like subunit (NMDA-L) in the rodent brain, *Journal of Neuroscience*, 15: 6509-6520.

Suchanek B, Seeburg PH, Sprengel R, 1995, Gene structure of the murine N-methyl-D-aspartate receptor subunit NR2C, *Journal of Biological Chemistry* 270: 41-44.

Sun L, Margolis FL, Shipley MT, Lidow MS, 1998, Identification of a long variant of mRNA encoding the NR3 subunit of the NMDA receptor: its regional distribution and developmental expression in the rat brain. *FEBS Lett* 441: 392-396.

Sundstrom E, Whittemore S, Mo LL, Seiger A, 1997, Analysis of NMDA receptors in the human spinal cord, *Experimental Neurology*, 148: 407-413.

Takai H, Katayama K, Uetsuka K, Nakayama H, Doi K, 2003, Distribution of N-methyl-D-aspartate receptors (NMDARs) in the developing rat brain, *Experimental and Molecular Pathology*, 75: 89-94.

Takanishi K, Tsuchida K, Tanabe Y, Masu M, Nakanishi S, 1993, Role of the large extracellular domain of metabotropic glutamate receptors in agonist selectivity determination, *Journal of Biological Chemistry*, 268: 19341-19345.

Tan PH, Yang LC, Shih HC, Lan KC, Cheng JT, 2005, Gene knockdown with intrathecal siRNA of NMDA receptor NR2B subunit reduces formalin-induced nociception in the rat, *Gene Therapy*, 12: 59-66.

Taniguchi K, Shinjo K, Mizutani M, Shimada K, Ishikawa T, Meniti FS, Nagahisa A, 1997, Antinociceptive activity of CP-101606, an NMDA receptor NR2B subunit antagonist, *British Journal of Pharmacology*, 122: 809-812.

Tao YX, Huang YZ, Mei L, Johns RA, 2000, Expression of PSD-95/SAP90 is critical for N-methyl-D-aspartate receptor-mediated thermal hyperalgesia in the spinal cord, *Letters to Neuroscience*, 98 No.2: 201-206.

Thomas CG, Miller AJ, Westbrook GL, 2006, Synaptic and extrasynaptic NMDA receptor NR2 subunits in cultured hippocampal neurons, *Journal of Neurophysiology*, 95: 1727-1734.

Thompson CL, Drewery DL, Atkins HD, Stephenson FA, Chazot PL, 2000, Immunohistochemical localization of N-methyl-D-Aspartate receptor NR1, NR2A, NR2B and NR2C/D subunits in the adult mammalian cerebellum, *Neuroscience Letters*, 283: 85-88.

Thompson CL, Drewery DL, Atkins HD, Stephenson FA, Chazot PL, 2002, Immunohistochemical localization of N-methyl-D-Aspartate receptor subunits in the

adult murine hippocampal formation: evidence for a unique role of the NR2D subunit, *Molecular Brain Research*, 102: 55-61.

Tolle TR, Berthele A, Zieglgansberger W, Seeburg PH, Wisden W, 1993, The differential expression of 16 NMDA and non-NMDA receptor subunits in the rat spinal cord and in Periaqueductal gray, *Journal of Neuroscience*, 13: 5009-5028.

Tortora GJ, Grabowski SR, 2003, Principles of Anatomy and Physiology 10th Edition, John Wiley and Sons, Inc, New York: 464-465.

Tovar KR, Westbrook GL, 1999, The incorporation of NMDA receptors with a distinct subunit composition at nascent hippocampal synapses in vitro, *Journal of Neuroscience*, 19: 4180-4188.

Tovar KR, Sprouffske K, Westbrook GL, 2000, fast NMDA receptor-mediated synaptic currents in neurons from mice lacking the ε2 (NR2B) subunit, *Journal of Neurophysiology*, 83: 616-620.

Toyoda H, Zhao MG, Zhuo M, 2006, NMDA receptor-dependent long-term depression in the anterior cingulated cortex, *Reviews In Neurosciences*, 17 (4): 403-413.

Tracey I, Ploghaus A, Gati JS, Clare S, Smith S, Menon RS, Matthews PM, 2002, Imaging Attentional Modulation of Pain in the Periaqueductal Gray in Humans, *The Journal of Neuroscience*, 22(7): 2748-2752.

Tsuchida E, Rice M, Bullock RJ, 1997, The neuroprotective effect of the forebrain-selective NMDA antagonist CP-101606 upon focal ischemic brain damage caused by subdural hematoma in the rat, *Neurotrauma,* 14 (6): 409-417.

Tymianski M, Charlton MP, Carlen PL, Tator CH, 1993, Source specificity of early calcium neurotoxicity in cultured embryonic spinal neurons, *Journal of Neuroscience*, 13: 2085-2104.

Ulas J, Weihmuller FB, Brunner LC, Joyce JN, Marshall JF, Cotman CW, 1994, Selective Increase of NMDA-sensitive glutamate binding in the striatum of Parkinson's disease, Alzheimer's disease and mixed Parkinson's disease/Alzheimer's disease patients: An autoradiographic study, *The Journal of Neuroscience*, 14 (11): 6317-6324.

Ultenius C, Linderoth B, Meyerson BA, Wallin J, 2006, Spinal NMDA receptor phosphorylation correlates with the presence of neuropathic signs following peripheral nerve injury in the rat, *Neuroscience Letters*, 399: 85-90.

Van Damme P, Dewil M, Robberecht W, van den Bosch L, 2005, Excitotoxicity and Amyotrophic Lateral Sclerosis, *Neurodegenerative Diseases*, 2: 147-159.

Van Zundert B, Yoshii A, Constantine-Paton M, 2004, Receptor compartmentalization and trafficking at glutamate synapses: a developmental proposal, *Trends in Neurosciences*, 27 (7): 428-437.

Verkhratsky A, Kirchoff F, 2007, NMDA receptors in glia, *The Neuroscientist*, 13 (1): 28-37.

Vicini S, Wang JF, Li JH, Zhu WJ, Wang YH, Luo JH, Wolfe BB, Grayson DR, 1998, Functional and pharmacological differences between recombinant N-methyl-D-aspartate receptors, *Journal of Neurophysiology*, 79: 555-566.

Virgo L, DeBelleroche J, 1995, Induction of the immediate early gene c-jun in human spinal cord in amyotropic lateral sclerosis with concomitant loss of NMDA receptor NR1 and glycine transporter mRNA, *Brain Research*, 676: 196-204.

Virgo L, Dekkers J, Mentis GZ, Navarrete R, De Belleroche J, 2000, Changes in expression of NMDA receptor subunits in the rat lumbar spinal cord following neonatal nerve injury, *Neuropathology and Applied Neurobiology*, 26: 258-272.

Wada A, Takahashi H, Lipton SA, Vincent Chen HS, 2006, NR3A modulates the outer vestibule of the NMDA receptor channel, *The Journal of Neuroscience*, 26 (51): 13156-13166.

Wafford KA, Bain CJ, Le Bourdelles B, Whiting PJ, Kemp JA, 1993, Preferential co-assembly of recombinant NMDA receptors composed of three different subunits, *Neuroreport*, 4: 1347-1349.

Wang YH, Bosy TZ, Yasuda RP, Grayson DR, Vicini S, Pizzorusso T, Wolfe BB, 1995, Characterisation of NMDA receptor subunit-specific antibodies: distribution of NR2A and NR2B receptor subunits in rat brain and ontogenic profile in the cerebellum, *Journal of Neurochemistry*, 65: 176-183.

Wang R, Zhang D, 2005, Memantine prolongs survival in an amyotrophic lateral sclerosis mouse model, *European Journal of Neuroscience*, 22: 2376-2380.

Wang CX, Shuaib A, 2005, NMDA/NR2B selective antagonists in the treatment of ischemic brain injury, *Current Drug Targets*, 4: 143-151.

Watanabe M, Mishine M, Inoue Y, 1994, Distinct spatiotemporal distributions of the N-methyl-D-aspartate receptor channel subunit mRNAs in the mouse cervical cord, *Journal Computational Neurology*, 345: 314-319.

Wee KSL, Zhang Y, Khanna S, Low CM, 2007, Immunolocalisation of N-methyl-D-aspartate receptor subunits NR3B in selected structures in the rat forebrain, cerebellum and lumbar spinal cord, *Journal of Comparative Neurology*, 509 (1): 118-135.

Wei F, Wang GD, Kerchner GA, Kim SJ, Xu HM, Chen ZF, Zhuo M, 2001, Genetic enhancement of inflammatory pain by forebrain NR2B overexpression, *Nature Neuroscience*, 4 (5): 453-4.

Wenthold RJ, Yokotani N, Doi K, Wada K, 1992, Immunochemical characterisation of the non-NMDA glutamate receptor using subunit-specific antibodies. Evidence for a hetero-oligomeric structure in rat brain. *Journal Biological Chemistry*, 267: 501-507.

Wenzel A, Scheurer L, Kunzi R, Fritschy JM, Mohler H, Benke D, 1995, Distribution of NMDA receptor proteins NR2A, 2B, 2C and 2D in rat brain, *Neuroreport* 7: 45-48.

Wenzel A, Mohler VH, Benke D, 1996, Developmental and regional expression of NMDA receptor subtypes containing the NR2D subunit in rat brain, *Journal Neurochemistry* 66: 1240-1248.

Wessel RH, Ahmed SM, Menniti FS, Dunbar GL, Chase TN, Oh JD, 2004, NR2B selective NMDA receptor antagonist CP-101,606 prevents levodopa-induced motor response alterations in hemi-parkinsonian rats, *Neuropharmacology*, 47 (2): 184-194.

Williams K, 1993, Ifenprodil discriminates subtypes of the N-methyl-D-aspartate receptor: selectivity and mechanisms at recombinant heteromeric receptors, *Molecular Pharmacology*, 44: 851-859.

Williams K, 1997, Modulation and block of ion channels: A new biology of polyamines, *Cell Signalling*, 9 (1): 1-13.

Williams JM, Mason-Parker SE, Abraham WC, Tate WP, 1998, Biphasic changes in the levels of N-methyl-D-aspartate receptor-2 subunits correlate with the induction and persistence of long-term potentiation, *Brain Research and Molecular Brain Research*, 60: 21-27.

Williams.K, 2001, Ifenprodil, a novel NMDA receptor antagonist:site and mechanism of action, *Current Drug Targets*, 2: 285-298.

Wilson AW, Medhurst SJ, Dixon CI, Bontoft NC, Winyard LA, Brackenborough KT, de Alba J, Clarke CJ, Gunthorpe MJ, Hicks GA, Bountra C, McQueen DS, Chessell IP, 2005, An animal model of chronic inflammatory pain: Pharmacological and temporal differentiation from acute models, *European Journal of Pain*,

Woolf CJ, 1983, Evidence for a central component of post-injury pain hypersensitivity, *Nature*, 306: 686-688.

Woolf CJ, Salter MW, 2000, Neuronal plasticity: increasing the gain in pain, *Science*, 288: 1765-1769.

Wu LJ, Toyoda H, Zhao MG, Lee YS, Tang J, Ko SW, Jia YH, Shum FWF, Zerbinatti CV, Bu G, Wei F, Xu TL, Muglia LJ, Chen ZF, Auberson YP, Kaang BK, Zhuo M, 2005, Upregulation of forebrain NMDA NR2B receptors contributes to behavioural sensitisation after inflammation, *The Journal of Neuroscience*, 25 (48): 11107-11116.

Wyllie DJ, Behe P, Colquhoun D, (1998), Single-channel activations and concentration jumps: cmparison of recombinant NR1a/NR2A and NR1a/NR2D NMDA receptors. *(Journal of Physiology London)*, 510: 1-18.

Yang CH, Huang CC, Hsu KS, 2005, Behavioural stress enhances hippocampal CA1 long-term depression through the blockade of the glutamate uptake, *The Journal of Neuroscience*, 25 (17): 4288-4293.

Yao Y, Mayer ML, 2006, Characterisation of a soluble ligand binding domain of the NMDA receptor regulatory subunit NR3A, *Journal of Neuroscience*, 26: 4559-4566.

Young PA, Young PH, 1997, Basic Clinical Neuroanatomy, Williams and Wilkins, USA.

Zeron MM, Chen N, Moshaver A, Lee AT, Wellington CL, Hayden MR, Raymond LA, 2001, Mutant huntingtin enhances excitotoxic cell death, *Molecular Cell Neuroscience*, 17: 41-53.

Zeron MM, Hansson O, Chen N, Wellington CL, Leavitt BR, Brundin P, Hayden MR, Raymond LA, 2002, Increased sensitivity to N-methyl-D-aspartate receptor-mediated excitotoxicity in a mouse model of Huntington's Disease, *Neuron*, 33: 849-860.

Zheng F, Zhang L, Wang AP, Bennett MV, Zukin RS, 1999, Protein kinase C potentiation of N-methyl-D-aspartate receptor activity is not mediated by phosphorylation of N-methyl-D-aspartate receptor subunits, *PNAS*, 96:15262-15267.

Zhang L, Rzigalinski BA, Ellis EF, Satin LS, 1996, Reduction of voltage-dependent $Mg^{2+}$ blockade of NMDA current in mechanically injured neurons, *Science,* 274: 1921-1923.

Zhao J, Peng Y, Xu Z, Chen RQ, Gu QH, Chen Z, Lu W, 2008, Synaptic metaplasticity through NMDA receptor lateral diffusion, *The Journal of Neuroscience*, 28 (12): 3060-3070.

Zhen X, Zhang L, Wang AP, Bennett MVL, Zukin RS, 1997, $Ca^{2+}$ influx amplifies protein kinase C potentiation of recombinant NMDA receptors, *Journal of Neuroscience* 17: 8676-86.

Zhuo M, 2002, Glutamate receptors and persistent pain:targeting forebrain NR2B subunits, *Drug Discovery Today*, No.4: 259-267.

Zigmond MJ., et. al., eds. 1999, *Fundamental Neuroscience*. Illustrations by Robert S. Woolley. Part III. San Diego, CA: Academic Press, 1999, pp. 417-517, and 547-654. ISBN.

Zou X, Lin Q, Willis WD, 2000, Enhanced phosphorylation of NMDA receptor 1 subunits in spinal cord dorsal horn and spinothalamic tract neurons after intradermal injection of capsaicin in rats, *Journal of Neuroscience*, 20: 6989-6997.